ROZPRAWY NAUKOWE
478

Marcin Schmidt

Characteristics of biological processes influenced by gut bacteria

POZNAŃ 2015

CHARACTERISTICS OF BIOLOGICAL PROCESSES INFLUENCED BY GUT BACTERIA

ABSTRACT

Introduction. Microbial community inhabiting gastrointestinal tract greatly outnumbers host cells and encodes hundreds-times more genes than human genome. Despite enormous qualitative and quantitative variation in human gut microbiota composition it shares surprisingly similar functional gene profiles. The similarity may reflect its importance for adaptation to the ecological niche and for development of interactions with host. An impact of specific microbial strain on human health is mainly deduced from epidemiological data. However, there is still little evidence available on molecular background of the host-microbe interactions.

Material and methods. Differentiated Caco-2 cells in culture were used as *in vitro* gut model. The enterocytes were stimulated with probiotic, commensal or pathogenic bacterial strains. Total RNA isolated from the epithelial cells was reverse-transcribed and investigated employing microarrays hybridization. Normalysed microarray data was used to generate lists of differentially expressed genes, which were further analysed to recognise biological processes influenced by the bacteria used. For gene expression pattern comparisons an unsupervised hierarchical cluster analysis applying Euclidean distance measures was used. Data mining was performed exploiting KEGG pathways database and Gene Ontology annotations. Modulation of virus infection-related processes was examined using rotavirus infected Caco-2 cells. Rotavirus genome replication/transcription and cellular genes expression in enterocytes treated with bacteria was analysed with RT-qPCR. Infected and/or bacteria treated cells' health was investigated with apoptosis (caspase-3/7), cell viability and cytotoxicity assays.

Results. Analysis of transcriptional responses to 6 single strains and 1 mixture of probiotic, 3 single strains of commensal and pathogenic strains revealed a large variation in enterocytes' response to bacteria ($R^2 \leqslant 0.66$). Single microorganism was able to modulate 1.1 thousands of human genes on an average. For the 13 experimental conditions tested the total number of 10.7 thousand genes were shown responsive to bacterial stimulation. The bacteria tested modulated up to 25% of the same genes. The KEGG pathway database search indicated that although the stimulation resulted in modulation of different genes

the gene products were involved in similar processes. Data mining using Gene Ontology annotations uncovered that the tested strains were able to significantly modulate a total number of 1735 specific biological processes. Whereas single strain altered 169 biological processes on average. Considering enterocyte responses in specific categories of biological processes the expression pattern of genes showed similarity of up to $R^2 = 0.97$. Number of biological processes recognised as overrepresented in a category indicated noteworthy action of specific bacterial strain. A category of virus infection-related biological processes was chosen for data mining results verification. In this process *E. coli* Nissle 1917 was proved to significantly modulate biological processes involved in rotavirus infection. The bacterial strain modulated expression of genes engaged in enterocyte's innate anti-viral response leading to decrease of rotavirus genome replication/transcription.

Conclusions. Employment of *in vitro* gut model of microbial-host interaction followed by microarray gene expression analysis and further data mining proved to be effective in recognising biological processes influenced by bacteria. The presented research describes an universal experimental procedure to indicate specific biological processes influenced by analysed microbial strain. The experimental data showed that despite strain-specific enterocyte's gene expression alternation the bacteria show convergence in modulation of specific biological pathways. Expanding annotation of human gene products may allow identification of novel biological processes modulated by microbial community. Results of this research might facilitate strain characterisation and development of targeted probiotic therapeutics.

Key words: bacteria-host interaction, probiotic, gene expression, enterocyte, rotavirus

CHARAKTERYSTYKA PROCESÓW BIOLOGICZNYCH MODULOWANYCH PRZEZ BAKTERIE JELITOWE

ABSTRAKT

Wprowadzenie. Mikroorganizmy zasiedlające układ pokarmowy znacznie przewyższają liczebnością komórki wchodzące w skład organizmu człowieka. Ich genomy łącznie kodują setki razy więcej genów niż genom ludzki. Pomimo wielkiej ilościowej i jakościowej różnorodności taksonomicznej mikroflory jelitowej człowieka charakteryzuje się ona zadziwiającą zbieżnością funkcji produktów genowych. Świadczy to o zakresie adaptacji do warunków panujących w zasiedlonej niszy ekologicznej i możliwości oddziaływań z organizmem gospodarza. Znaczenie poszczególnych mikroorganizmów dla zdrowia człowieka poznawane jest głównie na podstawie danych epidemiologicznych. Istnieje jednak niewiele dostępnych danych eksperymentalnych dotyczących molekularnego podłoża oddziaływań pomiędzy mikroorganizmami a gospodarzem.

Materiał i metody. Zróżnicowane komórki Caco-2 w hodowli zostały wykorzystane jako model *in vitro* nabłonka jelitowego. Enterocyty stymulowano szczepami bakterii probiotycznych, komensalnych i patogennych. Całkowite RNA izolowane z komórek nabłonkowych, po odwrotnej transkrypcji, poddano analizie mikromacierzowej. Uzyskane dane po normalizacji posłużyły do wygenerowania list genów różnicujących, które następnie wykorzystano do identyfikacji procesów biologicznych modulowanych przez stosowane bakterie. W porównaniu profilów ekspresji genów posługiwano się nienadzorowaną hierarchiczną analizą skupień, stosując odległości euklidesowe. Eksplorację danych przeprowadzono, wykorzystując zasoby bazy danych szlaków metabolicznych i regulatorowych KEGG oraz metasłownika ontologii genowych. Modulowanie procesów biologicznych związanych z infekcją wirusową badano z zastosowaniem infekcji komórek Caco-2 rotawirusem. Replikacja/transkrypcja genomu rotawirusa i ekspresja genów komórkowych w enterocytach stymulowanych bakteriami była analizowana z wykorzystaniem techniki RT-qPCR. Stan komórek infekowanych wirusem i/lub stymulowanych bakteriami analizowano testami określającymi aktywację kaspazy-3/7 (apoptoza), żywotność i cytotoksyczność komórek.

Wyniki. Analiza odpowiedzi transkrypcyjnej enterocytów na probiotyki (6 szczepów i 1 mieszaninę) oraz po 3 szczepy komensalne i patogenne wykazała duże

zróżnicowanie ($R^2 \leqslant 0{,}66$). Pojedynczy szczep modulował średnio 1,1 tysiąca ludzkich genów. Dla badanych 13 warunków eksperymentalnych całkowita liczba genów regulowanych pod wpływem bakterii wynosiła 10,7 tysiąca genów. Badane bakterie modyfikowały do 25% tych samych genów. Porównanie wyników z danymi zawartymi w bazie danych KEGG wykazało, że pomimo stymulacji różnych genów, ich produkty były zaangażowane w podobne procesy. Eksploracja danych z wykorzystaniem metasłownika ontologii genowych dowiodła, że testowane szczepy bakterii modulowały 1735 różnych procesów biologicznych. Jednak pojedynczy szczep zmieniał średnio 169 procesów biologicznych. Profile ekspresji grup genów w kontekście wybranych kategorii procesów biologicznych wykazywały korelację dochodzącą do $R^2 = 0{,}97$. Liczba zmienionych procesów biologicznych przewyższająca średnią dla danej kategorii wskazała znaczną aktywność badanych szczepów bakterii. Kategoria związana z infekcją wirusową została wybrana dla weryfikacji wyników eksploracji danych. W tym procesie potwierdzono rolę stymulacji *E. coli* Nissle 1917 w regulacji procesów związanych z infekcją rotawirusową. Szczep ten modulował ekspresję genów enterocytów, których produkty były zaangażowane w przeciwwirusową odpowiedź wrodzoną, prowadząc do zmniejszenia wydajności replikacji/transkrypcji genomu rotawirusa.

Wnioski. Zastosowanie modelu nabłonka jelitowego *in vitro* do badań oddziaływań gospodarz-mikroorganizm z wykorzystaniem analizy mikromacierzowej i eksploracji danych umożliwia ukazanie procesów biologicznych modulowanych przez bakterie. W prezentowanych badaniach przedstawiono procedurę eksperymentalną pozwalającą na wskazanie procesów biologicznych modulowanych przez badany szczep. Wyniki opisanych badań wykazały, że pomimo specyficznych dla szczepu zmian ekspresji genów w enterocytach badane bakterie wpływały na te same szlaki procesów biologicznych. Rozszerzenie opisu funkcji ludzkich genów pozwoli na identyfikację nowych procesów biologicznych, na które wywiera wpływ mikroflora. Wyniki tych badań mogą ułatwić charakterystykę właściwości szczepów i rozwój ukierunkowanych terapii probiotycznych.

Słowa kluczowe: oddziaływania bakterie-gospodarz, probiotyk, ekspresja genów, enterocyt, rotawirus

ISSN 1896-1894
ISBN 978-83-7160-770-7

Opracowanie redakcyjne
Maria Moczko

Redakcja językowa
Janina M. Kapuścińska

Skład i łamanie
perfekt sp.j.

WYDAWNICTWO UNIWERSYTETU PRZYRODNICZEGO W POZNANIU
ul. Witosa 45, 61-693 Poznań
tel./faks 61 848 78 08, e-mail: wydawnictwo@up.poznan.pl
http://www.wydawnictwo.up-poznan.net

Wydanie I. Ark. wyd. 16,2. Ark. druk. 11,0.

Wydrukowano w Zakładzie Graficznym Uniwersytetu Przyrodniczego w Poznaniu
ul. Wojska Polskiego 67, 60-625 Poznań
e-mail: zakgraf@up.poznan.pl

Table of contents

Abbreviations

ADHD – attention deficit-hyperactivity disorder
BDNF – brain derived neurotrophic factor
$CCID_{50}$ – 50% cell culture infectious dose
cfu – colony forming units
CNS – central nervous system
ELISA – enzyme-linked immunosorbent assay
GALT – gut-associated lymphoid tissue
GF – germ-free
HDL – high-density lipoprotein
HHBSS – HEPES buffered Hank's balanced salts solution
IFN – interferon
LDL – low-density lipoprotein
LPS – lipopolysaccharides
MOI – multiplicity of infection
N/A – not applicable
OD – optical density
PGN – peptidoglycans
pi – post infection
ROS – reactive oxygen species
SCFA – short chain fatty acids
SPF – specific pathogen free
T1D – type 1 diabetes, insulin-dependent
T2D – type 2 diabetes, insulin-independent
TEER – transepithelial electrical resistance

1. Introduction

1.1. THE SUPERORGANISM

A human organism is inhabited by a diverse microbial community composed of mainly bacteria but also archea, fungi, protozoa and viruses. The sum of microorganisms that reside inside and on their host is called a microbiota. The human body provides a number of microenvironments for various microbial ecosystems. The largest and the most numerously inhabited ecosystem is the lumen of the gastrointestinal tract. The gut environment dynamically responds to introduced foods with accompanying microorganisms and drugs. It also depends on a physiological state of the host-person. Environment of the stomach and duodenum forms a barrier which is reducing the number and the diversity of microorganisms entering downstream into intestine. Many microorganisms adapted themselves to ecological niches formed in intestines where they have convenient conditions for multiplication up to 10^{12} cells per gram of intestinal content. The bacteria inhabiting our intestines (the gut microbiota) are no longer perceived as accidental and indifferent guests. In 2000, the Nobel Laureate Joshua Lederberg introduced the concept of the 'superorganism' to describe this intricate association of the host with its microbiota (Lederberg, 2000). The microbiota forms an additional organ supplementing processes encoded by the human genome (O'Hara and Shanahan, 2006). However, some normal flora bacteria, considered commensal, can act as opportunistic pathogens in cases of impaired immunity (Tenaillon et al., 2010).

The total number of genes stored in the intestinal microbiome is estimated to be 360-times higher than the content of our genome. The Human Microbiome Project, launched in 2007, so far has explored the genomes of 600 reference microorganisms, 70 million of 16S rRNA coding sequences (used in molecular taxonomy of bacteria) representing thousands of species, 700 metagenomes and over 60 million of genes of microbiomes from healthy persons (Human Microbiome Project Consortium, 2012a; Markowitz et al., 2012).

It is estimated that human gut microbiome consists of over a thousand species with approximately 160 species present in all tested specimens (Fig. 1).

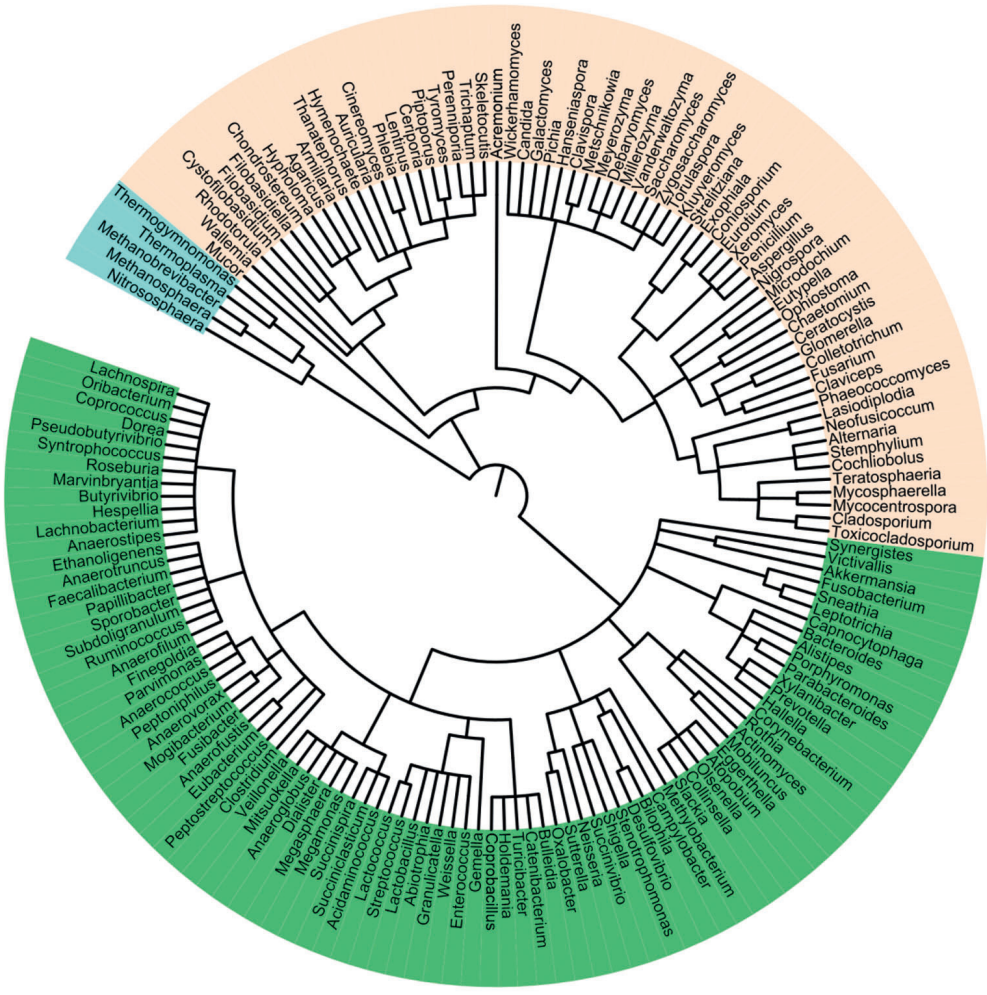

Fig. 1. A taxonomic tree of an exemplary human gut microbiome (to genus level) of Bacteria (green), Archea (blue) and Eukaryota (beige) identified by next-generation sequencing analysis by Hoffmann et al. (2013). The tree was generated using Interactive Tree of Life application (Letunic and Bork, 2011)

Ryc. 1. Drzewo taksonomiczne przykładowego ludzkiego mikrobiomu (do poziomu rodzaju) zawierające przedstawicieli bakterii, archeonów i eukariontów (zaznaczone kolorami – odpowiednio – zielonym, niebieskim i beżowym). Drzewo taksonomiczne zostało stworzone na podstawie danych z sekwencjonowania nowej generacji opublikowanych przez Hoffmanna i in. (2013) z wykorzystaniem aplikacji Interactive Tree of Life (Letunic i Bork, 2011)

Among these, from 75% to 82%, is expected to remain uncultivable. The abundance of 57 dominant species is characterised by 12- to 2200-fold variation (Qin et al., 2010). Up to 90% of gut bacteria are members of two phyla: the *Bacteroidetes* (e.g. *Bacteroides*, *Prevotella*) and the *Firmicutes* (e.g. *Clostridium*, *Enterococcus*, *Lactobacillus*, *Ruminococcus*), followed by the *Actinobacteria* (e.g. *Bifidobacterium*) and the *Proteobacteria* (e.g. *Helicobacter*, *Escherichia*). The dominant groups consist of anaerobic bacteria, represented by the genera *Bacteroides*, *Eubacterium*, *Bifidobacterium*, *Peptostreptococcus*, *Ruminococcus*, *Clostridium* and *Propionibacterium*, and sub-dominant bacteria of the *Enterobacteriaceae* family, especially *Escherichia coli*, and the genera *Streptococcus*, *Enterococcus*, *Lactobacillus*, *Fusobacterium*, *Desulfovibrio* and *Methanobrevibacter* (Eckburg et al., 2005).

A microbiome of an individual human organism is characterised by qualitative and quantitative diversity that complements the genetic variability resulting from its genome. The establishment of the intestinal microbiota is a gradual process. The increasing diversity of gut bacteria community is required for proper development of human organism and his overall health. A colonisation of the gastrointestinal tract begins in the first hours after birth. The succession of microbes inhabiting the intestinal tract is most noticeable during early stages of infant development. It is most noticeable when feeding changes from breast- or formula-feeding to weaning and later during introduction of solid foods. In the first year of life, the microbiota develops rapidly, but becomes more stable later on. The process is influenced by several factors such as: the manner of delivery (natural or by Caesarean section), the living environment microflora, gestational age and genotype of the infant (Martin et al., 2010; Reid et al., 2011; Shi and Walker, 2004). Diet, history of diseases and current illnesses, completed antibiotic therapies, and stress are other factors shaping the composition and diversity of the intestinal microflora (Mai, 2004). Antibiotics cause dramatic decline in abundance of specific groups, disturb the groups proportions and reduce overall bacterial diversity. Although the gut microflora subsequently recovers to resemble the pretreatment state, the microbiota remains perturbed in some cases for up to four years after treatment (Jakobsson et al., 2010; Ladirat et al., 2013). The composition of intestinal microflora also changes significantly with age. However, the age related differences are mainly manifested by differences in abundance of particular microbial groups. The total bacterial count in infant feces is nearly ten-times lower in $\log_{10}$ values comparing to adults and seniors. The *Bifidobacterium* genus represents a major fraction of the dominant bacterial species found in the infant fecal microbiota, which heavily outnumbers *Firmicutes* and *Bacteroidetes*. The fraction harbours an *E. coli* population at a level typical of

a dominant group (contrary to the level observed in adults). *Clostridium leptum* and *Clostridium coccoides* groups are only observed at a sub-dominant level in infants while they constitute one of the major dominant group in adults and elderly. In adults, the *Bacteroidetes* and *Firmicutes* are the most prevalent phyla present, with the *C. leptum* and *C. coccoides* groups belonging to the dominant group as well. The sub-dominant group consists of genera *Lactobacillus* and *Bifidobacterium*. Also *E. coli* is found to be in sub-dominant population in adults. Feces of the elderly show no significant differences when compared with those of adults with the exception of *C. leptum*, and *C. coccoides* groups that decrease in number and *E. coli*, which as in infants, show counts characteristic of a dominant group. The *Firmicutes*-to-*Bacteroidetes* ratio show significant differences between infants and adults (0.4 and 10.9, respectively) and between adults and elderly (10.9 and 0.6, respectively). However, no significant differences were found between infants and elderly (Mariat et al., 2009).

Despite enormous complexity a preliminary metagenomic analysis showed that the human gut microbiomes separate into three robust clusters – enterotypes (Arumugam et al., 2011). Each of the three enterotypes was supposed to be identifiable by the relative enrichment and variation in the levels of one of three main genera: *Bacteroidetes* (enterotype 1), *Prevotella* (enterotype 2) and *Ruminococcus* (enterotype 3). This suggested the existence of a limited number of well-balanced host-microbial symbiotic states (Arumugam et al., 2011). However, more detailed study revealed that the microbiota form gradients and most people fall at the extreme ends of the gradient, defined by *Bacteroides* and *Prevotella*, respectively (Koren et al., 2013). Another study proposed that the enterotypes reflect diet. The *Bacteroides* enterotype is associated with a high-fat or high-protein diet, while the *Prevotella* enterotype is associated with diet high in carbohydrates (Wu et al., 2011). Yet, another research indicated that a rural diet high in fiber leads to dominance of *Prevotella* and *Xylanibacter* (belonging to *Bacteroidetes*) and depletion of *Firmicutes*. Whereas a western diet, high in animal protein, sugar, starch, and fat and low in fiber, promotes *Firmicutes* and *Bacteroides* (De Filippo et al., 2010; Lozupone et al., 2012). Consumption of prebiotic inulin increases the levels of *Faecalibacterium prausnitzii* and *Bifidobacterium* sp. (Ramirez-Farias et al., 2009), and diet supplemented with resistant starch rises faecal levels of *Ruminococcus bromii* and *Eubacterium rectale* (Walker et al., 2011). The most recent study indicated that diet rapidly and reproducibly alters the human gut microbiome. Consumption of animal-based diet results in enrichment of *Alistipes*, *Bilophila*, and *Bacteroides*, which are bile resistant taxa. Whereas plant-based diet results in increase of the abundance of saccharolytic microbes belonging to *Eubacterium*, *Roseburia*, and *Ruminococ-*

cus, as well as *F. prausnitzii* (David et al., 2014). Although the bacterial composition changes in the individual, over 70% of the same strains can still be detected after 1 year, and a core set remains constant over longer time scales (Faith et al., 2013). The intestinal microbiota composition maintains a subject-specific pattern for longer than a decade. The pattern is constituted by a core community of permanent colonisers that resist various and aggressive environmental factors. The core consists of subject-specific phylotypes that include *Allistipes*, *Bifidobacterium*, *Bacteroides*, *Faecalibacterium*, *Blautia*, *Dorea* and *Ruminococcus*. These bacteria are most likely to be found in any human indicating their pivotal role in the ecosystem and the host (Rajilić-Stojanović et al., 2012). Even though the microbiota show tremendous abundance diversity across individuals they have remarkably similar functional gene profiles (Human Microbiome Project Consortium, 2012a). The similarities between microbiomes (collective gene profiles) may reflect importance of the gene-holders for their host. While the differences, which are in minority contribute, to changes in health status.

Glycosaminoglycan degradation and the related uronic acid metabolism pathways are present in high abundance in the gut microbiota. These are involved in animal proteoglycan (mucus) and indigestible dietary polysaccharides degradation for microbial carbohydrate utilization. Beta-glucuronidase, an enzyme engaged in the processes, is highly prevalent in the gut. The enzyme is involved in metabolism of both food matter and pharmaceuticals. This enzyme also links uronic acid metabolism with the rest of pentose and glucuronate processing. Other highly enriched microbial metabolic activities are gluconeogenesis and 2-oxoglutarate:ferredoxin oxidoreductase, but also biosynthesis of fatty acids, proline, lipopolysaccharides, pantothenates, tetrahydrofolates, degradation of histidine, methionine, and vitamin B6- taurine and hypotaurine- metabolism. These pathways are needed for microbial life within gut niches so they remain relatively stable (Abubucker et al., 2012). It was revealed that animal--based diet increased expression of bacterial genes for vitamin biosynthesis, degradation of polycyclic aromatic hydrocarbons and β-lactamase genes. The diet modulates expression of genes involved in amino acid metabolism and central metabolism, but also determines composition of short-chain fatty acids (SCFA) secreted by microbiota. Plant-based diet results in increased production of acetate and butyrate whereas animal-based diet of isovalerate and isobutyrate (David et al., 2014). Growing number of evidence suggests that richness of gut microbial genes and microbial composition inversely correlates with body weight, and metabolic markers (e.g. fat mass, glucose and lipid metabolism, inflammation). The composition of gut microbial population (especially fibre-degrading and SCFA-producing bacteria) can determine the efficacy of energy

harvest from food. On the other hand, a diet modification changes the composition of the gut microbiota.

Bacterial population in the human gut shows a bimodal distribution of genes. Individuals can be divided into "low gene count" (LGC) and "high gene count" (HGC) groups according to the number of genes present in their gut microbiota and thereby different microbial communities. The groups have, on average, 380,000 and 640,000 genes, and harbour less and more the rich microbiota, respectively. The two groups were found to differ significantly in abundances of 120,723 genes, which could not be precisely assigned to a known bacterial genome. The LGC-individuals are characterised by higher weight-gain, adiposity, insulin resistance and inflammation, compared to HGC-individuals. Less diverse gut microbiota has been reported in inflammatory bowel disease patients, elderly people with gut inflammation and in obese individuals. Patients with LGC respond significantly better to dietary intervention than those with HGC. The dietary intervention improves gut microbial richness and clinical results of the LGC patient. Interestingly, forty-six genera differed significantly in abundance between the LGC and HGC individuals. Although *Bacteroides*, *Parabacteroides*, *Ruminococcus*, *Campylobacter*, *Dialister*, *Porphyromonas*, *Staphylococcus* and *Anaerostipes* were more dominant in LGC, 36 genera, including *Faecalibacterium*, *Bifidobacterium*, *Lactobacillus*, *Butyrivibrio*, *Alistipes*, *Akkermansia*, *Coprococcus* and *Methanobrevibacter*, were significantly related to HGC. At the phylum level, a higher abundance of *Proteobacteria* and *Bacteroidetes* was observed in LGC individuals versus increased populations of *Verrucomicrobia*, *Actinobacteria* and *Euryarchaeota* in HGC individuals (Le Chatelier et al., 2013; Cotillard et al., 2013). These data suggests that each person possesses a distinct and highly variable microbiota, although a conserved set of gut colonisers (the core gut microbiota) and genes (the core microbiome) are shared among individuals. The core set of microbes and genes may determine the proper functioning of the gut or even entire organism.

1.2. METABOLIC ACTIVITY OF GUT BACTERIA

The intestinal microbiota provides many metabolic services to the human body. The most important are the syntheses of vitamins (LeBlanc et al., 2013) and amino acids (Metges et al., 2006). Bile acids biotransformation provided by bacteria is significantly linked to cholesterol and glucose metabolism. Furthermore, the gut microbiota not only regulates metabolism but also synthesis of bile acid (Hu et al., 2014; Sayin et al., 2013). Important contribution of the in-

testinal bacteria metabolism to the functioning of the human organism is metabolism of xenobiotics, which changes bioavailability of phytochemicals (e.g. polyphenols and alkaloids) and pharmaceuticals (Klünemann et al., 2014; Li and Jia, 2013). Enzymes provided by gut microorganisms allow fermentation of indigestible plant saccharides (oligo- and polysaccharides, like resistant starch and inulin) and mucus leading to generation of SCFA (e.g. acetic, butyric, lactic and propionic) and other metabolites (such as succinates, valerates and capronates). Fermentation products are adsorbed in large intestine together with resorbed salts and water. This way, the gut microbiota produces energy substrates for the host epithelium from indigestible dietary compounds. A variety of complex glycans are being degraded by bacteria mainly of *Bacteroides*, *Prevotella*, and *Xylanibacter* genera. However, *Eubacterium*, *Faecalibacterium* and *Roseburia* are recognised as the major butyrate producers. Recently discovered Verrucomicrobia, which includes *Akkermansia*, which was found to be specialised in mucus degradation, is also an important acetate and propionate producer (Tremaroli and Bäckhed, 2012). Beyond their trophic function on the intestinal epithelium, SCFAs act as signaling molecules (Layden et al., 2013; Wong et al., 2006). There is an increasing number of evidence that gut microbiota not only help gain energy-nutrients from the diet, but also regulate energy storage by increasing lipogenesis (Cani and Delzenne, 2009). Animal studies indicate that gut microbiota contributes to higher energy availability to the host and increase its metabolism. Conventionally raised mice as compared to germ-free (GF) animals have higher levels of serum metabolites from glycolysis and the tricarboxylic acid cycle while levels of cholesterol and fatty acids were reduced. The microbiota modifies a variety of lipid molecules in the serum, adipose tissue, and liver. Especially triglycerides and phosphatidylcholine molecules are affected (Velagapudi et al., 2010). Research of Bäckhed et al. (2007) indicated that germ-free C57BL/6J mice, in contrast to conventional mice, fed a high-fat and sugar-rich ("western") diet failed to develop obesity or insulin resistance, thus supporting a role for gut bacteria in the development of diet-induced obesity. In contrast, study of Fleissner et al. (2010) showed that germ-free C3H mice were not resistant to the obesigenic effects of high fat diet indicating that diet composition and/or genetic background influence the protection from diet-induced obesity conferred by GF status (Shen et al., 2013). Studies on energy harvest in humans revealed that changes in dietary calorie load were associated with rapid alteration in the gut bacterial composition, especially in *Firmicutes*-to-*Bacteroidetes* ratio (Jumpertz et al., 2011). The gut bacteria ferment indigestible polysaccharides into SCFAs which serve directly as energy substrates but also function as regulators of energy intake and energy metabolism (Conter-

no et al., 2011) increasing host satiety and reducing food intake. The SCFAs are recognised by G protein-coupled receptors Free Fatty Acid Receptor-2 and -3 (FFAR2, GPR43 and FFAR3, GPR41, respectively). The SCFA-signalling influence the gut peptide hormones level causing increase of glucagon-like peptide-1 (GLP1) and peptide YY (PYY), and decrease of ghrelin. It was also shown that appetite is affected through bacterial flagellin recognised by Toll like Receptor-5 (TLR5) involving NFκB-signalling pathway (Shen et al., 2013).

The closest insight in the role of the gut microbiota in metabolism is viewed through its involvement in metabolic disorders. The gut microbiota is involved in the control of energy metabolism (increasing energy storage) being a determinant of body weight and the size of adipose tissue. Obesity is a complex medical condition associated with a number of other metabolic disorders characterised by chronic, systemic, low-grade inflammation. One of them is metabolic endotoxemia, a common consequence of high-fat diet. It is a condition of elevated plasma levels of bacterial lipopolysaccharide (LPS), an endotoxin derived from the membrane of Gram-negative bacteria that reside in the gut. This is a result of passage of the bacterial cell fragments through the intestinal barrier into systemic circulation, either through increase in intestinal paracellular permeability or through LPS internalisation by enterocytes followed by chylomicron secretion (Boroni Moreira and de Cassia Goncalves Alfenas, 2012). The condition is accompanied by raised low-density lipoprotein (LDL)-to-high-density lipoprotein (HDL) ratio (dyslipidemia). The lipoproteins are proposed to buffer LPS in response to septic shock, and trigger metabolic diseases (Serino et al., 2009). Moreover, the gut microbiota has lower counts of *Bifidobacterium* species, which are known to strengthen mucosal barrier function against bacterial antigens (Shen et al., 2013). Lipopolysaccharides bind to toll-like receptor 4 and trigger inflammation, but also alter several stages of insulin signalling (Boroni Moreira and de Cassia Goncalves Alfenas, 2012). This led to gain of whole body, liver and adipose tissue weights, adipose and liver inflammation followed by fasted hyperglycemia and insulinemia (Shen et al., 2013). Another consequence of increased intestinal permeability is metabolic bacteremia. Amar et al. (2011a) showed that high-fat diet increase adherence of Gram-negative bacteria to the intestinal mucosa and facilitate transmucosal bacterial translocation. Later the same research group demonstrated that blood microbiota is mostly composed of the *Proteobacteria* phylum (85-90%) and such individuals have increased risk of developing the type 2 diabetes (T2D) and obesity (Amar et al., 2011b).

The most recent research indicates a role of gut microbiota also in atherosclerosis (Brown and Hazen, 2014; Koeth et al., 2013) and type 1 diabetes (T1D) (Nielsen et al., 2014; Peng et al., 2014).

1.3. ROLE OF GUT MICROBIOTA IN HOST PROTECTION

Many bacterial metabolites, such as SCFAs, bacteriocins and hydrogen peroxide provide antagonistic action against pathogenic bacteria. Also, competition for nutrients and adhesion space on epithelial cells surface plays a significant role in defense against harmful microorganisms (Sekirov et al., 2010). However, protective functions of the gut bacteria are mainly displayed by their impact on the growth, maturation and activity of immune cells. These cells are numerously represented in the tissues forming gastrointestinal tract establishing an organ called gut-associated lymphoid tissue (GALT) (Forchielli and Walker, 2005; Koboziev et al., 2010). Mucosal immune system has to be tolerant towards the huge number of mutualistic microorganisms that reside in the intestinal lumen. Yet, it has to assure a beneficial microbiota composition distinguishing and specifically eliminating pathobionts. At the same time it must restrict microbial overgrowth and react to penetrating microorganisms that breach the intestinal chemical and physical barriers. These barriers are composed of such factors as secreted soluble immunoglobulins A (sIgA), antimicrobial peptides (AMPs), the mucus layer, and the tightly interconnected enterocyte lining (Fig. 2).

The indigenous gut microbiota is considered to be a trigger stimulus leading to the generation of immuno-physiological response. The intestinal microbiota is indispensable for the myeloid and lymphoid cells to form organised lymphoid tissues and develop ability to produce secretory immunoglobulins (IgA) and intraepithelial CD8αβ lymphocytes. Homeostasis in the gut mucosa is maintained by a balance between potentially proinflammatory (T_H1, T_H17) and anti-inflammatory regulatory (T_{regs}) T cells. The impact of the gut microbiota extends over the immune system at a systemic level. A disturbance of gut microbiota contributes to systemic autoimmune and allergic diseases at sites distal to the intestinal mucosa (e.g. reduces the serum IgE-response, increase number of circulating CD4 T cells and circulating T_H1 cell frequencies; Hooper et al., 2012).

The body's protective mechanisms are also strengthened by microorganisms through intestinal barrier fortification. This is accomplished by tightening of epithelial intercellular connections and changing the properties of secreted mucus (Lam et al., 2007; Putaala et al., 2008, Resta-Lenert and Barrett, 2003). A study involving conventional and germ-free animals indicated that microbiota induce a repair of damaged intestinal epithelium (Hooper et al., 2012).

The symbiotic nature of the intestinal host-microbial relationship depends on maintenance of homeostatic relationship between the parties. This is achieved through host control over microbiota localization and community composition. Mucus layer coating the intestinal epithelial cells, antibacterial proteins secreted

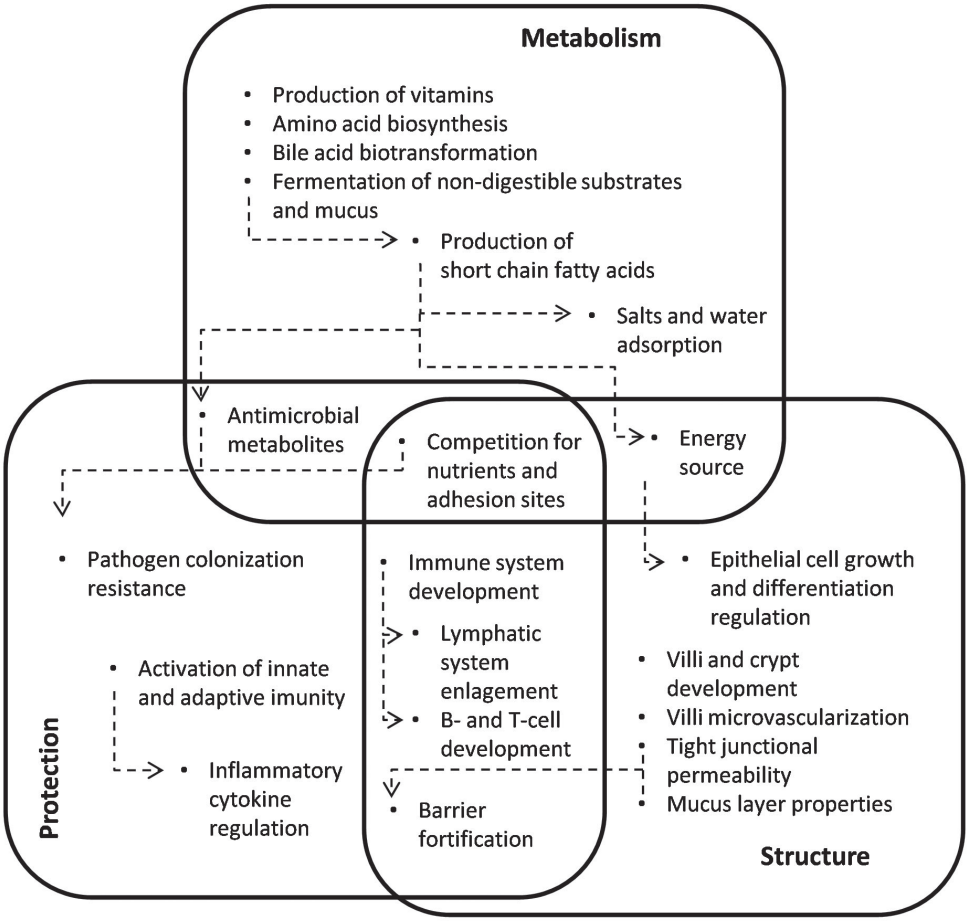

Fig. 2. Positive impact of normal gastrointestinal microflora on human health. The rounded rectangles represent the three basic sets of health-related activities of gut microbes: metabolic, protective and structural functions [according to Prakash et al. (2011), modified]

Ryc. 2. Pozytywny wpływ mikroflory przewodu pokarmowego na zdrowie człowieka. Zaokrąglone prostokąty reprezentują trzy podstawowe zestawy aktywności drobnoustrojów jelitowych związanych z ochroną zdrowia: funkcje metaboliczne, ochronne i strukturalne [według Prakasha i in. (2011), zmodyfikowana]

by them and IgA specific for intestinal bacteria (produced by plasma cells) function together to stratify luminal microbes and to minimize bacterial-epithelial contact (Hooper et al., 2012). One of the major functions of the immune system is a management of microbiota composition, diversity, and location (Costello et

al., 2012). However, the microbiota also spots its host making the host-microbes interaction is bidirectional. The bacteria eavesdrop on mammalian host signalling systems such as neuroendocrine stress hormones for their successful adaptation and survival within the host (Karavolos et al., 2013).

Microbiota imbalance is considered to be a key factor in development of several diseases. It is believed to trigger inflammatory signalling deregulation leading to the two main forms of inflammatory bowel disease (Crohn's disease and ulcerative colitis). The disease represents abnormal immune responses of the gastrointestinal tract associated with overproduction of pro-inflammatory cytokines. An excess activation of immune system by microbial antigens is a predisposing factor leading to a T-cell-mediated autoimmune disease that results in destruction of the insulin-producing beta cells of the pancreas, known as insulin-dependent diabetes (T1D). The T1D is associated with increased intestinal permeability (leaky gut syndrome) and lymphocytic infiltration in the mucosa. A highly proinflammatory substances such as lipopolysaccharides (LPS) and peptidoglycans (PGN) might be able to cross the epithelial barrier and reach the immune system to increase an inflammatory response (Serino et al., 2009).

Recently, the gut microbiota has been shown capable to modulate processes localized in distant tissues, such as intestinal angiogenesis (Reinhardt et al., 2012) and bone-mass density (Sjögren et al., 2012).

1.4. MICROBIOTA IN GUT-BRAIN AXIS INTERACTION

Recent studies have revealed a bidirectional communication between the central nervous system (CNS) and the gastrointestinal system. This interaction is termed "gut-brain axis". The communication is comprised of neural and humoral pathways. These connect CNS through vagus and/or spinal afferents with enteric nervous system and involve cytokines, hormones, neuropeptides, and microbial bioactive substances signalling (Forsythe and Kunze, 2013). The majority of research data linking gut microbes with behaviour comes from animal studies indicating a role for the gut microbiota in the regulation of anxiety, mood, cognition, pain and appetite (Bercik et al., 2012; Cryan and Dinan, 2012; Norris et al., 2013). Several animal studies and clinical trials with probiotics indicated influence of gut microorganisms in visceral perception including pain. Although the mechanisms of action remain unknown in case of IBS patients, the pro- and anti-inflammatory cytokine balance was improved. These data were obtained mainly with using strains belonging to *Lactobacillus* and *Bifidobacte-*

rium genera, however strains of *E. coli*, *Enterococcus faecalis*, and *Bacteroides coagulans* were also effective (Bercik et al., 2012).

Even more intriguing are studies revealing influence of microbiota on animal behaviour. Commensal bacteria of fruit fly (*Drosophila melanogaster*) are responsible for diet-induced mating preference of the fly (Sharon et al., 2010, 2011). The signalling initiates at peptidoglycan sensing receptor in the *Drosophila* gut (Royet and Charroux, 2013). The fruit fly mating preference research indicates that potentially beneficial bacteria lost by antibiotic treatment can be reintroduced to provide back a health benefit or behaviour (Sharon et al., 2010, 2011). Research of Goehler at al. (2008) on mice showed that the neural system can detect a change in the gut microbiota composition and can identify an occurrence of pathogen in the gut lumen. The studied animals displayed anxiety--like behaviour during the early phase of acute *Camplyobacter jejuni* infection. The pathogen triggered activity of vagal ascending pathways resulting in a specific activation of several brain regions already associated with anxiety-like behaviour. Another example comes from study on chronic *Helicobacter pylori* infection in mice. The infection led to abnormal feeding behaviour (in form of smaller but more frequent meals), as well as delayed gastric emptying and visceral sensitivity. This was shown to involve up-regulation of sensory nerves in the stomach and the spinal cord (Bercik et al., 2009). Moreover, it was shown that colonization by gut microbiota impacted mammalian brain development and subsequent adult behaviour. Germ-free (GF) mice displayed higher exploratory and lower anxiety-like behaviour than specific pathogen free (SPF) mice (Diaz Heijtz et al., 2011; Neufeld et al., 2011b). Similar findings were drawn from studies on rats (Crumeyrolle-Arias et al., 2014). The effect of microbiota colonization of GF mice depends on microbiota composition. This assumption can be drawn from study where colonization of germ-free BALB/c mice with microbiota from NIH Swiss mice increased exploratory behaviour, whereas colonization of germ-free NIH Swiss mice with BALB/c microbiota reduced the behaviour. Changes in colonic microflora composition in SPF mice induced by non-absorbable antibiotics caused an increase in exploratory behaviour and altered brain derived neurotrophic factor (BDNF) levels in the hippocampus and amygdala (Bercik et al., 2011). The gut-brain interactions seem to be important to CNS development of stress systems as introduction of normal gut microbiota to the adult GF mice did not normalize the behavioural phenotype (Neufeld et al., 2011a). Monoassociation of germ-free BALB/c mice with *Blautia coccoides* reduced the anxiety level, but did not affect the locomotor activity. Whereas colonization with *Bifidobacterium infantis* decreased the locomotor activity, but having no effect on the anxiety level (Nishino et al., 2013). Administration of

B. infantis (strain 35624) to rat pups in maternal separation model caused reduction of depression that was accompanied by restoration of basal noradrenaline concentrations in the brainstem (Desbonnet et al., 2008, 2010). Yet another study on depression in mice showed that administration of *Bifidobacterium longum* NCC3001 normalized the behaviour. However, *Lactobacillus rhamnosus* NCC4007 did not show such an effect (Bercik et al., 2010). Different study showed that strain JB-1 of *L. rhamnosus* was able to reduce anxiety- and depression-related behaviour (Bravo et al., 2011).

These examples indicate that intestinal dysbiosis might contribute to psychiatric disorders in patients with gut disorders. There is an increasing evidence of a link between autism and abnormalities in gut microbial functions. Analysis of fecal DNA samples indicated that the presence of autistic symptoms was associated with less diverse gut microbiomes. The autistic samples showed significantly lower abundances of the genera *Prevotella*, *Coprococcus*, and unclassified *Veillonellaceae* – carbohydrate-fermenting bacteria (Kang et al., 2013), yet another study indicated lower levels of *Bifidobacterium* spp. and higher levels of *Lactobacillus* spp. (Adams et al., 2011). As diet inevitably affects gut microbiota composition and there are numerous reports of diet altering various manifestations of psychiatric disorders, therefore, with no surprise we shall expect findings on the microbiota involvement in schizophrenia, attention deficit-hyperactivity disorder (ADHD), and other categories of Autistic Spectrum Disorders (e.g. Asperger syndrome, Rett syndrome; Gonzalez et al., 2011).

Most of bacterial species reside in the lumen of the gastrointestinal tract, whereas fewer, but well-adapted species (e.g. *Faecalibacterium prausnitzii*, *Akkermansia muciniphila* and several *Bacteroides* sp. and *Ruminococcus* sp.) adhere and reside within the mucus layer close to the gut tissue. The ability of microbes to bind to mucus increases their colonization capacity. Several beneficial microbes display the ability for prolonged intestinal residency (including probiotic ones, like *L. rhamnosus* GG, *L. plantarum* WCFS1 or *B. infantis*; Ouwerkerk et al., 2013). This allows them for easier contact to enterocytes in the small intestine where mucus layer is permeable for bacteria. The mucus organisation of the distal large intestine forms two layers where inner one is bacteria impermeant (Johansson et al., 2011). However in case of several disorders (eg. ulcerative colitis) the inner mucus layer is broken or penetrable by bacteria (Jäger et al., 2013; Johansson and Hansson, 2013). Most recent research focuses on bacterial protein signals associated with diseased states (Juste et al., 2014). Recognition of direct influence of bacterial species on intestinal epithelium may provide guidance for development of modern pharmacological concept for using bacterial molecules/lysates when application of live microorganism is contraindicated.

Microbiota influences human organism through direct interaction of bacterial cell with host cell (either enterocyte or immune cell e.g. dendritic cell) or through secreted products or metabolites (called postbiotics, e.g. SCFA, peptides, exopolysaccharides). Some effects of bacteria on human organism may be mediated by direct interaction with intestinal cells, while other effects may be mediated indirectly via modulation of gut microbiota (Fig. 2). However, there are several *in vitro* actions of bacteria (mainly probiotic) which do not translate into clinical effects and clinical observations which cannot be satisfactorily explained at the cellular level. There is a wide range of possible mechanisms which are only just being discovered and need further investigations. A large number of these mechanisms cannot easily be measured in humans for ethical or feasibility reasons. Thus an *in vitro* model provides a good solution to the problem.

2. Scientific hypothesis

There is a growing number of evidence on biological processes that are influenced by gut bacteria. The bacteria from medical perspective are classified into three major groups: probiotic, commensal and pathogenic. The boundaries of the groups are blurred. Some commensals in case of impaired immunity can act as pathogens. Whereas probiotic strains can be perceived as commensals with proven health benefits. These health benefits need to be experimentally demonstrated, most preferably in clinical studies. This poses a bottle-neck in strain characteristic. Microarray gene expression studies give a broad view on cell responsiveness to certain stimulus. The technique is widely used to recognise differentially regulated genes. Further employment of data mining allows to identify biological processes that are influenced by the stimulus. Therefore adaptation of proper *in vitro* cellular model and use of microarray technique followed by bioinformatic analysis should allow to indicate biological processes influenced by specific microbial strain.

According to widely accepted definition probiotic is a live and well characterised mircoorganism. However, there are effective treatments involving use of dead bacteria, often in form of lysate. Therefore the aim of this study was to analyse an early impact of selected probiotic microorganisms, but also commensal and pathogenic ones on intestinal epithelial cells' gene expression, and to recognise biological outcomes of that modulation. The research concentrated on the early intestinal epithelial cells' responses to dissect reactions mediated by bacterial antigens (of proteinaceous, lipopolysaccharide, peptidoglycan or exopolysacchardie nature) rather than by accumulation of common low-molecular-weight fermentation products.

WORKFLOW

The research performed was organised into four parts (see diagram below). The host-microbe interaction was simulated in *in vitro* gut model where differentiated Caco-2 enterocytes were exposed to bacterial cells. To identify differentially

expressed genes in response to bacteria a global transcriptome investigation was performed using microarray hybridisation. Gene expression analysis was performed on background corrected and normalised data to allow data mining for bacteria-mediated host biological processes. To validate characterised biological processes, a virus infection-related process was subjected to verification.

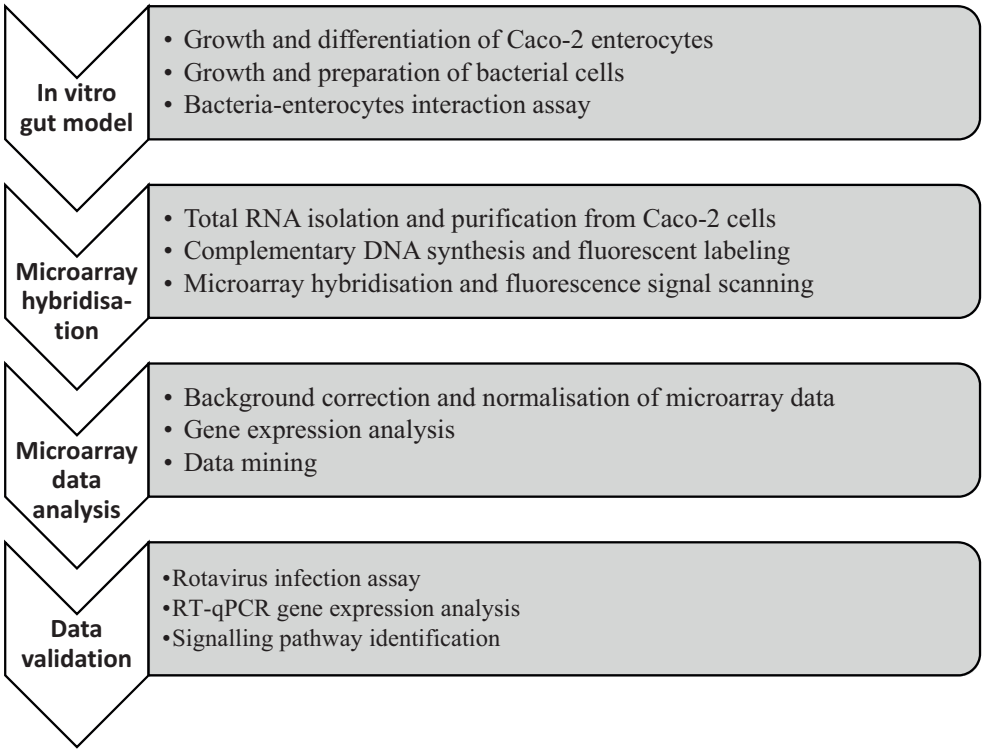

3. Materials and methods

3.1. MICROORGANISMS

In the presented studies microorganisms belonging to three functional groups: probiotic, commensal and pathogenic bacteria were used. The microorganisms used in this study are listed in Table 1.

Table 1. Strains of microorganisms used in the study
Tabela 1. Szczepy mikroorganizmów stosowane w badaniach

Group	Strain	Source	Designation
1	2	3	4
Probiotic [prob]	*Lactobacillus rhamnosus* GG (ATCC 53103)	Dicoflor, Vitis Pharma, Poland	LGG
	Bifidobacterium animalis subsp. *lactis* BB12	Linex Forte, Lek S.A., Poland	BB12
	Lactobacillus acidophilus LA-5	Linex Forte, Lek S.A., Poland	Lc5
	Lactobacillus plantarum PL02	Lactoral Junior, IBSS Biomed, Poland	mix (together with Lc5 and BB12)
	Lactobacillus rhamnosus KL53A	Lactoral Junior, IBSS Biomed, Poland	
	Lactobacillus delbruecki subsp. *bulgaricus* LBY-27	Probiolac, Polfarmex S.A., Poland	
	Lactococcus lactis PB411	ProBacti 4 Enteric, ZiołoFarmacja Sp. z o.o., Poland	
	Lactobacillus casei Shirota	Yakult, Holland	LcS
	Lactobacillus casei DN114001	Actimel, Danone, Poland	LcD

Table 1 cont.

1	2	3	4
	Escherichia coli Nissle 1917 (DSM 6601, serotype O6:K5:H1)	Mutaflor, Ardeypharm, Germany	EcN
Commensal [kom]	*Bifidobacterium animalis* MK2	departmental cell culture collection	Ba
	Bacteroides thetaiotaomicron ATCC 29741	Oxoid, UK	Bt
	Peptostreptococcus anaerobius ATCC 27337	Oxoid, UK	Pa
Pathogenic [pat]	*Salmonella enterica* serovar Typhimurium (*S*. Typhimurium) ATCC 14028	Oxoid, UK	St
	Escherichia coli ATCC 10536 (serotype O59:H21)	Oxoid, UK	EcF
	Escherichia coli O157:H7 VT-negative (NCTC 12900)	Sterbios, Poland	EcOH
	Human Rotavirus A G1P[8] strain RIX4414	Rotarix, GlaxoSmithKline, Poland	RV

In order to standardize the growth conditions, the strains were grown in glucose-free Brain and Heart Infusion broth (BTL) supplemented with fructooligosaccharides (2% w/v, Sigma-Aldrich) as the primary source of carbon. Except for *Peptostreptococcus anaerobius*, which was grown in Wilkins-Chalgren broth (Oxoid). The cultures were incubated at 37°C for 18-20 hours under anaerobic conditions (85% N_2, 10% CO_2, 5% H_2) obtained with use of Anoxomat Mark II System (Mart Microbiology BV). Bacterial cells were washed twice and resuspended in HHBSS buffer (HEPES buffered Hanks balanced salts solution), then an optical density of cell suspension was measured using wavelength of $\lambda = 600$ nm (OD_{600}). The cell density was determined by means of OD-to-cfu dependency.

3.2. RESEARCH MODEL BASED ON DIFFERENTIATED INTESTINAL EPITHELIAL CELL LINE CACO-2

Caco-2 cell line propagation and differentiation. The Caco-2 cell line was derived from colon adenocarcinoma. The cell line is widely used as a model of the intestinal barrier in clinical pharmacology (Sambuy et al., 2005) and studies of adhesion of microorganisms to the intestinal epithelium (Tuomola et al., 2001). The cells spontaneously differentiate and form a monolayer with many morphological and functional characteristics of mature enterocytes (Sambuy et al., 2005). Polarisation, development of the brush border and selective permeability obtained by the formation of close intercellular connections called tight junctions are typical attributes of functional intestinal epithelial cells. These attributes are displayed by differentiated Caco-2 cells. The cell line (ECACC Cat. No. 86010202; Sigma-Aldrich) was subcultured in Dulbecco's Modified Eagle's Minimal Essential Medium (Sigma-Aldrich) supplemented with: 2 mM Glutamine (Sigma-Aldrich), 1% Non-Essential Amino Acids (Sigma-Aldrich), and 10% Fetal Bovine Serum (Life Technologies). Cells were used between passage numbers 49 to 52. They were seeded in Millicell cell culture inserts (PTFE membrane, 0.4 μm pore size; Merck-Millipore) at 4×10^5 cells/cm^2 and cultured for 20 days with media changed every two or three days. The cells were being gradually adapted to buffering agent HEPES at the apical site and increased CO_2 content in the atmosphere (final concentrations: 25 mM and 10%, respectively), beginning from the 14th day of culture differentiation.

Bacterial stimulation of enterocytes. Bacterial cells were added to the apical site of the differentiated Caco-2 cell monolayer at multiplicity of 1-to-300 followed by incubation for 4 h at 37ºC, in 10% CO_2 atmosphere (with HHBSS change after 2 h).

Rotavirus infection. Fully differentiated Caco-2 cells were infected with attenuated Human Rotavirus A G1P[8] strain RIX4414 (Rotarix vaccine, GlaxoSmithKline). The infection was done with dialyzed and trypsin activated virus (0.5 μg/ml trypsin in HBSS at 37°C for 1 h) at $CCID_{50} = 0.5$. In the postinfection treatment procedure the Caco-2 cells were infected with rotavirus for 4 hours then exposed to bacteria (in the same amount as described previously) for another 4 hours (in total 8 hours-rotavirus and 4 hours-bacterial action). Also the Caco-2 cells were exposed to bacteria for 4 hours and then infected with rotavirus followed by 4 hours incubation (preinfection treatment, in total 8 hours-bacterial and 4 hours-rotavirus action). Control cells were infected with rotavirus in the same regime as described previously but not exposed to bacterial cells or exposed to bacteria but not infected with rotavirus. After total 8 hours of incubation the Caco-2 cells were used to isolate total RNA. For the study of viability, cytotoxicity and

apoptosis the cells were treated as described above but examined after 18 h. Three to four biological replicates were performed for each experimental condition.

3.3. ISOLATION AND PURIFICATION OF TOTAL RNA

The isolation of total RNA was performed using a modified Chomczynski and Sacchi method using TRI Reagent solution (Sigma-Aldrich). Samples of total RNA were analysed spectrophotometrically using NanoDrop ND-1000 spectrophotometer. The total RNA samples were DNase digested with TURBO free DNase Kit (Life Technologies). Purified total RNA preparations were analysed qualitatively using Bioanalyzer 2100 (Agilent) automatic analyser to determine the degree of RNA integrity. All samples used for cDNA synthesis had the RIN values above 9.4.

3.4. COMPLEMENTARY DNA SYNTHESIS AND FLUORESCENT LABELING, MICROARRAY HYBRIDISATION

Microarrays were hybridised with 1-2 μg of cDNA synthetised in reverse transcription reaction with oligo$(dT)_{20}$ primer using 20 μg of total RNA isolated from Caco-2 cells (control and bacteria treated). Complementary DNAs of the treated and control samples were two-colour fluorescently labelled (AlexaFluor 555 or AlexaFluor 647) using SuperScript Plus Indirect cDNA Labeling System (LifeTechnologies). A degree of label incorporation to cDNA samples was measured using NanoDrop ND-1000 spectrophotometer. The labelled cDNAs of Caco-2 cells after treatment with tested strains of bacteria and control cells were hybridised to Human Whole Genome OneArray microarrays (v. 4; Phalanx Biotech). The microarray contains 32,050 oligonucleotides (30,968 human genome probes, and 1082 experimental control probes). Each probe is 60-mer oligonucleotide designed to hybridise to a specific target gene described in the current public domain content validated by the Human Genome Sequencing Project. Hybridisation was performed in automatic hybridisation station HybArray12 (PerkinElmer) under the following conditions:

- pre-hybridisation (1 hour in 5 × SSPE, 0.1% SDS, 0.1 mg/ml BSA at 42°C),
- hybridisation (16 hours in SlideHyb Glass Array Hybridization Buffer #3 (LifeTechnologies, Poland) at 42°C,
- three washes: (1st wash) 2 × SSC, 0.5% SDS (5 min, 42°C); (2nd wash) 0.5 × SSC, 0.5% SDS (5 min, 42°C); (3rd wash) 0.05 × SSC (1 min, at RT).

Caco-2 cells transcriptome after interaction with bacterial cells (probiotic, commensal and pathogenic – the total of 13 strains) were analysed on microarrays in duplicate (26 microarrays). The duplicate was made with dye-swap to allow fluorescence intensity compensation of both dyes.

Microarray images after hybridisation were acquired using a laser scanner ScanArray Express (Perkin Elmer) at 5 μm density in two channels for fluorescence at 555 nm and 647 nm wavelengths. Quantitative analysis of fluorescence intensity signals from microarrays was performed using GenePix Pro v. 6.0 software (Axon Instruments Inc.).

3.5. QUANTITATIVE RT-PCR ANALYSIS

To evaluate the level of selected human genes expression and rotavirus genome segments and transcripts amount, RT-qPCR assays were performed in biological triplicates of differentiated Caco-2 cells after contact with bacteria preinfected or postinfected with attenuated Human Rotavirus A G1P[8] strain RIX4414. Rotavirus RNA segments analysis was performed with primers (Table 2) designed with PriFi (Fredslund et al., 2005) based on DNA sequence alignments to select primers annealing sites to conservative motifs (for universal thermal conditions of Ta = 60°C and optimal amplicon length of 90 to 150 base pairs, where possible). Primers for human transcripts (Table S1) were selected from qPrimerDepot database (Cui et al., 2007), except for *MAP3K1* (PrimerBank ID 153945764b1 (Wang X. et al., 2012b)), and *B2M*, *HPRT1*, *RPLPO*, *GAPDH*, *ACTB*, *TBP*, *RN18S1* (Lossos et al., 2003). The reaction condition was optimized for best performing qPCR master mix and primers concentration in universal thermal conditions. PCR efficiencies were calculated from the slopes of standard curves (Pfaffl, 2001) for designed primer pairs and were found to be within the acceptable range of E = 1.9-2.1. Total RNA (7.5 ng/μl of reaction mixture) was reverse transcribed with an oligo(dT) and random hexamer primer mix using High Capacity RNA-to-cDNA Kit (LifeTechnologies). Complementary DNA (0.02 μl of RT reaction/μl of qPCR reaction mix) was analysed using GoTaq qPCR Master Mix (Promega) for human transcript analysis. Maxima SYBR Green qPCR Master Mix (Thermo Scientific) was used for quantification of rotavirus targets. The Applied Biosystems 7500 System with 7500 Software v. 2.0.5 (Applied Biosystems) was used for quantitative PCR. Primers for human genes transcripts were used at 0.15 μM each and for rotavirus segments at 0.2 μM each.

Table 2. Primers designed for quantitative Real-Time PCR analysis of rotavirus segments
Tabela 2. Startery zaprojektowane do ilościowej analizy segmentów rotawirusowych metodą Real-Time PCR

Gene symbol	GenBank accession no.	Gene description	Primer pair sequence	Amplicon size
1	2	3	4	5
NSP1	Seq.set 1	rotavirus A genotype G1P[8] segment 5 non-structural protein NSP1 gene	TGTACCATGTATCATGTATGTCAGTGGTG TTTTGTCACTTCATTTTTAAAAGTTCTCAT	108
NSP3	Seq.set 2	rotavirus A genotype G1P[8] segment 7 non-structural protein NSP3 gene	TGCACTAGACTTATGAAGGATAAAATAGAACGTGG AACGAGATTTCCAATCAATAGTATCAATTTCC	106
NSP4	Seq.set 3	rotavirus A genotype G1P[8] segment 10 non-structural protein NSP4 gene	CGTGCGGAAAGATGGATAAACTTGC CAGATGCAATATATGGAAAATACGCCATTCCAGG	126
NSP56	Seq.set 4	rotavirus A genotype G1P[8] segment 11 non-structural proteins NSP5 and NSP6 genes	AATGAATCGTCTTCTACAACGTCAACTCTTTCTGG GGTGAGTGGATCGTTTGAAGCAGAATCAGATGGTC	159
VP1	Seq.set 5	rotavirus A genotype G1P[8] segment 1 RNA-directed RNA polymerase VP1 gene	AAACAAATGGTCCAAGATGTGTCAAACGATGTGAG GCTATATATCTTTTCGCTATTTCAATACCGACTG	116
VP2	Seq.set 6	rotavirus A genotype G1P[8] segment 2 RNA viral genome binding protein VP2 gene	AGAGACAGACTTAGATTATTACCAGTTGAAAGACG CTCCTTGAGCAATTTTATCTGAAGCTC	112
VP3	Seq.set 7	rotavirus A genotype G1P[8] segment 3 guanylyltransferase VP3 gene	AAGCATGAAAGTATTAGCTTTAAGACACAGTGTGG AGATTAGAAATGAGAAATGCATTTTCATACTCATC	117

1	2	3	4	5
VP4	Seq.set 8	rotavirus A genotype G1P[8] segment 4 outer capsid protein VP4 gene	GATGATTATCAGACTCCAATTATGAATTCAG AAATCAATCAATTGTGCCATAGCTATTTCTTGTG	128
VP6	Seq.set 9	rotavirus A genotype G1P[8] segment 6 inner capsid protein VP6 gene	AAGTGAGGACCAGACTAACCATCTGGTATCCAATC ATCATTCATGCAGTTACTCTACGTAGCGAACATG	126
VP7	Seq.set 10	rotavirus A genotype G1P[8] segment 9 glycoprotein VP7 gene	GAGAGAATGATGAGAGTGAATTGG GGTCACATCATACAATTCTAATCTAAGATATATC	171

Seq.set 1 – GenBank accession nos.: HM773836, HM773814, HM773792, HM773770, HM773748, HM773847, HM773825, HM773803, HM773781, HM773759, JN258407, JN258377, JN258355, JN258337, JN258395, JN258372, JN258352.

Seq.set 2 – GenBank accession nos.: HM773816, HM773794, HM773772, HM773750, HM773849, HM773827, HM773805, HM773783, HM773761, JN258391, JN258369, JN258347, JN258402, JN258381, JN258358, JN258334.

Seq.set 3 – GenBank accession nos.: HM773841, HM773819, HM773797, HM773775, HM773753, HM773852, HM773830, HM773808, HM773786, HM773764, JN258400, JN258379, JN258357, JN258339, JN258389, JN258367, JN258345.

Seq.set 4 – GenBank accession nos.: HM773842, HM773820, HM773798, HM773776, HM773754, HM773853, HM773831, HM773809, HM773787, HM773765, JN258399, JN258378, JN258356, JN258333, JN258388, JN258366, JN258344.

Seq.set 5 – GenBank accession nos.: HM773832, HM773810, HM773788, HM773766, HM773744, HM773843, HM773821, HM773799, HM773777, HM773755, JN258397, JN258375, JN258353, JN258331, JN258386, JN258364, JN258342.

Seq.set 6 – GenBank accession nos.: HM773833, HM773811, HM773789, HM773767, HM773745, HM773844, HM773822, HM773800, HM773778, HM773756, JN258406, JN258385, JN258363, JN258341, JN258396, JN258374, JN258350, FJ152128.

Seq.set 7 – GenBank accession nos.: HM773834, HM773812, HM773790, HM773768, HM773746, HM773845, HM773823, HM773801, HM773779, HM773757, JN258394, JN258373, JN258351, JN258405, JN258384, JN258361, JN258336.

Seq.set 8 – GenBank accession nos.: JN849151, JN849121, JN849155, JN849147, JN849153, JN849135, JN849119, JN849149, JN849125, HM773835, HM773813, HM773791, HM773769, HM773747, HM773846, HM773824, HM773802, HM773780, HM773758, JN258393, JN258371, JN258349, JN258404, JN258383, JN258360, JN258340, EU839956, EU839958, EU839955, EU839957.

Seq.set 9 – GenBank accession nos.: HM773837, HM773815, HM773793, HM773771, HM773749, HM773848, HM773826, HM773804, HM773782, HM773760, JN258403, JN258382, JN258359, JN258335, JN258392, JN258370, JN258348.

Seq.set 10 – GenBank accession nos.: HQ650885, HQ650883, HQ650881, HQ650879, HQ650877, HQ650875, HQ650873, HQ650871, GU377205, GU377203, GU377201, GU377199, GU377197, GU377195, GU358446, GU358444, GU358442, GU358440, GU358438, GU358436, GU358434, GU358432, GU358430, GU358428, GU358426, GU358424, GU358422, GU358420, HQ650886, HQ650884, HQ650882, HQ650880, HQ650878, HQ650876, HQ650874, HQ650872, GU377204, GU377202, GU377200, GU377198, GU377196, GU358445, GU358443, GU358441, GU358439, GU358437, GU358435, GU358433, GU358431, GU358429, GU358427, GU358425, GU358423, GU358421, GU358419, HM773840, HM773818, HM773796, HM773774, HM773752, HM773851, HM773829, HM773807, HM773785, HM773763, JN258390, JN258368, JN258346, JN258401, JN258380, JN258362, JN258338, HQ650887, FJ348350, FJ348348, FJ348349.1, GU358417, GU358415, GU358413, GU358411, GU358418, GU358416, GU358414, GU358412, GU377206.

3.6. ENTEROCYTES VIABILITY, CYTOTOXICITY AND APOPTOSIS ASSAY

Fully differentiated Caco-2 cells either infected with rotavirus and/or exposed to bacteria were tested for viability, cytotoxicity and apoptosis with ApoTox-Glo Triplex Assay (Promega). The assay determines viability and cytotoxicity by measuring two differential protease biomarkers simultaneously by addition of a single nonlytic reagent containing two peptide substrates. The live-cell protease activity is restricted to intact viable cells and is measured using a fluorogenic, cell-permeant peptide substrate that enters intact cells. It is cleaved to generate a fluorescent signal proportional to the number of living cells. The live--cell protease activity marker loses its activity upon loss of membrane integrity and leakage into the surrounding culture medium. A second, cell-impermeant, fluorogenic peptide substrate is used simultaneously to measure dead-cell protease activity that has been released from cells that have lost membrane integrity. The ratio of viable cells to dead cells is independent of cell number and, therefore, can be used to normalise data. The second reagent contains luminogenic DEVD-peptide substrate for caspase-3/7 and recombinant luciferase. Caspase-3/7 cleavage of the substrate releases luciferin, which is a substrate for luciferase and generates light. The light output, measured with a luminometer, correlates with caspase-3/7 activation as a key indicator of apoptosis. For the cell viability, cytotoxicity and apoptosis studies Caco-2 cells were seeded (at 4×10^5 cells/cm^2 density) and grown and differentiated in 96-well-plate (BRANDplates cellGrade-premium, Millipore-Merck). The differentiated enterocytes were treated with selected bacterial strains and/or rotavirus as described previously. Viability, cytotoxicity and apoptosis of Caco-2 cells after 18 h of rotavirus infection and/or bacterial treatment were tested as recommended by manufacturer. Briefly – to each well containing cell monolayer in 100 µl of culture medium 20 µl of Viability/Cytotoxicity Reagent was added, briefly mixed and incubated in Thermomixer Comfort (Eppendorf; 400 rpm, orbital shaking, 30 sec and 1 h at 37°C, respectively). Fluorescence was measured at two wavelength sets: $400_{Ex}/505_{Em}$ (for Viability) and $485_{Ex}/520_{Em}$ (for Cytotoxicity). Then 100 µl of Caspase-Glo 3/7 Reagent was added to all wells, and briefly mixed (in the same conditions as previously) and incubated for 1 h at 25°C, followed by luminescence measurement (caspase activation, a hallmark of apoptosis). Fluorescence and luminescence intensities were measured in Infinite M200 (Tecan) microplate reader.

3.7. REAL-TIME LABEL-FREE MONITORING OF CELL FATE

Non-differentiated Caco-2 cells' fate was analysed upon either infection with rotavirus or exposure to bacteria or both. The analysis determined changes in cells density, morphology, adhesion and cell-to-cell connections in real-time by dynamic measurement of electrode impedance. The Caco-2 cells were seeded (at 4×10^5 cells/cm^2 density) on microelectronic biosensor plate equipped with electrodes on the surface of growth area (E-Plate 16, ACEA Biosciences). The enterocytes were treated with selected bacterial strains and/or rotavirus as described previously. The electrodes allowed measurement of impedance in continuous regime and the readings were recorded by the xCelligence System equipped with RTCA DP Analyzer (ACEA Biosciences). Presence of the cells on top of the electrodes, adhesion to surface and changes in their morphology, as well as development of connections between cells affected local ionic environment at the electrode/solution interface leading to an increase of the electrode impedance (Atienza et al., 2006).

3.8. PROCEDURES FOR DATA ANALYSIS: NORMALISATION AND DIFFERENTIAL ANALYSIS, IDENTIFICATION AND SELECTION OF BIOLOGICAL PROCESSES MODULATED UPON CONTACT WITH BACTERIAL CELLS

Numerical values of fluorescence intensities were normalised and analysed for differential gene expression in Bioconductor package (Gentleman et al., 2004) running in "R" environment (http://www.r-project.org/). Normalisation eliminates disturbances occurring in case of cDNA labelled with varying intensity (Siatkowski and Zyprych, 2008; Stępniak et al., 2008). Raw data (Fig. S1) was subjected to various combinations of pre-treatment processes including: background correction ["Normexp" (Ritchie et al., 2007)), within-slide normalisation ("Print-tip loess"; Smyth and Speed, 2003, Yang et al., 2002)), and between slide normalisation ("Aquantile"; Yang and Thorne, 2003)]. Comparison of the results of these combinations (Fig. S2-S6) shown that it was best to normalise the data without background correction and normalisation between arrays. Therefore, the microarray datasets were subjected to within-slide normalisation only – "Print-tip loess" (Fig. S5). This technique uses the majority of genes for data normalisation. It is based on the two major assumptions: that most genes are not differentially expressed, and that there is approximately an equal number of up- and down-regulated genes (Smyth and Speed, 2003; Yang et al., 2002).

Then, based on a linear model ("Limma") an analysis of gene expression was performed to generate differential gene lists. For statistical analysis and assessing differential expression, "Limma" uses an empirical Bayes method to moderate the standard errors of the estimated log-fold changes. This results in more stable inference and improved power, especially for experiments with small numbers of arrays (Smyth, 2004, 2005).

Cluster analysis. In order to obtain information about the similarity of individual transcriptomes of enterocytes in response to microorganisms a sample oriented cluster analysis was performed. For this purpose, the Cluster 3.0 program (Human Genome Center, University of Tokyo) with "C Clustering" library version 1.5 (de Hoon et al., 2004) was used. Unsupervised hierarchical cluster analysis was applied based on the determination of the distance between clusters using average linkage (UPGMA, unweighted pair group method with averaging) with the Euclidean distance as a measure of similarity between the expression datapoints. Cluster analysis of samples was performed on the full lists of genes or genes involved in a specific category of biological process. The analysis uses the quotient value of $\log_2$(FC) and the weight factor (w) as an indicator of increased or decreased gene expression. Weighting factor was $w = 1$ for genes with $p < 0.05$, while for $p \geq 0.05$ weight ratio was calculated on the basis of the p-value for a specific gene expression level (p) by the quadratic equation (1):

$$w = a \cdot p^2 + b \cdot p + c \tag{1}$$

where:

$$a = -84.21052632$$
$$b = 192.6315789$$
$$c = -8.421052632$$

Such a conversion approached the $\log_2$(FC) value to zero with increasing p-value (decreasing statistical significance). The result of the unsupervised hierarchical cluster analysis was returned in form of dendrogram of similarity. The end of each branch indicates a particular sample (experimental variant). The branches converge at the nodes, the lower a node is located the greater similarity between expression profiles of samples was calculated (correlation coefficient higher – ranging from 0 to 1). The two most diverging branches (having no node) separate samples showing no correlation of gene expression profile (correlation coefficient $R^2 = 0$).

Microarray data mining. Exploration of microarray data was carried out using the ErmineJ v. 2.1 program (Gillis et al., 2010; Lee et al., 2005) with the use of "Gene Score Resampling" (GSR) algorithm (Pavlidis et al., 2004). This

program performs analyses of large gene lists from gene expression profiling data to determine functionally interesting patterns in the data. ErmineJ clusters genes in microarray analysis into functional groups on the basis of universal classification and categorisation of biological processes, molecular function and cellular component in relation to the identified gene products (based on the gene ontology; Ashburner et al., 2000). Gene ontologies (GO) are structured in a hierarchical manner, superior processes can group several thousand genes (e.g. regulation of metabolic process – GO:0019222 – 2894 genes), and detailed processes, at least two genes (e.g. heat generation – GO:0031649). In this way information on biological processes influenced by the test bacteria acting on enterocytes can be obtained. The complete list of genes with their *p*-values of statistical significance of their recorded expression level changes was subjected to further analysis. GSR uses all the gene scores for the genes in a biological process-gene set to produce a score for the biological process. This means that genes that do not meet a statistical threshold for selection can contribute to the score (Pavlidis et al., 2004).

Quantitative PCR data analysis. The relative fold change in human genes expression or amount of rotavirus segments and transcripts was calculated based on the relative comparative Ct (ΔΔCt) method (Schmittgen and Livak, 2008) using DataAssist v. 3.01 software (Life Technologies) based on a two-sample, two-tailed Student's t-test with the RN18S1 selected as the most stable ($\Delta Ct < 2$) endogenous control gene.

4. Results

4.1. GENE EXPRESSION RESPONSE TO BACTERIA STRAINS

In order to discover an early response of human intestinal epithelial cells to selected bacteria strains the *in vitro* gut model based on differentiated Caco-2 cells was used. The Human Whole Genome OneArray (Phalanx Biotech) transcriptome analysis microarrays were employed to investigate the mRNA obtained from Caco-2 cells before and after treatment with selected bacterial strains:

- probiotic – *L. rhamnosus* GG (ATCC 53103), *B. animalis* subsp. *lactis* BB12, a mixture of strains (*L. acidophilus* LA-5, *L. plantarum* PL02, *L. rhamnosus* KL53A, *L. delbruecki* subsp. *bulgaricus* LBY-27, *L. lactis* PB411 and *B. animalis* BB12), *L. acidophilus* LA-5, *L. casei* Shirota, *L. casei* DN114001, *E. coli* Nissle 1917,
- commensal – *B. animalis* MK2, *B. thetaiotaomicron* ATCC 29741, *P. anaerobius* ATCC 27337, and
- pathogenic – *S.* Typhimurium ATCC 14028, *E. coli* ATCC 10536, *E. coli* O157:H7 (NCTC 12900).

This experiment allowed the identification of a total number of approximately 10.7 thousand different genes undergoing differential expression ($p < 0.05$) in Caco-2 cells under the influence of the microorganisms used. However, a single microorganism influenced on average 1.1 thousand genes, with a maximum of 2.8 thousand and a minimum of 380 genes in the case of *L. acidophilus* LA-5 and *E. coli* ATCC 10536, respectively (Table 3).

Based on the linear model "Limma" an analysis of gene expression patterns was performed in order to search for differential genes common to the analysed groups of microorganisms (probiotics, commensal and pathogenic). This would allow a determination of species' impact on human health. For this purpose, the individual microarray datasets of strains belonging to the specific group were treated as biological replicates. The results, with 14 (for probiotic), 6 (for commensal) and 6 (for pathogenic) microarrays have revealed a large variation in response of enterocytes to different strains of the same group by giving small numbers of differentially expressed genes for a group (see Table 3).

Table 3. Number of genes with statistically significantly ($p < 0.05$) increased and decreased expression level in human enterocytes (differentiated Caco-2 cell monolayer) treated with selected strains of microorganisms

Tabela 3. Liczba genów o statystycznie istotnie ($p < 0,05$) podwyższonym lub obniżonym poziomie ekspresji w ludzkich enterocytach (zróżnicowanych komórkach Caco-2) po stymulacji wybranymi szczepami mikroorganizmów

Group	Strain [designation]	Number of differentially expressed genes ($p < 0.05$)	
		upregulated	downregulated
Probiotic	*Lactobacillus rhamnosus* GG (ATCC 53103) [LGG]	345	402
	Bifidobacterium animalis subsp. *lactis* BB12 [BB12]	257	292
	Lactobacillus acidophilus LA-5 [Lc5]	1 564	1 299
	mixture of: *Lactobacillus plantarum* PL02 *Lactobacillus rhamnosus* KL53A *Lactobacillus delbruecki* subsp. *bulgaricus* LBY-27 *Lactococcus lactis* PB411 *Lactobacillus acidophilus* LA-5 *Bifidobacterium animalis* subsp. *lactis* BB12 [mix]	327	608
	Lactobacillus casei Shirota [LcS]	289	349
	Lactobacillus casei DN114001 [LcD]	477	451
	Escherichia coli Nissle 1917 [EcN]	220	339
	all probiotic together [prob]	43	207
Commensal	*Bifidobacterium animalis* MK2 [Ba]	363	226
	Bacteroides thetaiotaomicron ATCC 29741[Bt]	993	1 217
	Peptostreptococcus anaerobius ATCC 27337 [Pa]	746	934
	all commensal together [kom]	26	55
Pathogenic	*Salmonella* Typhimurium ATCC 14028 [St]	553	619
	Escherichia coli ATCC 10536 [EcF]	319	61
	Escherichia coli O157:H7 (NCTC 12900) [EcOH]	712	672
	all pathogenic together [pat]	114	233
An average number of genes*		551	575

* Excluding group analysis (prob, kom, pat).

* Nie uwzględnia analiz grupowych (prob, kom, pat).

Comparison of lists of genes with significantly changed expression showed that the tested bacteria modulated from 1% to 25% of the same genes (7% on average; by analysing the percentage in relation to the whole list of genes modulated by the microorganism; Table 4). These percentages refer to 13 and 137 genes, respectively (with an average of 69 genes, Table S2). In the case of transcriptomes modulated by bacteria moderating a long list of genes (e.g. *L. acidophilus* LA-5 – 2863 genes and *B. thetaiotaomicron* ATCC29741 – 2210 genes, Table 3) the longest list of 397 joint differentially expressed genes gives a small percentage as compared to the whole lists (14% and 18%, respectively; Table 4).

Within the joint group of genes modulated by two compared bacteria strains from 23% to 98% of genes (average 64%) showed the same direction of changes in expression. Such a comparison of responsomes to strains within probiotic, commensal and pathogenic group gave both maximum and average percentage of joint differentially modulated genes in the same pattern of: 91% and 66%, 58% and 46%, and 82% and 72%, respectively (Table 4). This indicates that the highest consistency in joint differentially expressed genes in the same pattern remains within pathogenic strains and the most divergent are probiotic strains.

Comparison of groups revealed both maximum and average percentage of joint differentially modulated genes in the same manner at: 97% and 68% (probiotic vs. commensal strains), 98% and 58% (probiotic vs. pathogenic strains), and 88% and 62% (commensal vs. pathogenic strains).

Lactobacillus acidophilus LA-5 and *L. casei* DN114001, in contrast to other probiotic strains, did not influence all genes commonly modulated by probiotics in the same manner (95% and 80%, respectively; Table 4). The same can be observed for genes modulated by *B. animalis* MK2 (91%) in respect to genes commonly influenced by commensals. Only *E. coli* ATCC 10536 modulated all differentially expressed genes of enterocytes in the same pattern as for pathogens' group. *Lactobacillus casei* Shirota and *L. casei* DN114001 influenced all the joint differential gene expression in the same fashion as compared to the commensal group. *Lactobacillus acidophilus* LA-5 displayed the smallest concordance (31%) of joint differentially expressed genes in comparison to the commensal group. Within the probiotic strains the *B. animalis* BB12 displayed the lowest similarity in the pattern of gene regulation of joint differential genes common with pathogens group (27%).

In order to determine similarities between transcriptomes of differentiated Caco-2 enterocytes exposed to bacteria strains an unsupervised hierarchical cluster analysis was applied. The analysis generated a dendrogram (Fig. 3) displaying similarities between bacterial strains influence on enterocytes' whole genome activity. Euclidean distance was used as a measure of similarity. This

method clusters samples of similar shape or trend of gene expression profile taking into account level of expression changes. Cluster analysis confirmed, demonstrated earlier by the "Limma" linear model, a large variation in response of enterocytes to the bacteria tested. This is demonstrated by the long-drawn branches and high located nodes in the dendrogram (Fig. 3).

The cluster analysis showed that the greatest similarity in transcriptional response of differentiated Caco-2 enterocytes was observed in case of two strains of the *B. animalis*: BB12 and MK2 (marked in Figure 3 as BB12 and Ba, respectively). The correlation coefficient of expression pattern of all genes analysed for the two strains was $R^2 = 0.66$. Whereas the response of enterocytes to the strains of *E. coli*: Nissle 1917, ATCC 10536 and NCTC 12900 (marked on Figure 3 as: EcN, EcF and EcOH, respectively), and *L. casei* strains: DN114001 and Shirota (marked on Figure 3 as LcD and LcS, respectively) showed more similarities to the response to other species tested than within the studied strains of fecal coliforms and *L. casei*. The profile of gene activity in differentiated Caco-2 enterocytes after the stimulation with *E. coli* NCTC 12900 showed no correlation with gene expression profiles identified in the remaining experimental variants.

Comparison of enterocytes' responsomes did not show any considerable group of genes modulated by any collection of the bacteria tested. The list of all significantly modulated genes by all the bacterial strain tested was analysed with Kyoto Encyclopedia of Genes and Genomes (KEGG) Pathway database (Kanehisa et al., 2012). The list was composed of over 6.2 thousand unique genes and over 2.6 thousands were modulated by more than one of the strains used. The KEGG Pathway database contained entries on only 2016 genes from the list which were assigned to pathway maps (Table S3). The highest number of genes (n = 370) were assigned to metabolic pathways map (KEGG id: hsa01100) indicating that the bacteria used modulate cell metabolism. Other targets were located in signal transduction pathway maps revealing that bacteria modify cell sensitivity and reaction to stimuli through changing expression of pathways' components. The phosphatidylinositol 3'-kinase (PI3K)-Akt signalling pathway had 125 members differentially expressed. The pathway is activated by many types of cellular stimuli or toxic insults. It regulates fundamental cellular functions such as transcription, translation, proliferation, growth, and survival. Signal molecules such as growth factors bind to their receptor tyrosine kinase (RTK) or G protein-coupled receptors (GPCR). This stimulates PI3K isoforms, that catalyse the production of phosphatidylinositol-3,4,5-triphosphate (PIP3), a second messenger that activate Akt. The Akt controls key cellular processes by phosphorylating substrates involved in apoptosis, protein synthesis, metabolism, and cell cycle (Fig. 4).

Table 4. Overview of the percentages of joint differentially expressed genes ($p < 0.05$) in differentiated Caco-2 enterocytes under the influence of *L. rhamnosus GG* ATCC 53103 (LGG), *B. animalis* BB12 (BB12), *L. acidophilus* LA-5 (Lc5), mixture (mix) of selected strains (*L. acidophilus* LA-5, *L. plantarum* PL02, *L. rhamnosus* KL53A, *L. delbruecki* subsp. *bulgaricus* LBY-27, *L. lactis* PB411, *B. animalis* BB12), *L. casei* Shirota (LcS), *L. casei* DN114001 (LcD), *E. coli* Nissle 1917 (EcN), *B. animalis* MK2 (Ba), *B. thetaiotaomicron* ATCC 29741 (Bt), *P. anaerobius* ATCC 27337 (Pa), *S.* Typhimurium ATCC 14028 (St), *E. coli* ATCC 10536 (EcF), *E. coli* O157:H7 (EcOH). The upper half of the table shows the percentages of total number of joint genes in pairs of experimental conditions in relation to total number of genes modulated by strain designated in: upper row-header of the table (↑, top in a cell) and left column-header of the table (←, bottom in a cell). The lower half of the table shows the percentages of joint genes that display the same expression pattern in pairs of experimental conditions (≈). The overview includes probiotics (prob), commensal (kom) and pathogenic (pat) groups analysis. The values were rounded to integer numbers except values of less than 0.5

Tabela 4. Odsetek genów różnicujących ($p < 0,05$) w zróżnicowanych enterocytach Caco-2 po stymulacji: *L. rhamnosus GG* ATCC 53103 (LGG), *B. animalis* BB12 (BB12), *L. acidophilus* LA-5 (Lc5), mieszaniną (mix) wybranych szczepów (*L. acidophilus* LA-5, *L. plantarum* PL02, *L. rhamnosus* KL53A, *L. delbruecki* subsp. *bulgaricus* LBY-27, *L. lactis* PB411, *B. animalis* BB12), *L. casei* Shirota (LcS), *L. casei* DN114001 (LcD), *E. coli* Nissle 1917 (EcN), *B. animalis* MK2 (Ba), *B. thetaiotaomicron* ATCC 29741 (Bt), *P. anaerobius* ATCC 27337 (Pa), *S.* Typhimurium ATCC 14028 (St), *E. coli* ATCC 10536 (EcF), *E. coli* O157:H7 (EcOH). Prawa połowa tabeli przedstawia odsetki całkowitej liczby wspólnych genów różnicujących dla par warunków eksperymentalnych w odniesieniu do całkowitej liczby genów różnicujących modulowanych przez szczepy, których symbole umieszczono w rzędzie nagłówka tabeli (↑, górna liczba w komórce) lub kolumnie nagłówka tabeli (←, dolna liczba w komórce). Dolna połowa tabeli przedstawia odsetki genów różnicujących o tym samym charakterze zmiany ekspresji dla pary porównywanych warunków eksperymentalnych (≈). Porównanie zawiera analizy grupowe dla szczepów probiotycznych (prob), komensalnych (kom) i patogennych (pat). Wartości zostały zaokrąglone do liczb całkowitych z wyjątkiem wartości mniejszych niż 0,5

≈	↑ / ←	Probiotic								Commensal				Pathogenic			
		LGG	BB12	Lc5	mix	LcS	LcD	EcN	prob	Ba	Bt	Pa	kom	St	EcF	EcOH	pat
1	2	3	4	5	6	7	8	9	10	11	12	13	14	15	16	17	18
	LGG		3	4	5	4	5	4	5	5	4	3	2	4	6	3	1
			3	15	6	3	6	3	2	4	12	6	0.3	6	3	6	1
	BB12	68		3	4	5	4	6	7	4	3	3	6	3	4	2	3
				15	6	5	7	6	3	4	13	8	1	7	3	6	2

1	2	3	4	5	6	7	8	9	10	11	12	13	14	15	16	17	18
Probiotic	Lc5	82	46		12 4	11 2	13 4	19 4	23 2	20 4	18 14	10 6	16 0.4	12 5	23 3	18 9	20 2
	mix	55	74	65		9 6	3 3	5 3	5 1	6 4	3 7	5 10	9 1	3 4	9 4	4 6	2 1
	LcS	88	76	54	70		2 3	9 8	15 6	3 3	3 12	4 11	19 2	5 10	5 3	3 5	4 2
	LcD	48	56	50	52	61		4 3	4 1	6 4	6 13	4 6	5 0.4	6 8	3 1	5 7	5 2
	EcN	67	91	61	82	90	63		41 18	5 5	5 19	5 16	36 5	12 25	9 6	4 11	14 9
	prob	100	100	95	100	100	80	100		1 3	3 30	3 21	46 15	6 29	2 4	2 12	18 24
Commensal	Ba	74	73	79	63	63	52	78	88		3 12	4 11	14 2	4 7	8 5	4 7	4 2
	Bt	41	70	86	46	82	33	94	84	27		10 7	59 2	16 9	12 2	10 6	19 3
	Pa	65	67	66	65	78	58	97	98	58	54		44 2	11 8	7 1	8 6	10 2
	kom	50	80	31	71	100	100	93	95	91	100	100		3 41	1 5	1 17	7 28
Pathogenic	St	67	65	30	47	85	49	98	94	37	82	88	100		7 2	9 10	19 6
	EcF	68	38	88	69	42	31	56	56	79	23	64	75	68		2 9	10 9
	EcOH	74	35	63	51	60	60	56	69	71	37	77	86	67	82		28 7
	pat	80	27	74	43	93	65	78	80	77	58	91	96	98	100	77	

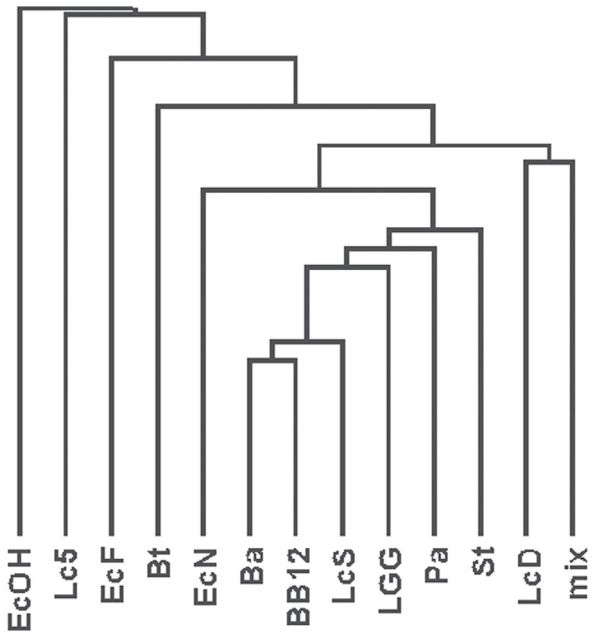

Fig. 3. Dendrogram of the experimental variants determined by an unsupervised hierarchical cluster analysis using Euclidean distance measures in determining the global similarity between the level of expression within all analysed genes. The compared transcriptomes were of differentiated Caco-2 cells in response to microorganisms: *L. rhamnosus GG* ATCC 53103 (LGG), *B. animalis* BB12 (BB12), *L. acidophilus* LA-5 (Lc5), mixture (mix) of selected strains (*L. acidophilus* LA-5, *L. plantarum* PL02, *L. rhamnosus* KL53A, *L. delbruecki* subsp. *bulgaricus* LBY-27, *L. lactis* PB411, *B. animalis* BB12), *L. casei* Shirota (LcS), *L. casei* DN114001 (LcD), *E. coli* Nissle 1917 (EcN), *B. animalis* MK2 (Ba), *B. thetaiotaomicron* ATCC 29741 (Bt), *P. anaerobius* ATCC 27337 (Pa), *S.* Typhimurium ATCC 14028 (St), *E. coli* ATCC 10536 (EcF), *E. coli* O157:H7 (EcOH)
Ryc. 3. Dendrogram podobieństwa ekspresji genów dla poszczególnych warunków eksperymentalnych uzyskany z zastosowaniem nienadzorowanej hierarchicznej analizy skupień i wykorzystaniem odległości euklidesowej przy określaniu globalnego podobieństwa pomiędzy poziomem ekspresji wszystkich analizowanych genów. Porównano profile ekspresji genów w zróżnicowanych komórkach Caco-2 po stymulacji: *L. rhamnosus GG* ATCC 53103 (LGG), *B. animalis* BB12 (BB12), *L. acidophilus* LA-5 (Lc5), mieszaniną (mix) wybranych szczepów (*L. acidophilus* LA-5, *L. plantarum* PL02, *L. rhamnosus* KL53A, *L. delbruecki* subsp. *bulgaricus* LBY-27, *L. lactis* PB411, *B. animalis* BB12), *L. casei* Shirota (LcS), *L. casei* DN114001 (LcD), *E. coli* Nissle 1917 (EcN), *B. animalis* MK2 (Ba), *B. thetaiotaomicron* ATCC 29741 (Bt), *P. anaerobius* ATCC 27337 (Pa), *S.* Typhimurium ATCC 14028 (St), *E. coli* ATCC 10536 (EcF), *E. coli* O157:H7 (EcOH)

The mitogen-activated protein kinase (MAPK) cascade had 88 members differentially expressed in response to bacteria (Fig. 5). The signalling pathway is involved in cell proliferation, differentiation and migration in response to e.g. pro-inflammatory stimuli. Human cells express at least four distinctly regulated groups of MAPKs: extracellular signal-related kinases (ERK)-1/2, Jun amino--terminal kinases (JNK1/2/3), p38 proteins (p38alpha/beta/gamma/delta) and ERK5. These are activated by specific MAPK kinases (MAPKKs). Each MAPKK, however, can be activated by more than one MAPKK kinase (MAPKKK), increasing the complexity and diversity of MAPK signalling.

The Rap1 signalling pathway controls diverse processes, such as cell adhesion, cell-cell junction formation and cell polarity. The pathway is centered over G protein, Rap1 that plays a dominant role in the control of cell-cell and cell-matrix interactions by regulating the function of integrins and other adhesion molecules in various cell types. Rap1 also regulates MAP kinase (MAPK) and Act activity in a manner highly dependent on the context of cell types. Stimulation of enterocytes by bacteria used changed expression of 84 members of the pathway (Fig. 6).

The tested bacteria modulated also expression of 72 members of the Ras signalling pathway (involved in regulating cell proliferation, survival, growth, migration, differentiation or cytoskeletal dynamism), 59 members of the forkhead box O (FOXO) signalling pathway (involved in regulation of apoptosis, cell--cycle control, glucose metabolism, oxidative stress resistance, and longevity), and many other signal transduction pathways (see Table 5). Signalling pathways are complex network of interactions where stimuli from various sources are integrated. Microorganisms modulating expression of different counterparts of the same signalling pathway influence an effect of the same process (Gilbert, 2000).

The bacteria used for stimulation of Caco-2 cells influenced also expression of 80 gene products involved in regulation of actin cytoskeleton (Fig. 7) and closely related cellular processes like: focal adhesion, tight junctions, and adherens junction with 74, 58, and 31 genes modulated, respectively.

Beside signalling pathways and cellular processes the bacteria modulated genes were identified in genetic information processing, organismal systems, and diseases. Altogether the KEGG database search revealed involvement of the bacteria modulated genes in many general and several disease molecular interaction pathway maps (Table 5). This indicate that although the bacteria modulate different genes in strain specific fashion their action is aimed to similar host cell processes, as it was shown on exemplary pathway maps (Figs 4-7).

In analyses regarding lists of genes modulated by single strains of the bacteria used the commensals (*B. thetaiotaomicron* ATCC 29741 and *P. anaerobius* ATCC 27337), and pathogens (*S.* Typhimurium ATCC 14028 and *E. coli* O157:H7)

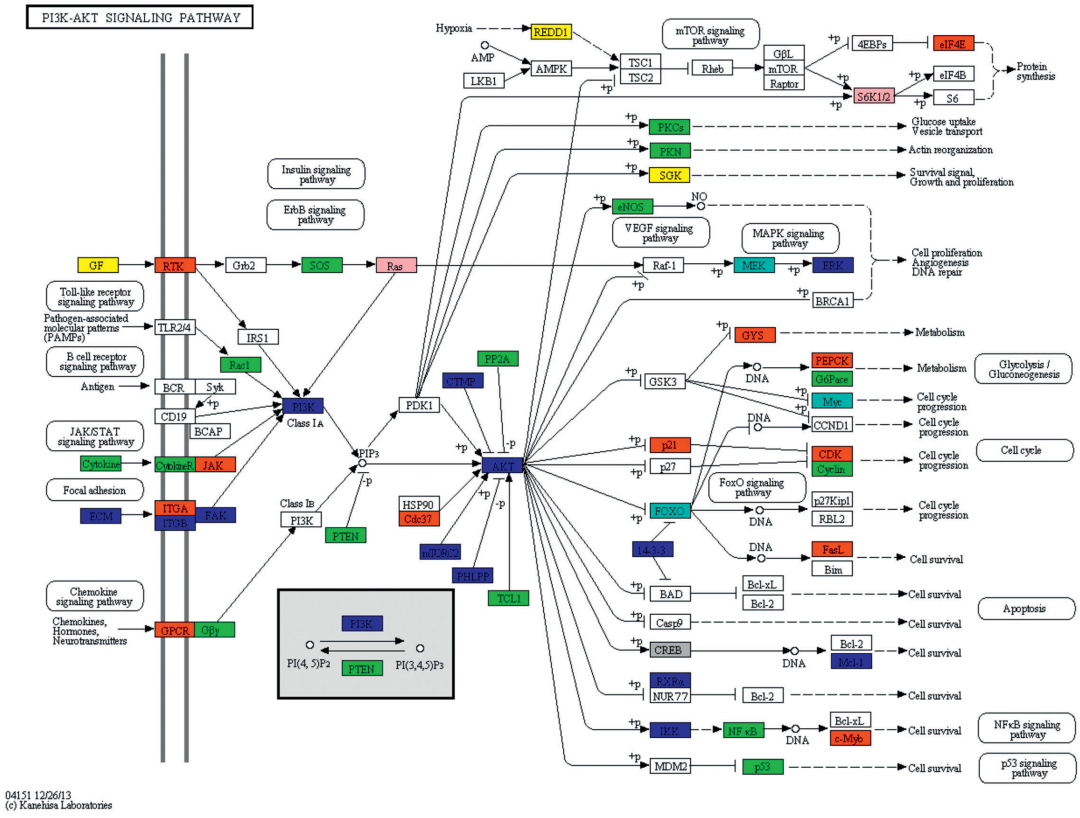

Fig. 4. Pathway map of the phosphatidylinositol 3'-kinase (PI3K)-Akt signalling. Members of the pathway which expression was modulated by specific group of bacteria used were coloured: green (probiotic), blue (commensal), red (pathogens), cyan (probiotic and commensal), yellow (probiotic and pathogens), pink (commensal and pathogens), and gray (probiotic and commensal and pathogens). For notation used in pathways maps see Figure S7 in supplementary materials

Ryc. 4. Mapa szlaku sygnalizacyjnego 3'-kinazy fosfatydyloinozytolu (PI3K) i serynowo-treoninowej kinazy białkowej Akt. Składniki szlaku, których ekspresja była modulowana przez bakterie z danej grupy, oznaczono kolorem: zielonym (probiotyki), niebieskim (komensalne), czerwonym (patogeny), turkusowym (probiotyki i komensalne), żółtym (probiotyki i patogeny), różowym (komensalne i patogeny) i szarym (probiotyki, komensalne i patogeny). Oznaczenia stosowane na mapach zostały opisane na rycinie S7 w materiałach pomocniczych

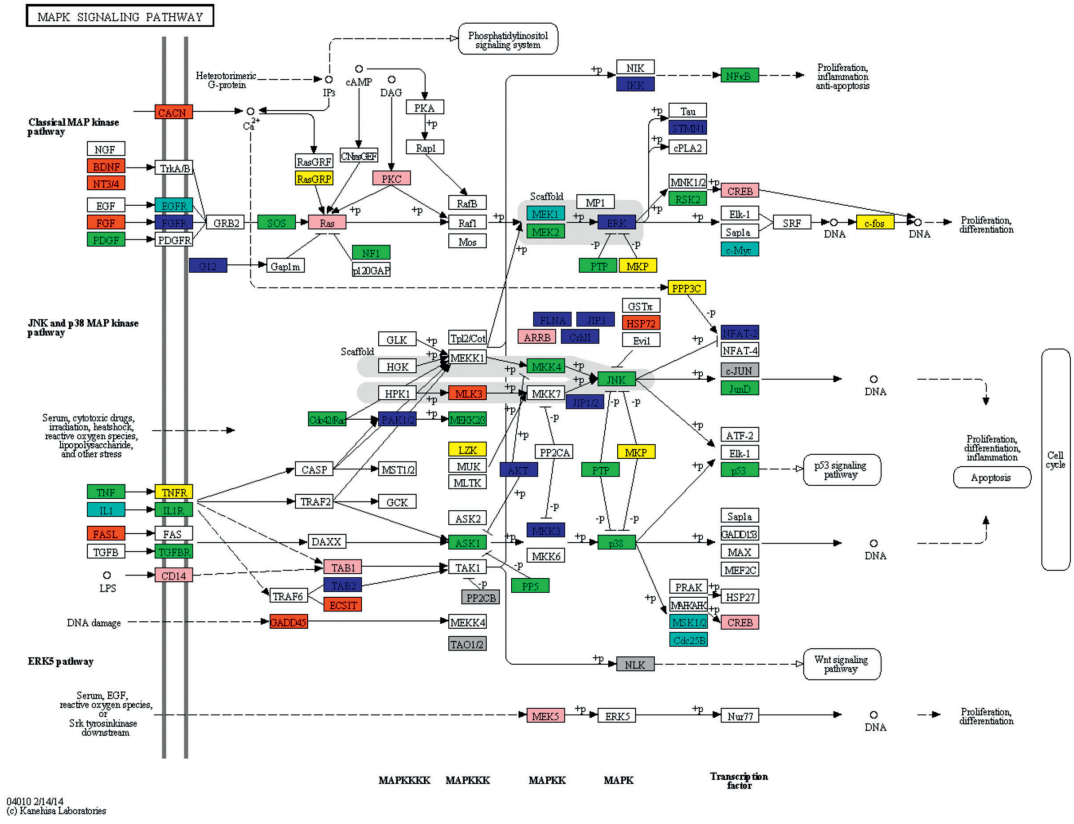

Fig. 5. Pathway map of the mitogen-activated protein kinase signalling. Members of the pathway which expression was modulated by specific group of bacteria used were coloured: green (probiotic), blue (commensal), red (pathogens), cyan (probiotic and commensal), yellow (probiotic and pathogens), pink (commensal and pathogens), and gray (probiotic and commensal and pathogens). For notation used in pathways maps see Figure S7 in supplementary materials

Ryc. 5. Mapa szlaku sygnalizacyjnego kinazy aktywowanej przez mitogeny. Składniki szlaku, których ekspresja była modulowana przez bakterie z danej grupy, oznaczono kolorem: zielonym (probiotyki), niebieskim (komensalne), czerwonym (patogeny), turkusowym (probiotyki i komensalne), żółtym (probiotyki i patogeny), różowym (komensalne i patogeny) i szarym (probiotyki, komensalne i patogeny). Oznaczenia stosowane na mapach zostały opisane na rycinie S7 w materiałach pomocniczych

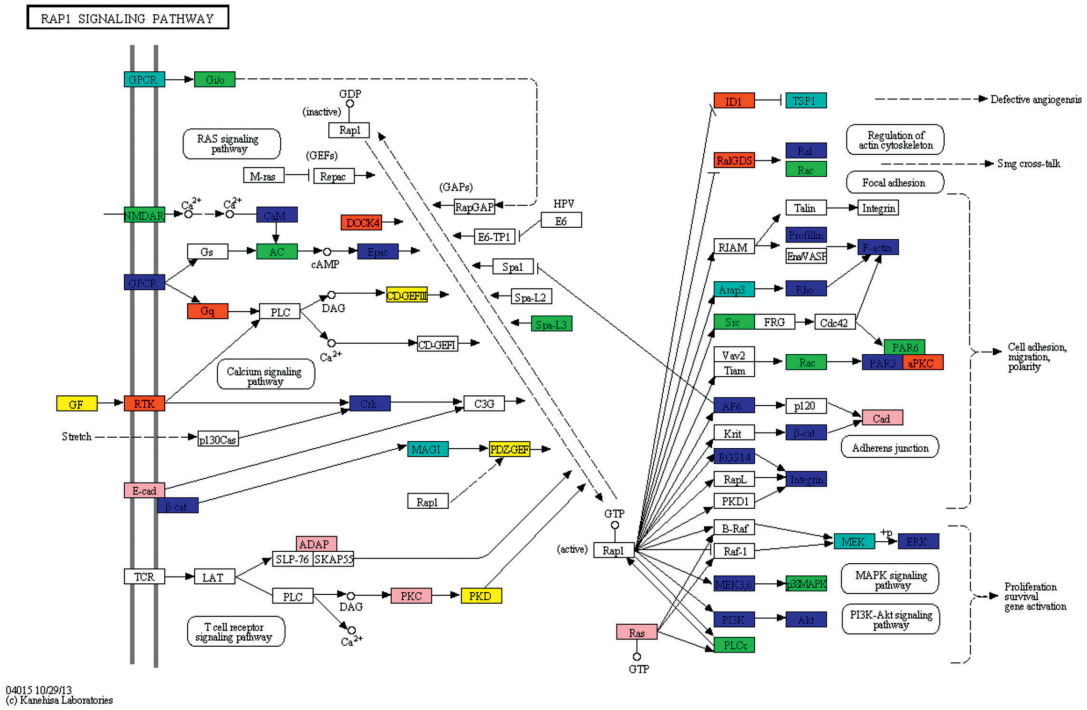

Fig. 6. Pathway map of the Rap1 signalling. Members of the pathway which expression was modulated by specific group of bacteria used were coloured: green (probiotic), blue (commensal), red (pathogens), cyan (probiotic and commensal), yellow (probiotic and pathogens), pink (commensal and pathogens), and gray (probiotic and commensal and pathogens). For notation used in pathways maps see Figure S7 in supplementary materials

Ryc. 6. Mapa szlaku sygnalizacyjnego białka Rap1. Składniki szlaku, których ekspresja była modulowana przez bakterie z danej grupy, oznaczono kolorem: zielonym (probiotyki), niebieskim (komensalne), czerwonym (patogeny), turkusowym (probiotyki i komensalne), żółtym (probiotyki i patogeny), różowym (komensalne i patogeny) i szarym (probiotyki, komensalne i patogeny). Oznaczenia stosowane na mapach zostały opisane na rycinie S7 w materiałach pomocniczych

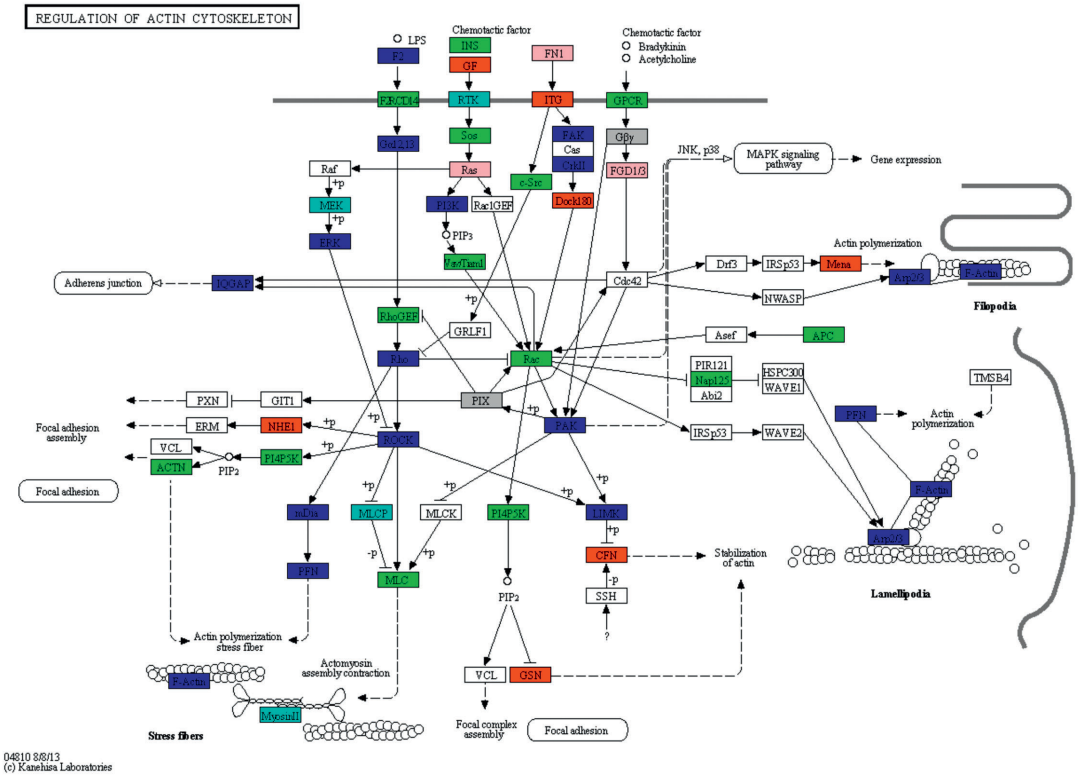

Fig. 7. Pathway map of the regulation of actin cytoskeleton. Members of the pathway which expression was modulated by specific group of bacteria used were coloured: green (probiotic), blue (commensal), red (pathogens), cyan (probiotic and commensal), yellow (probiotic and pathogens), pink (commensal and pathogens), and gray (probiotic and commensal and pathogens). For notation used in pathways maps see Figure S7 in supplementary materials

Ryc. 7. Mapa szlaku regulacji cytoszkieletu aktynowego. Składniki szlaku, których ekspresja była modulowana przez bakterie z danej grupy, oznaczono kolorem: zielonym (probiotyki), niebieskim (komensalne), czerwonym (patogeny), turkusowym (probiotyki i komensalne), żółtym (probiotyki i patogeny), różowym (komensalne i patogeny) i szarym (probiotyki, komensalne i patogeny). Oznaczenia stosowane na mapach zostały opisane na rycinie S7 w materiałach pomocniczych

Table 5. List of selected pathway maps where at least 20 differentially expressed genes involved in response to the bacteria used were identified by KEGG database (Kanehisa and Goto, 2000). Number of genes identified are given in parenthesis

Tabela 5. Lista map szlaków, w których co najmniej 20 genów różnicujących w odpowiedzi na bakterie zostało zidentyfikowanych w zasobach bazy danych KEGG (Kanehisa i Goto, 2000). Liczba zidentyfikowanych genów różnicujących została umieszczona w nawiasach

Metabolism
Metabolic pathways (370), Purine metabolism (47), Carbon metabolism (43), Biosynthesis of amino acids (32), Glycerophospholipid metabolism (31), Pyrimidine metabolism (28), Metabolism of xenobiotics by cytochrome P450 (28), Oxidative phosphorylation (27), Glycolysis / Gluconeogenesis (22), Inositol phosphate metabolism (22), Glycerolipid metabolism (22), Drug metabolism – cytochrome P450 (20)

Genetic Information Processing
Protein processing in endoplasmic reticulum (56), Ubiquitin mediated proteolysis (53), RNA transport (46), Spliceosome (41), mRNA surveillance pathway (32)

Environmental Information Processing
PI3K-Akt signalling pathway (125), MAPK signalling pathway (88), Rap1 signalling pathway (84), Cytokine-cytokine receptor interaction (83), Ras signalling pathway (72), Chemokine signalling pathway (66), FoxO signalling pathway (59), Calcium signalling pathway (57), Hippo signalling pathway (55), Insulin signalling pathway (53), TNF signalling pathway (52), Jak-STAT signalling pathway (51), HIF-1 signalling pathway (47), Wnt signalling pathway (44), Thyroid hormone signalling pathway (43), ErbB signalling pathway (42), NF-kappa B signalling pathway (39), GnRH signalling pathway (35), TGF-beta signalling pathway (33), Phosphatidylinositol signalling system (31), ECM-receptor interaction (26), mTOR signalling pathway (25), VEGF signalling pathway (25), p53 signalling pathway (23), PPAR signalling pathway (20)

Cellular Processes
Regulation of actin cytoskeleton (80), Focal adhesion (74), Endocytosis (71), Tight junction (58), Cell adhesion molecules (CAMs) (48), Cell cycle (47), Phagosome (46), Lysosome (44), Apoptosis (34), Adherens junction (31), Peroxisome (26), Ribosome (25), Gap junction (25)

Organismal Systems
Leukocyte transendothelial migration (43), Toll-like receptor signalling pathway (43), Inflammatory mediator regulation of TRP channels (34), Protein digestion and absorption (28), RIG-I-like receptor signalling pathway (26), NOD-like receptor signalling pathway (22), Antigen processing and presentation (22), Mineral absorption (21)

Human Diseases
Pathways in cancer (115), Proteoglycans in cancer (92), Viral carcinogenesis (78), Transcriptional misregulation in cancer (73), Herpes simplex infection (67), MicroRNAs in cancer (67), Hepatitis B (65), Epstein-Barr virus infection (64), Influenza A (60), Tuberculosis (58), Hepatitis C (57), Chagas disease (*American trypanosomiasis*) (44), Measles (43), Toxoplasmosis (43), Amoebiasis (39), Salmonella infection (36), Pertussis (34), Bacterial invasion of epithelial cells (29), Leishmaniasis (27), Epithelial cell signalling in *Helicobacter pylori* infection (31), *Staphylococcus aureus* infection (26), Colorectal cancer (26), Chemical carcinogenesis (26), Shigellosis (25), Inflammatory bowel disease (IBD) (21)

modulated the highest number of genes assigned to KEGG pathway maps. Interestingly commensal *B. animalis* MK2 and pathogenic *E. coli* ATCC 10536 modulated the smallest number of genes annotated in the KEGG pathway maps.

The KEGG is a collection of manually curated databases. Therefore the amount of interactions it contains is limited. To further characterise general differences and similarities between the transcriptomes of the differentiated Caco-2 cells exposed to selected bacterial strains the GO slim terms of the complex Gene Ontology annotations (Ashburner et al., 2000) were used (Table 6). Significant over- and underrepresentation of GO slim terms in the comparison of the 13 analysed strains were determined by a Grubbs' test (Grubbs, 1969) on percentages of differential genes within each GO Slim term. The analysis was performed for total percent of differential genes within each GO Slim term, and separately for percent of up- and down-regulated genes to see whether any of the strains modulate genes in different proportions. Among the strains tested three showed a derogation from the general trend. The most divergent response was observed in case of *E. coli* Nissle 1917 treatment. The strain was causing modulation of genes in elevated number in GO slim terms associated with regulation and transcription like 'biological regulation', 'response to stimulus', 'nucleic acid binding', 'transcription regulator activity', 'nucleus', and 'cellular component organisation'. Within those terms significantly overrepresented were down-regulated genes involved in nucleic acid binding and up-regulated genes engaged in transcription regulator activity. Overrepresented GO Slim terms in the group of genes with up-regulated expression were implicated in 'multi-organism process' and 'chromosome'. Also 'ion binding' and 'oxygen binding' GO Slim terms regarding downregulated genes were overrepresented (Table 6).

Another strain that triggered deviation from the global trend in enterocyte gene expression in comparison to other strains was *E. coli* ATCC 10536. The strain modulated significantly smaller percentage of genes associated with endosome and down-regulated genes associated with cytoskeleton (underrepresentation in GO slim terms). Together with over-representation of up-regulated genes involved in 'cell projection' (Table 6) those terms indicate influence of the strain on cellular architecture. Moreover it triggered overrepresentation of up-regulated genes related to 'hydrolase activity' and 'electron carrier activity' indicating its activity on metabolic processes. It also caused overrepresentation of up-regulated genes and underrepresentation of down-regulated genes in GO slim term of 'cell communication' (keeping the total number of differential genes related to this term within total range). Overrepresentation of down-regulated genes related to 'chromosome' was also associated with action of this strain. The *E. coli* ATCC 10536 caused up-regulation of significant number of unclassified genes indicating that the strain may hold properties so far unidentified (Table 6).

Table 6. Percentages of differentially expressed genes (upregulated – top in a cell, downregulated– bottom in a cell) in Caco-2 enterocytes under the influence of tested microorganisms as categorised by GO Slims. The GO Slims give a broad overview of the ontology content without the detail of the specific fine grained terms. The bacterial strains used in the study were designated: LGG – *L. rhamnosus GG* ATCC 53103, BB12 – *B. animalis* BB12, Lc5 – *L. acidophilus* LA-5, mix – mixture of selected strains (*L. acidophilus* LA-5, *L. plantarum* PL02, *L. rhamnosus* KL53A, *L. delbruecki* subsp. *bulgaricus* LBY-27, *L. lactis* PB411, *B. animalis* BB12), LcS – *L. casei* Shirota, LcD – *L. casei* DN114001, EcN – *E. coli* Nissle 1917, Ba – *B. animalis* MK2, Bt – *B. thetaiotaomicron* ATCC 29741, Pa – *P. anaerobius* ATCC 27337, St – *S.* Typhimurium ATCC 14028, EcF – *E. coli* ATCC 10536, EcOH – *E. coli* NCTC 12900. Significant over- and under-represented genes in GO slim terms were determined by selecting outliers in percentages of differential genes by a Grubbs' test regarding percentage of total differential genes in a category (indicated by double-lined cell border) or in separate calculations of up- and down-regulated genes percentages (in bold numbers). The total number of differentially expressed genes is shown in Table S4

Tabela 6. Odsetek genów różnicujących ($p < 0,05$, o podwyższonej ekspresji – górny wiersz w komórce, o obniżonej ekspresji – dolny wiersz w komórce) sklasyfikowanych w kategoriach określeń GO Slim. Określenia GO Slim dają ogólny pogląd na powiązania genów z procesami (ontologie). Szczepy bakterii stosowane do stymulacji komórek Caco-2 mają następujące oznaczenia: LGG – *L. rhamnosus GG* ATCC 53103, BB12 – *B. animalis* BB12, Lc5 – *L. acidophilus* LA-5, mix – mieszanina wybranych szczepów (*L. acidophilus* LA-5, *L. plantarum* PL02, *L. rhamnosus* KL53A, *L. delbruecki* subsp. *bulgaricus* LBY-27, *L. lactis* PB411, *B. animalis* BB12), LcS – *L. casei* Shirota, LcD – *L. casei* DN114001, EcN – *E. coli* Nissle 1917, Ba – *B. animalis* MK2, Bt – *B. thetaiotaomicron* ATCC 29741, Pa – *P. anaerobius* ATCC 27337, St – *S.* Typhimurium ATCC 14028, EcF – *E. coli* ATCC 10536, EcOH – *E. coli* NCTC 12900. Liczby genów dla danego określenia GO Slim odbiegające od trendu zaobserwowanego dla wszystkich badanych warunków eksperymentalnych wyznaczono na podstawie wartości odstających od średniego odsetka liczby genów, stosując test Grubbsa i zaznaczając podwójną linią ramki komórki (dla całkowitej liczby genów) lub stosując pogrubioną czcionkę dla obliczeń uwzględniających tylko odsetek genów o podwyższonej lub obniżonej ekspresji. Liczba genów różnicujących należących do danego procesu została ujęta w Tabeli S4

GO Slim term		Percentage of up-regulated genes in a term Percentage of down-regulated genes in a term												
		probiotic							commensal			pathogenic		
		LGG	BB12	Lc5	mix	LcS	LcD	EcN	Ba	Bt	Pa	St	EcF	EcOH
1	2	3	4	5	6	7	8	9	10	11	12	13	14	15
	metabolic process	13.65 20.75	18.03 17.12	17.53 24.62	10.7 23.64	13.64 19.91	15.84 16.38	17.71 29.16	19.86 14.09	18.96 16.29	13.69 19.94	17.24 16.04	20 8.16	17.7 21.75

1	2	3	4	5	6	7	8	9	10	11	12	13	14	15
Biological process	biological regulation	12.99 18.21	15.66 15.66	15.86 18.79	9.2 21.5	13.79 18.65	15.41 15.63	16.99 26.3	17.49 12.05	15.34 15.75	12.68 17.8	17.32 16.55	22.63 5	17.05 16.91
	multicellular organismal process	9.37 8.57	7.29 7.83	8.8 7.58	6.31 10.8	8.15 9.72	8.08 7.22	11.63 9.84	11.88 5.77	7.15 10.05	7.92 7.5	10.67 8.87	13.42 3.68	9.1 7.66
	cell communication	7.36 9.77	7.65 7.1	8.63 7.65	5.67 11.12	9.4 9.25	8.19 7.76	9.3 11.99	9.34 6.96	8.37 8.78	7.14 7.8	10.15 8.79	**15** **2.11**	9.61 8.09
	response to stimulus	6.69 9.5	8.56 5.46	6.67 6.11	5.24 10.59	6.43 7.37	5.93 5.5	11.81 9.3	9.51 4.07	6.88 6.29	5.42 6.79	8.87 6.74	12.63 3.95	7.59 5.42
	developmental process	6.43 7.9	5.83 5.65	6.99 6.29	4.81 7.49	6.43 7.52	5.93 5.39	10.02 6.08	9.17 4.41	5.66 7.15	5.77 5.36	8.45 6.66	9.74 3.42	7.23 5.71
	cellular component organization	3.88 7.36	5.46 5.46	5.69 7.33	3.64 8.24	5.33 6.74	5.28 5.5	7.87 7.16	6.62 3.74	7.29 5.2	4.82 4.46	6.83 4.95	7.37 6.58	6.65 6.14
	localization	5.22 6.96	8.38 6.01	5.73 8.66	3.32 8.45	6.58 6.74	7.11 5.39	6.8 8.77	7.47 4.58	7.92 6.38	5.42 5.89	7.42 5.38	11.58 2.37	6.21 8.02
	cell proliferation	1.34 2.68	2.55 2	1.99 2.51	1.82 3.64	2.82 2.51	1.51 1.72	4.83 1.97	3.9 1.53	2.26 1.95	2.32 1.67	2.73 2.3	5 1.05	2.1 1.66
	death	1.87 3.21	2.55 3.46	2.34 3.18	1.6 2.57	2.19 2.51	2.26 1.83	5.01 1.97	2.21 0.85	3.35 1.86	1.9 2.74	3.67 2.05	4.21 1.05	2.96 2.02
	multi-organism process	1.47 2.01	1.46 0.55	1.19 1.61	1.18 1.71	1.57 1.57	1.29 0.75	**4.11** 0.89	2.04 1.02	1.67 1.31	1.37 1.19	2.73 1.37	2.37 2.11	2.67 0.79
	growth	0.54 1.61	1.09 2	0.94 0.91	1.07 1.18	0.31 1.72	0.54 1.19	0.36 0.89	1.53 0.68	1.09 0.9	0.71 1.07	1.11 1.02	1.58 1.05	1.01 0.58
	reproduction	1.74 1.87	1.46 2.19	1.64 1.33	0.86 1.93	2.51 1.88	1.29 1.08	3.76 1.43	2.55 0.51	1.63 1.67	1.19 1.43	2.05 1.02	2.89 1.05	2.02 1.23
	unclassified	22.89 20.21	17.3 27.5	13.59 13.41	17.97 27.91	21.63 24.14	23.38 23.17	10.55 21.82	30.39 16.47	15.02 29.73	21.25 26.49	16.64 26.11	**43.16** 6.84	20.59 16.62

Table 6 cont.

1	2	3	4	5	6	7	8	9	10	11	13	14	15	16
Molecular function	protein binding	14.73 19.54	16.76 16.39	16.24 21.66	10.16 21.5	14.89 19.28	16.81 15.95	19.86 22	18.68 12.05	20.45 15.66	13.93 14.52	20.82 15.78	23.95 7.89	18.28 18.86
	ion binding	6.29 8.43	7.47 9.84	9.64 10.86	5.13 10.37	8.93 10.03	10.13 8.62	6.26 **19.14**	9.68 7.98	8.33 9	8.93 11.9	9.39 8.62	11.58 2.63	8.09 11.05
	hydrolase activity	3.35 5.89	5.28 3.46	4.54 6.15	3.21 5.67	3.13 5.64	4.74 3.88	3.4 5.9	5.6 3.74	6.56 3.71	3.63 4.58	4.18 3.24	**8.42** 1.05	3.9 5.2
	nucleic acid binding	5.09 8.3	6.56 8.93	6.18 10.2	2.99 8.34	3.45 7.99	7.11 6.68	9.48 16.82	7.13 5.09	5.75 6.15	5.77 9.64	6.4 6.57	5 5.79	7.8 8.38
	nucleotide binding	3.88 5.62	4.37 3.46	5.2 6.71	2.35 6.1	2.51 5.33	4.74 3.45	2.86 9.12	6.62 3.74	6.83 4.3	3.39 5	5.8 3.5	7.37 2.37	4.48 5.71
	transferase activity	3.35 4.82	5.1 3.46	4.19 4.72	2.35 4.92	2.51 3.13	3.45 2.48	3.76 4.11	5.77 2.38	3.35 3.67	3.04 3.39	3.58 3.41	5 1.32	3.68 5.49
	molecular transducer activity	4.28 5.22	3.46 3.28	4.16 2.65	1.82 4.49	3.45 5.17	3.34 3.88	3.04 5.19	4.07 2.21	2.67 4.75	3.39 2.86	4.1 4.61	**6.32** 0.26	3.68 2.6
	transcription regulation activity	2.14 3.88	2.73 3.1	3.25 3.46	1.71 5.03	1.88 4.23	2.91 3.02	**5.55** 6.08	2.89 2.04	2.58 3.03	2.8 3.57	4.27 3.33	2.63 0.26	3.54 3.9
	enzyme regulator activity	2.28 1.87	2 1.46	1.96 1.71	1.28 3.21	2.19 1.41	1.94 2.16	1.97 3.4	1.87 2.21	1.58 2.13	1.49 1.96	2.39 3.07	2.63 1.58	2.38 1.81
	transporter activity	1.87 1.87	2.55 2.19	2.03 2.93	0.96 2.35	2.98 0.78	2.48 1.72	1.97 3.22	2.04 1.19	2.94 2.13	1.96 2.32	3.07 1.71	4.47 0.79	2.1 2.67
	electron carrier activity	0.67 0.54	0.73 0.36	0.28 0.21	0.75 0.32	0.31 0.16	0.54 0.22	0.18 0.72	0.17 0.17	0.54 0.45	0.3 0.54	0.17 0.26	**1.32** 0	0.36 0.22
	structural molecule activity	0.8 0.67	0.55 0.36	0.91 1.99	0.53 1.6	0.94 0.63	0.97 0.75	0.72 1.97	0.34 1.36	1.99 1.22	1.01 0.77	1.54 1.37	0.53 1.58	1.23 1.01

1	2	3	4	5	6	7	8	9	10	11	13	14	15	16
Molecular function	lipid binding	1.07 0.8	0.73 0.73	1.08 0.8	0.43 1.5	0.63 1.57	0.32 0.97	0.54 1.79	0.34 0.51	0.72 1.36	0.71 1.13	0.94 0.85	1.05 0.26	0.72 1.23
	oxygen binding	0.4 0.13	0.36 0	0.07 0.07	0.43 0	0.31 0	0.11 0.11	0.36 **0.36**	0.34 0.17	0.09 0.05	0.18 0.18	0.17 0	0.53 0	0.07 0
	carbohydrate binding	0.8 0.67	1.82 0	0.7 0.24	0.32 0.53	1.57 0.94	0.22 0.97	0.54 0.36	0.85 0.51	0.81 1.22	0.6 0.42	0.68 0.85	0.53 0.53	1.16 0.65
	molecular adaptor activity	0 0.27	0.18 0	0.24 0.28	0.11 0.32	0.31 0	0.22 0.11	0 0	0.51 0.17	0.14 0.09	0.18 0	0.26 0.09	0.53 0	0.07 0.14
	chromatin binding	0.27 0.54	0.18 0.36	0.35 0.38	0.11 0.64	0.16 0.94	0.22 0.54	0.18 1.07	**0.68** 0	0.36 0.32	0.42 0.54	0.17 0.51	0 0	0.14 0.43
	antioxidant activity	0 0.27	0.18 0	0 0.17	0 0	0.31 0.16	0 0.11	0 0.36	0.17 0	0.27 0.09	0 0.24	0 0.09	0 0	0.22 0.07
	protein tag	0 0	0 0	0 0	0 0	0 0	0 0	0 0	0.17 0	0 0	0.06 0	0 0	0 0	0 0
	translation regulation activity	0.13 0.27	0 0	0.03 0.17	0 0	0 0	0 0.11	0 0	0.17 0.17	0.05 0	0.06 0	0 0.09	0 0	0.07 0.07
	nutrient reservoir activity	0 0	0 0	0 0	0 0	0 0	0 0	0 0	0.17 0	0 0	0.06 0	0 0	0 0	0 0
	unclassified	21.95 18.88	15.85 26.23	11.18 11.77	17.54 26.84	21.32 21.16	21.77 22.52	9.84 17.89	29.37 16.64	13.62 25.2	19.35 25.24	15.36 24.57	**43.42** 6.32	19.87 14.74
	membrane	10.71 17.4	16.39 11.48	13.34 14.18	7.81 17.43	13.79 15.2	15.09 12.61	13.42 16.46	14.77 9.17	15.43 15.29	10.83 12.8	15.61 12.37	18.68 4.74	15.46 14.74
	nucleus	7.9 13.52	9.65 11.29	9.95 16.03	4.06 15.61	7.52 12.85	11.75 10.78	14.67 19.5	12.56 9.85	10.72 9.73	9.46 13.51	10.92 9.98	10 6.32	11.99 13.08

Table 6 cont.

1	2	3	4	5	6	7	8	9	10	11	13	14	15	16
Cellular component	macromolecular complex	4.95 7.76	6.92 4.55	5.31 9.92	2.89 8.77	4.86 4.86	6.79 5.93	7.69 8.77	5.43 4.58	8.42 6.02	5.65 5.12	7.51 4.69	7.11 6.58	7.3 7.3
	cytosol	1.87 2.28	2.55 2	2.13 4.61	1.82 3.32	2.66 3.13	1.83 2.26	2.15 3.4	2.72 2.38	4.71 2.13	2.02 2.32	3.16 2.13	4.47 3.16	2.75 3.68
	cytoskeleton	1.87 2.81	1.64 2.37	2.65 3.18	1.5 3.53	1.1 2.04	2.37 2.69	2.86 3.22	3.4 2.72	4.3 2.94	3.04 1.79	3.5 2.22	4.21 **0.26**	2.89 2.24
	membrane-enclosed lumen	3.48 5.62	3.83 2.37	3.49 6.29	1.5 5.78	3.13 3.76	3.45 3.23	4.47 6.62	4.24 2.38	5.66 3.39	3.45 3.33	3.33 3.5	3.68 2.89	3.83 4.84
	extracellular matrix	1.2 0.54	0.91 0.18	0.91 0.35	1.28 0.21	1.41 0.63	0.32 0.54	0.36 0.72	1.19 0.51	0.41 0.59	0.77 0.6	0.51 0.68	1.32 0.53	0.87 0.79
	Golgi apparatus	1.34 2.95	2.73 0.73	1.92 3.04	1.28 3.85	1.72 2.66	1.94 2.26	1.97 2.15	3.06 1.19	3.12 1.76	1.13 1.85	2.3 1.62	2.37 0.79	1.59 1.95
	extracellular space	2.01 1.07	2.37 1.09	1.5 0.52	1.18 1.28	2.19 1.57	1.08 0.86	2.86 2.15	3.06 1.02	1.31 1.4	1.13 1.07	1.28 1.45	4.21 1.05	1.73 1.16
	endoplasmic reticulum	1.74 3.21	2.55 1.09	1.57 3.35	1.07 2.99	2.19 1.72	1.62 1.72	2.5 2.33	1.87 1.36	2.81 1.81	1.67 1.55	2.22 1.71	2.63 1.84	1.81 3.11
	mitochondrion	0.94 2.54	2.55 1.82	1.92 3.53	1.07 2.25	2.04 1.88	2.26 1.62	1.97 1.97	1.87 2.21	3.53 1.4	1.43 1.61	1.45 1.45	2.63 1.58	2.31 3.03
	cell projection	0.54 2.01	0.91 1.46	1.36 1.54	0.96 2.03	1.25 1.72	0.97 1.29	0.72 3.22	2.38 0.51	1.27 1.31	1.43 1.49	1.11 0.85	**3.16** 0.26	1.81 0.72
	endomembrane system	1.07 1.2	2.37 1.28	1.29 2.51	0.86 2.25	1.41 0.78	1.29 1.62	2.15 1.61	1.53 0.85	2.22 1.67	1.19 0.95	1.71 1.45	0.79 0.53	1.66 3.03
	vesicle	1.61 1.61	2.19 0.55	1.26 1.71	0.75 1.71	1.41 0.63	1.72 1.08	1.43 1.07	1.36 0.68	2.17 1.72	1.25 0.89	2.13 0.94	0.53 1.05	1.52 1.59
	chromosome	0.8 1.61	1.28 0.55	0.7 1.57	0.43 1.6	1.1 1.1	0.75 1.4	**3.76** 0.72	1.7 0.68	0 1.09	0.77 0.77	0.94 0.77	0.79 **3.95**	2.1 1.23
	endosome	1.07 0.4	0.55 0.91	0.7 1.26	0.21 1.07	1.1 0.63	1.19 0.75	1.07 1.07	1.02 0.17	1.09 0.54	0.54 0.42	0.94 0.68	0.26 0	0.72 0.72

1	2	3	4	5	6	7	8	9	10	11	13	14	15	16
Cellular component	envelope	0.54 1.34	1.82 0.91	0.87 2.34	0.11 1.28	1.25 0.94	1.62 1.19	1.79 1.43	0.85 0.51	1.9 0.81	0.89 0.71	1.02 1.11	1.05 0.53	1.16 2.02
	vacuole	0.54 0.54	0.18 0.18	0.38 0.8	0.11 0.53	0.78 0.63	0.65 0.54	0.54 1.07	0.85 0.51	1 0.23	0.36 0.6	1.11 0.51	0.53 0	0.65 0.36
	ribosome	0.13 0.4	0.18 0.18	0.17 1.19	0 0.32	0.16 0.31	0.22 0.11	0 0.72	0.17 0.51	0.5 0.36	0.18 0.18	0.26 0.17	0 1.05	0.29 0.36
	lipid particle	0 0	0 0.18	0.03 0.03	0 0.11	0.16 0	0 0	0 0	0 0	0.05 0	0 0	0 0	0 0	0 0
	microbody	0 0.4	0.18 0	0.21 0.31	0 0.11	0 0.16	0.22 0.11	0.36 0.54	0 0	0.36 0.09	0.12 0.18	0.17 0	0 0.26	0.36 0.22
	external encapsulating structure	0 0	0 0	0 0	0 0	0 0	0 0	0.18 0	0 0	0 0	0 0	0.09 0	0 0	0 0
	unclassified	24.36 20.08	18.03 28.23	12.75 13.45	17.54 26.74	19.75 24.45	23.6 22.31	7.87 24.51	27.67 16.47	14.48 26.29	20.65 26.31	14.08 27.39	**45.79** 6.32	20.3 16.55

Modulation of genes dissimilar to global trends was also identified in case of *B. animalis* MK2 treatment. It showed overrepresentation of up-regulated genes regarding GO Slim term of 'chromatin binding' (Table 6) indicating the strain influence on chromatin organisation during interphase.

4.2. DATA MINING FOR BIOLOGICAL SIGNIFICANCE OF BACTERIAL STIMULI

To discover bacterial action on the human body description of function of differentially expressed genes' product was analysed. Study of known specific gene actions was performed to search for biological processes influenced by tested strains. This could also reveal any similarity patterns on higher than gene expression level. Many biological processes are encoded by multiple genes and regulated through alternative pathways. Therefore lack of similarity in the expression level of individual genes does not exclude a similar end-point effect. In order to identify biological processes that are affected by tested strains, the microarray datasets were explored using a structured vocabulary of biological terms (gene ontology). Full lists of genes with statistical significance coefficients (*p*-values) of changes in the level of expression were analysed using the ErmineJ program (Lee et al., 2005) to look for altered biological processes. Individual experimental variants indicated potential changes in the 110 to 350 specific biological processes ($p < 0.05$; with an average of 169). The significantly influenced biological processes comprise of 3.2% to 10.6% (with an average of 5.0%) of total identified processes. A total number of 1735 specific biological processes was changed significantly ($p < 0.05$) in response to tested microorganisms (Table 7). However, low similarity in the profiles of expressed genes resulted in the absence of widely altered biological processes for the group of probiotic microorganisms, Gram-positive and Gram-negative bacteria, or those belonging to the *Lactobacillus* genus. The number of processes changed will rise as new annotations will be assigned to gene products. However, there is still a lot of human genes of unknown function, and many may have several functions still undiscovered.

In case of the commensal and pathogenic bacteria only two common specific biological processes, altered by the representatives within these two groups were identified. In the case of *B. animalis* MK2, *B. thetaiotaomicron* ATCC 29741 and *P. anaerobius* ATCC 27337 (commensal group) these were 'negative regulation of Ras protein signal transduction' (GO:0046580) and 'negative regulation of small GTPase mediated signal transduction' (GO:0051058). Whereas pathogenic bacteria (*S.* Typhimurium ATCC 14028, *E. coli* ATCC 10536 and

Table 7. Number of identified biological processes that are affected by microorganisms. The analysis was performed with ErmineJ software using full lists of genes with significance coefficients of their expression level changes

Tabela 7. Liczba zidentyfikowanych procesów biologicznych zmienionych przez mikroorganizmy. Analizie w programie ErmineJ zostały poddane pełne listy genów ze współczynnikami istotności statystycznej oznaczonych wartości zmian poziomu ekspresji genów

Group	Strain [designation]	Number of affected biological processes	
		$p < 0.05$	total identified
Probiotic	*Lactobacillus rhamnosus* GG (ATCC 53103) [LGG]	129	3 391
	Bifidobacterium animalis subsp. *lactis* BB12 [BB12]	110	3 417
	Lactobacillus acidophilus LA-5 [Lc5]	121	3 212
	mixture of: *Lactobacillus plantarum* PL02 *Lactobacillus rhamnosus* KL53A *Lactobacillus delbruecki* subsp. *bulgaricus* LBY-27 *Lactococcus lactis* PB411 *Lactobacillus acidophilus* LA-5 *Bifidobacterium animalis* subsp. *lactis* BB12 [mix]	166	3 310
	Lactobacillus casei Shirota [LcS]	182	3 322
	Lactobacillus casei DN114001 [LcD]	116	3 036
	Escherichia coli Nissle 1917 [EcN]	350	3 302
	all probiotic strains[1]	73	2 111
Commensal	*Bifidobacterium animalis* MK2 [Ba]	167	3 487
	Bacteroides thetaiotaomicron ATCC 29741[Bt]	217	3 397
	Peptostreptococcus anaerobius ATCC 27337 [Pa]	206	3 553
	all commensal strains[1]	82	2 111
Pathogenic	*Salmonella* Typhimurium ATCC 14028 [St]	165	3 386
	Escherichia coli ATCC 10536 [EcF]	158	3 359
	Escherichia coli O157:H7 (NCTC 12900) [EcOH]	113	3 319
	all pathogenic strains[1]	143	2 111
Number of different[2] processes for all strains		1 735	4 273
Number of different[2] processes for all probiotic strains		1 011	3 919

Table 7 cont.

Number of different[2] processes for all commensal strains	546	3 862
Number of different[2] processes for all pathogenic strains	409	3 700
Number of joint[3] processes for all strains	0	2 519
Number of joint[3] processes for all probiotic strains	0	2 583
Number of joint[3] processes for all commensal strains	2	3 106
Number of joint[3] processes for all pathogenic strains	2	3 021
Number of joint[3] processes for Gram-positive bacteria	0	2 575
Number of joint[3] processes for Gram-negative bacteria	0	2 879
Number of joint[3] processes for *Lactobacillus* sp.	0	2 658
Number of joint[3] processes for *E. coli*	3	2 996

1 – analysis of gene lists obtained by treating the strains from the group as biological replicates, 2 – full repertoire of altered biological processes, 3 – altered biological processes joint for the entire group of microorganisms analysed.
1 – wykorzystując listę genów uzyskaną przy traktowaniu analiz poszczególnych szczepów z danej grupy jako powtórzenia biologiczne, 2 – wszystkie zmienione procesy biologiczne, 3 – zmienione procesy biologiczne wspólne dla danej grupy analizowanych mikroorganizmów.

E. coli NCTC 12900) modulated 'homophilic cell adhesion' (GO:0007156) and 'toll-like receptor 4 signalling pathway' (GO:0034142).

The analysed *E. coli* strains modified biological processes of 'response to superoxide' (GO:0000303), 'response to oxygen radical' (GO:0000305), and 'homophilic cell adhesion' (GO:0007156).

Comparison of biological processes altered in differentiated Caco-2 cells in response to single microbial strains (and a mixture) showed that the strains revealed their influence on up to 28 of the same specific biological process (with the average of 10, at the statistical significance of $p < 0.05$, Table 8). To increase a chance of detecting subtle effects (McDonald, 2009) biological processes influenced at the statistical significance of $p < 0.1$ were also analysed. This approach showed that maximum number of the same biological processes affected by the strains increased to 80 (with the average of 31).

The probiotic strains in a group analysis did not revealed any common biological process changed. The single probiotic strain influenced on an average 8.8 of the same biological processes with another probiotic strain. However, the probiotic strains share on an average 11.5 of the same biological processes with the commensal strains. Comparison of the probiotic and pathogenic strains indicates that the strains influence on an average 8.7 of the same biological pro-

Table 8. Number of significantly altered biological processes joint to Caco-2 enterocytes under the influence of tested microorganisms. Right-upper half shows the number of joint biological processes altered at the level of statistical significance of $p < 0.05$, left-lower half shows the number of common biological processes altered at the level of statistical significance of $p < 0.1$. The comparison includes the analyses of probiotics, commensal and pathogenic groups. Strain designations as in the Table 7

Tabela 8. Liczba statystycznie istotnie zmienionych procesów biologicznych wspólnych dla enterocytów Caco-2 stymulowanych badanymi mikroorganizmami. Prawa górna połowa przedstawia liczbę wspólnych procesów biologicznych zmienionych dla $p < 0{,}05$. Lewa dolna połowa przedstawia liczbę wspólnych procesów biologicznych zmienionych dla $p < 0{,}1$. Porównanie zawiera analizy grupowe dla probiotyków, komensali i patogenów. Oznaczenia szczepów jak w tabeli 7

	$p < 0.05$	Probiotic								Commensal				Pathogenic			
	$p < 0.1$	LGG	BB12	Lc5	mix	LcS	LcD	EcN	prob	Ba	Bt	Pa	kom	St	EcF	EcOH	pat
Probiotic	LGG		5	4	15	12	4	19	3	7	11	15	1	6	7	4	5
	BB12	20		3	6	2	8	5	5	7	3	8	1	4	9	2	6
	Lc5	12	13		13	6	3	11	2	4	20	3	5	0	6	6	5
	mix	29	17	23		8	7	16	2	17	10	11	3	5	5	7	1
	LcS	40	12	16	28		15	16	3	11	17	19	9	18	9	4	9
	LcD	18	19	17	16	36		6	3	4	8	8	0	6	6	3	3
	EcN	40	28	27	55	66	32		18	17	15	26	15	28	25	22	30
	prob	6	12	10	11	15	14	35		4	3	3	10	2	7	4	19
Commensal	Ba	39	23	16	45	33	19	51	11		16	12	7	10	8	4	4
	Bt	37	30	39	38	57	31	70	13	45		18	14	9	15	8	10
	Pa	50	36	17	31	61	29	79	12	45	58		5	25	11	14	14
	kom	4	7	16	6	19	4	46	27	15	31	26		4	2	6	17
Pathogenic	St	28	17	9	25	60	20	80	13	32	47	72	24		18	6	14
	EcF	28	29	31	22	34	29	71	19	27	48	38	21	41		5	17
	EcOH	18	7	19	16	26	15	52	10	11	34	29	17	30	19		13
	pat	22	21	17	15	25	15	67	38	17	35	34	39	36	31	32	

cesses which is similar to comparisons within the probiotic group. *Escherichia coli* Nissle 1917 share the highest number of the same biological processes with other tested strains. *Bifidobacterium animalis* BB12 or *L. casei* DN114001 share the lowest number of the same biological processes with the other strains. With an exception of *L. casei* Shirota, which the latter strain shares close taxonomical relationship. Unlike the *L. casei* strains, the two strains of *B. animalis* share a below-average number of biological processes influenced. This may confirm why one belongs to the probiotic and the other to commensal group.

To better illustrate the similarities and differences in the impact of the examined microorganisms on the specific biological processes in enterocytes, the processes were grouped into 37 commonsense categories (Table 9). The categories (general biological processes) were selected based on current knowledge of processes that are possibly influenced by microbiota. Such an approach allows to distinguish specific attributes of the analysed microorganisms on enterocyte and whole organism biology, as the global transcriptome comparison did not reveal striking similarities. The largest influence on general biological processes in enterocytes was observed in case of the *E. coli* Nissle 1917. The strain altered above median number of specific biological processes in 34 categories. Whereas, the least potent was *L. acidophilus* LA-5, which altered above median a number of specific biological processes in only six categories (Table 9).

Number of biological processes changed in the category (general biological process) indicates an impact of a strain on a general process. To investigate whether a strain that influences a general process modulates it similarily to the other or in the opposite fashion, expression patterns of genes assigned to that process were compared. Although the enterocytes' response to bacteria is strain specific some species-specific traits can be clearly seen. A similar response to both *B. animalis* strains BB12 and MK2 can be observed in gene expression patterns regarding biological processes such as i.e. structure and function of gastrointestinal tract ($R^2 = 0.925$, Fig. 8.27), viral infection ($R^2 = 0.900$, Fig. 8.8), metabolism ($R^2 = 0.884$, Fig. 8.9), reactive oxygen species and redox potential ($R^2 = 0.863$, Fig. 8.17), detoxification ($R^2 = 0.857$, Fig. 8.5), aging ($R^2 = 0.852$, Fig. 8.22), healing and regeneration ($R^2 = 0.825$, Fig. 8.6), and homeostasis ($R^2 = 0.823$, Fig. 8.7). Even more species-specific similarity in biological processes--specific gene expression pattern can be seen in response to *L. casei* strains: Shirota and DN114001. These are i.e. structure and function of gastrointestinal tract ($R^2 = 0.972$, Fig. 8.27), identification of microorganisms ($R^2 = 0.963$, Fig. 8.18), metabolism ($R^2 = 0.950$, Fig. 8.9), detoxification ($R^2 = 0.933$, Fig. 8.5), cell cycle ($R^2 = 0.926$, Fig. 8.4), cell differentiation ($R^2 = 0.923$, Fig. 8.20), apoptosis ($R^2 = 0.921$, Fig. 8.2), and development and morphogenesis ($R^2 = 0.904$,

Table 9. Number of altered biological processes in Caco-2 cells under influence of the tested strains combined into arbitrary categories of biological processes. The substantial numbers of biological processes changed significantly (for $p < 0.05$) by specific strain were identified as those with greater than median for the category are indicated in bold numbers. Strains designations as in Table 7

Tabela 9. Liczba zmienionych procesów biologicznych zachodzących w komórkach Caco-2 pod wpływem stosowanych komórek bakterii, zebranych w subiektywne kategorie. Pogrubioną czcionką oznaczono liczby procesów biologicznych ($p < 0,05$), które zostały zmienione w ilości większej niż wartość mediany dla wszystkich analizowanych mikroorganizmów w danej kategorii. Oznaczenia szczepów jak w tabeli 7

Categories of biological processes (number of processes in category)	Number of modified biological processes $p < 0.05$ $p < 0.1$												
	probiotic							commensal			pathogenic		
	LGG	BB12	Lc5	mix	LcS	LcD	EcN	Ba	Bt	Pa	St	EcF	EcOH
1	2	3	4	5	6	7	8	9	10	11	12	13	14
Adhesion (47)	1 3	0 1	0 1	**5** 15	0 1	0 1	**6** 7	0 5	**2** 7	1 1	**3** 4	**2** 2	**4** 6
Apoptosis (48)	**5** 7	1 3	2 2	**8** 12	0 1	2 3	2 3	**5** 5	**4** 5	2 8	1 3	1 2	0 2
Blood pressure (35)	0 1	**4** 6	**7** 7	2 2	1 1	0 0	**3** 5	0 0	**5** 8	**3** 6	0 2	2 4	0 1
Cell cycle (153)	4 15	1 3	1 3	1 3	**8** 17	1 1	**14** 20	**8** 12	**10** 16	**7** 17	5 13	3 4	**7** 16
Detoxification (15)	1 1	1 1	0 1	0 1	**2** 3	0 0	**2** 3	**2** 4	**3** 3	**2** 2	1 1	**4** 4	0 1
Healing and regeneration (15)	0 1	0 0	**1** 1	0 0	**3** 5	0 0	**6** 9	0 0	0 1	0 0	**2** 2	0 0	**2** 2
Homeostasis (58)	0 2	**4** 4	1 3	0 0	0 0	**4** 7	**5** 6	1 1	**7** 10	**7** 9	1 3	1 3	0 2
Viral infection (90)	**4** 7	0 2	0 0	2 2	**10** 15	**5** 9	**24** 31	0 1	1 8	3 10	**8** 9	3 8	1 4

Table 9 cont.

1	2	3	4	5	6	7	8	9	10	11	12	13	14
Extracellular matrix (17)	0 2	0 0	0 3	0 0	0 0	**1** 3	**1** 3	**3** 3	**1** 3	0 0	**1** 3	**2** 4	0 0
Metabolism (535)	5 15	7 21	**35** 49	7 17	**13** 18	9 14	**36** 57	**14** 31	**42** 59	10 21	9 26	**20** 44	12 31
Cell migration (57)	**7** 15	0 0	0 1	0 7	**11** 17	**6** 7	**10** 13	4 6	3 9	**8** 12	4 5	**5** 8	1 2
Blood and lymphatic vessels (27)	1 4	0 0	2 2	1 2	**3** 5	0 1	**4** 6	**3** 5	2 6	**3** 7	2 2	1 2	**3** 3
DNA repair (42)	0 0	0 1	**2** 2	1 4	**2** 3	0 1	**4** 5	1 3	**2** 3	**6** 8	0 1	0 0	0 3
Necrosis (4)	0 0	**1** 1	0 0	0 0	0 0	0 1	**2** 2	0 1	0 1	0 0	0 0	**1** 1	0 1
Acquired immunity (455)	11 21	4 17	6 11	**36** 67	**43** 57	**21** 42	**47** 70	15 29	13 23	16 38	**26** 39	**26** 43	2 6
Innate immunity (32)	**5** 7	**3** 3	**2** 4	1 3	0 2	**2** 2	1 3	0 2	**2** 5	1 1	**4** 5	0 2	1 4
Inflammation (28)	**6** 7	1 1	1 2	**3** 4	0 2	0 1	**3** 5	**2** 2	0 0	**6** 9	1 1	0 1	0 0
Cytoskeleton organization (90)	0 0	0 4	0 3	**4** 7	1 3	**5** 8	0 5	1 4	**6** 9	0 1	1 2	**2** 6	1 4
Cell polarization (6)	0 0	0 0	0 0	0 0	0 0	0 0	0 0	**1** 1	**1** 1	0 0	0 0	0 0	0 0
Reactive oxygen species and redox potential (37)	3 3	2 2	**4** 4	1 1	2 2	3 3	**4** 5	0 0	**5** 9	0 0	0 1	**9** 12	**6** 7
Identification of microorganisms (29)	1 1	0 0	0 0	0 1	0 2	**4** 6	**3** 10	1 2	2 4	**5** 6	**10** 11	**5** 5	**5** 6
Morphogenesis and development (416)	16 48	9 20	8 13	9 17	**27** 45	8 13	**23** 43	**34** 65	15 31	16 35	**19** 34	**23** 38	9 20

1	2	3	4	5	6	7	8	9	10	11	12	13	14
Cell differentiation (201)	**10**	2	4	7	**11**	**10**	8	8	**12**	6	**10**	5	3
	13	5	7	11	17	17	16	17	22	10	21	7	6
Circadian rhythm (12)	**2**	**2**	0	0	**1**	0	**1**	0	0	**5**	0	0	0
	3	2	0	0	2	2	2	0	0	7	1	0	0
Secretion (59)	2	3	1	3	1	2	3	**6**	1	**8**	**4**	1	3
	2	4	1	3	4	11	6	7	3	9	7	5	6
Aging (20)	**1**	0	0	**1**	**1**	**1**	**2**	0	0	0	0	0	0
	1	1	1	1	1	2	2	0	0	1	0	0	0
Steroid metabolism (57)	0	**3**	0	1	1	0	**13**	2	**4**	2	1	**7**	2
	1	3	0	1	3	3	15	2	7	3	1	8	4
Stress (36)	1	1	0	2	2	2	**7**	1	**3**	**5**	**4**	**3**	2
	2	1	2	4	7	5	8	1	4	8	5	3	3
Chromatin structure (67)	0	0	**4**	**4**	**6**	1	**9**	**3**	0	1	1	0	0
	2	0	5	10	15	3	15	5	2	9	2	2	5
Structure and function of epithelium	1	1	0	0	**7**	1	**6**	**3**	**3**	0	1	1	0
(84)	5	5	0	3	12	2	11	7	8	2	6	5	1
Structure and function of the	1	1	0	**3**	**3**	0	**9**	0	0	**2**	**3**	1	**2**
gastrointestinal tract (44)	2	2	0	4	5	3	13	2	1	4	7	1	5
Symbiosis (14)	**3**	0	0	**4**	0	0	**2**	0	**4**	**1**	0	0	0
	3	0	0	4	1	0	2	0	4	3	0	0	0
Signalling (489)	19	18	13	19	**24**	15	**35**	15	**33**	**31**	**27**	12	**23**
	29	30	25	37	41	28	49	28	57	61	55	33	39
Transport (198)	1	**10**	5	3	1	5	**16**	4	**10**	**11**	3	5	3
	4	30	8	3	4	10	23	12	16	26	5	14	5
Nerve system (90)	3	3	3	**9**	3	**6**	**11**	**4**	1	**4**	3	**6**	2
	8	4	10	12	9	10	13	8	2	10	6	11	6
Lipid absorption and metabolism (36)	0	1	0	**3**	1	**2**	**12**	0	1	**2**	**2**	1	**2**
	0	1	1	4	1	2	14	0	1	3	3	1	2
Vitamin metabolism (23)	2	2	1	0	**3**	1	**5**	2	0	2	0	1	**3**
	2	4	1	0	3	4	5	2	3	3	0	3	5

Fig. 8.19). The process-specific gene expression patterns in response to *L. casei* DN114001 and *L. casei* Shirota (or both) often cluster with response to *L. rhamnosus* GG (the three strains belong to *Lactobacillus* group *Casei*, which are phylogenetically closely related (Sato et al., 2012)) and/or to the mixture of probiotic strains used ($R^2 > 0.872$, Figs 8.4, 8.5, 8.9, 8.17, 8.18, 8.20, 8.27). On the other hand a biological process-related gene expression patterns specific to response to the *E. coli* strains did not display species-specific similarities. In gene expression patterns of the analysed categories of biological processes (Fig. 8) the responses to *B. animalis* strains and *L. casei* strains displayed species-specific similarities showing median value of correlation coefficients of $R^2 = 0.771$ and $R^2 = 0.787$, respectively. The most similar pair of *E. coli* strains was the Nissle 1917 and ATCC 10536 (median value of $R^2 = 0.218$). Moreover, dendrograms of gene expression patterns related to general biological process categories, indicate that the *E. coli* strains induced the extremely different gene expression patterns as compared to the rest of all the strains tested ($R^2 = 0$). This applies to selected biological process categories in respect to: the Nissle 1917 strain – apoptosis (Fig. 8.2), viral infection (Fig. 8.8), cytoskeleton organisation (Fig. 8.16), aging (Fig. 8.22), the ATCC 10536 strain – chromatin structure (Fig. 8.25), nerve system (Fig. 8.30), and the NCTC 12900 strain – healing and regeneration (Fig. 8.6), homeostasis (Fig. 8.7), cell migration (Fig. 8.10), blood and lymphatic vessels (Fig. 8.11), innate immunity (Fig. 8.14), steroids (Fig. 8.23), transport (Fig. 8.29). The second most frequent outlier was *L. acidophilus* LA-5 generating the extremely different response in case of following biological process categories: cell cycle (Fig. 8.4), metabolism (Fig. 8.9), identification of microorganisms (Fig. 8.18), development and morphogenesis (Fig. 8.19), cell differentiation (Fig. 8.20), structure and function of gastrointestinal tract (Fig. 8.27), signalling (Fig. 8.28). In case of the *L. acidophilus* LA-5 strain the difference was even more noteworthy since all the other strains tested induced quite similar gene expression pattern in categories of: cell cycle ($R^2 > 0.606$, Fig. 8.4), metabolism ($R^2 > 0.579$, Fig. 8.9), identification of microorganisms ($R^2 > 0.696$, Fig. 8.18), development and morphogenesis ($R^2 > 0.541$, Fig. 8.19), cell differentiation ($R^2 > 0.656$, Fig. 8.20), structure and function of gastrointestinal tract ($R^2 > 0.646$, Fig. 8.27). The most divergent gene expression patterns (indicated by long branches and high located nodes) were observed in processes like: adhesion ($R^2 < 0.779$, Fig. 8.1), DNA repair ($R^2 < 0.770$, Fig. 8.12), cytoskeleton organization ($R^2 < 0.702$, Fig. 8.16), structure and function of epithelium ($R^2 < 0.777$, Fig. 8.26), transport ($R^2 < 0.732$, Fig. 8.29), and nerve system ($R^2 < 0.740$, Fig. 8.30). Large similarities in responsomes to majority (70%) of the tested strains (low situated nodes and short branches) can be noticed in pro-

cesses such as: apoptosis ($R^2 > 0.808$, Fig. 8.2), healing and regeneration ($R^2 > 0.754$, Fig. 8.6), metabolism ($R^2 > 0.772$, Fig. 8.9), innate immunity ($R^2 > 0.781$, Fig. 8.14), inflammation ($R^2 > 0.772$, Fig. 8.15), development and morphogenesis ($R^2 > 0.712$, Fig. 8.19), and structure and function of gastrointestinal tract ($R^2 > 0.854$, Fig. 8.27).

4.3. VERIFICATION OF MICROARRAY DATA

4.3.1. Rotavirus infection – a model for enterocyte response to virus infection

The microarray analysis gave a broad view to biological processes that are influenced by bacteria. One of the category identified was response to virus infection. To verify the accuracy of the microarray analysis the response to virus infection biological process was chosen for further study. Two bacterial strains were used in the experiment: *B. animalis* BB12 and *E. coli* Nissle 1917. The microarray data mining showed no influence of *Bifidobacterium* ssp. ($p > 0.05$) and the effect of the *E. coli* Nissle 1917 ($p < 0.05$) on biological processes in category of virus infection (Table 9). Since virus-induced gastroenteritis is a common problem among children worldwide and rotavirus infection is the most common cause of the gastrointestinal disorders a modulation of expression of genes involved in response to viral infection at cellular level was selected for validation of microarray data. According to Greenberg and Estes (2009) the rotaviruses infect nondividing differentiated enterocytes near the tips of the villus because mature enterocytes express factors required for efficient infection and/or replication. The diarrhea occurs due to virus-mediated destruction of absorptive enterocytes and changes in tight junctions that lead to paracellular leakage. However, the rotavirus infection triggers little inflammation in infected intestines that distinguishes viral-induced diarrhea from bacterial-induced diarrhea. After the incubation period lasting 18-36 h shedding of massive quantities of virus occurs (Glass et al., 2006; Greenberg and Estes, 2009).

4.3.2. *Escherichia coli* Nissle 1917 but not *Bifidobacterium animalis* BB12 interferes with rotavirus replication

The primary goal of virus genetic information is replication to disseminate infection. Microarray data mining gives insight into biological processes mainly on cellular level. Therefore the outcome of *E. coli* Nissle 1917 modulation of

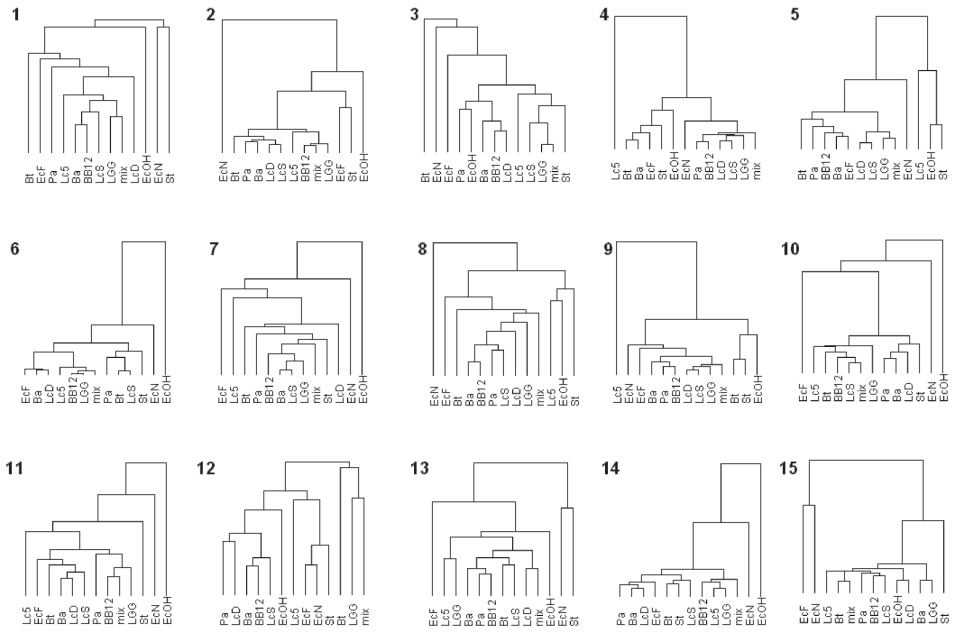

Fig. 8. Dendrograms of similarities in gene expression of genes grouped in categories of biological processes were generated with unsupervised hierarchical cluster analysis based on the determination of the distance between clusters using average linkage with the Euclidean distance as a measure of similarity between the expression datapoints. Expression of genes (n > 126) belonging to the following categories of biological processes were analysed: adhesion (1), apoptosis (2), blood pressure (3), cell cycle (4), detoxification (5), healing and regeneration (6), homeostasis (7), viral infection (8), metabolism (9), cell migration (10), blood and lymphatic vessels (11), DNA repair (12), acquired immunity (13), innate immunity (14), inflammation (15), cytoskeleton organisation (16), reactive oxygen species and redox potential (17), identification of microorganisms (18), development and morphogenesis (19), cell differentiation (20), secretion (21), aging (22), steroids (23), stress (24), chromatin structure (25), structure and function of epithelium (26), structure and function of gastrointestinal tract (27), signalling (28), transport (29), and nerve system (30). Strains designations as in Table 7

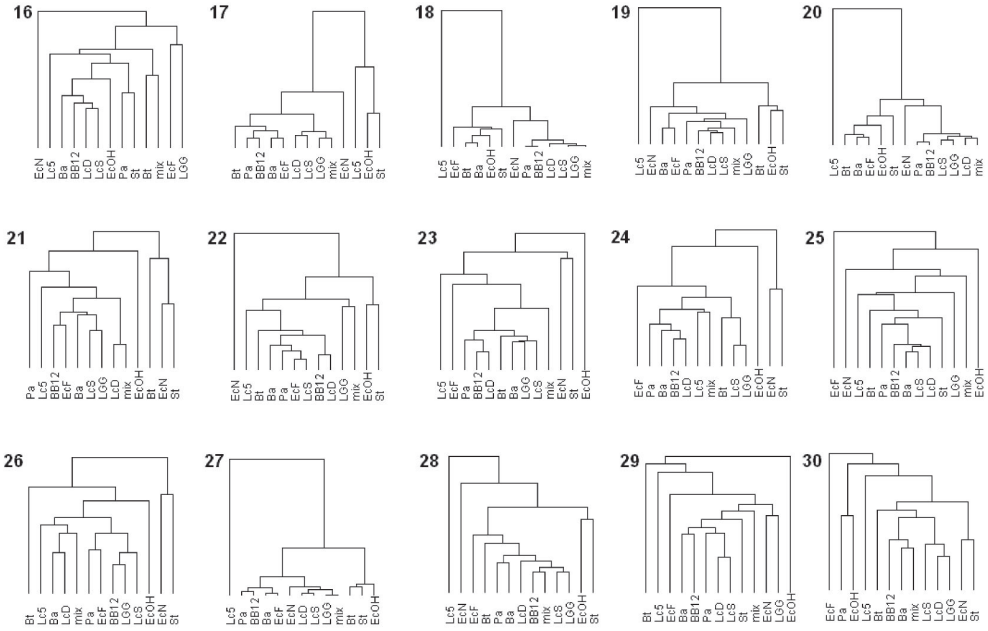

Ryc. 8. Dendrogramy podobieństwa ekspresji genów zgrupowanych w kategoriach procesów biologicznych utworzono z zastosowaniem nienadzorowanej hierarchicznej analizy skupień, wykorzystując odległość euklidesową przy określaniu globalnego podobieństwa pomiędzy poziomem ekspresji analizowanych genów należących do danej grupy. Analizie poddano poziomy ekspresji genów (n > 126) przypisanych do następujących kategorii: adhezja (1), apoptoza (2), ciśnienie krwi (3), cykl komórkowy (4), detoksyfikacja (5), gojenie i regeneracja (6), homeostaza (7), infekcja wirusowa (8), metabolizm (9), migracja komórek (10), naczynia krwionośne i limfatyczne (11), naprawa DNA (12), odporność nabyta (13), odporność wrodzona (14), stan zapalny (15), organizacja cytoszkieletu (16), wolne rodniki tlenowe i potencjał redoks (17), rozpoznawanie mikroorganizmów (18), rozwój i morfogeneza (19), różnicowanie komórek (20), wydzielanie (21), starzenie (22), steroidy (23), stres (24), struktura chromatyny (25), struktura i funkcje nabłonka (26), struktura i funkcje układu pokarmowego (27), sygnalizacja (28), transport (29) i układ nerwowy (30). Oznaczenia szczepów jak w tabeli 7

genes involved in response to virus infection should influence virus genome replication, transcription or other cellular processes implicated in antiviral response (e.g. apoptosis). To address the problem an *in vitro* model with differentiated Caco-2 cells infected with Human Rotavirus A G1P[8] strain RIX4414 was used. The enterocytes were either preincubated with the bacteria for 4 h and then infected with rotavirus followed by further 4 h incubation (preinfection bacterial treatment) or infected with rotavirus and after 4 h exposed to the bacteria for another 4 h (postinfection bacterial treatment). Next the total RNA was isolated from Caco-2 cells, which was primed with a mixture of poly(dT) and random hexamer primers for reverse transcription. Obtained complementary DNA was used to quantitate rotavirus genomic segments and transcripts with qPCR. The analysis was performed with ΔΔCt method using 18S rRNA as a reference, which maintained high consistency across all samples (Fig. 9).

In both pre- and postinfection *B. animalis* BB12 treatment (see Figure 10 and Figure 11, respectively) the quantity of rotavirus genomic segments and transcripts were not changed significantly. Whereas treatment with *E. coli* Nissle 1917 lead to significant decrease in rotavirus RNA. The preinfection treatment of differentiated Caco-2 cells with the Nissle 1917 strain lead to significant decrease in NSP3, NSP56, and VP4 RNAs (Fig. 10). Whereas postinfection treatment with the same strain caused reduction in all rotavirus RNAs level. The NSP1, VP1, VP2, VP6, and VP7 were the most significantly declined (Fig. 11). This indicates that the probiotic strain of *E. coli* does modify enterocytes' biology to counteract rotavirus infection. The result validates also the microarray data mining noticing that *E. coli* Nissle 1917 modifies cellular response to virus.

4.3.3. Bacteria treatment of rotavirus infected cells did not change viability and cytotoxicity of enterocytes

The quantitative PCR analysis of rotavirus segments (Figure 10 and Figure 11) in differentiated Caco-2 cells showed that both preinfection and postinfection treatment with probiotic *E. coli* Nissle 1917 reduced virus replication and/or transcription as compared to the control cells. This might be seen as a reduction of virus replication rate. To better recognise the biological background of the bacterial treatment, enterocytes' condition was analysed using a measure of viability, cytotoxicity, and apoptosis (caspase-3 and -7 activation). Enterocytes' parameters 4 or 8 h after infection with rotavirus either with or without *B. animalis* BB12 or *E. coli* Nissle 1917 treatment (both pre- and post-infection) did not displayed significant differences (data not shown). However the same parameters

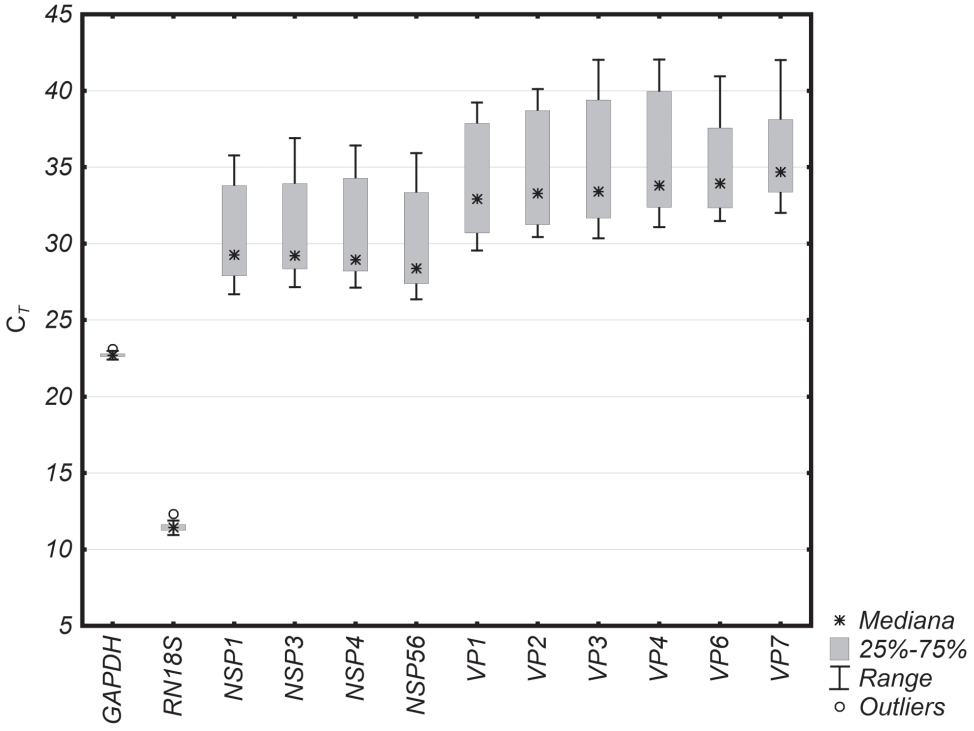

Fig. 9. Box plot displaying the overall range of Ct distribution for each target in qPCR analysis. Cellular transcripts encoding glyceraldehyde-3-phosphate dehydrogenase (*GAPDH*) and 18S rRNA (*RN18S*), and Rotavirus segments (NSP1, NSP3, NSP4, NSP56, VP1, VP2, VP3 VP4, VP6, and VP7) were analysed. The plot shows high consistency between analyses of biological replicates as indicated by very narrow box for cellular transcripts Ct (GAPDH, RN18S) and high variation in rotavirus targets quantity among the experimental conditions. The box contains the middle 50% of the data (Ct values). The asterisk within box denote the median Ct value. The whiskers indicate the minimum and maximum Ct values fitting within 1.5 × IQR (the interquartile range), otherwise would be indicated as outliers by open circles

Ryc. 9. Wykres pudełkowy przedstawiający zakres rozkładu Ct dla transkryptów analizowanych techniką qPCR. Ilościowemu oznaczeniu poddano komórkowe transkrypty kodujące dehydrogenazę gliceraldehydo-3-fosforanową (*GAPDH*) i 18S rRNA (*RN18S*) oraz segmenty rotawirusa (NSP1, NSP3, NSP4, NSP56, VP1, VP2, VP3 VP4, VP6, VP7). Wykres pokazuje dużą spójność analizowanych powtórzeń biologicznych, o czym świadczy bardzo mały rozrzut wartości Ct dla komórkowych RNA (GAPDH, RN18S) i wysoką zmienność w ilości RNA rotawirusa pomiędzy porównywanymi warunkami eksperymentalnymi. Prostokąt zawiera środkowe 50% danych (wartości Ct). Gwiazdka w obrębie prostokąta oznacza wartość mediany Ct. Wąsy wskazują minimalne i maksymalne wartości Ct mieszczące się w 1,5 × IQR (zakresu międzykwartylowego), wartości odstające zostały oznaczone przez otwarte kółka

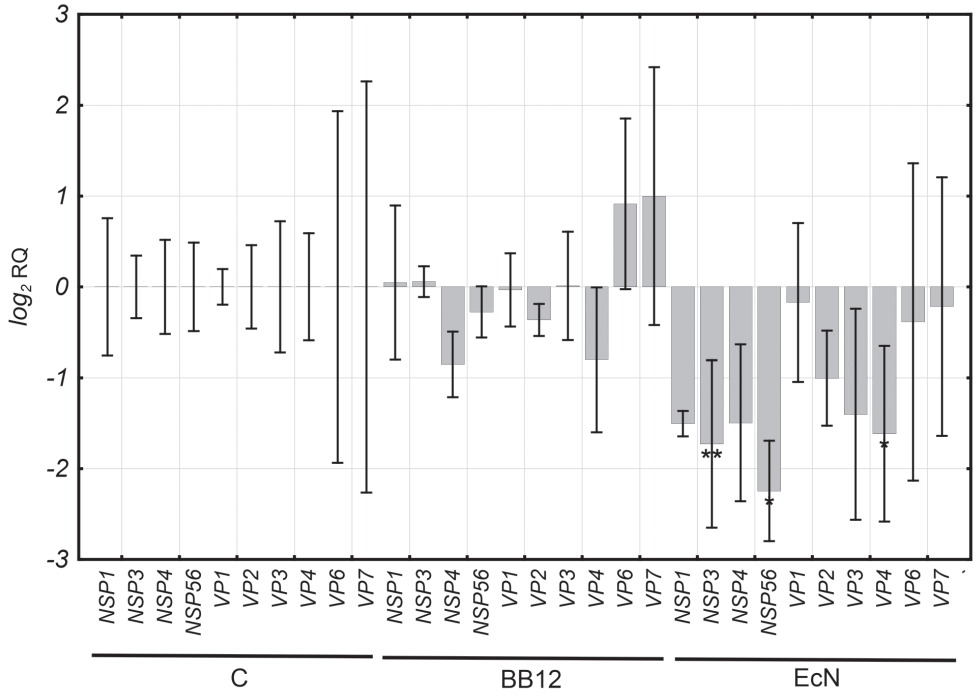

Fig. 10. Changes of rotavirus genomic segments and transcripts level in Caco-2 cells treated with bacteria: *B. animalis* BB12 (BB12), *E. coli* Nissle 1917 (EcN) for 4 h and untreated (control cells, C). Subsequently infected with rotavirus and further incubated for another 4 h (preinfection bacterial treatment). The decrease of rotavirus genomic segments and transcripts level is observed in case of *E. coli* Nissle 1917 treatment for NSP3 ($p < 0.05$; designated with double-asterisk **), NSP56 and VP4 ($p < 0.1$; designated with asterisk *). The data was obtained from biological replicates performed in triplicate

Ryc. 10. Zmiany ilości segmentów genomowych i transkryptów rotawirusa w komórkach Caco-2 stymulowanych bakteriami: *B. animalis* BB12 (BB12), *E. coli* Nissle 1917 (EcN) przez 4 h i komórek kontrolnych (C) niepoddanych działaniu bakterii. Po stymulacji bakteriami komórki enterocytów były poddane infekcji rotawirusem i inkubowane przez kolejne 4 h (stymulacja bakteriami poprzedzająca infekcję). Spadek poziomu segmentów genomowych i transkryptów rotawirusa został zaobserwowany w przypadku działania *E. coli* Nissle 1917 dla NSP3 ($p < 0,05$; oznaczone podwójną gwiazdką **), NSP56 i VP4 ($p < 0,1$; oznaczone pojedynczą gwiazdką *). Dane uzyskano, prowadząc analizę trzech biologicznych powtórzeń

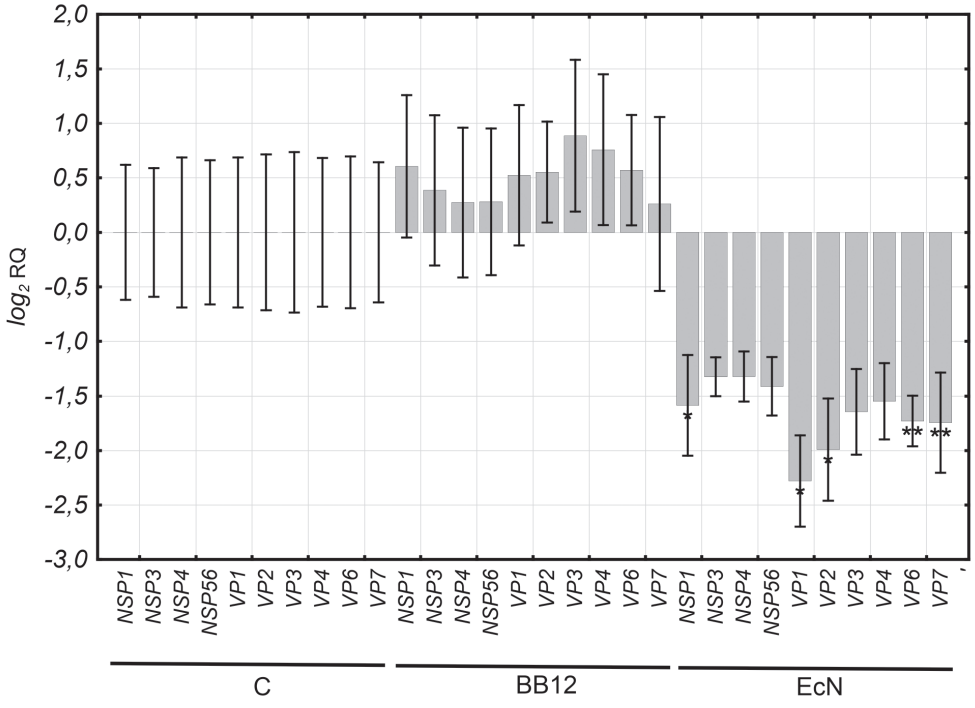

Fig. 11. Changes of rotavirus genomic segments and transcripts level in Caco-2 cells infected with rotavirus and incubated for 4 h then treated with bacteria (postinfection bacterial treatment): *B. animalis* BB12 (BB12), *E. coli* Nissle 1917 (EcN) for another 4 h and not treated (control cells, C). The clear overall decrease of rotavirus genomic segments and transcripts level is observed in case of *E. coli* Nissle 1917 treatment. The statistical analysis indicated that level of VP6 and VP7 was decreased at $p < 0.05$ confidence level (designated with double-asterisk **) and NSP1, VP1 and VP2 at $p < 0.1$ confidence level (designated with asterisk *). The data was obtained from biological replicates performed in triplicate

Ryc. 11. Zmiany ilości segmentów genomowych i transkryptów rotawirusa w komórkach Caco-2 infekowanych rotawirusem, po czym inkubowanych przez 4 h, a następnie poddanych stymulacji bakteriami (stymulacja bakteriami po infekcji): *B. animalis* BB12 (BB12), *E. coli* Nissle 1917 (EcN) przez 4 h i komórek kontrolnych (C) nie poddanych działaniu bakterii. Wyraźny spadek liczby segmentów i transkryptów rotawirusa zaobserwowano po działaniu *E. coli* Nissle 1917. Analiza statystyczna wykazała istotny ($p < 0,05$) spadek poziomu VP6 i VP7 (oznaczone podwójną gwiazdką **) oraz NSP1, VP1, VP2 ($p < 0,1$; oznaczone pojedynczą gwiazdką *). Dane uzyskano, prowadząc analizę trzech biologicznych powtórzeń

analysis 14 or 18 h after infection with rotavirus showed significant ($p < 0.05$) viability differences only between non-infected and rotavirus pre- and post-infected cells, which showed 62% and 38% reduction in viability, respectively. There was also a significant difference in viability (63%) regarding 4 hours-shift of infection time (between pre-infected and post-infected regime). No significant changes in viability was observed considering bacteria action (Fig. 12).

Significant 4-fold increase in cytotoxicity ($p < 0.05$; Fig. 13) was observed only between infected and non-infected cells regardless of treatment with bacteria or 4 hours-shift of infection time (between pre-infection and post-infection regime). The bacteria treatment neither influenced rotavirus-mediated cytotoxicity nor caused cytotoxicity itself to the differentiated Caco-2 cells after 14 or 18 h post treatment.

4.3.4. Preinfection bacteria treatment enhances caspase-3/7 activation in rotavirus infected enterocytes

A typical cellular response to virus infection is an apoptosis induction. A common hallmark of the process is activation of caspase pathway. The caspase-3 and -7 are 'downstream caspases', activated by other initiator caspases activated by different stimuli, thus an universal marker of apoptosis (Kurokawa and Kornbluth, 2009). The rotavirus infection raised significantly caspase-3/-7 activity by up to 81% ($p < 0.05$) in comparison to non-infected cells 18 h pi. Moreover, rotavirus-infected differentiated Caco-2 cells pretreated with *B. animalis* BB12 or *E. coli* Nissle 1917 showed increased caspase-3/-7 activity by 24% and 16% (respectively, $p < 0.05$) in comparison to rotavirus-infected differentiated Caco-2 cells not treated with the bacteria. However, neither significant differences were observed regarding type of bacterial strain used for pretreatment of Caco-2 cells prior to infection, nor in case of post-infection treatment (Fig. 14). This indicates that contact with bacteria enhances infected enterocytes' susceptibility to apoptosis. The non-infected differentiated Caco-2 cells treated with the bacterial strains did not show difference in caspase-3/-7 activity to control cells indicating that contact with the bacteria did not trigger apoptosis itself. Together with the finding that *E. coli* Nissle 1917 reduces replication rate of rotavirus prompt infected cell apoptosis may enhance the bacterial strain capability to shorten rotavirus infection outcome.

4.3.5. Rotavirus infected undifferentiated Caco-2 cells preinfection treated

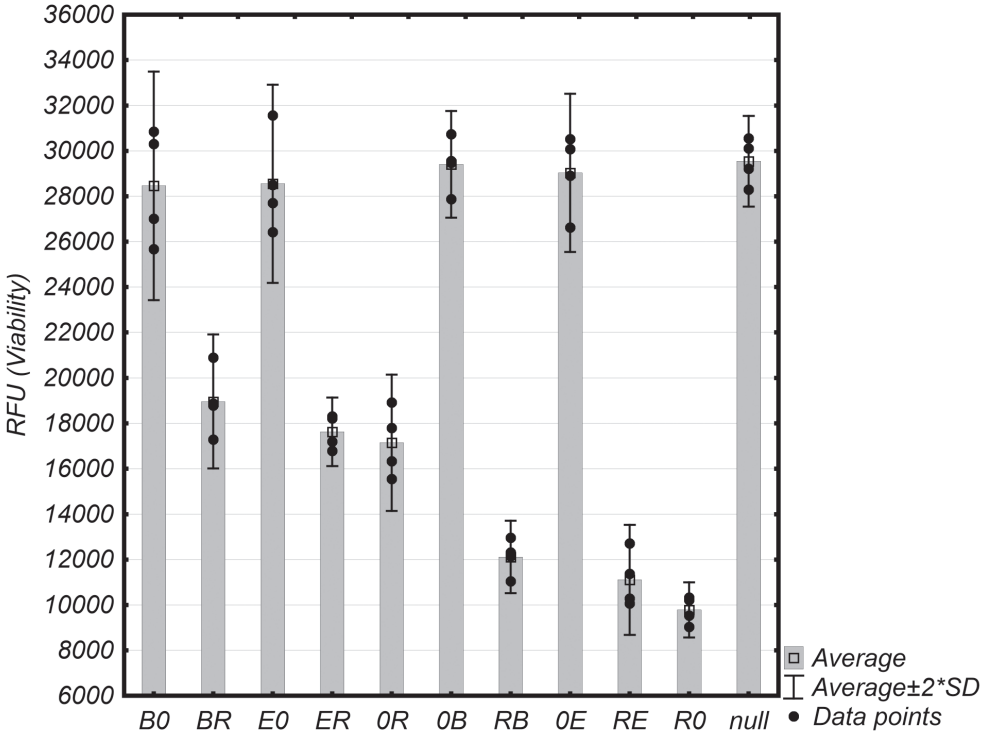

Fig. 12. Viability of differentiated Caco-2 cells after 14 h (BR, ER, 0R) or 18 h (RB, RE, R0) of infection with rotavirus. The enterocytes were either pre-treated with *B. animalis* BB12 (B0, BR) or *E. coli* Nissle 1917 (E0, ER), or post-treated with *B. animalis* BB12 (0B, RB) or *E. coli* Nissle 1917 (0E, RE). The control cells neither rotavirus--infected nor treated with bacteria were designated 'null'. The viability was measured in live-cell protease assay and displayed in relative fluorescence units (RFU)

Ryc. 12. Żywotność zróżnicowanych komórek Caco-2 po 14 h (BR, ER, 0R) lub 18 h (RB, RE, R0) od infekcji rotawirusem. Komórki enterocytów zostały poddane działaniu bakterii *B. animalis* BB12 (B0, BR) lub *E. coli* Nissle 1917 (E0, ER) przed infekcją albo po infekcji *B. animalis* BB12 (0B, RB) lub *E. coli* Nissle 1917 (0E, RE). Komórki kontrolne niepoddane infekcji ani działaniu bakterii oznaczono 'null'. Żywotność komórek mierzono z zastosowaniem analizy proteazy żywych komórek i przedstawiono jako wartości intensywności fluorescencji (RFU)

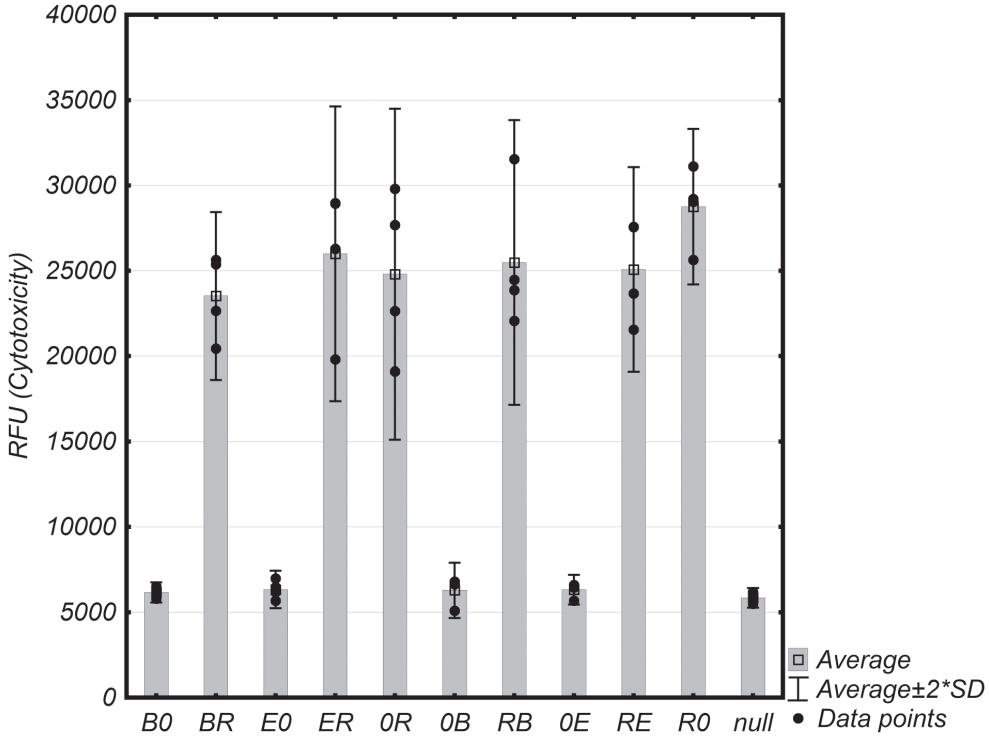

Fig. 13. Cytotoxicity of differentiated Caco-2 cells after 14 h (BR, ER, 0R) or 18 h (RB, RE, R0) of infection with rotavirus. The cells were either pre-treated with *B. animalis* BB12 (B0, BR) or *E. coli* Nissle 1917 (E0, ER), or post-treated with *B. animalis* BB12 (0B, RB) or *E. coli* Nissle 1917 (0E, RE). The control cells neither rotavirus-infected nor treated with bacteria were designated 'null'. The cytotoxicity was measured in dead--cell protease assay and displayed in relative fluorescence units (RFU)

Ryc. 13. Cytotoksyczność zróżnicowanych komórek Caco-2 po 14 h (BR, ER, 0R) lub 18 h (RB, RE, R0) od infekcji rotawirusem. Komórki enterocytów zostały poddane działaniu bakterii *B. animalis* BB12 (B0, BR) lub *E. coli* Nissle 1917 (E0, ER) przed infekcją albo po infekcji *B. animalis* BB12 (0B, RB) lub *E. coli* Nissle 1917 (0E, RE). Komórki kontrolne nie poddane infekcji ani działaniu bakterii oznaczono 'null'. Cytotoksyczność komórek mierzono z zastosowaniem analizy proteazy martwych komórek i przedstawiono jako wartości intensywności fluorescencji (RFU)

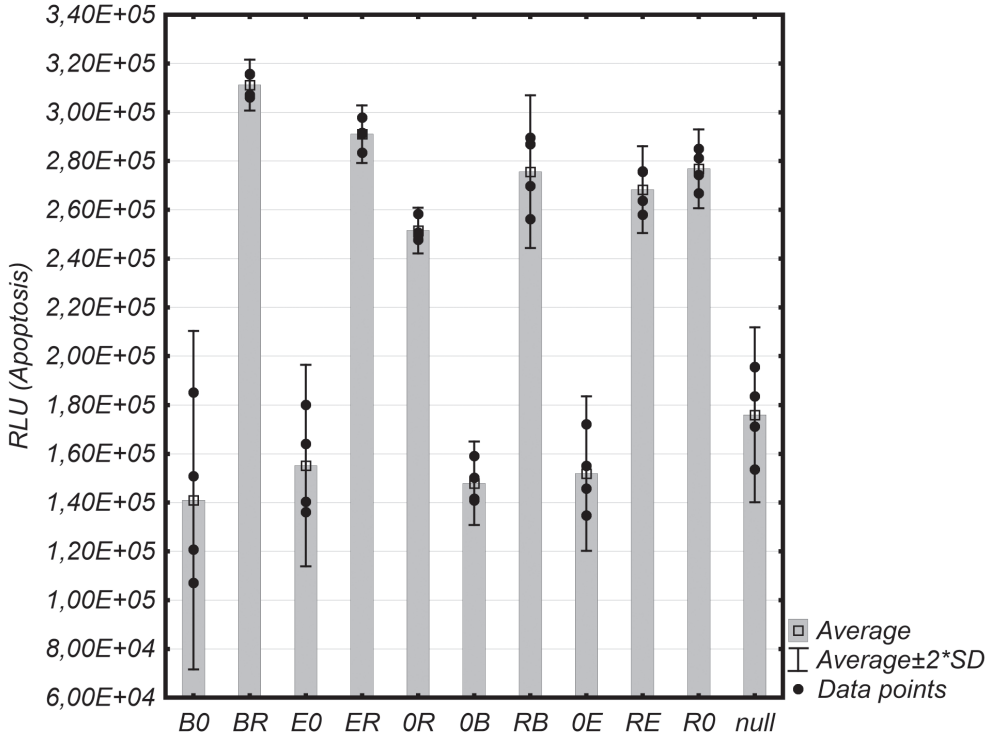

Fig. 14. Caspase-3 and -7 activity (a measure of apoptosis) in differentiated Caco-2 cells after 14 h (BR, ER, 0R) or 18 h (RB, RE, R0) of infection with rotavirus. The cells were either pre-treated with *B. animalis* BB12 (B0, BR) or *E. coli* Nissle 1917 (E0, ER), or post-treated with *B. animalis* BB12 (0B, RB) or *E. coli* Nissle 1917 (0E, RE). The control cells neither rotavirus-infected nor treated with bacteria were designated 'null'. The caspase-3/7 activity was measured in luminescence assay and displayed in relative luminescence units (RLU)

Ryc. 14. Aktywność kaspazy-3 i -7 w komórkach Caco-2 po 14 h (BR, ER, 0R) lub 18 h (RB, RE, R0) od infekcji rotawirusem. Komórki enterocytów zostały poddane działaniu bakterii *B. animalis* BB12 (B0, BR) lub *E. coli* Nissle 1917 (E0, ER) przed infekcją albo po infekcji *B. animalis* BB12 (0B, RB) lub *E. coli* Nissle 1917 (0E, RE). Komórki kontrolne niepoddane infekcji ani działaniu bakterii oznaczono 'null'. Aktywność kaspazy-3 i -7 mierzono z zastosowaniem analizy luminescencyjnej i przedstawiono jako wartości intensywności luminescencji (RLU)

with *E. coli* Nissle 1917 do not undergo cell death

To further investigate possible differences between *B. animalis* BB12 and *E. coli* Nissle 1917 pre- and post-infection enterocyte treatments on rotavirus infection dynamics, a real-time label-free monitoring of cells fate was performed. In this experiment, due to technical limitations, a confluent but non-differentiated Caco-2 cells were used. Normalized cell index (CI) of Caco-2 cells showed that the attachment and establishment of fully confluent cell monolayer was achieved after 58 h of cell culture (Fig. 15, plot A). The cells were maintained for another 31 h to ensure culture stability.

After 90 h of culture the Caco-2 monolayer was either infected with rotavirus RIX4414, or treated with *B. animalis* BB12 or *E. coli* Nissle 1917 and further cultivated. After another 4 h the cells were postinfection treated with either of the two bacterial strains, or post-bacterial treatment infected with the rotavirus to reproduce infection/treatment timings from previous experiments. Based on the dynamic monitoring for 48 h pi of the Caco-2 cells infected with the rotavirus RIX4414 showed no change in CI. Similarly, no change in CI was observed in control cells (neither treated with a bacteria nor infected with virus) and cells treated with the bacterial strains only, and cells treated with the Nissle 1917 strain followed by infection with the rotavirus (Fig. 15, plot B). The cells postinfection treated with either *B. animalis* BB12 or *E. coli* Nissle 1917, and preinfection treated with *B. animalis* BB12 exhibited different onset times and appearance of cytopathic kinetic patterns (Fig. 15, plot B: RB, RE, and BR, respectively). The postinfection treatement with *E. coli* Nissle 1917 lead to rapid rise of CI with maximum at 12 h pi followed by steady decline of CI till complete culture death at 38 h pi (Fig. 15, plot B: RE). The preinfection treatment with *E. coli* Nissle 1917 caused a minute rise of CI. However there was no difference in CI curve shape as compared to non-infected cells or infected but not treated with any bacteria (Fig. 15, plot B: ER vs C or R). In both cases of the *E. coli* Nissle 1917 treatment of infected Caco-2 cells they showed caspase-3/-7 activation (Fig. 14). However only in the case of postinfection treatment the activation of the caspases triggered cell death. In case of the preinfection treatment cell culture did not display any cytopathic characteristic for 48 h pi as analysed with xCelligence system. The *B. animalis* BB12 treatment of infected Caco-2 cells caused increase of CI followed by its decline (Fig. 15, plot B: BR and RB). The increase of CI in case of the *B. animalis* BB12 treatments were much slower as compared to the *E. coli* Nissle 1917 posttreatment, reaching maximum at 26 h pi (the pretreatment) and 30 h pi (the posttreatment). The decline of CI of the preinfection *B. animalis* BB12 treated Caco-2 cells was rapid, step-like curve.

The *B. animalis* BB12 treated Caco-2 cells, both pre- and postinfection, showed caspase-3/-7 activation however cytopathic effects occurred in much later onset than the *E. coli* Nissle 1917 postinfection treatment.

4.3.6. *Escherichia coli* Nissle 1917 modifies expression of virus infection--related genes

To further investigate the biological processes involved in reduction of rotavirus RNA level by the *E. coli* Nissle 1917 strain expression level of cellular genes involved in response to virus was verified using qPCR which gives more precise results than microarrays. The complementary DNA obtained from differentiated Caco-2 cells treated with *B. animalis* BB12 and *E. coli* Nissle 1917 prior to and after infection with the RIX4414 rotavirus were used for cellular gene expression level analysis. The qPCR assay using ΔΔCt method with 18S rRNA as a reference gene was performed. The transcript levels in pre- and post-infection bacteria treated cells were compared to infected but non-treated with bacteria enterocytes. The results of the assay on 93 virus response related genes (Table 10) showed significant changes in transcript level of 39 genes ($p < 0.05$). Raising the statistical significance level to $p = 0.1$ yields ten more differentially expressed genes. The preinfection bacterial treatment modified cellular gene expression in an opposite direction under influence of the two bacterial strains only in case of 13 genes for $p < 0.05$. These are: *AIM2*, *APOBEC3G*, *CCL3*, *CCL5*, *CD40*, *IFI44L*, *IFNA2*, *IFNB1*, *IL12B*, *NLRP3*, *NOD2*, *PSTPIP1*, *TLR9*. Considering statistical significance at $p < 0.1$ the list includes also: *AZI2*, *CARD8*, *CASP1*,*CASP8*. An additional 13 gene products ($p < 0.05$; *CXCL11*, *FADD*, *HSP90AA1*, *IFIH1*, *IL8*, *IRAK1*, *MAP3K1*, *PIN1*, *PYDC1*, *RIPK1*, *TBP*, *TNF*, *TRIM25*) might contribute to protective *E. coli* Nissle 1917 action as their expression was significantly changed by the Nissle 1917 strain but not by the BB12 strain. Genes *HPRT1* and *IRF9* join that list for $p < 0.1$. These genes are involved in several biological processes related to virus infection that are more precisely categorised in Table 11. Some of the genes communicate the enterocyte with surrounding cells (e.g. immune cells) informing on the ongoing virus infection. Thus the analysed response reaches further than cellular level only.

Table 10. Gene expression changes (relative quantity; RQ) in Caco-2 cells after treatment

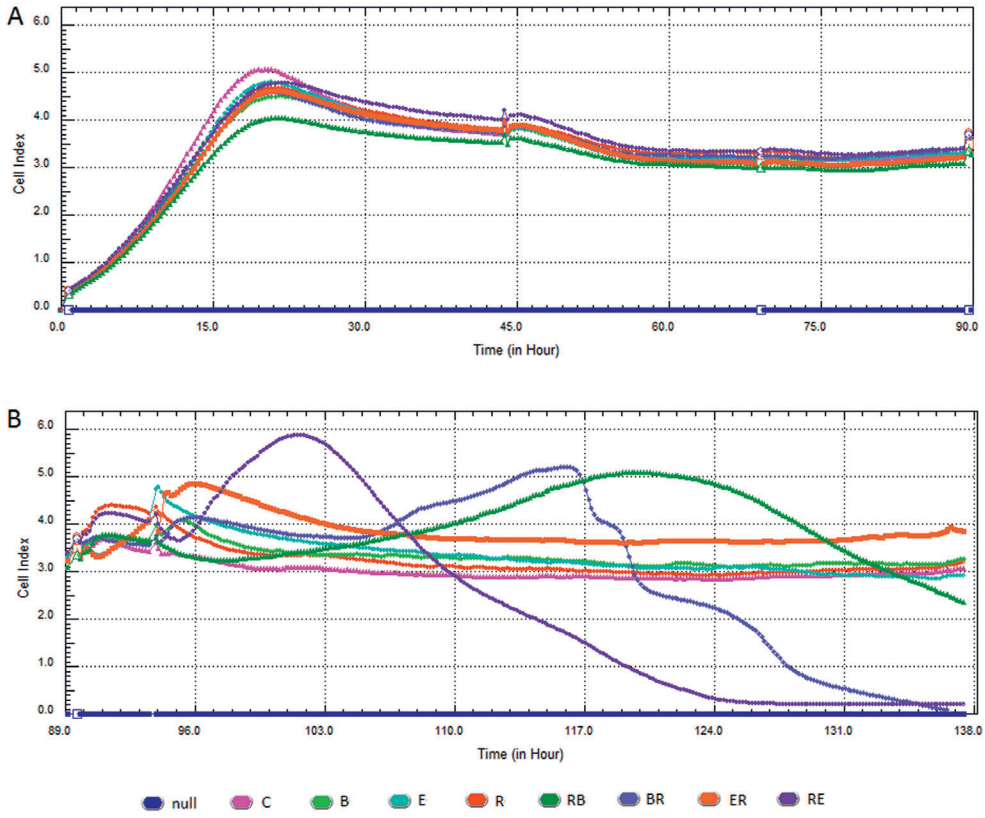

Fig. 15. Dynamic monitoring of Caco-2 cells attachment to growth surface and establishment of fully confluent monolayer (plot A, time 0 to 89 h), and cells fate during rotavirus infection and bacterial treatment (plot B, time 89 to 137.5 h). Resistance of the growth medium was used as a baseline (null, blue) for cell index calculation. Control Caco-2 cells (C, magenta) neither infected nor treated with bacteria displayed stable CI value. Both *B. animalis* BB12 (B, green), *E. coli* Nissle 1917 (E, cyan) treated, and rotavirus RIX4414 infected (R, red) Caco-2 cells did not differed in CI value from control cells for the duration time of the experiment. *Escherichia coli* Nissle 1917 pretreated and than infected with the rotavirus Caco-2 cells (ER, coral) displayed stable but slightly elevated CI. Whereas *B. animalis* BB12 pre- and postinfection treated (BR, slate blue and RB, dark green, respectively), and postinfection *E. coli* Nissle 1917 treated (RE, blue violet) Caco-2 cells showed increase of CI followed by its decline. Results are presented as average values from a quadruplicate measurements

Ryc. 15. Wykres przedstawiający przyżyciowy monitoring przyczepu komórek Caco-2 do powierzchni naczynia hodowlanego i utworzenia monowarstwy o pełnej konfluencji (wykres A, czas od 0 do 89 h) oraz zmian w tych procesach podczas przebiegu infekcji rotawirusowej i stymulacji bakteriami (wykres B, czas od 89 do 137,5 h). Oporność pożywki hodowlanej została użyta jako wartość bazowa (oznaczone 'null', kolor niebie-

with *B. animalis* BB12 (BB12) or *E. coli* Nissle 1917 (EcN) either preinfected or postinfected with Human Rotavirus A G1P[8] strain RIX4414 as normalised to 18S rRNA level. Values in bold numbers represent significantly altered ($p < 0.05$) gene expression fold-change

Tabela 10. Względne zmiany ekspresji genów (RQ) w komórkach Caco-2 stymulowanych *B. animalis* BB12 (BB12) lub *E. coli* Nissle 1917 (EcN). Enterocyty zostały zainfekowane ludzkim rotawirusem A G1P[8] szczep RIX4414 przed lub po stymulacji komórkami bakterii. Zmiany ekspresji genów były normalizowane względem ilości transkryptów 18S rRNA. Wartości statystycznie istotne ($p < 0,05$) zostały zapisane pogrubioną czcionką

Gene symbol	Preinfection bacterial treatment				Postinfection bacterial treatment			
	BB12		EcN		BB12		EcN	
	RQ	*p*-value	RQ	*p*-value	RQ	*p*-value	RQ	*p*-value
1	2	3	4	5	6	7	8	9
ACTB	**3.81**	0.0336	1.00	0.993	0.13	0.4231	0.14	0.4273
AIM2	**0.88**	0.0432	**1.27**	0.0083	0.35	0.4638	0.26	0.4118
APOBEC3G	**0.88**	0.0432	**1.27**	0.0083	1.20	0.3118	0.88	0.3275
ATG5	**2.72**	0.0063	0.55	0.1222	0.48	0.1303	0.68	0.4518
AZI2	1.91	0.0962	0.59	0.0671	0.71	0.0878	**0.53**	0.0239
B2M	1.01	0.9793	0.79	0.3592	0.97	0.89	0.82	0.4237
CARD8	2.30	0.0849	0.42	0.0609	1.55	0.2807	1.24	0.6797
CASP1	**1.83**	0.0054	0.58	0.081	0.65	0.2611	0.54	0.1726
CASP10	**3.97**	0.0141	3.13	0.0823	0.78	0.2046	0.56	0.0678
CASP8	1.58	0.0523	**0.64**	0.0005	0.95	0.892	1.00	0.9887
CCL3	**0.88**	0.0432	**11.79**	0.0066	0.42	0.4482	0.96	0.9641
CCL5	**0.88**	0.0432	**1.27**	0.0083	1.20	0.3118	0.88	0.3275

Table 10 cont.

←

ski) dla ustalenia indeksu komórkowego (CI). Komórki kontrolne Caco-2 niepoddane infekcji ani stymulacji bakteriami dawały stały odczyt indeksu komórkowego (C, kolor karmazynowy). Komórki Caco-2 stymulowane *B. animalis* BB12 (B, kolor zielony), *E. coli* Nissle 1917 (E, kolor turkusowy) oraz infekowane rotawirusem RIX4414 (R, kolor czerwony) nie wykazywały odmiennych wartości CI od wartości odnotowanych dla komórek kontrolnych w czasie przebiegu eksperymentu. Komórki Caco-2 stymulowane *E. coli* Nissle 1917, po czym infekowane rotawirusem (ER, kolor koralowy) uzyskały podwyższony, ale stabilny indeks komórkowy. Komórki Caco-2 stymulowane *B. animalis* BB12 przed lub po infekcji (odpowiednio BR, szaroniebieski i RB, ciemnozielony) oraz stymulowane *E. coli* Nissle 1917 po infekcji (RE, niebieskofioletowy) wykazywały wzrastający, a następnie opadający indeks komórkowy. Krzywe zostały wykreślone jako średnia z czterech wartości pomiarowych

1	2	3	4	5	6	7	8	9
CD40	**0.88**	0.0432	**1.27**	0.0083	2.61	0.3997	5.22	0.4312
CD80	1.11	0.9154	1.67	0.5742	0.35	0.3785	0.07	0.2452
CD86	0.27	0.4055	0.38	0.4715	1.20	0.3118	0.88	0.3275
CHUK	2.59	0.1753	2.02	0.4073	0.32	0.5005	0.32	0.5047
CTSB	9.35	0.193	0.56	0.5952	0.80	0.6063	1.72	0.2994
CTSL1	1.24	0.3686	0.86	0.1292	1.30	0.0886	1.17	0.2587
CTSS	9.42	0.0577	1.95	0.3212	0.59	0.3889	0.54	0.3437
CXCL10	**75.73**	0.0387	**160.15**	0.0129	0.86	0.7309	0.65	0.4185
CXCL11	3.61	0.2127	**1.27**	0.0083	1.02	0.9846	1.90	0.3113
CXCL9	7.26	0.1552	0.53	0.4072	2.13	0.4434	0.49	0.5248
CYLD	**6.78**	0.0482	1.61	0.5499	0.92	0.9079	0.68	0.6559
DAK	16.04	0.335	1.39	0.6497	0.19	0.2823	0.26	0.3116
DDX3X	1.36	0.4679	0.46	0.2912	1.02	0.9479	0.70	0.2617
DDX58	7.08	0.1638	1.79	0.4913	0.29	0.2257	0.16	0.1791
DHX58	3.80	0.2728	0.32	0.4903	0.37	0.4526	0.15	0.3347
FADD	1.41	0.6242	**0.23**	0.0094	0.89	0.8933	0.76	0.7548
FOS	2.08	0.2817	1.37	0.3683	1.36	0.4929	1.02	0.968
GAPDH	0.89	0.2929	0.96	0.8062	1.00	0.9735	0.87	0.2672
HERC5	1.47	0.1201	0.75	0.3456	1.1216	0.3126	0.90	0.6614
HPRT1	3.35	0.2312	0.60	0.0786	1.04	0.8434	0.67	0.2401
HSP90AA1	1.32	0.3807	**0.39**	0.0445	1.84	0.2061	1.08	0.6851
IFI44L	**0.88**	0.0432	**1.27**	0.0083	1.20	0.3118	0.88	0.3275
IFIH1	2.09	0.1734	**0.35**	0.004	5.45	0.4592	0.79	0.7546
IFNA1	0.25	0.4009	1.06E+8	0.4226	0.14	0.4258	0.51	0.6338
IFNA2	**0.88**	0.0432	**1.27**	0.0083	1.20	0.3118	3.04	0.4563
IFNAR1	0.64	0.6588	2.90	0.2914	1.18	0.8549	0.63	0.7229
IFNB1	**0.88**	0.0432	**1.27**	0.0083	1.20	0.3118	0.88	0.3275
IKBKB	3.99	0.3294	0.81	0.5773	4.59	0.3692	0.79	0.7377
IKBKG	0.20	0.1344	0.12	0.1203	3.00	0.1768	3.91	0.3094
IL12A	1.87	0.3765	1.30	0.4606	2.62	0.0831	5.19	0.163
IL12B	**0.88**	0.0432	**1.27**	0.0083	1.20	0.3118	0.88	0.3275
IL15	1.10	0.8833	0.29	0.1408	1.49	0.624	0.93	0.8558
IL18	3.43	0.0649	0.93	0.9121	0.47	0.4987	0.48	0.5027
IL1B	6.51	0.129	17.66	0.139	0.96	0.9373	0.73	0.6143
IL6	3.04	0.2424	10.23	0.1824	0.93	0.881	1.59	0.2192
IL8	57.94	0.1119	**445.69**	0.0252	**6.78**	0.0035	**13.98**	0.0109

1	2	3	4	5	6	7	8	9
IRAK1	3.20	0.328	**0.46**	0.0001	1.69	0.35	0.72	0.5331
IRF3	1.65	0.6258	0.11	0.1494	0.61	0.5108	0.13	0.2099
IRF5	0.28	0.1642	0.85	0.7732	1.69	0.4636	2.04	0.2556
IRF7	0.52	0.3816	0.13	0.1768	0.86	0.8339	0.78	0.7153
IRF9	2.45	0.1802	0.33	0.0623	1.39	0.2645	0.77	0.4765
ISG15	0.94	0.8763	1.92	0.5647	1.23	0.7284	0.99	0.9875
JUN	2.29	0.119	3.37	0.1888	1.02	0.9595	0.78	0.5396
MAP2K1	1.99	0.2591	0.98	0.9258	0.61	0.2569	0.43	0.1499
MAP2K3	1.87	0.1133	0.92	0.6694	0.78	0.6289	0.55	0.362
MAP3K1	1.39	0.4683	**1.78**	0.0214	0.44	0.3381	1.16	0.5681
MAP3K7	0.86	0.8685	0.35	0.1657	0.90	0.8517	0.53	0.3919
MAPK1	0.77	0.6857	0.39	0.1272	0.005	0.0812	0.004	0.081
MAPK14	0.74	0.6856	0.21	0.2175	0.34	0.2942	0.16	0.2182
MAPK3	0.72	0.4451	0.45	0.2807	4.33	0.39	1.00	0.9943
MAPK8	3.76	0.179	0.79	0.5034	0.54	0.3723	0.47	0.32
MAVS	1.84	0.1991	0.89	0.7761	1.06	0.7364	0.83	0.1674
MEFV	7.79	0.1746	1.25	0.6026	2.41	0.3484	0.78	0.4768
MX1	3.74	0.2871	5.53	0.4402	1.41	0.6094	0.65	0.3351
MYD88	3.70	0.3435	0.55	0.4574	5.11	0.0638	3.96	0.1084
NFKB1	**1.79**	0.0186	1.91	0.5649	2.48	0.1465	**2.46**	0.0193
NFKBIA	2.12	0.3601	11.30	0.4181	6.51	0.3756	**10.28**	0.0272
NLRP3	**0.88**	0.0432	**1.27**	0.0083	1.20	0.3118	0.88	0.3275
NOD2	**0.88**	0.0432	**1.27**	0.0083	2.91	0.3484	0.88	0.3275
OAS2	2.18	0.2621	1.88	0.423	1.52	0.6234	3.49	0.4316
PIN1	1.20	0.4649	**0.60**	0.0309	1.04	0.7297	0.74	0.2469
PSTPIP1	**0.88**	0.0432	**1.27**	0.0083	1.20	0.3118	0.88	0.3275
PYCARD	2.60	0.3138	1.02	0.9115	0.15	0.2569	0.34	0.3537
PYDC1	2.80	0.4441	**1.27**	0.0083	1.20	0.3118	0.88	0.3275
RELA	1.39	0.2867	0.92	0.8313	3.96	0.1432	1.48	0.2207
RIPK1	1.22	0.5297	**0.23**	0.0351	1.25	0.6855	0.33	0.3395
RIPK2	15.43	0.3729	2.30	0.1695	1.01	0.9739	0.76	0.4373
RPLPO	3.30	0.3823	0.3696	0.115	0.58	0.204	0.67	0.3094
SPP1	0.76	0.8071	1.04	0.9711	1.01	0.9445	5.45	0.449
STAT1	**1.74**	0.0179	1.19	0.7217	0.98	0.88	0.73	0.0704
SUGT1	6.30	0.2315	1.53	0.6755	0.75	0.7558	0.37	0.466
TBK1	3.66	0.3735	0.67	0.4476	1.98	0.2122	1.14	0.6572

Table 10 cont.

1	2	3	4	5	6	7	8	9
TBP	3.46	0.1036	**0.37**	0.0197	1.34	0.5901	1.01	0.9926
TICAM1	15.66	0.2626	6.58	0.1891	5.31	0.1759	**4.14**	0.0106
TLR3	0.90	0.8992	0.79	0.6399	2.02	0.3663	1.51	0.3499
TLR7	1.94	0.3344	1.53	0.5264	**3.19**	0.0016	2.79	0.1396
TLR8	0.52	0.5342	0.34	0.4037	1.73	0.6101	1.70	0.4602
TLR9	**0.88**	0.0432	**1.27**	0.0083	0.31	0.4568	0.22	0.4135
TNF	11.58	0.2242	**30.53**	0.0089	2.79	0.3022	2.22	0.2415
TRADD	0.80	0.3491	0.81	0.5104	1.51	0.345	0.99	0.9859
TRAF3	2.65	0.2112	2.21	0.2106	0.91	0.863	0.84	0.709
TRAF6	7.64	0.354	1.31	0.353	2.10	0.0902	1.72	0.1621
TRIM25	1.32	0.2835	**1.57**	0.0127	1.24	0.4193	0.88	0.4681

Table 11. Selected biological processes related to virus infection and genes involved in these processes which expression level was significantly changed by *B. animalis* BB12 and/or *E. coli* Nissle 1917 during rotavirus infection of differentiated Caco-2 cells (Huang da et al., 2009)

Tabela 11. Wybrane procesy biologiczne związane z infekcją wirusową i geny, których produkty uczestniczą w tych procesach, o istotnie zmienionym poziomie ekspresji przez *B. animalis* BB12 i/lub *E. coli* Nissle 1917 podczas infekcji rotawirusem zróżnicowanych komórek Caco-2 (Huang da i in., 2009)

Biological process	Genes
1	2
Antiviral defense	*APOBEC3G, IFIH1, IFNA2, IFNB1, IRF9, STAT1, TICAM1, TRIM25*
Apoptosis	*ATG5, CARD8, CASP1, CASP10, CASP8, FADD, IFIH1, IFNA2, IFNB1, IL12A, IL12B, IRAK1, MAP3K1, MAPK1, MYD88, NFKB1, NFKBIA, NLRP3, NOD2, RIPK1, STAT1, TICAM1, TNF, TRAF6*
Cytokine production and cytokine signaling	*CARD8, CASP1, CCL3, CCL5, CD40, CXCL10, CXCL11, IL12A, IL12B, IL18, IL8, MAPK1, MYD88, NFKB1, NFKBIA, NLRP3, NOD2, PYDC1, STAT1, TICAM1, TLR7, TLR9, TNF, TRAF6*
Cytokine-cytokine receptor interaction	*CCL3, CCL5, CD40, CXCL10, CXCL11, IFNA2, IFNB1, IL12A, IL12B, IL18, IL8, TNF*

1	2
Defense response	*APOBEC3G, CCL3, CCL5, CD40, CXCL10, CXCL11, IFIH1, IFNA2, IFNB1, IL12A, IL8, MYD88, NFKB1, NLRP3, NOD2, PYDC1, TICAM1, TLR7, TLR9, TNF*
Host-virus interaction	*APOBEC3G, FADD, IFIH1, MAPK1, NFKBIA, STAT1, TBP, TRIM25*
Immune response	*AIM2, APOBEC3G, CCL3, CCL5, CD40, CTSS, CXCL10, CXCL11, IFI44L, IFIH1, IL12A, IL12B, IL18, IL8, IRAK1, MAPK1, MYD88, NFKBIA, NLRP3, NOD2, PYDC1, TICAM1, TLR7, TLR9, TNF, TRAF6, TRIM25*
Inflammatory response	*CCL3, CCL5, CD40, CXCL10, CXCL11, IFNA2, IL8, MYD88, NFKB1, NLRP3, TICAM1, TLR7, TLR9, TNF*
Innate immune response	*APOBEC3G, IFIH1, IFNB1, IL12A, IL12B, IRAK1, MYD88, NFKBIA, NOD2, PYDC1, TICAM1, TLR7, TLR9*
Jak-STAT signalling	*IFNA2, IFNB1, IL12A, IL12B, IRF9, STAT1*
Lipopolysaccharide-mediated signalling	*IRAK1, MAPK1, NFKBIA, STAT1, TICAM1*
MAPKinase signalling	*MAP3K1, MAPK1, NFKB1, NFKBIA, RIPK1, STAT1*
NF-kB signalling	*AZI2, CARD8, CASP1, CASP8, CD40, FADD, IRAK1, MAP3K1, MYD88, NFKB1, NFKBIA, NOD2, RIPK1, STAT1, TICAM1, TLR7, TLR9, TNF, TRAF6*
NOD-like receptor signalling	Receptors and signalling: *CARD8, CASP1, CASP8, CCL5, HSP90AA1, MAPK1, NFKB1, NFKBIA, NLRP3, NOD2, PSTPIP1, PYDC1, TRAF6* Responsive genes: *IL18, IL8, TNF*
Pattern recognition receptor signalling	*IRAK1, MYD88, NFKBIA, NOD2, TICAM1, TLR7*
Protein kinase cascade	*AZI2, CARD8, CASP1, CASP8, CD40, FADD, IL12A, IRAK1, MAP3K1, MAPK1, MYD88, NFKBIA, NOD2, RIPK1, STAT1, TICAM1, TLR7, TLR9, TNF, TRAF6*
Regulation of transcription	*IFNB1, IRAK1, IRF9, MAP3K1, MAPK1, MYD88, NFKB1, NFKBIA, NLRP3, NOD2, PYDC1, RIPK1, STAT1, TBP, TICAM1, TNF*
Regulation of viral reproduction	*APOBEC3G, CCL3, CCL5, IFNB1, IL8, MAP3K1, TNF*
Response to bacterium	*CCL5, IFNB1, IL12A, IRAK1, MAPK1, MYD88, NFKBIA, NOD2, STAT1, TICAM1, TLR9, TNF*
Response to exogenous dsRNA	*MAPK1, NFKBIA,NOD2, STAT1, TICAM1*

Table 11 cont.

1	2
Response to virus	*APOBEC3G, CCL5, IFIH1, IFNA2, IFNB1, IRF9, NLRP3, STAT1, TICAM1, TLR7, TLR9, TNF*
RIG-I-like receptor signalling	Receptors and chaperones: *CYLD, IFIH1, TRIM25* Downstream signalling: *ATG5, AZI2, CASP10, CASP8, FADD, MAP3K1, NFKB1, NFKBIA, PIN1, RIPK1, TNF, TRAF6* Responsive genes: *CXCL10, IFNA2, IFNB1, IL12A, IL12B, IL8*
Toll-like receptor signalling	Receptors and chaperones: *TLR7, TLR9* Downstream signalling: *CASP8, FADD, IRAK1, MAP3K1, MAPK1, MYD88, NFKB1, NFKBIA, RIPK1, STAT1, TICAM1, TNF, TRAF6* Responsive genes: *CCL3, CCL5, CD40, CXCL10, CXCL11, IFNA2, IFNB1, IL12A, IL12B, IL8*

5. Discussion

5.1. ENTEROCYTE GENE EXPRESSION RESPONSE TO BACTERIA

Data published by other research groups reports that microorganisms are capable of changing the level of expression from 0.35% to 13% of genes in epithelial cells (Belcher et al., 2000; Eckmann et al., 2000; Fukushima et al., 2003; Panigrahi et al., 2007; Pedron et al., 2003; Rosenberger et al., 2000). However, different methodological approaches used by different research groups to analyse results (such as a biased cut-off point) might have impact on the data. Results presented in this work, using the same methodology for all tested microorganisms, show that depending on the strain considered the responses affected from 1.23% to 9.26% of genes (Table 3). This follows the data from the literature.

All available meta-data analyses bear unavoidable ambiguity of differences in methodological approach of experimental procedure and data analysis (Schmidt et al., 2011). Therefore this might be the first research that covers such a large number of microorganisms analysed with the same methodology.

Comparison of the number of differential genes did not provide any correlation in terms of groups of the studied microorganisms that could be set with the current state of knowledge. For the number of microorganisms studied the transcriptional response of the enterocytes was specific for the strain used. A total number of 10.7 thousands genes were responsive to the microorganisms studied. However, 3.9 thousands genes were modulated by more than one strain.

The highest consistency in joint differentially expressed genes modulated in the same pattern of expression remained between probiotic and commensal strains and the most divergent were probiotic and pathogenic strains. This was the most expected result since the border between probiotic and commensal is blurred in contrast to probiotic versus pathogen. Similarly, the groups of commensals and pathogens may share a portion of the same traits. It is widely known that some commensal bacteria can cause disease in case of immune system failure becoming opportunistic pathogens. Pathogens are defined as microorganisms that encode virulence factors in their genomes. The factors allow the microorganism to colonize host, modulate its immune response, and damage

tissues. Some of the virulence factors are toxins that are potent immunestimulators (e.g. LPS) or interfere with certain biochemical pathways in the host (Keen, 2012). Except of destructive enzymes and toxins the other virulence factors may have their analogous components in non-pathogenic bacteria. Therefore some similarities in responses to bacteria regardless their overall influence on host can be expected.

Comparison of single strain responsome to group responsome may specify outlier to a group that it was assigned to. Conversely, a similarity of gene expression pattern of specific group to single microorganism assigned to a different group can indicate somehow similar action (e.g. *L. casei* DN114001 or *L. casei* Shirota vs. commensals). An opposite action identified for probiotic versus pathogenic strain may indicate a strain of choice for preventing the pathogen's action. In case of two probiotic strains of opposite gene modulation scheme such knowledge suggests that they should not be put together in dietary supplement as they may deliver an antagonistic action.

The cluster analysis of gene expression showed low similarity in the response of the epithelial cells to the tested strains. The responsomes did not reflect the taxonomic relationship of the strains in any manner. This was clearly visible in the examples of strains of the *E. coli* and *L. casei* strains, and of *Lactobacillus* sp. The only exception was for *B. animalis* strains. There were also no significant differences between the responses of differentiated Caco-2 enterocytes to the strains of probiotic, pathogenic, and commensal nature. Such a variation in response of the epithelial cells to microorganisms may result from the enormous diversity observed in the bacterial kingdom.

The highest similarity was observed between responsomes derived from differentiated Caco-2 enterocytes interacting with strains of *B. animalis*. This may result from the high homogeneity of genomes of this species, which is clonal and genetic variation is limited to intergenic regions and short palindromic repeats (Bottacini et al., 2010). Comparison of complete genome sequences of six strains of *B. animalis* subsp. *lactis* showed their similarity ranging from 82.5% to 99.5% at a very low diversity of genome sizes from 1.915 to 1.944 Mbp and capacity from 1528 to 1642 protein coding genes. Analysis of complete genome sequences of 19 members of the *Bifidobacterium* genus showed that the core genome consists of 724 gene families (approximately 46% of the capacity of the *B. animalis* genome), while the pan-genome was estimated to be 6980 gene families (Bottacini et al., 2010; Lukjancenko et al., 2012). Much higher genetic diversity can be observed within the *Lactobacillus* genus, where the analysis of full genome sequences of 21 representatives showed that this genus has a common gene pool of 363 gene families (core genome), and pan-genome extends

over 13 069 gene families. Similarity of the genomes of strains of: *L. casei* is approximately 70% (with a capacity of their genomes ranging from 2771 to 3044 genes), *L. casei* and *L. rhamnosus* – from 55.5% to 59.3% (with a capacity of *L. rhamnosus* strain genomes from 2834 to 2944 genes). However, similarity of the genomes of strains of *L. casei* or *L. rhamnosus* to *L. acidophilus* is only about 13% (with the volume of *L. acidophilus* WNCF genome consisting of 1862 genes; Lukjancenko et al., 2012). Strains of *E. coli* contain larger genomes (ranging from 4.557 to 5.933 Mbp with their capacity from 4084 to 5803 genes) that gives 1472 gene families constituting the core genome and pan-genome consisting of 13 296 gene families (data obtained from the analysis of the complete genomic sequences of the 53 strains of *E. coli*; Lukjancenko et al., 2010). With the individual differences between strains of up to 1459 genes (Sun et al., 2005). Such a large diversity of genetic information of even taxonomically very closely related microorganisms may explain the lack of correlation between human cells' responsomes treated with the selected bacterial strains. The finding is in agreement to the European Food Safety Authority (EFSA) group of experts scientific opinion in relation to health claims proposed for some probiotics "…that owing to the strain-specificity of the effects, the evidence obtained for one strain cannot be extrapolated to another…" (EFSA, 2009). Therefore an outcome of host-microbe interaction is highly strain specific. There is a tremendous work to be done to correlate a specific trait to bacterial genetic information. Even though a whole genome sequence knowledge indicating that a genome harbours an orthologous gene does not prove the gene is functional. A comparative genomic and functional analysis of 100 *L. rhamnosus* strains showed that, despite a group of 11, strains share the same set of genes and display significant phenotypic variations. These differences might be due to i.e. single nucleotide polymorphisms, insertions and deletions not usually addressed in multiple genome comparison. Moreover, use of a reference genome for assembly of sequences obtained by next generation sequencing may cause oversight of strain-specific genes present in different isolates (Douillard et al., 2013).

The KEGG Pathway database search returned the highest number of genes assigned to metabolic pathways map. However, it might be a result of excellent knowledge on metabolic pathways and cycles, as well as thorough annotation of gene products involved in them; not necessarily due to the most potent influence of bacteria on this kind of biological processes. Several targets of the bacteria tested were identified in diseases directly connected to gastrointestinal tract (e.g. *Salmonella* infection, bacterial invasion of epithelial cells, *H. pyroli* infection, colorectal cancer, Shigellosis and IBD). Modulation of genes involved in diseases indicates possible use of bacterial strains in

treatment. But also may point etiology agent or reveal therapeutic targets in case of diseases induced by pathogens.

Analysis of GO Slim terms showed that *E. coli* Nissle 1917 produced the most divergent response. Overrepresentation of GO Slim term 'multi-organism process' suggests that mechanisms to react to alterations of external conditions or presence of different species and to adapt the transcriptome accordingly were more active in presence of the *E. coli* Nissle 1917 strain than the other. Another explanation of the response, further supported by overrepresented GO Slim term 'chromosome', could be the genotoxic action of the strain. This feature was indicated as essential for probiotic action of the strain (Olier et al., 2012). The *E. coli* Nissle 1917 induces a transient DNA damage response in enterocytes leading to formation of phosphorylated H2AX foci (Cuevas-Ramos et al., 2010) a principal component of chromatin involved in the detection, signalling, and repair of DNA double-strand breaks (Chen et al., 2013). Overrepresentation of GO slim terms regarding down-regulated expression of genes implicated in 'ion binding' and 'oxygen binding' indicates also the strain's metabolic modulatory activity.

Enterocytes' responsome to *E. coli* ATCC 10536 was characterised by overrepresentation of up-regulated genes involved in GO Slim term 'cell projection'. This action is characteristic for pathogenic bacteria to target cytoskeletal components, these include actin, microtubules, dynein, and endocytosis-associated protein dynamin. The pathogenic bacteria action results in the formation of a 'pedestal' on the host-cell surface, where the pathogen resides (Bhavsar et al., 2007). Whereas significant changes in GO Slim term 'cell communication' indicate that the strain mediates interaction between an enterocyte and its surroundings.

The responsomes to the three strains: *B. animalis* MK2, *E. coli* Nissle 1917, and *E. coli* ATCC 10536 characterised by over- and under-representation of certain GO Slim terms were encountered in case of the strains that modulated lower than an average number of differentially expressed genes in differentiated Caco-2 enterocytes (see Table 3). The underrepresentation of a GO Slim term might be explained by low number of differentially modulated genes, whereas the overrepresentation might not. Therefore, this kind of exploration may have significant potential.

5.2. BIOLOGICAL SIGNIFICANCE OF BACTERIAL STIMULI

The host cell response is strain specific and bacteria tested were shown to modulate approximately 30% of human genes.The KEGG pathway results uncovered that despite enormous diversity of modulated genes bacteria target similar biolog-

ical pathways. Due to manual curation of the KEGG database it contains limited number of entries. Therefore, for more informative results, Gene Ontology (GO) was used. The GO is structured and controlled vocabulary (ontology) that describes gene products in terms of their associated biological processes (also cellular components and molecular function). The *Homo sapiens* Reference genome GO Annotation contained 18426 gene products annotated with total 298243 annotations for Jun 11, 2014 (according to Gene Ontology website 2014).

Data mining of Gene Ontologies for specific biological processes modified by groups of microorganisms indicated two processes for both commensals and pathogens. Commensals modified signal transduction components (GO:0046580, GO:0051058). Both processes are involved in signalling pathways of many possible outcomes. Among others they are involved in regulation of cell communication, apoptosis, development, metabolism, cell cycle, cell adhesion, and immune system processes primarily through EGF, FGF and PDGF signalling pathways (Thomas et al., 2006). Whereas pathogens influenced homophilic cell adhesion (GO:0007156) and toll-like receptor 4 signalling pathway (GO:0034142). The first process plays important role in cell-cell adhesion and signal transduction. It is crucial for organism to keep epithelial barrier integrity to prevent pathogen invasion (Vereecke et al., 2011). The toll-like receptor 4 is involved in detection of lipopolysaccharides from Gram-negative bacteria and is thus important in the activation of the innate immune system. It is the main Toll-like receptor involved in the control of *Salmonella* and *Escherichia* infections (de Jong et al., 2012; Tapping et al., 2000). All the pathogenic bacterial strains tested belong to Gram-negative group, however in the study there were two more Gram-negative strains (*E. coli* Nissle 1917 and *B. thetaiotaomicron* ATCC 29741) which did not influence toll-like receptor 4 signalling pathway. Interestingly the two latter strains belong to probiotic and commensal group thus might have adopted to gut environment and do not trigger innate immune response. Commensal and probiotic bacteria are proposed to have the ability to regulate mucosal and systemic immunity (Diehl et al., 2013; Karlsson et al., 2004; Lathrop et al., 2011; Rizzello et al., 2011). Intestinal epithelial cells, on the other hand, were shown to be largely unresponsive to the gut flora. They acquire TLR tolerance immediately after birth by exposure to exogenous endotoxin to facilitate microbial colonization and the development of a stable intestinal host-microbe homeostasis (Lotz et al., 2006). In this experiment the *in vitro* model was used that does not include immune cells. So the lack of TLR4 activation may indicate that the tolerance for specific group of microorganisms can be administered on the epithelial cell level, or those microorganisms adopted to the intestinal niche do not induce innate responses.

The 'homophilic cell adhesion' (GO:0007156) was also commonly modified by the *E. coli* strains. The process was also changed by the studied pathogenic strain group which is assembled by *E. coli* strains in two-thirds. The modulation of GO:0007156 process seems significant for all Gram-negative strains tested except for *B. thetaiotaomicron* ATCC 29741. The *Bacteroides* species is distinct from the other Gram-negative species tested. It belongs to dominant group of the human gut microbiome and was shown to have multiple positive effects on post-natal gut development. The species stimulates angiogenesis and establishment of the intestinal mucosal barrier, furthermore it was shown to affect acquisition and storage of lipids by adipocytes. Although it lacks proteins with detectable homology to known adhesins or flagellar components a large repertoire of outer membrane polysaccharide-binding proteins aid *B. thetaiotaomicron* to maintain residency in its niche in the absence of these components. It interacts with and harvests nutrients from the mucus layer that overlies the intestinal epithelium (Wexler, 2007; Xu and Gordon, 2003). The unique interactions that manage *B. thetaiotaomicron* adhesion to gut epithelium lead to distinct perception of the bacteria by the enterocytes. The characteristic role of *B. thetaiotaomicron* for human gut and its noticeable adaptation to the niche must be the reason for not influencing homophilic cell adhesion process as other Gram-negative bacteria studied did.

The fecal coliforms influenced additionally 'response to superoxide' (GO:0000303) and 'response to oxygen radical' (GO:0000305). The latter processes are child terms of 'response to reactive oxygen species' (GO:0000302). The term describes any process that results in a change in state or activity of a cell as a result of a reactive oxygen species (ROS) stimulus. The response might be primary in nature in case the bacteria are the source of ROS (Korshunov and Imlay, 2010) or secondary as enterocytes' response to self-generated ROS in response to other stimulus. Oxidative defense mechanisms involving production of reactive oxygen species have important role in innate immunity and inflammatory processes. Reactive oxygen species are generated in response to bacterial lipopolysaccharides by colon epithelial cells (Rada and Leto, 2008). Also LPS-activated platelets (Aktan et al., 2013), neutrophils (Khanfer et al., 2012), vein (Barbeiro et al., 2009) and lung (Wang et al., 2007) endothelial cells can contribute to host defense through release of reactive oxygen species for bactericidal actions. Even though the *E. coli* strains used in this study display opposite action on human organism (the ATCC 10536 and NCTC 12900 strains are pathogens, whereas Nissle 1917 is probiotic strain) the Nissle 1917 strain exhibits genotoxic activity that is required for its probiotic action through modulating the immunomodulatory properties (Guerra et al., 2011; Olier et al.,

2012). The property of the Nissle 1917 strain might also be a remainder of its postulated pathogenic ancestry (Hancock et al., 2010). It is also proposed that the commensal bacteria can be the major trigger of ROS in the adult intestines (Kajino-Sakamoto et al., 2010).

The average number of joint biological processes in comparison between single probiotic strains was lower than between probiotic and commensal strains. This indicates that the outcome of probiotics action is somehow targeted onto the same processes as of commensals rather than the other probiotics. It is not surprising since any commensal strain when proved to be safe and with documented beneficial action on human health can become probiotic.

Interestingly, in the case of the *L. acidophilus* LA-5 strain compared to some of the other strains tested (*L. rhamnosus* GG, *L. casei* DN114001, *B. animalis* MK2, *P. anaerobius* ATCC 27337, *S.* Typhimurium ATCC 14028 and *E. coli* NCTC 12900), they share unexpectedly low number of joint processes (Table 8). This is intriguing as the strain pairs share above-average number of joint differentially expressed genes (Table S2). The discrepancy can be a result of two factors: modulation of not annotated genes and use of data mining algorithm that takes into account genes being described with significance coefficient above 0.05 threshold (Pavlidis et al., 2004).

It has to be kept in mind that the biological processes indicated as joint for a pair of strains are not necessarily changed in the same way. The biological processes were selected based on a list of genes with significance coefficient of an expression change, but not with fold-change value. Therefore additional specific experiments are needed to verify the biological significance of a given interaction. It remains to be discovered whether certain strain has beneficial or harmful influence on the particular health aspect. It can be hypothesised that effect exerted by probiotic or commensal strain is positive and by pathogenic strain – negative. Furthermore in case that both probiotic/commensal and pathogenic strains affect the same process they constitute a first choice pair for more detailed studies of possible contradictory action. Especially in case where they are characterised by divergent enterocytes' gene expression response. On the other hand, a different transcriptional response may indicate unique mode of influence and not necessarily an opposite action.

Comparison of category related gene expression patterns revealed species--specific (regarding *B. animalis* and *L. casei*) and genus-specific (regarding *Lactobacillus* sp.) modulation of general biological processes. Interestingly responsomes to the *E. coli* strains did not show such similarities. The *E. coli* strains used belong to probiotic and pathogen groups, however the Nissle 1917 strain has pathogen ancestry (Hancock et al., 2010).

Some general processes (e.g. apoptosis, healing and regeneration, metabolism, innate immunity, inflammation, development and morphogenesis, and structure and function of gastrointestinal tract) revealed large similarities ($R^2 > 0.7$) in category related gene expression pattern of responses to majority of strains. This can be explained by adaptation of the strains to ecological niche of gastrointestinal tract where the processes take place.

The divergent responses to the bacterial strains tested regarding some of the biological process categories considered indicated that there are presumably strain-specific traits that mediate genes expression in different way. On the other hand, the processes that are mediated in very similar fashion by a group of microorganisms suggest a common traits or lack of influence on gene expression. However, the lack of response is slightly possible where an above-average number of specific processes is influenced within the considered category. Such similarities in dendrogram shape can be easily seen in case of cell cycle (Fig. 8.4), identification of microorganisms (Fig. 8.18), and cell differentiation (Fig. 8.20) or metabolism (Fig. 8.9), development and morphogenesis (Fig. 8.19), and structure and function of gastrointestinal tract (Fig. 8.27). Altogether the data may indicate that some of the biological processes are highly strain-dependent, and other simply influenced by presence of microbes with minor reliant on strain-specific traits. Similarities of dendrograms regarding different biological processes were in part due to substantial number of the same genes involved in the processes but also similar action of the strains.

The intestinal epithelium is a monolayer of columnar cells which form a tight barrier separating gut content from inner tissues. The selective permeability, important for absorption of nutrients while preventing invasion of microorganisms, is achieved by tight adhesion of enterocytes to each other fortified by specialized structures called tight junctions, adherence junctions and desmosomes (Natividad and Verdu, 2013). Regulation of the cellular structures is important in the maintenance of the epithelial architecture and, thereby, in the preservation of intestinal barrier (Sharma et al., 2010). Comparison of enterocytes gene expression pattern regarding 'adhesion' category shows high divergence in gene response to the bacterial strains tested (Fig. 8.1). The responses to Gram-positive probiotic strains cluster together, however according to data mining with gene ontology only the mixture of probiotic strains influenced substantial number of the biological processes in significant manner. The ability of probiotic *Lactobacillus* and *Bifidobacterium* strains to affect intestinal permeability has been already shown. Furthermore such beneficial effects on the host possess also *B. thetaiotaomicron* and *E. coli* Nissle 1917 (Natividad and Verdu, 2013; both microbes modulated substantial number of biological processes in the

'adhesion' category). Interestingly transcriptional response of adhesion related genes to probiotic *E. coli* Nissle 1917 and pathogenic *S. enterica* ATCC14028 forms an outlier group, yet with very low similarity (Fig. 8.1). It was already demonstrated that enteric pathogens, such as enteropathogenic *E. coli* strains (Liu et al., 2005) and *S. enterica* (Jepson et al., 2000), can disrupt the tight junctions of enterocytes through a number of different virulence factors which is in agreement with the indication that the pathogenic strains tested in this study modulate substantial number of biological processes categorised into 'adhesion' (Table 9). Enterocytes covering intestinal villi undergo coordinated regulation of proliferation, differentiation and apoptosis. They originate from stem cells in crypt and shed at the tip of villus. The balance between enterocyte proliferation and apoptosis is crucial for maintenance of mucosal barrier equilibrium. Recent work from a variety of laboratories has demonstrated a role for receptors of the innate immune system (including TLRs and PRR) in the initiation of enterocyte apoptosis (Siggers and Hackam, 2011) therefore indicating role of microorganisms in the process. Substantial involvement of commensal group in 'cell cycle' category was observed in this study where probiotic group represents highly similar pattern in gene expression but *L. acidophilus* LA-5 constitutes an outlier (Fig. 8.4). Relatively similar patterns of gene expression can be observed for additional categories: 'differentiation' (Fig. 8.20), and 'development and morfogenesis' (Fig. 8.19) still with slight fluctuations in strains that influenced substantial number of significantly changed processes. In case of apoptosis the gene expression pattern as influenced by the strains tested display high similarities for probiotics and commensals with pathogens indicating higher divergence but probiotic *E. coli* Nissle 1917 constituting an outlier (Fig. 8.2).

Gene expression similarity dendrograms may serve also for discerning probiotic-specific traits. In case the same species (e.g. *B. animalis* in this study) is represented by a probiotic strain (BB12) and a commensal strain (MK2) the high similarity in enterocyte transcriptional response may display reaction to species-specific traits but divergent response indicates strain-specific traits. Considering the 'blood pressure' category, for example, the BB12 strain is influencing a substantial number of biological processes whereas the MK2 strain none. The gene expression pattern of enterocytes in response to both strains remain similar ($R^2 = 0.748$, Fig. 8.3). This indicate that overall regulation of the genes involved in the process in both cases was the same but not equally strong. On the other hand, in case of 'blood and lymphatic vessels' category, the MK2 strain influences a substantial number of biological processes whereas the BB12 none ($R^2 = 0.637$). Here the strains are more divergent in generating transcriptomic response in enterocytes (Fig. 8.11). The two *B. animalis* strains share

a below-average number of biological processes influenced despite very similar global Caco-2 responsome generated. This may explain why one of the strains belongs to the probiotic and the other to commensal group. Taking into account the high genomic homogeneity of *B. animalis* strains (Bottacini et al., 2010) the divergent action of the BB12 and MK2 strains might be explained by quantitative differences in specific molecule present on bacterial surface rather than an unique trait. Anyhow, for greater confidence in such an assumption, an analysis of more strains of the same species should be performed.

The *in silico* analysis, so far, has not taken into account signalling pathways cross-talk that influences biological consequence of a signal (Claudio et al., 2013; Karavolos et al., 2013), and the transcriptome analysis do not reveal regulatory processes occurring at posttranscriptional level. Microbial cells belong to exogenous stress factors. These regulate also mRNA translation and posttranslational modifications that play an important role in stress responses. Moreover, other processes like splicing and mRNA decay are also stress-regulated (Claudio et al., 2013). It should be noted that apart from moderating gene expression, the microbiota can modulate expression of microRNAs (miRNAs) in the host. The small RNAs can repress expression of proteins without affecting the mRNA levels (Dalmasso et al., 2011).

5.3. ANTI-VIRAL PROPERTIES OF *E. COLI* NISSLE 1917

5.3.1. Rotavirus replication impaired by *E. coli* Nissle 1917

Several probiotic strains were characterised by their ability to prevent acute inflammation of the gastro-intestinal tract caused by viral infection (rotaviruses, noroviruses) or shortening the time and intensity of the course of infection. The most significant data of such an action was documented for: *L. rhamnosus* GG, *L. casei* Shirota, *L. casei* DN114001, *L. acidophilus* NCFM (Grandy et al., 2010; Liu et al., 2010; Maragkoudakis et al., 2010; Nagata et al., 2011, Pedone et al., 2000). Three of the strains mentioned were included in the study and were shown to significantly alter biological processes in the category of virus infection. In addition, there are more and more reports about the impact of probiotics on the incidence and course of other viral diseases such as flu (Davidson et al., 2011; Kawase et al., 2010; Takeda et al., 2011,), rhinitis (Berggren et al., 2011, Leyer et al., 2009) or AIDS (Bolton et al., 2008; Hummelen et al., 2010).

Rotaviruses belong to *Reoviridae* family. They are non-enveloped viruses containing double-stranded (ds) RNA genome divided into 11 segments. There

are five species of rotavirus (A, B, C, D, and E), however Rotavirus A causes over 90% of rotavirus infections in humans. It is a contagious virus that can cause gastroenteritis. Infants and young children are most likely to get rotavirus disease. Adults usually develop immunity. Symptoms include severe watery diarrhea, often with vomiting, fever, and abdominal pain. The virus spreads by the fecal-oral route. Children can shed the virus both before and after they become sick with diarrhea. They shed the virus in their feces (stool) mostly when they are sick and during the first three days after recovery. Rotaviruses infect enterocytes of the villi of the small intestine. The virus enters cells by receptor mediated endocytosis. The virus proteins VP4 and VP7 disrupt endosome membrane and genomic segments protected in the VP2 and VP6 viral proteins shell undergo transcription by the viral RNA-dependent RNA polymerase. Produced mRNA are used both for protein synthesis and replication. Most of the rotavirus proteins accumulate in viroplasm, where replication is finished and dual-layered particles are assembled. Virion maturation completes in endoplasmic reticulum where third layer is formed. The progeny viruses are released from the cell by lysis (Bernstein, 2009; Ruiz et al., 2009).

Both *B. animalis* BB12 and *E. coli* Nissle 1917 are approved for administration to infants and both were shown to reduce acute diarrhea in infants (Henker et al., 2007; Jungersen et al., 2014). However, microarray data mining indicated that the *B. animalis* BB12 does not influence biological processes involved in viral infection whereas *E. coli* Nissle 1917 does. The rotavirus RNA quantification in Caco-2 cells treated with the bacteria verified the microarray data. This indicates that the microarray data does provide functional information of biological importance and might serve as guidance for discovering microbial strain effect on host cell or even organism.

Study of Ayala-Breton et al. (2009) showed that qPCR is sensitive enough to measure rotavirus RNA level increase as early as 2 h pi in cells infected at MOI = 0.1. During the first 4 h the amount of rotavirus RNA increase linearly, later a logarithmic increase of viral RNA level is observed. However, the two treatment regimens indicate both prophylactic and therapeutic capacity of the *E. coli* Nissle 1917 probiotic strain to reduce the outcome of rotavirus infection. This finding shows that the antiviral probiotic action of the strain is managed on a cellular level. However, it does not exclude the possibility that the strain can exert its action through direct involvement of systemic responses like inflammation, and/or acquired immunity.

Rotavirus replication cycle is restricted to the cell cytoplasm where double-layered particles, containing genomic dsRNA segments, function as molecular machines, producing caped viral (+)RNAs that are extruded from transcribing

particles into the cytoplasm. The proteins in the core of the virion possess the enzymatic activity of RNA polymerase dependent on dsRNA templates. The nascent rotavirus (+)RNAs act as mRNAs for protein synthesis and as a template for genome replication (Trask et al., 2012). The rotavirus hijacks the cellular metabolism to translate its mRNAs while simultaneously blocks cellular protein synthesis by impeding nucleocytoplasmic transport of host mRNAs. This process depends on vial nonstructural protein NSP3. Inhibition of host cell protein synthesis allows the virus to regulate cellular stress and antiviral response (Rubio et al., 2013). Small interfering RNA (siRNA)-blockage of NSP3 expression has no effect on the translation of viral proteins, but restores translation of cellular proteins in rotavirus infected cells, but also increase synthesis of viral dsRNA (Chung and McCrae, 2011). Therefore reduction in NSP3 RNA by the Nissle 1917 strain preinfection treatment may allow host-cell to develop antiviral response. Although depletion of NSP3 should increase virus genome replication this was not observed in this study. Quantitative PCR analysis indicated also that Caco-2 cells preinfection treatment with the Nissle 1917 strain significantly decreased NSP5 transcript (primer pair used target NSP5 coding sequence) and/or genomic segment 11 (coding for NSP5 and NSP6). The NSP5 is a major building block of viroplasm. The protein recruits viral polymerase VP1, the core protein VP2, and the NSP2 (ATPase) inside the viroplasm to form the viral replication complex (Martin et al., 2013). Small interfering RNA targeting genome segment 11 treatment of rotavirus infected cells results in inhibition of viroplasm formation, decreased production of structural and nonstructural proteins, synthesis of viral genomic dsRNA and production of infectious particles. These effects were shown not to be caused by inhibition of NSP6 (Campagna et al., 2005). Therefore the decrease in NSP5 RNA induced by the bacterial treatment should impair overall replicative cycle of the virus. Another viral RNA decreased by the Nissle 1917 strain preinfection treatment of Caco-2 cells was coding for VP4 protein. The protein has a key role in infectivity, as it forms spikes protruding from the virion particle surface and function in virion attachment to permissive host cell. The VP4 is involved in outer capsid assembly (Trask et al., 2013) therefore reduction of its amount should block generation of nascent infectious particles.

The Caco-2 postinfection treatment with the Nissle 1917 strain resulted in significant decrease of NSP1, VP1, VP2, VP6, and VP7 RNAs. The NSP1 protein is a virulence factor responsible for proteasome-mediated degradation of: interferon regulatory factors (IRF3, IRF5, and IRF7; Arnold et al., 2013a), TNF receptor-associated factor 2 (TRAF2; Bagchi et al., 2013a), tumor protein p53 (TP53; Bhowmick et al., 2013), and mitochondrial antiviral signalling pro-

tein (MAVS; Nandi et al., 2014). Degradation of these proteins cause inhibition of interferon and interferon stimulated genes (ISGs) expression (Arnold et al. 2013a; Nandi et al., 2014), inhibition of interferon mediated non-canonical NFκB activation (Bagchi et al., 2013a), and inhibition of apoptosis during initial stages of infection (Bhowmick et al., 2013). In addition, NSP1 can block *IFNB* promoter activation by DEAD (Asp-Glu-Ala-Asp) box polypeptide 58 (DDX58, also known as RIG-I) through interaction with the DDX58 protein and inhibit DDX58-mediated type I interferon responses (Qin et al., 2011). Research of Graff et al. (2009) showed that the virus protein inhibits activation of NFκB by another mechanism. It induces proteasome-dependent degradation of beta--transducin repeat containing E3 ubiquitin protein ligase (BTRC) a substrate recognition protein recruiting nuclear factor of kappa light polypeptide gene enhancer in B-cells inhibitor, alpha (NFKBIA) for polyubiquitination. Arnold and Patton (2011) revealed that various rotavirus strains employ diverse interferon antagonist activities mediated by NSP1 proteins due to their immense sequence variation. Rotavirus NSP1 was reported also to interact with PI3K regulatory subunit p85, a member of PI3K/Akt pathway. The interaction results in efficient activation of this pathway. Phosphoinositide 3-kinases (PI3Ks) regulate diverse cellular processes like cell survival, proliferation, inflammation, and immunity (Bagchi et al., 2013b). This way virus may modulate inflammatory, apoptosis, and both innate and adaptive immune response signalling. Decrease in NSP1 RNA may restore antiviral signalling allowing cell to overcome infection or enter apoptosis to prevent spread of infection.

The VP1 protein is dsRNA-dependent, RNA polymerase, enclosed along with the 11 dsRNA segments within the VP2 shell. The polymerase can operate either in replicative mode generating a dsRNA genomic product (when the template is the plus strand) or in transcriptional mode producing a ssRNA(+) (mRNA, when the template is the minus strand; Silvestri et al., 2004). The decrease in VP1 RNA results in decrease of the VP1 protein, that is required for virus genome packaging (Trask et al., 2012). This should prevent progeny virion assembly, that is further jammed by the decrease in capsid proteins VP6 and VP7. The Nissle 1917 strain action is directed both to prevent virus from hijack cellular control and decrease virus replication. It remains to be revealed whether the Nissle 1917 strain derived signalling inhibited rotavirus RNA synthesis or induced its degradation. The latter possibility seems to be more probable as the RNA polymerase (VP1) is entrapped within virus core shell therefore protected from action of cytoplasmic proteins.

5.3.2. Cellular responses of enterocytes to bacteria treatment and rotavirus infection

Dynamic monitoring of enterocytes fate was performed on undifferentiated Caco-2 cells. The Caco-2 are able to differentiate on solid surfaces. However, the cells form gas-pockets causing detachement of the cell monolayer from growth surface. This would interfere with cell index measurement. Therefore, this experiment was performed on undifferentiated cells to prevent misinterpretation of monolayer detachment as cytopathic effects.

According to literature a development of the fully functional tight junctions takes place after 13 days of culture as indicated by trans-epithelial electric resistance (TEER) measurement. The TEER steadily raises from 0 ohm/cm^2 at day 3 to over 3000 ohm/cm^2 at day 13 (Johannessen et al., 2013). However, more detailed study with transmission electron microscopy of Caco-2 cells during the time course revealed the formation of localized electron-dense areas of closely opposing plasma membranes between cells characteristic of tight junctions by day 4. As well as, at the same time [^{3}H]inulin diffusion across the monolayer was dramatically reduced to a background level, indicative of the formation of functional tight junctions. Moreover, the temporal expression patterns of genes encoding tight junction integral membrane proteins (occludin and claudin-1) increased initially after cell-cell adhesion and peaked at a time coincident with formation of functional tight junctions (Halbleib et al., 2007). Since the experimental setup in both studies (Halbleib et al., 2007; Johannessen et al., 2013) did not show any major differences it is possible that tight junctions are formed by day 4 establishing a diffusion barrier but their full development takes a few more days. Despite both the TEER measurement and xCelligence system are resistance based assays the electrode arrangement are different. The xCelligence system recorded initial formation of tight junctions but is not able to quantify their tightness. Hence, it can be assumed that in this study after 90 h of culture Caco-2 cells monolayer already developed tight junctions since cell index (CI) did not show further change for the entire duration of the experiment. A rise of CI reflected probably cell swelling. Whereas, decline in CI indicated relaxation of cellular connections, cell-rounding and shrinking, and subsequent cell death (where CI approached baseline).

Apoptosis has been shown to promote degradation of tight junction proteins (Bojarski et al., 2004) in enterocytes leading to decrease of transepithelial resistance (Bojarski et al., 2001). Rotavirus infection leads to alternations in cytoskeleton of infected cell (Brunet et al., 2000) and promotes structural and functional injuries localized at the tight junctions (Obert et al., 2000). These cellular events

promote infection of polarized cells (Delorme-Axford and Coyne, 2011). Thus infection alone and undoubtedly subsequent apoptosis should precede increase in paracellular permeability. This assumption is not supported by the data obtained from undifferentiated Caco-2 cells infected with rotavirus. The cell index measured as a function of cell monolayer impedance does not differ between infected and not-infected control cells (Fig. 15). Results presented by other research group indicated that undifferentiated Caco-2 cells infected with simian rotavirus (strain SA11) at MOI = 0.5 did not exhibit apoptotic morphologies such as chromatin condensation or breakdown into apoptotic bodies at 24 h pi, and showed no significant activation of caspase-3, even at 48 h pi when MOI = 2.5 was used (Gac et al., 2010). In this study MOI of approximately 0.35 was applied. This may explain why the rotavirus RIX4414-infected undifferentiated Caco-2 cells did not show any cytopathic effects at 49 h pi (R vs. C; Fig. 15). Whereas fully differentiated Caco-2 cells infected with rhesus rotavirus (MOI = 10) showed 5-fold increase in number of apoptotic cells (with no significant difference regarding necrosis) at 24 h pi, however the cells did not display cell membrane damages yet. Only 5.82% of the infected cells were at late apoptotic stage at 24 h pi, but early signs of apoptosis (externalisation of phosphatydyl serine measured by Annexin V assay) were observed already at 4 h pi. The number of apoptotic-positive cells at 4 h pi was 3.9% and did not change significantly at least till 15 h pi, to reach 42% after 24 h pi. The maximum of virus yield is reached at 20 h pi (Chaibi et al., 2005), rotavirus release from fully-differentiated Caco-2 cells starts from 18 h pi before cell lysis, which occurs beyond 24 h pi, when total progeny viruses have been already released (Jourdan et al., 1997). The results of apoptosis induction measured with caspase-3/-7 assay at 14 or 18 h pi in this study comply with those of Chaibi group (Chaibi et al., 2005). Another reason that rotavirus RIX4414 did not lead to clearly visible cytopathic effects may be due to strain differences (Arnold and Patton, 2011) or its attenuation. The molecular basis for the attenuation of the strain is unknown (Greenberg and Estes, 2009). The rotavirus vaccine strain originates from child stool isolate that was serially passaged 26 times in primary African Green Monkey Kidney cells (AGMK), then 7 times in AGMK cell line giving vaccine strain designated 89-12. Then the strain was further passaged in Vero cells and cloned by limiting dilution and renamed RIX4414 (Bernstein, 2006). The assessment of clinical studies revealed that the RIX4414 is more attenuated than the parent strain 89-12 (Glass et al., 2006). The vaccine virus 89-12 was detected in 75%, whereas the RIX4414 in 38% to 65% of vaccine recipients' stool (Dang et al., 2012; Popp et al., 1991). The shedding data corresponds to rotavirus antigens detection in stool of vaccinated infants and children. Whereas more de-

tailed study of Zibrik et al. (2007) showed that the RIX4414 vaccinated adults does not shed live rotavirus (tested by cell culture) and only one individual shed a small amount of virus antigen (tested by ELISA).

According to research of Gac et al. (2010) the 4 h post infection time allows analysis of cellular responses of enterocyte to rotavirus infection as increased SOD2 protein level is already visible in rotavirus infected Caco-2 cells. However, at that datapoint, VP6 protein is not detectable via immunofluorescence suggesting that it is dependent on viral RNA or structural protein presence in infected cells (Gac et al., 2010). Thus the cellular genes expression change observed in qPCR analysis is of an early type response to virus infection.

Data obtained from animal models and clinical studies of rotavirus infection indicate that the virus is not by itself inherently cytopathic. Thus the rotavirus infections are not accompanied by significant inflammation (Chaibi et al., 2005).

Taken together the analyses indicate that the *E. coli* Nissle 1917 treatments block rotavirus RIX4414 replication and transcription. However, the postinfection treatment triggers rapid cell death regardless of the virus antiapoptotic actions and the preinfection treatment maintained cell viability (despite caspase-3/-7 activation). Although the *B. animalis* BB12 treated Caco-2 cells undergo cell death but allowing the rotavirus replication.

5.3.3. *Escherichia coli* Nissle 1917 modifies enterocyte's innate anti-viral responses

Several products of the differentially expressed genes under influence of the *E. coli* Nissle 1917 in respect to the rotavirus infection were described in details regarding their involvement in virus infection. This may pinpoint possible interactome cross-talk between bacteria and virus derived signals.

Detection of rotavirus infection in intestinal cells involves activation of cytoplasmic pattern recognition receptors (PRR): interferon induced with helicase C domain 1 (IFIH1, also known as MDA5) and DEAD (Asp-Glu-Ala-Asp) box polypeptide 58 (DDX58, also known as RIG-I) that detect viral RNA and signal through mitochondrial antiviral signalling protein (MAVS, also known as IPS-1) to stimulate the activation of interferon response factor-3 and -7 (IRF3/7), nuclear factor-kappa B (NFκB) and activator protein-1 (AP1) leading to interferons (IFN-α/β/λ) and proinflammatory cytokines (IL-1β, IL-6, IL-8, IL-18, and TNFα) expression. Cytokine expression results in attraction and activation of immune cells. An alternative pathway of rotavirus detection leads through endosomal/lysosomal PRR. Binding of virus RNA to the toll-like receptor 3 (TLR3)

passes the signal through toll-like receptor adaptor molecule 1 (TICAM1, also known as TRIF) to IRF3/7 leading to IFNs expression. The host defence following rotavirus infection triggers secretion from infected cells type I (IFN-α/β) and type III (IFN-λ) interferons. Receptors for IFN-α/β are expressed almost ubiquitously. Therefore type I interferons signal infection to hematopoietic cells as well (paracrine signalling). The receptor for IFN-λ is expressed primarily on epithelial cells. This signal is mainly received by bystander enterocytes to induce antiviral state (autocrine signalling). Activation of these receptors induce kinase signalling cascade resulting in phosporylation of signal transducer and activator of transcription (STAT) transcription factors. Heterodimer of activated STAT1 and STAT2 proteins associate with interferon regulatory factor-9 (IRF9). Resulting complex induces expression of interferon stimulated genes (ISGs). Products of these genes have the ability to directly inhibit replication of viruses but also posses immunostimulatory and immunomodulatory properties (reviewed in details by: Arnold et al., 2013b; Holloway and Coulson, 2013).

Gene expression analysis of Caco-2 cells treated with *E. coli* Nissle 1917 prior or after rotavirus infection lead to modulation of genes already recognised to be involved in innate cellular responses to rotavirus infection but also indicated other genes involved in pathogen recognition signalling (Fig. 16). The bacterial strain triggered upregulation of several pattern recognition receptor genes responsible for detection of pathogens (*AIM2*, *NLRP3*, *NOD2*, *TLR9*).

The absent in melanoma 2 gene (*AIM2*) was shown to be IFN-inducible and involved in the sensing of dangerous cytosolic DNA produced by infection with DNA viruses and of intracellular bacteria leading to production and caspase--1-mediated activation of pro-inflammatory cytokines (Rathinam et al., 2010). Although the AIM2 protein is involved in inflammasome formation and activation in response to DNA viruses (Gram et al., 2012) its uppregulation by *E. coli* Nissle 1917 may contribute to nonconventional antiviral action triggered by the bacterial strain. NLR family, pyrin domain containing 3 (NLRP3) gene encodes a member of the NALP3 inflammasome complex. This complex functions as an upstream activator of NFκB signalling, and plays a role in the regulation of inflammation, the immune response, and apoptosis. The inflammasome also mediates maturation of the pro-inflammatory cytokines (e.g. IL-1β and IL-18) via the caspase-1-mediated cleavage of the cytokine pro-forms (Lupfer and Kanneganti, 2013; Yu and Levine, 2011). The NALP3 inflammasome complex interacts with heat shock protein 90kDa alpha (cytosolic), class A member 1 protein (HSP90AA1). The heat shock protein positively regulate rotavirus replication by modulating virus induced PI3K/Akt and NFκB signalling pathways. Moreover the HSP90 was reported to actively participate in the folding and stabilization

of rotavirus NSP3 protein. The inhibition of HSP90 lead to depletion of NSP3 protein due to its degradation, but had no influence on NSP3 transcript level (Dutta D. et al., 2011). The Nissle 1917 strain preinfection treatment of Caco-2 cells lead to both significant decrease in rotavirus NSP3 RNA level and cellular *HSP90AA1* mRNA level indicating that the bacterial strain predispose enterocyte to antiviral response through two independent pathways. The downregulation of HSP90AA1 expression abrogates rotavirus replication by hindering PI3K/Act and NFκB signalling and causes depletion of rotavirus NSP3 protein.

Both AIM2 and NLRP3 interact with caspase-1 through PYCARD. The caspase-1 action is regulated by PYD (pyrin domain) containing 1 (PYDC1) protein that interacts with PYCARD. The PYDC1 appears to function as a dominant-negative inhibitor which can suppress caspase-1 activation and CFLAR protein. The latter protein is involved in regulating apoptosis by affecting the recruitment of caspase-8 to tumor necrosis factor family death receptors (Natarajan et al., 2006). Recent research has indicated that proteins belonging to the same protein family inhibits inflammasome and regulates responses to infection with DNA viruses (Khare et al., 2014). The *E. coli* Nissle 1917 treatment upregulated expression of PYDC1. This may explain inhibition of apoptiosis and point out activation of innate response generally assigned to detection of DNA viruses (as it involves also *AIM2*, which was upregulated as well). The action of PYCARD is negatively regulated by proline-serine-threonine phosphatase interacting protein 1, encoded by PSTPIP1 gene. Its product is a scaffold protein and a negative regulator of the actin cytoskeleton polymerization. Mutations within the gene are associated with autoinflammatory syndromes. Pyrin (MEFV) is a cytosolic receptor for PSTPIP1 required for recruitment and activation of caspase-1 to inflammasome, and suspected to restrict viral replication (Yu et al., 2007). Upregulation of *PSTPIP1* expression by the *E. coli* Nissle 1917 might contributed to reduction of rotavirus replication.

Nucleotide-binding oligomerization domain containing 2 (*NOD2*) gene encodes a cytoplasmic receptor with caspase recruitment (CARD) domains. It plays a role in the immune response to intracellular bacterial lipopolysaccharides (LPS) and activating the NFκB protein. Recent studies have shown that RNA (Lupfer et al., 2013; Sabbah et al., 2009) and DNA (Kapoor et al., 2014; Suzuki et al., 2011) viruses can also activate NOD2 leading to increased expression of IFN-β and IL8 (Kapoor et al., 2014). Virus induced NOD2 signalling negatively regulate NLRP3 inflammasome activation and IL-18 release, and leads to induction of type I interferons through MAVS and IRF3 (Lupfer et al., 2013). The *E. coli* Nissle 1917 was shown to upregulate *NOD2* expression therefore sensitizing the cell to pathogen.

A subgroup of endosomal toll-like receptors (TLR3, TLR7, TLR8 and TLR9) are specialized in recognition of microbial nucleic acids. TLR3 senses double-stranded (ds) RNA, TLR7 and TLR8 – ssRNA, whereas TLR9 – DNA (especially bacterial, containing CpG motifs). Upon binding their ligand they initiate a signalling cascade via the adaptor molecules: MYD88 (TLR7, 8 and 9) or TICAM1 (TLR3) leading to activation of NFκB/AP1 and IRF3/7 transcription factors (Saitoh and Miyake, 2009). Although TLR9 is recognized as DNA receptor (for both bacterial and virus genomes), Wang H. et al. (2012) showed increased expression of TLR9 in case of multiple RNA virus (rotavirus, astrovirus and enterovirus) infection of Caco-2. Therefore the *E. coli* Nissle 1917 treatment of Caco-2 cells upregulation of TRL9 gene expression confirms involvenment of this PRR in rotavirus detection. The TLR3-mediated signalling pathway was also modified by the bacterial strain treatment. The Nissle 1917 strain upregulated transcription of *TICAM1* and downregulated transcription of *IRAK1*. The toll-like receptor adaptor molecule 1 (TICAM1) protein is an intracellular signalling domain that mediates interactions between the toll-like receptor 3 (TLR3) and signal-transduction components. It mediates dsRNA induction of interferon-β through activation of NFκB, during an antiviral immune response. Some virus proteins target TICAM1 and lead to their degradation (Hyun et al., 2013). The most recent study indicates that interleukin-1 receptor-associated kinase 1 (IRAK1) protein inhibits TICAM- and DDX58--mediated the TLR3–IFN-β and proinflammatory cytokine response (Bruni et al., 2103). Downstream to TICAM1 is TRAF6 also inhibited by IRAK1. Therefore downregulation of *IRAK1* by the Nissle 1917 strain relieves TLR3-signalling of rotavirus infection (Alexopoulou et al., 2001). Further downstream to TRAF6 is receptor (TNFRSF)-interacting serine-threonine kinase 1 (RIPK1), a signalling component involved in programmed cell death. RIPK1 upon association with Fas-associated protein with death domain (FADD) and caspase-8 contributes to cell death by apoptosis. However, depletion or inhbition of caspase-8 and FADD favours necroptosis, a programmed form of necrotic cell death (Kaczmarek et al., 2013; Salvesen and Walsh, 2014). Depending on cell type and stimulus, additional proteins can trigger ubiquitylation of RIPK1, targeting it to proteasomal degradation. This modification further contributes to pro-survival signalling as it enables RIPK1-mediated activation of NFκB and induction of pro-survival transcriptional programmes (Darding and Meier, 2012; Mocarski et al., 2011). Therefore downregulation of *RIPK1* expression by the *E. coli* Nissle 1917 treatment similarily to ubiquitin degradation may contribute to cell survival.

Signals from endosomal (TLR3/9) and cytoplasmic (DDX58 and IFIH1) pattern recognition receptors, through RIPK1 and MAVS, respectively, contribute

to the activation of MAP3K1. The kinase activation is leading to the activation of transcription factors NFκB and AP-1 (Yoshida et al., 2008). Nuclear factor of kappa light polypeptide gene enhancer in B-cells 1 (*NFKB1*) gene encodes a 105 kD protein which can undergo proteolytic cleavage to produce a 50 kD protein. The 105 kD protein is a REL protein-specific transcription inhibitor and the 50 kD protein is a DNA binding subunit of the NFκB (NFKB) protein complex. Whereas nuclear factor of kappa light polypeptide gene enhancer in B-cells inhibitor, alpha (*NFKBIA*) gene encodes a member of the NFκB inhibitor family, which interacts with REL dimers to inhibit NFκB/REL complexes involved in inflammatory responses. The NFKB complex is a transcription regulator activated by various intra- and extra-cellular stimuli including viral products. The *E. coli* Nissle 1917 treatment also upregulated transcription of genes encoding MAP3K1, NFKB1 and NFKBIA. Those are other locations where the bacterial strain modulate innate anti-viral response signalling. Interleukin-8 promoter contains NFKB-binding site that may explain upregulation of *IL8* (Kunsch and Rosen, 1993). Interleukin-8 overexpression in case of pre- and postinfection *E. coli* Nissle 1917 treatment may result in different signalling pathways, since the preinfection treatment did not upregulate the *NFKB*. The *NFKBIA* was 4-fold higher upregulated in respect to *NFKB1*. The research of Marchant et al. (2014) showed that the *NFKBIA* encoded IκBα mediates the export of IFNα from virus--infected cells. Therefore, the upregulation of the genes may induce inflammatory response through upregulation of *IL8* and release of IFNα.

Another important PRR is DDX58 (RIG-I), although its expression was not changed by the Nissle 1917 strain, the bacteria upregulated gene encoding its activator (TRIM25). Tripartite motif containing 25 protein ubiquitinates DDX58 resulting in a marked increase in its downstream signalling activity. The activator is essential for DDX58-mediated IFN-β production and antiviral activity in response to RNA virus infection (Maelfait and Beyaert, 2012). TRIM family proteins have been shown to have antiviral activity and virus proteins target them to evade recognition by the host viral RNA pattern recognition receptors (Munir, 2010).

Expression of one of the PRR (*IFIH1*) was downregulated by the *E. coli* Nissle 1917. Interferon induced with helicase C domain 1 (IFIH1) protein is a viral double-stranded RNA (dsRNA) receptor sharing sequence similarity and signalling pathways with DDX58 (Wu et al., 2013). It was shown to be able to restrict positive-strand RNA virus replication (Nikonov et al., 2013). Activation of the receptor leads to induction of Bax/Bak-independent apoptosis pathway via mitochondrial antiviral signalling (MAVS) and caspase-8. Caspase-8 recruited to mitochondria forms a new death inducing signaling complex (DISC) that acti-

vates caspase-3 and apoptosis in a death receptor- and FADD-independent manner. This pathway is thought to help RNA viruses to kill cells which are usually protected by Bcl-2 overexpression (El Maadidi et al., 2014). Preinfection treatment of Caco-2 with *E. coli* Nissle 1917 lead to downregulation of *IFIH1* gene that may result in inhibition of apoptosis.

Another cellular protein involved in apoptosis signalling is Fas (TNFRSF6)--associated via death domain protein (FADD). It is an adaptor molecule that interacts with various receptors and mediates cell apoptotic signals. Such interaction allows it to recruit and activate caspase-8 (Grunert et al., 2012). Expression of *FADD* gene was downregulated by *E. coli* Nissle 1917 therefore should reduce ability of enterocyte to enter apoptosis in case of rotavirus infection. Moreover, the bacterial strain also caused downregulation of *CASP8* gene. Although it does not explain reduction of rotavirus genome replication and/or transcription, it may justify lack of cytopathic effect observed in label-free dynamic monitoring of undifferentiated Caco-2 cells fate. However, measurement of downstream caspase-3 and -7 activity did not show significant difference regarding infected differentiated Caco-2 cells that were not treated with bacteria. Even though the data obtained in the two experiments appear inconsistent, it has to be kept in mind that one study concerned *CASP8* gene transcript level and the other CASP3/7 enzymatic activity. Furthermore in death signalling CASP3 is downstream to CASP8 and can be activated through alternative pathway (Iwai et al., 2013). Cells infected by viruses usually undergo apoptotic death. This is an innate defence system to reduce spread of infection. Viruses evolved mechanisms dampening apoptosis at early stages of infection to allow their replication. On the other hand, some viruses induce apoptosis at the end of replication cycle to facilitate progeny release. Caspase-8 plays a central role in the execution-phase of cell apoptosis. It can also be induced via DDX58-like receptor signalling pathway by viral dsRNA (Thompson et al., 2011) through Bax/Bak-independent action (El Maadidi et al., 2014). Innate anti-viral response pathway passing signals from several PRR (DDX58, IFIH1, and NOD2) through MAVS leads to activation of interferon response factor-3/7 that promote expression of interferon genes. Upstream of IRF3/7 in the signalling pathway is 5-azacytidine induced 2 (*AZI2*) gene product (Zhao et al., 2012). It was shown to enhance IFN-β promoter activation, but suppress IRF3 activation in response to poly(I:C) or LPS. The protein is involved also in TLR3/4-mediated TICAM1 pathway signalling (Funami et al., 2007; Sasai et al., 2005). It can activate NFκB-dependent gene expression by activating IκB kinase-related kinases, and may protect cells from TNF-α-induced apoptosis by promoting NFκB activation (Fujita et al., 2003). The mentioned AZI2 functions are involved in recognition of RNA virus

through TLR and DDX58-like receptor leading to rapid expression of type I interferons (Zhao et al., 2012). The AZI2 protein was found to be associated with TAX1BP1 (Goncalves et al., 2011) which was found to inhibit antiviral signalling (Parvatiyar et al., 2010). Therefore, downregulation of the *AZI2* gene by *E. coli* Nissle 1917 may explain antiviral action of the bacterial strain. However, the downstream signalling leading to upregulation of IFN expression might be a result of an alternative pathway. Moreover, the bacterial strain downregulated peptidylprolyl cis/trans isomerase, NIMA-interacting 1 protein (*PIN1*) gene expression. The protein was shown to negatively regulate activation of IRF3 and lead to proteasome-dependent degradation of IRF3 (Saitoh et al., 2006). It was also shown that similar protein (PIN3) interacts with virus proteins resulting in efficient, productive replication of such viruses like: EBV (Narita et al., 2013), HCV (Lim et al., 2011), and HIV-1 (Watashi et al., 2008). Therefore, downregulation of PIN1 expression by the Nissle 1917 strain may contribute to reduction of rotavirus replication. This might be acheieved by release of IRF3 activation and/or reduction of interacting partner for a viral protein.

Activated by phosphorylation IRF3/7 transcription factors bind IFNα/β gene promoters to stimulate transcription of the cytokines. Interferons are major molecules that mediate signalling of viral infection. They induce hundreds of genes called interferon-stimulated genes (ISGs) that are responsible for innate and acquired immunity, and inflammatory, and cellular response to viral infection. These responses are mainly of antiviral and antiproliferative nature (Schoggins, 2014). Preinfection treatement of Caco-2 cells with *E. coli* Nissle 1917 upregulated expression of interferon alpha 2 (*IFNA2*) and interferon beta 1 (*IFNB1*) genes. Therefore action of the *E. coli* Nissle1917 on expression of the several members of innate anti-viral signalling pathway results in enhancement of the type I interferon-mediated signalling (Fig. 16). One of the ISGs upregulated by the Nissle 1917 strain is the interferon-induced protein 44-like protein (IFI44L), which was shown to affect virus replication (Schoggins et al., 2011). However, some viruses counteract this action by downregulating its transcription (Wie et al., 2013). The apolipoprotein B mRNA editing enzyme, catalytic polypeptide--like 3G (APOBEC3G) is a member of the cytidine deaminase protein family. The protein coding gene also belongs to ISGs family. Its product was found to be a specific inhibitor of RNA viruses like: human immunodeficiency virus-1 (Gillick et al., 2013) and xenotropic murine leukemia virus (MLV)-related virus (Dey et al., 2011). Although its expression is strongly induced by influenza A virus, it does not negatively affect this virus propagation (Pauli et al., 2009). The APOBEC3G protein was shown to inhibit viral replication by a mechanism involving specific binding of the protein to single-stranded DNA (ssDNA) or

RNA (ssRNA) but not to double-stranded nucleotides (Imahashi et al., 2012). Expression of APOBEC3G was upregulated by *E. coli* Nissle 1917. In case of rotavirus infection the protein may act on viral transcripts preventing their translation and incorporation into progeny virions.

Preinfection *E. coli* Nissle 1917 treatment of Caco-2 cells lead to upregulation of several cytokines. The chemokine (C-C motif) ligand 3 (*CCL3*) and chemokine (C-X-C motif) ligand 10 (*CXCL10*) were overexpressed 12- and 160-fold. Whereas *CCL5* and *CXCL11* only 1.3-fold both. All these cytokines play a role in inflammatory responses. The cytokines expression is induced by several stimuli e.g. IFNγ, TNFα, IL-1β, LPS, virus DNA or RNA (Biasin et al., 2010; Wang J. et al., 2013) through MAPK, NFκB and C/EBPβ signaling pathways (Guzzo et al., 2012). Their expression can be blocked by EBV (Jabs et al., 2002) and HIV-1 (Zhao et al., 2007) to evade the host's immune system favouring persistent infection. Secretion of the cytokines is proposed to be an alternative mechanism to prevent viral infection (Menten et al., 2002; von der Ohe et al., 2001). Several papers indicate role of the cytokines (especially CCL3 and CXCL10) in lowering virus titer during viral infection. However, these data come from *in vivo* studies (reviewed in Melchjorsen et al., 2003) that should rather be associated with their proinflammatory action. Casola et al. (1998) showed that rotavirus infection of Caco-2 cells insignificantly increase expression of *CCL3* and *CCL5*. However, preinfection treatment of Caco-2 cells with the *E. coli* Nissle 1917 strain produced significant upregulation of genes encoding those cytokines.

Interleukin (IL)-12 is a key cytokine in promoting anti-viral Th1 responses. It is a heterodimer of p35 and p40 subunits encoded by *IL12A* and *IL12B* genes, respectively. However, p40 subunit can form a homodimer IL12 p80 to function as a macrophage chemoattractant, as well as a competitive antagonist of IL-12. It was shown that IL12 p80 expression causing the consequent recruitment of macrophages is critical regulatory processes for an appropriate antiviral immune response. Moreover, IL12 p80 overexpression may contribute to the localized excessive inflammation (Gunsten et al., 2009). Preinfection treatement of Caco-2 cells with *E. coli* Nissle 1917 upregulated expression of *IL12B* that may produce IL12 p80 homodimers. Therefore the bacterial signals may contribute to enhancement of inflammatory response as rotavirus infection in precived as trigerring weak inflammatory response (Greenberg and Estes, 2009).

Interleukin-8 (IL-8, CXCL8) is a pro-inflammatory chemokine able to elicit granulocytes, NK cells and T cell chemotaxis at the inflammatory site. It is a principal mediator of the inflammatory response to many viruses and bacteria. However, it may also interfere with the antiviral effect of IFN-α (Pollicino et al.,

2013). The *IL-8* was highly upregulated in both pre- and postinfection treatment of Caco-2 cells with *E. coli* Nissle 1917. Sheth et al. (1996) showed that rotavirus infection of cultured intestinal epithelial cells stimulates IL-8 expression and secretion. Among the cell lines tested the Caco-2 cells demonstrated the lowest increase in IL-8 expression (1.9-fold). Whereas in HT-29 and T84 cells the production of the cytokine incerased 16.8- and 9.7-fold, respectively (Sheth et al., 1996). Similar data was obtained by Casola et al. (1998). The Nisle 1917 strain boosted expression of the cytokine dramatically in case of preinfection treatment of Caco-2 cells. Tumor necrosis factor-alpha (TNF) gene was also upregulated by the bacterial strain. It encodes a multifunctional proinflammatory cytokine involved in the regulation of a wide spectrum of biological processes including cell proliferation, differentiation, and apoptosis. This cytokine has also antiviral properties. Its expression is regulated by NFκB/AP1 in positive feedback (Bartee et al., 2009). Research of Sheth et al. (1996) showed no influence of rotavirus infection of intestinal epithelial cells (HT-29) on expression of IL-6, IL1A, IL1B and TNF. The results were further confirmed by Casola et al. (1998) and Rodríguez et al. (2009) regarding both HT-29 and Caco-2 cells. However, rotavirus infection of gnobiotic pigs led to raise of IL-6 and TNF in serum of study animals (Azevedo et al., 2006). Clinical studies of rotavirus gastroenteritis in young children also indicated increase of IL-6 and TNF serum levels (Jiang et al., 2003). This might be due to secondary reaction of other e.g. immune cells in response to infection. The *E. coli* Nissle 1917 caused increase of *TNF* expression in Caco-2 cells indicating a role of the bacterial strain in modulation of signalling pathway leading to upregulation of the cytokine. In this case expression of *TNF* by intestinal epithelial cells might contribute to earlier response to virus leading to faster clearance of infection.

The inflammatory signalling involves also CD40 molecule, TNF receptor superfamily member 5. The *CD40* was also upregulated in Caco-2 cells by the Nissle 1917 strain prior to rotavirus infection. The receptor was found to be expressed on numerous immune cells but also endothelial cells, fibroblasts, smooth muscle cells, and epithelial cells. It plays a central role in the regulation of humoral and cell-mediated immunity, and inflammatory mediator production (Dugger et al., 2009) therefore, its upregulation may contribute to the Nissle 1917 strain modulation of innate anti-viral action.

The TATA box binding protein (TBP) is a member of multiprotein complex (TFIID) involved in initiation of transcription by RNA polymerase II. The complex is target to a number of viral proteins (Berk et al., 1998; Qadri et al., 1995). Recent research has shown that TBP is mainly localized at sites of viral DNA replication and transcription (Lester and DeLuca, 2011; Mainz et al.,

2014; Quadt et al., 2006). Common strategy of RNA viruses is virus-induced inhibition of host gene expression to prevent the host antiviral responses (Lyles, 2000; Weidman et al., 2003). Yet, the hepatitis delta virus (HDV) containing genome composed of a single-stranded circular RNA utilizes TBP for its replication (Greco-Stewart et al., 2009). The *E. coli* Nissle 1917 preinfection treatment resulted in downregulation of *TBP* gene transcription. However, at the current state of knowledge it is not possible to give a rational explanation of the importance of *TBP* downregulation for host cell. There is no data allowing to connect TBP with rotavirus biology. Rotaviruses block expression of host proteins on mRNA export from nucleus level (Rubio et al., 2013), not at initiation of transcription.

The Caco-2 response to Rotarix vaccine may not be of pure rotavirus origin since it was demonstrated that the vaccine contains porcine circovirus-1 (PCV1). This is a highly prevalent nonpathogenic pig virus, which has not been shown to be infectious in humans (Victoria et al., 2010). It was shown that the PCV1 DNA is protected from DNases indicating presence of viral capsids. However, Rotarix derived PCV1 was not able to infect PS, HEK293 and Vero cells, suggesting that the high amount of PCV1 DNA present in vaccine does not correspond to biologically active particles (Baylis et al., 2011). The Rotarix vaccine was shown to contain 4.1×10^7 to 5.5×10^8 PCV1 DNA copies in the final doses, and that the PCV1 genome is near full-length and contained two mutations in cap gene (Gilliland et al., 2012). The PCV1 virus belongs to smallest known viruses, has 1.7 kb circular ssDNA genome encoding only two genes (Finsterbusch and Mankertz, 2009). In case the PCV1 contributed to Caco-2 anti-viral responses the *E. coli* Nissle 1917 modulation of the responses show that the bacterial strain posseses wide anti-viral properties.

Most of the genes involved in response to virus infection (n = 37; *ACTB*, *AIM2*, *APOBEC3G*, *ATG5*, *CARD8*, *CASP1*, *CASP10*, *CASP8*, *CCL3*, *CCL5*, *CD40*, *CTSS*, *CXCL11*, *CYLD*, *HPRT1*, *HSP90AA1*, *IFI44L*, *IFIH1*, *IFNA2*, *IFNB1*, *IL12B*, *IRAK1*, *MAP3K1*, *MYD88*, *NFKB1*, *NFKBIA*, *NLRP3*, *NOD2*, *PSTPIP1*, *RIPK1*, *STAT1*, *TBP*, *TICAM1*, *TLR7*, *TLR9*, *TNF*, *TRIM25*) were described as polymorphic in human population. This can contribute to individuals' differences in phenotypic response (Huang da et al., 2009) and disease outcome.

Rotavirus infection is considered as the most frequent cause of diarrhea in children. The illness usually lasts several days and is self-limiting, therefore an oral rehydration is the conventional treatment for the condition. No specific medication was developed to shorten the period of illness. However, it was shown that certain strains of probiotic can reduce the duration of diarrhea and rotavirus shedding. Numerous randomized controlled trials have demonstrated probiotics

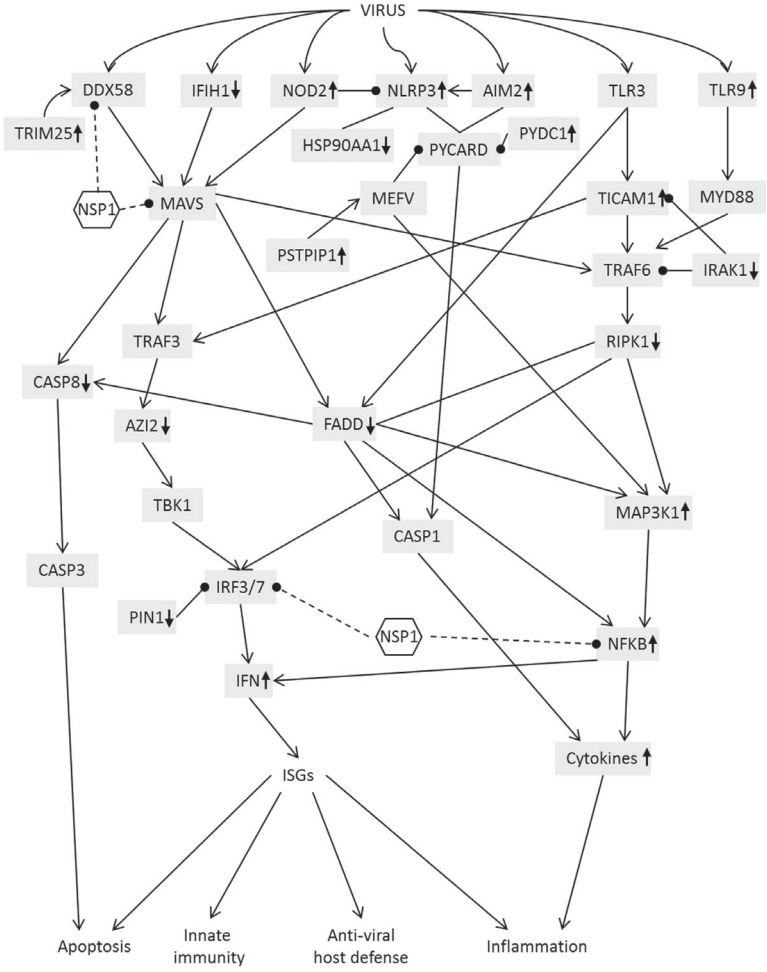

Fig. 16. Signalling and regulatory pathways in rotavirus detection and modulation of anti-viral responses. Lines connecting cellular gene products (gray boxes) represent: interactions, and activation (arrowheads) or inhibition (roundheads) involved in signal transduction. Arrows within boxes indicate upregulation (↑) or downregulation (↓) of the gene transcription in case of the bacterial stimulation. Rotavirus protein NSP1 inhibition of cellular anti-viral responses were also indicated

Ryc. 16. Szlaki sygnalizacyjne i regulatorowe uczestniczące w detekcji infekcji rotawirusowej i modulowania odpowiedzi przeciwwirusowej. Linie łączące produkty genów (szare prostokąty) przedstawiają fizyczne oddziaływania o charakterze aktywacyjnym (zakończone strzałką) lub inhibitorowym (zakończone kropką). Wzrost (↑) lub obniżenie (↓) poziomu ekspresji genów modulowanych przez badane bakterie zaznaczono strzałkami w obrębie prostokątów oznaczających produkty genów. Blokowanie komórkowej odpowiedzi przeciwwirusowej przez białko NSP1 rotawirusa (oznaczone sześcianem) zaznaczono liniami przerywanymi

effectiveness in virus induced gastroenteritis e.g.: *B. animalis* subsp. *lactis* B94 (Erdogan et al., 2012) and HN019 (Shu et al., 2001), *B. bifidum* (Duffy et al., 1994; Saavedra et al., 1994), *L. acidophilus* (Kolader et al., 2013), *L. paracasei* ST11 (Sarker et al., 2005), *L. rhamnosus* GG (Basu et al., 2009, Fox and Dang, 2004; Guandalini, 2011; Szajewska et al., 2011), *L. rhamnosus* 35 (Fang et al., 2009), *L. sporogenes* (Dutta et al., 2011b), *S. cerevisiae* subsp. *boulardi* (Guandalini, 2011), and probiotic mixtures (Dubey et al., 2008; Grandy et al., 2010; Szymański et al., 2006; Teran et al., 2009). There are reports available on efficacy of *E. coli* Nissle 1917 on acute diarrhea. Double-blind clinical trial showed a statistically significant reduction of the duration of acute diarrhea by 2.3 days (Henker et al., 2007) or 3.3 days (Henker et al., 2008) after administration of the probiotic. However, neither of the studies in focus mentions etiology of the diahrrea.

Although *B. animalis* BB12 did not induce antiviral cellular responses in enterocytes the probiotic strain was shown to possess viral-infection-preventing properties in clinical trials (Chouraqui et al., 2004; Phuapradit et al., 1999). Its antiviral activity is attributed to immunomodulating effects on GALT. The strain was shown to increase concentration of fecal total IgA in infants (Mohan et al., 2008; Rautava et al., 2006) and adults (Kabeerdoss et al., 2011), and anti-rotavirus- and anti-poliovirus-specific IgA following immunization (Fukushima et al., 1998; Holscher et al., 2012). Such an activity might be a common feature of *Bifidobacterium* species since *B. longum*, *B. infantis* and *B. breve* were also shown to boost levels of antipoliovirus IgA after vaccination (Mullie et al., 2004). Significantly delayed onset and early resolution of diarrhea were observed in *B. bifidum* ATCC 15696- and *B. infantis* ATCC 15697- treated, rotavirus-infected mice. Analysis of rotavirus-specific IgA and IgG in serum, and IgA in feces, mucosal total IgA and IgG levels in Peyer's patches suggests that bifidobacteria may act as an adjuvant by modulating early mucosal and strong humoral rotavirus-specific immune responses (Qiao et al., 2002). Furthermore, the elevated immune response after administration of *B. animalis* BB12 exerts to whole body as it was demonstrated to reduce respiratory infections as well (Rautava et al., 2009; Taipale et al., 2011). It was demonstrated that *B. bifidum* Bb11 can act as a lipopolysaccharide-like polyclonal activator for B cells. The strain enable B cells to respond to TGFβ1 and IL-5 for the IgA production (Ko et al., 1999, Sonoda et al., 1992). *Bifidobacterium bifidum* Bb11 significantly induces the synthesis of total IgA by mucosal lymphoid cells. Nevertheless, the strain itself does not induce its own specific antibody responses, implying that the strain does not provoke unnecessary immune reaction (Park et al., 2002). IgA-inducing properties possess also other commensal bacteria. Both *Bacteroides* and *Lactobacillus* strains have such feature, however *Bacteroides acidifaciens* induces IgA more

remarkably than *Lactobacillus johnsoni* (Yanagibashi et al., 2009, 2013). Such an activity has important implications for the primary defense against pathogens in the gastrointestinal tract. Another way probiotics can contribute to antiviral response is by altering cytokine production (e.g. TNFα, IL-6, IFNβ (Wang Y. et al., 2013), IL-1β (Miettinen et al., 2012), TNFα, IFNγ (Khani et al., 2012), IFNγ, IL-10, TGFβ (Wen et al., 2012), IL-12, IFNβ (Weiss et al., 2011). However, comparison of the capacity of 27 lactobacilli and 16 bifidobacteria strains to stimulate bone marrow-derived dendritic cells indicated that lactobacilli can be divided into two groups of bacteria featuring contrasting effects, while all bifidobacteria exhibit uniform effects. *Lactobacillus acidophilus*, *L. gasseri*, *L. casei* and *L. plantarum*, induced strong IL-12 and TNFα production and up-regulation of maturation markers. In contrast, all bifidobacteria and certain lactobacilli strains were low IL-12 and TNFα inducers (Weiss et al., 2011). *Bifidobacteria* antiviral properties are not solely related to immune system action modulation. *Bifidobacterium longum* CECT 7210 was shown to inhibit *in vitro* rotavirus replication and protect cells from virus infection. Furthermore, the strain was demonstrated to act *in vivo* on murine model (Munoz et al., 2011).

6. Summary

The results of the study indicate that the impact of microorganisms on host intestinal epithelial cells is strain-specific. Response of the enterocytes to 12 bacterial strains and mixture of several strains showed ability of microbial species to modulate 10.7 thousands human genes in total. Average number of differentially expressed genes modulated by single strain was 1.1 thousands. The highest similarity in gene expression pattern was observed for group of pathogenic strains. Whereas the most divergent were probiotic strains. Between-group comparison revealed the highest consistency in joint differentially expressed genes modulated in the same pattern of expression for probiotic and commensal strains. Whereas the most divergent were probiotic and pathogenic strains. Responsome analysis showing an opposite gene modulation scheme may be used as guidelines for further tests on probiotic strain to be used for treatment of disorder caused by specific pathogen. In case where two probiotics modulate substantial number of the same genes in opposite way such a knowledge suggests they should not be used in the same dietary supplement. The microarray data does provide information of biological importance and might serve as guidance for discovering microbial strain effect on host cells or even organism. Although bacteria can modulate different genes in strain specific fashion, their action is sometimes aimed to similar host cell processes. Genes which products are involved in metabolic pathways were mostly modulated. Within this general pathway the most targeted was purine metabolism. Regarding genetic information processing the protein processing in endoplasmic reticulum was most responsive to bacteria tested. Among signalling pathways involved in environmental information processing the PI3K-Akt, MAPK, and Rap1 signalling pathways were changed by the bacteria. Also cellular processes such as: regulation of actin cytoskeleton, focal adhesion, and endocytosis were most influenced. Data mining indicated also a possible influence of bacteria on organismal systems. These concerned for example leukocyte transendothelial migration and toll-like receptor signalling pathway. Bacterial action on enterocytes additionally revealed

their possible participation in diseases development mainly through regulation of signalling during carcinogenesis (including virus induced) and modification of proteoglycans in cancer cells. Modulation of genes involved in diseases indicate possible use of bacterial strains in treatment or specify therapeutic targets in case of diseases induced by pathogens.

Microarray results data mining revealed biological processes that the bacterial strains are capable to modify. One of them was response to viral infection. Among bacterial strains tested the *E. coli* Nissle 1917 was identified as most probable to interfere with viral processes. More detailed study showed that the strain possesses both prophylactic and therapeutic capacity to reduce the outcome of rotavirus infection. The Nissle 1917 strain action is directed both to prevent virus from hijack cellular control and prevent virus replication. Rotavirus infected differentiated Caco-2 cells pre- and postinfection treated with *E. coli* Nissle 1917 provided decreased virus replication. Preinfection treatment changed expression of genes involved in apoptosis regulation to redirect cells to necroptosis. It also enhanced innate anti-viral responses and pro-inflammatory paracrine signalling.

The challenges for understanding host-microbial interactions are intimately connected with human health. The first question arising is: how a specific strain modulates gene expression and metabolism of intestinal epithelial cells? There is a good evidence from animal models that microbiota is indispensable for health and wellbeing, as well as can trigger number of pathologies. However, little is known about molecular mechanisms of host-microbe interactions and their outcome on local and systemic level. What microbial molecules drive modulation of biological processes in intestinal epithelial cells? What is the molecular basis for the differential ability of distinct commensal and pathogenic species to trigger different signalling pathways? Why do some strains of given species exert powerful effect on specific process, whereas others of the same species are essentially mute for it?

It must be remembered that gut microbiota also include viruses, and eukaryotes (fungi and protozoa). These other elements of the microbial community have coevolved in this environment and undoubtedly provide fascinating targets for further exploration of host-microbe relationships. Deeper insight into the relationships will certainly grant exciting new opportunities to improve human health.

The bacteria alone affect our life in ways no one ever expected. The future of personalized nutrition and medicine will not be complete until we understand our microbiome. Recently proposed enterotypes are just a prologue to customised medical treatments as bacteria influence our metabolism and metabolise

xenobiotics. The personal bacterial community may be both a diagnostic marker and treatment target as its balance is important to health. A potential therapy may be composed of bacteria, but also viruses and fungi. However, therapy may apply to the whole microbiota. It was found to be the most effective in case of recurrent *Clostridium difficile*-infection. However, a list of diseases treated with bacteriotherapy (called also fecal microbiota transplantation) is growing (Guo et al., 2012; Khoruts and Sadowsky, 2011). As the personal microbiome is dynamic it would need to be updated many times in a lifetime to serve for its therapeutical purpose.

7. Conclusions

1. Enormous genetic diversity regarding strains of bacterial species results in strain-specific transcriptomic responses of intestinal epithelial cells stimulated with bacteria. Approximately 30% of the human protein coding genes were shown to be modulated by bacterial species, where single species were capable to influence transcription from 0.38 to 2.8 thousand genes.
2. Although the bacterial strains modulate diverse sets of genes, products of the genes are involved in similar metabolic, signalling, cellular and disease pathways. This indicates convergence in targeted processes, components and functions of the host cells. Therefore there are groups of genes involved in specific host biological processes that show traits of species- or genus-specific regulation.
3. The *in vitro* gut model used to simulate bacteria-host interactions and microarray analysis of gene transcription followed by data mining proved to allow identification of biological processes in host cells influenced by microorganisms. The only limiting factor is extent of gene products annotation to recognise modified biological processes.
4. Overrepresentation of biological processes belonging to general biological process category in analysis of strain influence on enterocytes demonstrated to be informative in pointing health aspects that analysed strain effectively modulates.

References

Abubucker, S., Segata, N., Goll, J., Schubert, A. M., Izard, J., Cantarel, B. L., Rodriguez-Mueller, B., Zucker, J., Thiagarajan, M., Henrissat, B., White, O., Kelley, S. T., Methe, B., Schloss, P. D., Gevers, D., Mitreva, M., Huttenhower, C. (2012). Metabolic reconstruction for metagenomic data and its application to the human microbiome. PLoS Comput Biol., 8(6); e1002358.

Adams, J. B., Johansen, L. J., Powell, L. D., Quig, D., Rubin, R. A. (2011). Gastrointestinal flora and gastrointestinal status in children with autism--comparisons to typical children and correlation with autism severity. BMC Gastroenterol., 11, 22.

Aktan, I., Dunkel, B., Cunningham, F. M. (2013). Equine platelets inhibit E. coli growth and can be activated by bacterial lipopolysaccharide and lipoteichoic acid although superoxide anion production does not occur and platelet activation is not associated with enhanced production by neutrophils. Vet. Immunol. Immunopathol., 152(3-4), 209-217.

Alexopoulou, L., Holt, A. C., Medzhitov, R., Flavell, R. A. (2001). Recognition of double-stranded RNA and activation of NF-kappaB by Toll-like receptor 3. Nature, 413(6857), 732-728.

Amar, J., Chabo, C., Waget, A., Klopp, P., Vachoux, C., Bermudez-Humaran, L. G., …, Burcelin, R. (2011a). Intestinal mucosal adherence and translocation of commensal bacteria at the early onset of type 2 diabetes: molecular mechanisms and probiotic treatment. EMBO Mol. Med., 3(9), 559-572.

Amar, J., Serino, M., Lange, C., Chabo, C., Iacovoni, J., Mondot, S.,…, Burcelin, R. (2011b). Involvement of tissue bacteria in the onset of diabetes in humans: evidence for a concept. Diabetologia, 54(12), 3055-3061.

Arnold, M. M., Barro, M., Patton, J. T. (2013a). Rotavirus NSP1 mediates degradation of interferon regulatory factors through targeting of the dimerization domain. J. Virol., 87(17), 9813-921.

Arnold, M. M., Patton, J. T. (2011). Diversity of interferon antagonist activities mediated by NSP1 proteins of different rotavirus strains. J. Virol., 85(5), 1970-1979.

Arnold, M. M., Sen, A., Greenberg, H. B., Patton, J. T. (2013b). The battle between rotavirus and its host for control of the interferon signaling pathway. PLoS Pathog., 9(1), e1003064.

Arumugam, M., Raes, J., Pelletier, E., Le Paslier, D., Yamada, T., Mende, D. R., …, Bork, P. (2011). Enterotypes of the human gut microbiome. Nature, 473(7346), 174-180.

Ashburner, M., Ball, C. A., Blake, J. A., Botstein, D., Butler, H., Cherry, J. M., …, Sherlock, G. (2000). Gene ontology: tool for the unification of biology. The Gene Ontology Consortium. Nat. Genet., 25, 25-29.

Atienza, J. M., Yu, N., Kirstein, S. L., Xi, B., Wang, X., Xu, X., Abassi, Y. A. (2006). Dynamic and label-free cell-based assays using the real-time cell electronic sensing system. Assay Drug. Dev. Technol., 4(5), 597-607.

Ayala-Breton, C., Arias, M., Espinosa, R., Romero, P., Arias, C. F., Lopez, S. (2009). Analysis of the kinetics of transcription and replication of the rotavirus genome by RNA interference. J. Virol., 83(17), 8819-8831.

Azevedo, M.,S., Yuan, L., Pouly, S., Gonzales, A. M., Jeong, K. I., Nguyen, T. V., Saif, L. J. (2006). Cytokine responses in gnotobiotic pigs after infection with virulent or attenuated human rotavirus. J. Virol., 80(1), 372-382.

Bäckhed, F., Manchester, J. K., Semenkovich, C. F., Gordon, J. I. (2007). Mechanisms underlying the resistance to diet-induced obesity in germ-free mice. Proc. Natl. Acad. Sci. USA, 104(3), 979-984.

Bagchi, P., Bhowmick, R., Nandi, S., Kant Nayak, M., Chawla-Sarkar, M. (2013a). Rotavirus NSP1 inhibits interferon induced non-canonical NF-kB activation by interacting with TNF receptor associated factor 2. Virology, 444(1-2), 41-44.

Bagchi, P., Nandi, S., Nayak, M. K., Chawla-Sarkar, M. (2013b). Molecular mechanism behind rotavirus NSP1-mediated PI3 kinase activation: interaction between NSP1 and the p85 subunit of PI3 kinase. J. Virol. 87(4), 2358--2362.

Barbeiro, H. V., Barbeiro, D. F., Debbas, V., Souza, H. P., Laurindo, F. R., Velasco, I. T., Soriano, F. G. (2009). Purine nucleotides reduce superoxide production by nitric oxide synthase in a murine sepsis model. Braz. J. Med. Biol. Res., 42(11), 1050-1057.

Bartee, E., Mohamed, M. R., Lopez, M. C., Baker, H. V., McFadden, G. (2009). The addition of tumor necrosis factor plus beta interferon induces a novel synergistic antiviral state against poxviruses in primary human fibroblasts. J. Virol., 83(2), 498-511.

Basu, S., Paul, D. K., Ganguly, S., Chatterjee, M., Chandra, P. K. (2009). Efficacy of high-dose Lactobacillus rhamnosus GG in controlling acute watery

diarrhea in Indian children: a randomized controlled trial. J. Clin. Gastroenterol., 43(3), 208-213.

Baylis, S. A., Finsterbusch, T., Bannert, N., Blümel, J., Mankertz, A. (2011). Analysis of porcine circovirus type 1 detected in Rotarix vaccine. Vaccine, 29(4), 690-697.

Belcher, C. E., Drenkow, J., Kehoe, B., Gingeras, T. R., McNamara, N., Lemjabbar, H., …, Relman, D. A. (2000). The transcriptional responses of respiratory epithelial cells to Bordetella pertussis reveal host defensive and pathogen counter-defensive strategies. Proc. Natl. Acad. Sci. USA, 97, 13847-13852.

Bercik, P., Collins, S. M., Verdu, E. F. (2012). Microbes and the gut-brain axis. Neurogastroenterol. Motil., 24(5), 405-413.

Bercik, P., Denou, E., Collins, J., Jackson, W., Lu, J., Jury, J., …, Collins, S. M. (2011). The intestinal microbiota affect central levels of brain-derived neurotropic factor and behavior in mice. Gastroenterology, 141(2), 599-609.

Bercik, P., Verdu, E. F., Foster, J. A., Lu, J., Scharringa, A., Kean, I., …, Collins, S. M. (2009). Role of gut-brain axis in persistent abnormal feeding behavior in mice following eradication of Helicobacter pylori infection. Am. J. Physiol. Regul. Integr. Comp. Physiol., 296(3), R587-594.

Bercik, P., Verdu, E. F., Foster, J. A., Macri, J., Potter, M., Huang, X., …, Collins, S. M. (2010). Chronic gastrointestinal inflammation induces anxiety-like behavior and alters central nervous system biochemistry in mice. Gastroenterology, 139(6), 2102-2112.

Berggren, A., Lazou Ahren, I., Larsson, N., Önning, G. (2011). Randomised, double-blind and placebo-controlled study using new probiotic lactobacilli for strengthening the body immune defence against viral infections. Eur. J. Nutr., 50(3), 203-210.

Berk, A. J., Boyer, T. G., Kapanidis, A. N., Ebright, R. H., Kobayashi, N. N., Horn, P. J., …, Triezenberg, S. J. (1998). Mechanisms of viral activators. Cold Spring Harb. Symp. Quant. Biol., 63, 243-252.

Bernstein, D. I. (2006). Live attenuated human rotavirus vaccine, Rotarix. Semin. Pediatr. Infect. Dis., 17(4), 188-194.

Bernstein, D. I. (2009). Rotavirus overview. Pediatr. Infect. Dis. J., 28(3 Suppl.), S50-53.

Bhavsar, A. P., Guttman, J. A., Finlay, B. B. (2007). Manipulation of host-cell pathways by bacterial pathogens. Nature, 449(7164), 827-834.

Bhowmick, R., Halder, U. C., Chattopadhyay, S., Nayak, M. K., Chawla-Sarkar, M. (2013). Rotavirus-encoded nonstructural protein 1 modulates cellular apoptotic machinery by targeting tumor suppressor protein p53. J. Virol., 87(12), 6840-6850.

Biasin, M., Piacentini, L., Lo Caputo, S., Naddeo, V., Pierotti, P., Borelli, M., …, Clerici, M. (2010). TLR activation pathways in HIV-1-exposed seronegative individuals. J. Immunol., 184(5), 2710-2717.

Bojarski, C., Gitter, A. H., Bendfeldt, K., Mankertz, J., Schmitz, H., Wagner, S., …, Schulzke, J. D. (2001). Permeability of human HT-29/B6 colonic epithelium as a function of apoptosis. J. Physiol., 535, 541-552.

Bojarski, C., Weiske, J., Schöneberg, T., Schröder, W., Mankertz, J., Schulzke, J. D., …, Huber, O. (2004). The specific fates of tight junction proteins in apoptotic epithelial cells. J. Cell. Sci., 117, 2097-2107.

Bolton, M., van der Straten, A., Cohen, C. R. (2008). Probiotics: potential to prevent HIV and sexually transmitted infections in women. Sex. Transm. Dis., 35(3), 214-225.

Boroni Moreira, A. P., de Cassia Goncalves Alfenas, R. (2012). The influence of endotoxemia on the molecular mechanisms of insulin resistance. Nutr. Hosp., 27(2), 382-390.

Bottacini, F., Medini, D., Pavesi, A., Turroni, F., Foroni, E., Riley, D., …, Ventura, M. (2010). Comparative genomics of the genus Bifidobacterium. Microbiology, 156(Pt 11), 3243-3254.

Bravo, J. A., Forsythe, P., Chew, M. V., Escaravage, E., Savignac, H. M., Dinan, T. G., Bienenstock, J., Cryan, J. F. (2011). Ingestion of Lactobacillus strain regulates emotional behavior and central GABA receptor expression in a mouse via the vagus nerve. Proc. Natl. Acad. Sci. USA, 108(38), 16050--16055.

Brown, J. M., Hazenm S. L. (2014). Metaorganismal nutrient metabolism as a basis of cardiovascular disease. Curr. Opin. Lipidol., 25(1), 48-53.

Brunet, J. P., Jourdan, N., Cotte-Laffitte, J., Linxe, C., Geniteau-Legendre, M., Servin, A., Quero, A. M. (2000). Rotavirus infection induces cytoskeleton disorganization in human intestinal epithelial cells: implication of an increase in intracellular calcium concentration. J. Virol., 74, 10801-10806.

Bruni, D., Sebastia, J., Dunne, S., Schröder, M., Butler, M. P. (2013). A novel IRAK1-IKKε signaling axis limits the activation of TAK1-IKKβ downstream of TLR3. J. Immunol., 190(6), 2844-2856.

Campagna, M., Eichwald, C., Vascotto, F., Burrone, O. R. (2005). RNA interference of rotavirus segment 11 mRNA reveals the essential role of NSP5 in the virus replicative cycle. J. Gen. Virol., 86, Pt 5, 1481-1487.

Cani, P. D., Delzenne, N. M. (2009). The role of the gut microbiota in energy metabolism and metabolic disease. Curr. Pharm. Des., 15(13), 1546-1558.

Casola, A., Estes, M. K., Crawford, S. E., Ogra, P. L., Ernst, P. B., Garofalo, R. P., Crowe, S. E. (1998). Rotavirus infection of cultured intestinal epithe-

lial cells induces secretion of CXC and CC chemokines. Gastroenterology, 114(5), 947-955.

Chaibi, C., Cotte-Laffitte, J., Sandre, C., Esclatine, A., Servin, A. L., Quero, A. M., Geniteau-Legendre, M. (2005). Rotavirus induces apoptosis in fully differentiated human intestinal Caco-2 cells. Virology, 332, 480-490.

Chen, W. T., Alpert, A., Leiter, C., Gong, F., Jackson, S. P., Miller, K. M. (2013). Systematic identification of functional residues in mammalian histone H2AX. Mol. Cell. Biol., 33(1), 111-126.

Chouraqui, J. P., Van Egroo, L. D., Fichot, M. C. (2004). Acidified milk formula supplemented with bifidobacterium lactis: impact on infant diarrhea in residential care settings. J. Pediatr. Gastroenterol. Nutr., 38, 288-292.

Chung, K. T., McCrae, M. A. (2011). Regulation of gene expression by the NSP1 and NSP3 non-structural proteins of rotavirus. Arch. Virol., 156(12), 2197-2203.

Claudio, N., Dalet, A., Gatti, E., Pierre, P. (2013). Mapping the crossroads of immune activation and cellular stress response pathways. EMBO J., 32(9), 1214-1224.

Conterno, L., Fava, F., Viola, R., Tuohy, K. M. (2011). Obesity and the gut microbiota: does up-regulating colonic fermentation protect against obesity and metabolic disease? Genes Nutr., 6(3), 241-260.

Costello, E. K., Stagaman, K., Dethlefsen, L., Bohannan, B. J., Relman, D. A. (2012). The application of ecological theory toward an understanding of the human microbiome. Science, 336(6086), 1255-1262.

Cotillard, A., Kennedy, S. P., Kong, L. C., Prifti, E., Pons, N., Le Chatelier, E., …, Ehrlich, S. D. (2013). Dietary intervention impact on gut microbial gene richness. Nature, 500(7464), 585-588.

Crumeyrolle-Arias, M., Jaglin, M., Bruneau, A., Vancassel, S., Cardona, A., Dauge, V., …, Rabot, S. (2014). Absence of the gut microbiota enhances anxiety-like behavior and neuroendocrine response to acute stress in rats. Psychoneuroendocrinology, 42, 207-217.

Cryan, J. F., Dinan, T. G. (2012). Mind-altering microorganisms: the impact of the gut microbiota on brain and behaviour. Nat. Rev. Neurosci., 13(10), 701-712.

Cuevas-Ramos, G., Petit, C. R, Marcq, I., Boury, M., Oswald, E., Nougayrède, J. P. (2010). *Escherichia coli* induces DNA damage in vivo and triggers genomic instability in mammalian cells. Proc. Natl. Acad. Sci. USA, 107(25), 11537-11542.

Cui, W., Taub, D. D., Gardner, K. (2007). qPrimerDepot: a primer database for quantitative real time PCR. Nucleic Acids Res., 35 (Database issue), D805-809.

Dalmasso, G., Nguyen, H. T., Yan, Y., Laroui, H., Charania, M. A., Ayyadurai, S., Sitaraman, S. V., Merlin, D. (2011). Microbiota modulate host gene expression via microRNAs. PLoS One, 6(4), e19293.

Dang, D. A., Nguyen, V. T., Vu, D. T., Nguyen, T. H., Nguyen, D. M., Yuhuan, Le, T. L. (2012). A dose-escalation safety and immunogenicity study of a new live attenuated human rotavirus vaccine (Rotavin-M1) in Vietnamese children. Vaccine. 30 Suppl 1. A114-121.

Darding, M., Meier, P. (2012). IAPs: guardians of RIPK1. Cell Death Differ, 19(1), 58-66.

David, L. A., Maurice, C. F., Carmody, R. N., Gootenberg, D. B., Button, J. E., Wolfe, B. E., …, Turnbaugh, P. J. (2014). Diet rapidly and reproducibly alters the human gut microbiome. Nature, 505(7484), 559-563.

Davidson, L. E., Fiorinom A. M., Snydmanm D. R., Hibberdm P. L. (2011). Lactobacillus GG as an immune adjuvant for live-attenuated influenza vaccine in healthy adults: a randomized double-blind placebo-controlled trial. Eur. J. Clin. Nutr., 65(4), 501-507.

De Filippo, C., Cavalieri, D., Di Paola, M., Ramazzotti, M., Poullet, J. B., Massart, S., …, Lionetti, P. (2010). Impact of diet in shaping gut microbiota revealed by a comparative study in children from Europe and rural Africa. Proc. Natl. Acad. Sci. USA, 107(33), 14691-14696.

Delorme-Axford, E., Coyne, C. B. (2011). The actin cytoskeleton as a barrier to virus infection of polarized epithelial cells. Viruses, 3(12), 2462-2477.

Desbonnet, L., Garrett, L., Clarke, G., Bienenstock, J., Dinan, T. G. (2008). The probiotic Bifidobacteria infantis: An assessment of potential antidepressant properties in the rat. J. Psychiatr. Res., 43(2), 164-174.

Desbonnet, L., Garrett, L., Clarke, G., Kiely, B., Cryan, J. F., Dinan, T. G. (2010). Effects of the probiotic Bifidobacterium infantis in the maternal separation model of depression. Neuroscience, 170(4), 1179-1188.

Dey, A., Mantri, C. K., Pandhare-Dash, J., Liu, B., Pratap, S., Dash, C. (2011). Downregulation of APOBEC3G by xenotropic murine leukemia-virus related virus (XMRV) in prostate cancer cells. Virol. J., 8, 531.

Diaz Heijtz, R., Wang, S., Anuar, F., Qian, Y., Björkholm, B., Samuelsson, A., …, Pettersson, S. (2011). Normal gut microbiota modulates brain development and behavior. Proc. Natl. Acad. Sci. U S A, 108(7), 3047-3052.

Diehl, G. E., Longman, R. S., Zhang, J. X., Breart, B., Galan, C., Cuesta, …, Littman, D. R. (2013). Microbiota restricts trafficking of bacteria to mesenteric lymph nodes by CX(3)CR1(hi) cells. Nature, 494(7435), 116-120.

Douillard, F. P., Ribbera, A., Kant, R., Pietilä, T. E., Järvinen, H. M., Messing, M., …, de Vos, W. M. (2013). Comparative genomic and functional analysis of 100 Lactobacillus rhamnosus strains and their comparison with strain GG. PLoS Genet., 9(8), e1003683.

Dubey, A. P., Rajeshwari, K., Chakravarty, A., Famularo, G. (2008). Use of VSL#3 in the treatment of rotavirus diarrhea in children: preliminary results. J. Clin. Gastroenterol., 42 Suppl. 3 Pt 1, S126-129.

Duffy, L. C., Zielezny, M. A., Riepenhoff-Talty, M., Dryja, D., Sayahtaheri-Altaie, S., Griffiths, E., …, Ogra, P. L. (1994). Effectiveness of Bifidobacterium bifidum in mediating the clinical course of murine rotavirus diarrhea. Pediatr. Res., 35, 690-695.

Dugger, K., Lowder, T. W., Tucker, T. A., Schwiebert, L. M. (2009). Epithelial cells as immune effector cells: the role of CD40. Semin. Immunol., 21(5), 289-292.

Dutta, D., Chattopadhyay, S., Bagchi, P., Halder, U. C., Nandi, S., Mukherjee, A., E., …, Chawla-Sarkar, M. (2011a). Active participation of cellular chaperone Hsp90 in regulating the function of rotavirus nonstructural protein 3 (NSP3). J. Biol. Chem., 286(22), 20065-20077.

Dutta, P., Mitra, U., Dutta, S., Rajendran, K., Saha, T. K., Chatterjee, M. K. (2011b). Randomised controlled clinical trial of Lactobacillus sporogenes (Bacillus coagulans)., used as probiotic in clinical practice., on acute watery diarrhoea in children. Trop. Med. Int. Health., 16(5), 555-561.

Eckburg, P. B., Bik, E. M., Bernstein, C. N., Purdom, E., Dethlefsen, L., Sargent, M., …, Relman, D. A. (2005). Diversity of the human intestinal microbial flora. Science, 308, 1635-1638.

Eckmann, L., Smith, J. R., Housley, M. P., Dwinell, M. B., Kagnoff, M. F. (2000). Analysis by high density cDNA arrays of altered gene expression in human intestinal epithelial cells in response to infection with the invasive enteric bacteria Salmonella. J. Biol. Chem., 275, 14084-14094.

EFSA. (2009). Scientific opinion on the substantiation of health claims related to non-characterised microorganisms pursuant to Article 13 of Regulation (EC) No 1924/2006 on request from the European Commission. EFSA J., 7(9), 1247. doi: 10.2903/j.efsa.2009.1247

El Maadidi, S., Faletti, L., Berg, B., Wenzl, C., Wieland, K., Chen, Z. J., …, Borner, C. (2014). A novel mitochondrial MAVS/Caspase-8 platform links RNA virus-induced innate antiviral signaling to Bax/Bak-independent apoptosis. J. Immunol., 192(3), 1171-1183.

Erdogan, O., Tanyeri, B., Torun, E., Gönüllü, E., Arslan, H., Erenberk, U., Oktem, F. (2012). The comparition of the efficacy of two different probiotics in rotavirus gastroenteritis in children. J. Trop. Med., 2012, 787240.

Faith, J. J., Guruge, J. L., Charbonneau, M., Subramanian, S., Seedorf, H., Goodman, A.L., Gordon, J. I. (2013). The long-term stability of the human gut microbiota. Science, 341(6141). doi: 10.1126/science.1237439

Fang, S. B., Lee, H. C., Hu, J. J., Hou, S. Y., Liu, H. L., Fang, H. W. (2009). Dose-dependent effect of Lactobacillus rhamnosus on quantitative reduction of faecal rotavirus shedding in children. J. Trop. Pediatr., 55(5), 297-301.

Finsterbusch, T., Mankertz, A. (2009). Porcine circoviruses – small but powerful. Virus Res., 143(2), 177-183.

Fleissner, C. K., Huebel, N., Abd El-Bary, M. M., Loh, G., Klaus, S., Blaut, M. (2010). Absence of intestinal microbiota does not protect mice from diet-induced obesity. Br. J. Nutr., 104(6), 919-929.

Forchielli, M. L., Walker, W. A. (2005). The role of gut-associated lymphoid tissues and mucosal defence. Br. J. Nutr., 93 Suppl. 1, S41-48.

Forsythe, P., Kunze, W. A. (2013). Voices from within: gut microbes and the CNS. Cell. Mol. Life Sci., 70(1), 55-69.

Fox, C. H., Dang, G. (2004). Probiotics in the prevention and treatment of diarrhea. J. Altern. Complement. Med., 10, 601-603.

Fredslund, J., Schauser, L., Madsen, L. H., Sandal, N., Stougaard, J. (2005). PriFi: using a multiple alignment of related sequences to find primers for amplification of homologs. Nucleic Acids Res., 33 (Web Server issue), W516-520.

Fujita, F., Taniguchi, Y., Kato, T., Narita, Y., Furuya, A., Ogawa, T., …, Nakanishi, M. (2003). Identification of NAP1., a regulatory subunit of IkappaB kinase-related kinases that potentiates NF-kappaB signaling. Mol. Cell. Biol., 23, 7780-7793.

Fukushima, K., Ogawa, H., Takahashi, K., Naito, H., Funayama, Y., Kitayama, T., …, Sasaki, I. (2003). Non-pathogenic bacteria modulate colonic epithelial gene expression in germ-free mice. Scand. J. Gastroenterol., 38, 626-634.

Fukushima, Y., Kawata, Y., Hara, H., Terada, A., Mitsuoka, T. (1998). Effect of a probiotic formula on intestinal immunoglobulin A production in healthy children. Int. J. Food. Microbiol., 42, 39-44.

Funami, K., Sasai, M., Ohba, Y., Oshiumi, H., Seya, T., Matsumoto, M. (2007). Spatiotemporal mobilization of Toll/IL-1 receptor domain-containing adaptor molecule-1 in response to dsRNA. J. Immunol., 179(10), 6867-6872.

Gac, M., Bigda, J., Vahlenkamp, T. W. (2010). Increased mitochondrial superoxide dismutase expression and lowered production of reactive oxygen species during rotavirus infection. Virology, 404(2), 293-303.

Gene Ontology website. accessed on Jun 30, 2014 at: http://www.geneontology.org/GO.current.annotations.shtml

Gentleman, R. C., Carey, V. J., Bates, D. M., Bolstad, B., Dettling, M., Dudoit, S., …, Zhang, J. (2004). Bioconductor: open software development for computational biology and bioinformatics. Genome Biol., 5, R80.

Gilbert, S. F. (2000). Cross-talk between pathways. In: Developmental biology. Sunderland (MA): Sinauer Associates. Available from: http://www.ncbi.nlm.nih.gov/books/NBK10087/

Gillick, K., Pollpeter, D., Phalora, P., Kim, E. Y., Wolinsky, S. M., Malim, M. H. (2013). Suppression of HIV-1 infection by APOBEC3 proteins in primary human CD4(+) T cells is associated with inhibition of processive reverse transcription as well as excessive cytidine deamination. J. Virol., 87(3), 1508-1517.

Gilliland, S. M., Forrest, L., Carre, H., Jenkins, A., Berry, N., Martin, J., …, Schepelmann, S. (2012). Investigation of porcine circovirus contamination in human vaccines. Biologicals, 40(4), 270-277.

Gillis, J., Mistry, M., Pavlidis, P. (2010). Gene function analysis in complex data sets using ErmineJ. Nat. Protoc., 5(6), 1148-1159.

Glass, R. I., Parashar, U. D., Bresee, J. S., Turcios, R., Fischer, T. K., Widdowson, M. A., Jiang, B., Gentsch, J. R. (2006). Rotavirus vaccines: current prospects and future challenges. Lancet, 368(9532), 323-332.

Goehler, L. E., Park, S. M., Opitz, N., Lyte, M., Gaykema, R. P. (2008). Campylobacter jejuni infection increases anxiety-like behavior in the holeboard: possible anatomical substrates for viscerosensory modulation of exploratory behavior. Brain Behav. Immun., 22(3), 354-366.

Goncalves, A., Bürckstümmer, T., Dixit, E., Scheicher, R., Górna, M. W., Karayel, E., …, Superti-Furga, G. (2011). Functional dissection of the TBK1 molecular network. PLoS One, 6(9), e23971.

Gonzalez, A., Stombaugh, J., Lozupone, C., Turnbaugh, P. J., Gordon, J. I., Knight, R. (2011). The mind-body-microbial continuum. Dialog. Clin. Neurosci., 13(1), 55-62.

Graff, J.W., Ettayebi, K., Hardy, M. E. (2009). Rotavirus NSP1 inhibits NFkappaB activation by inducing proteasome-dependent degradation of beta-TrCP: a novel mechanism of IFN antagonism. PLoS Pathog., 5(1), e1000280.

Gram, A. M., Frenkel, J., Ressing, M. E. (2012). Inflammasomes and viruses: cellular defence versus viral offence. J. Gen. Virol., 93(Pt 10), 2063-2075.

Grandy, G., Medina, M., Soria, R., Teran, C. G., Araya, M. (2010). Probiotics in the treatment of acute rotavirus diarrhoea. A randomized., double-blind., controlled trial using two different probiotic preparations in Bolivian children. BMC Infect. Dis., 10, 253.

Greco-Stewart, V. S., Schissel, E., Pelchat, M. (2009). The hepatitis delta virus RNA genome interacts with the human RNA polymerases I and III. Virology, 386(1), 12-15.

Greenberg, H. B., Estes, M. K. (2009). Rotaviruses: from pathogenesis to vaccination. Gastroenterology, 136(6), 1939-1951.

Grubbs, F. (1969). Procedures for detecting outlying observations in samples. Technometrics, 11(1), 1-21.

Grunert, M., Gottschalk, K., Kapahnke, J., Gündisch, S., Kieser, A., Jeremias, I. (2012). The adaptor protein FADD and the initiator caspase-8 mediate activation of NF-κB by TRAIL. Cell Death Dis., 3, e414.

Guandalini, S. (2011). Probiotics for prevention and treatment of diarrhea. J. Clin. Gastroenterol., 45 Suppl. S149-153.

Guerra, L., Guidi, R., Frisan, T. (2011). Do bacterial genotoxins contribute to chronic inflammation., genomic instability and tumor progression? FEBS J., 278(23), 4577-4588.

Gunsten, S., Mikols, C. L., Grayson, M. H., Schwendener, R. A., Agapov, E., Tidwell, R. M., Walter, M. J. (2009). IL-12 p80-dependent macrophage recruitment primes the host for increased survival following a lethal respiratory viral infection. Immunology, 126(4), 500-513.

Guo, B., Harstall, C., Louie, T., Veldhuyzen van Zanten, S., Dieleman, L. A. (2012). Systematic review: faecal transplantation for the treatment of Clostridium difficile-associated disease. Aliment. Pharmacol. Ther., 35(8), 865-875.

Guzzo, C., Ayer, A., Basta, S., Banfield, B. W., Gee, K. (2012). IL-27 enhances LPS-induced proinflammatory cytokine production via upregulation of TLR4 expression and signaling in human monocytes. J. Immunol., 188(2), 864-873.

Halbleib, J. M., Sääf, A. M., Brown, P. O., Nelson, W. J. (2007). Transcriptional modulation of genes encoding structural characteristics of differentiating enterocytes during development of a polarized epithelium in vitro. Mol. Biol. Cell., 18(11), 4261-4278.

Hancock, V., Vejborg, R. M., Klemm, P. (2010). Functional genomics of probiotic Escherichia coli Nissle 1917 and 83972., and UPEC strain CFT073: comparison of transcriptomes., growth and biofilm formation. Mol. Genet. Genomics, 284(6), 437-454.

Henker, J., Laass, M., Blokhin, B. M., Bolbot, Y. K., Maydannik, V. G., Elze, M., …, Schulze, J. (2007). The probiotic *Escherichia coli* strain Nissle 1917 (EcN) stops acute diarrhoea in infants and toddlers. Eur. J. Pediatr., 166(4), 311-318.

Henker, J., Laass, M. W., Blokhin, B. M., Maydannik, V. G., Bolbot, Y. K., Elze, M., …, Schulze, J. (2008). Probiotic *Escherichia coli* Nissle 1917 versus placebo for treating diarrhea of greater than 4 days duration in infants and toddlers. Pediatr. Infect. Dis. J., 27(6), 494-499.

Hoffmann, C., Dollive, S., Grunberg, S., Chen, J., Li, H., Wu, G. D., …, Bushman, F. D. (2013). Archaea and fungi of the human gut microbiome: correlations with diet and bacterial residents. PLoS One, 8(6), e66019.

Holloway, G., Coulson, B. S. (2013). Innate cellular responses to rotavirus infection. J. Gen. Virol., 94(Pt 6), 1151-1160.

Holscher, H. D., Czerkies, L. A., Cekola, P., Litov, R., Benbow, M., Santema, S., …, Tappenden, K. A. (2012). Bifidobacterium lactis Bb12 enhances intestinal antibody response in formula-fed infants: a randomized, double-blind, controlled trial. JPEN J. Parenter. Enteral. Nutr., 36(1 Suppl.), 106S-117S.

de Hoon, M. J., Imoto, S., Nolan, J., Miyano, S. (2004). Open source clustering software. Bioinformatics, 20, 1453-1454.

Hooper, L. V., Littman, D. R., Macpherson, A. J. (2012). Interactions between the microbiota and the immune system. Science, 336(6086), 1268-1273.

Hu, X., Bonde, Y., Eggertsen, G., Rudling, M. (2014). Muricholic bile acids are potent regulators of bile acid synthesis via a positive feedback mechanism. J. Intern. Med., 275(1), 27-38.

Huang da, W., Sherman, B. T., Lempicki, R. A. (2009). Systematic and integrative analysis of large gene lists using DAVID bioinformatics resources. Nat. Protoc., 4(1), 44-57.

Human Microbiome Project Consortium. (2012a). Structure, function and diversity of the healthy human microbiome. Nature, 486(7402), 207-214.

Human Microbiome Project Consortium. (2012b). A framework for human microbiome research. Nature, 486(7402), 215-221.

Hummelen, R., Vos, A. P., van't Land, B., van Norren, K., Reid, G. (2010). Altered host-microbe interaction in HIV: a target for intervention with pro- and prebiotics. Int. Rev. Immunol., 29(5), 485-513.

Hyun, J., Kanagavelu, S., Fukata, M. (2013). A unique host defense pathway: TRIF mediates both antiviral and antibacterial immune responses. Microbes Infect., 15(1), 1-10.

Imahashi, M., Nakashima, M., Iwatami, I. (2012). Antiviral mechanizm and biochemical basis of the human APOBEC3 family. Front. Microbiol., 3, 250 (e-journal).

Iwai, A., Shiozaki, T., Miyazaki, T. (2013). Relevance of signaling molecules for apoptosis induction on influenza A virus replication. Biochem. Biophys. Res. Commun., 441(3), 531-537.

Jabs, W. J., Wagner, H. J., Maurmann, S., Hennig, H., Kreft, B. (2002). Inhibition of macrophage inflammatory protein-1 alpha production by Epstein--Barr virus. Blood, 99, 1512-1526.

Jäger, S., Stange, E. F., Wehkamp, J. (2013). Inflammatory bowel disease: an impaired barrier disease. Langenbecks Arch. Surg., 398(1), 1-12.

Jakobsson, H. E., Jernberg, C., Andersson, A. F., Sjölund-Karlsson, M., Jansson, J. K., Engstrand, L. (2010). Short-term antibiotic treatment has differing long-term impacts on the human throat and gut microbiome. PLoS One, 5(3), e9836.

Jepson, M. A., Schlecht, H. B., Collares-Buzato, C. B. (2000). Localization of dysfunctional tight junctions in Salmonella enterica serovar typhimurium-infected epithelial layers. Infect. Immun., 68, 7202-7208.

Jiang, B., Snipes-Magaldi, L., Dennehy, P., Keyserling, H., Holman, R. C., Bresee, J., Gentsch, J., Glass, R. I. (2003). Cytokines as mediators for or effectors against rotavirus disease in children. Clin. Diagn. Lab. Immunol., 10(6), 995-1001.

Johannessen, L. E., Spilsberg, B., Wiik-Nielsen, C. R., Kristoffersen, A. B., Holst-Jensen, A., Berdal, K. G. (2013). DNA-fragments are transcytosed across CaCo-2 cells by adsorptive endocytosis and vesicular mediated transport. PLoS One, 8(2), e56671.

Johansson, M. E., Ambort, D., Pelaseyed, T., Schütte, A., Gustafsson, J. K., Ermund, A., Hansson, G. C. (2011). Composition and functional role of the mucus layers in the intestine. Cell. Mol. Life Sci., 68(22), 3635-3641.

Johansson, M. E., Hansson, G. C. (2013). Mucus and the goblet cell. Dig. Dis., 31(3-4), 305-309.

de Jong, H. K., Parrym C. M., van der Poll, T., Wiersinga, W. J. (2012). Host-pathogen interaction in invasive Salmonellosis. PLoS Pathog., 8(10), e1002933.

Jourdan, N., Maurice, M., Delautier, D., Quero, A. M., Servin, A. L., Trugnan, G. (1997). Rotavirus is released from the apical surface of cultured human intestinal cells through nonconventional vesicular transport that bypasses the Golgi apparatus. J. Virol., 71, 8268-8278.

Jumpertz, R., Le, D. S., Turnbaugh, P. J., Trinidad, C., Bogardus, C., Gordon, J. I., Krakoff, J. (2011). Energy-balance studies reveal associations between gut microbes., caloric load., and nutrient absorption in humans. Am. J. Clin. Nutr., 94(1), 58-65.

Jungersen, M., Wind, A., Johansen, E., Christensen, J. E., Stuer-Lauridsen, B., Eskesen, D. (2014). The science behind the probiotic strain *Bifidobacterium animalis* subsp. *lactis* BB-12. Microorganisms, 2, 92-110.

Juste, C., Kreil, D. P., Beauvallet, C., Guillot, A., Vaca, S., Carapito, C., …, Dore J. (2014). Bacterial protein signals are associated with Crohn's disease. Gut., 63(10), 1566-1577. doi: 10.1136/gutjnl-2012-303786

Kabeerdoss, J., Devi, R. S., Mary, R. R., Prabhavathi, D., Vidya, R., Mechenro, J., …, Ramakrishna, B. S. (2011). Effect of yoghurt containing Bifidobac-

terium lactis Bb12 on faecal excretion of secretory immunoglobulin A and human beta-defensin 2 in healthy adult volunteers. Nutr. J., 10, 138.

Kaczmarek, A., Vandenabeele, P., Krysko, D. V. (2013). Necroptosis: the release of damage-associated molecular patterns and its physiological relevance. Immunity, 38(2), 209-223.

Kajino-Sakamoto, R., Omori, E., Nighot, P. K., Blikslager, A. T., Matsumoto, K., Ninomiya-Tsuji, J. (2010). TGF-beta-activated kinase 1 signaling maintains intestinal integrity by preventing accumulation of reactive oxygen species in the intestinal epithelium. J. Immunol., 185(8), 4729-4737.

Kanehisa, M., Goto, S. (2000). KEGG: kyoto encyclopedia of genes and genomes. Nucleic Acids Res., 28, 27-30.

Kanehisa, M., Goto, S., Sato, Y., Furumichi, M., Tanabe, M. (2012). KEGG for integration and interpretation of large-scale molecular data sets. Nucleic Acids Res., 40 (Database issue), D109-114.

Kang, D. W., Park, J. G., Ilhan, Z. E., Wallstrom, G., Labaer, J., Adams, J. B., Krajmalnik-Brown, R. (2013). Reduced incidence of Prevotella and other fermenters in intestinal microflora of autistic children. PLoS One, 8(7), e68322.

Kapoor, A., Forman, M., Arav-Boger, R. (2014). Activation of nucleotide oligomerization domain 2 (NOD2) by human cytomegalovirus initiates innate immune responses and restricts virus replication. PLoS One, 9(3), e92704.

Karavolos, M. H., Winzer, K., Williams, P., Khan, C. M. (2013). Pathogen espionage: multiple bacterial adrenergic sensors eavesdrop on host communication systems. Mol. Microbiol., 87(3), 455-465.

Karlsson, H., Larsson, P., Wold, A. E., Rudin, A. (2004). Pattern of cytokine responses to gram-positive and gram-negative commensal bacteria is profoundly changed when monocytes differentiate into dendritic cells. Infect. Immun., 72, 2671-2678.

Kawase, M., He, F., Kubota, A., Harata, G., Hiramatsu, M. (2010). Oral administration of lactobacilli from human intestinal tract protects mice against influenza virus infection. Lett. Appl. Microbiol., 51(1), 6-10.

Keen, E. C. (2012). Paradigms of pathogenesis: targeting the mobile genetic elements of disease. Front. Cell. Infect. Microbiol., 2, 161.

Khanfer, R., Carroll, D., Lord, J. M., Phillips, A. C. (2012). Reduced neutrophil superoxide production among healthy older adults in response to acute psychological stress. Int. J. Psychophysiol., 86(3), 238-244.

Khani, S., Motamedifar, M., Golmoghaddam, H., Hosseini, H. M., Hashemizadeh, Z. (2012). In vitro study of the effect of a probiotic bacterium Lactobacillus rhamnosus against herpes simplex virus type 1. Braz. J. Infect. Dis., 16(2), 129-135.

Khare, S., Ratsimandresey, R. A., de Almeida, L., Cuda, C. M., Rellick, S. L., Misharin, A.V., …, Stehlik, C. (2014). The PYRIN domain-only protein POP3 inhibits ALR inflammasomes and regulates responses to infection with DNA viruses. Nat. Immunol., 15(4), 343-353.

Khoruts, A., Sadowsky, M. J. (2011). Therapeutic transplantation of the distal gut microbiota. Mucosal Immunol., 4(1), 4-7.

Klünemann, M., Schmid, M., Patil, K. R. (2014). Computational tools for modeling xenometabolism of the human gut microbiota. Trends Biotechnol., 32(3), 157-165.

Ko, E. J., Goh, J. S., Lee, B. J., Choi, S. H., Kim, P. H. (1999). Bifidobacterium bifidum exhibits a lipopolysaccharide-like mitogenic activity for murine B lymphocytes. J. Dairy Sci., 82, 1869-1876.

Koboziev, I., Karlsson, F., Grisham, M. B. (2010). Gut-associated lymphoid tissue, T cell trafficking, and chronic intestinal inflammation. Ann. NY Acad. Sci., 1207, Suppl. 1, E86-93.

Koeth, R. A., Wang, Z., Levison, B. S., Buffa, J. A., Org, E., Sheehy, B. T., …, Hazen, S. L. (2013). Intestinal microbiota metabolism of L-carnitine., a nutrient in red meat., promotes atherosclerosis. Nat. Med., 19(5), 576-585.

Kolader, M. E., Vinh, H., Ngoc Tuyet, P. T., Thompson, C., Wolbers, M., Merson, L., …, Baker, S. (2013). An oral preparation of Lactobacillus acidophilus for the treatment of uncomplicated acute watery diarrhoea in Vietnamese children: study protocol for a multicentre., randomised., placebo-controlled trial. Trials, 14, 27.

Koren, O., Knights, D., Gonzalez, A., Waldron, L., Segata, N., Knight, R., …, Ley, R. E. (2013). A guide to enterotypes across the human body: meta-analysis of microbial community structures in human microbiome datasets. PLoS Comput Biol., 9(1), e1002863.

Korshunov, S., Imlay, J. A. (2010). Two sources of endogenous hydrogen peroxide in Escherichia coli. Mol. Microbiol., 75(6), 1389-1401.

Kunsch, C., Rosen, C. A. (1993). NF-kappa B subunit-specific regulation of the interleukin-8 promoter. Mol. Cell. Biol., 13(10), 6137-6146.

Kurokawa, M., Kornbluth, S. (2009). Caspases and kinases in a death grip. Cell, 138(5), 838-854.

Ladirat, S. E., Schols, H. A., Nauta, A., Schoterman, M. H., Keijser, B. J., Montijn, R. C., …, Schuren, F. H. (2013). High-throughput analysis of the impact of antibiotics on the human intestinal microbiota composition. J. Microbiol. Meth., 92(3), 387-397.

Lam, E. K., Tai, E. K., Koo, M. W., Wong, H. P., Wu, W. K., Yu, L., …, Cho, C. H. (2007). Enhancement of gastric mucosal integrity by Lactobacillus rhamnosus GG. Life Sci., 80(23), 2128-2136.

Lathrop, S. K., Bloom, S. M., Rao, S. M., Nutsch, K., Lio, C. W., Santacruz, N., Peterson D. A., Stappenbeck, T. S., Hsieh, C. S. (2011). Peripheral education of the immune system by colonic commensal microbiota. Nature, 478(7368), 250-254.

Layden, B. T., Angueira, A. R., Brodsky, M., Durai, V., Lowe, W. L. Jr. (2013). Short chain fatty acids and their receptors: new metabolic targets. Transl. Res., 161(3), 131-140.

LeBlanc, J. G., Milani, C., de Giori, G. S., Sesma, F., van Sinderen, D., Ventura, M. (2013). Bacteria as vitamin suppliers to their host: a gut microbiota perspective. Curr. Opin. Biotechnol., 24(2), 160-168.

Le Chatelier, E., Nielsen, T., Qin, J., Prifti, E., Hildebrand, F., Falony, G., …, Pedersen, O. (2013). Richness of human gut microbiome correlates with metabolic markers. Nature, 500(7464), 541-546.

Lederberg, J. (2000). Infectious history. Science, 288, 287-293.

Lee, H. K., Braynen, W., Keshav, K., Pavlidis, P. (2005). ErmineJ: tool for functional analysis of gene expression data sets. BMC Bioinformatics, 6, 269.

Lester, J. T., DeLuca, N. A. (2011). Herpes simplex virus 1 ICP4 forms complexes with TFIID and mediator in virus-infected cells. J. Virol., 85(12), 5733-5744.

Letunic, I., Bork, P. (2011). Interactive Tree Of Life v2: online annotation and display of phylogenetic trees made easy. Nucleic Acids Res., 39 (Web Server issue), W475-478.

Leyer, G. J., Li, S., Mubasher, M. E., Reifer, C., Ouwehand, A. C. (2009). Probiotic effects on cold and influenza-like symptom incidence and duration in children. Pediatrics, 124(2), e172-179.

Li, H., Jia, W. (2013). Cometabolism of microbes and host: implications for drug metabolism and drug-induced toxicity. Clin. Pharmacol. Ther., 94(5), 574-581.

Lim, Y. S., Tran, H. T., Park, S. J., Yim, S. A., Hwang, S. B. (2011). Peptidyl--prolyl isomerase Pin1 is a cellular factor required for hepatitis C virus propagation. J. Virol., 85(17), 8777-8788.

Liu, F., Li, G., Wen, K., Bui, T., Cao, D., Zhang, Y., Yuan, L. (2010). Porcine small intestinal epithelial cell line (IPEC-J2) of rotavirus infection as a new model for the study of innate immune responses to rotaviruses and probiotics. Viral Immunol., 23(2), 135-149.

Liu, Z., Li, N., Neu, J. (2005). Tight junctions, leaky intestines, and pediatric diseases. Acta Paediatr., 94(4), 386-393.

Lossos, I. S., Czerwinski, D. K., Wechser, M. A., Levy, R. (2003). Optimization of quantitative real-time RT-PCR parameters for the study of lymphoid malignancies. Leukemia, 17, 789-795.

Lotz, M., Gütle, D., Walther, S., Menard, S., Bogdan, C., Hornef, M. W. (2006). Postnatal acquisition of endotoxin tolerance in intestinal epithelial cells. J. Exp. Med., 203(4), 973-984.

Lozupone, C. A., Stombaugh, J. I., Gordon, J. I., Jansson, J. K., Knight, R. (2012). Diversity, stability and resilience of the human gut microbiota. Nature, 489(7415), 220-230.

Lukjancenko, O., Ussery, D. W., Wassenaar, T. M. (2012). Comparative genomics of Bifidobacterium, Lactobacillus and related probiotic genera. Microb. Ecol., 63(3), 651-673.

Lukjancenko, O., Wassenaar, T. M., Ussery, D. W. (2010). Comparison of 61 sequenced Escherichia coli genomes. Microb. Ecol., 60(4), 708-720.

Lupfer, C., Kanneganti, T. D. (2013). The expanding role of NLRs in antiviral immunity. Immunol. Rev., 255(1), 13-24.

Lupfer, C., Thomas, P. G., Anand, P. K., Vogel, P., Milasta, S., Martinez, J., …, Kanneganti, T. D. (2013). Receptor interacting protein kinase 2-mediated mitophagy regulates inflammasome activation during virus infection. Nat. Immunol., 14(5), 480-488.

Lyles, D. S. (2000). Cytopathogenesis and inhibition of host gene expression by RNA viruses. Microbiol. Mol. Biol. Rev., 64(4), 709-724.

Maelfait, J., Beyaert, R. (2012). Emerging role of ubiquitination in antiviral RIG-I signaling. Microbiol. Mol. Biol. Rev., 76(1), 33-45.

Mai, V. (2004). Dietary modification of the intestinal microbiota. Nutr. Rev., 62, 235-242.

Mainz, D., Quadt, I., Stranzenbach, A. K., Voss, D., Guarino, L. A., Knebel-Mörsdorf, D. (2014). Expression and nuclear localization of the TATA-box-binding protein during baculovirus infection. J. Gen. Virol., 95(Pt 6), 1396-1407.

Maragkoudakis, P. A., Chingwaru, W., Gradisnik, L., Tsakalidou, E., Cencic, A. (2010). Lactic acid bacteria efficiently protect human and animal intestinal epithelial and immune cells from enteric virus infection. Int. J. Food. Microbiol., 141 Suppl. 1, S91-97.

Marchant, D. J., Bellac, C. L., Moraes, T. J., Wadsworth, S. J., Dufour, A., Butler, G.S., …, Overall, C. M. (2014). A new transcriptional role for matrix metalloproteinase-12 in antiviral immunity. Nat. Med., 20(5), 493-502.

Mariat, D., Firmesse, O., Levenez, F., Guimaraes, V., Sokol, H., Dore, J., Furet, J. P. (2009). The Firmicutes/Bacteroidetes ratio of the human microbiota changes with age. BMC Microbiol., 9, 123.

Markowitz, V. M., Chen, I. M., Chu, K., Szeto, E., Palaniappan, K., Jacob, B., …, Kyrpides, N. C. (2012). IMG/M-HMP: a metagenome compara-

tive analysis system for the Human Microbiome Project. PLoS One, 7(7), e40151.

Martin, D., Charpilienne, A., Parent, A., Boussac, A., D'Autreaux, B., Poupon, J., Poncet, D. (2013). The rotavirus nonstructural protein NSP5 coordinates a [2Fe-2S] iron-sulfur cluster that modulates interaction to RNA. FASEB J., 27(3), 1074-1083.

Martin, R., Nauta, A. J., Ben Amor, K., Knippels, L. M., Knol, J., Garssen, J. (2010). Early life: gut microbiota and immune development in infancy. Benef. Microbes, 1(4), 367-382.

McDonald, J. H. (2009). Handbook of biological statistics. Baltimore, Maryland. Sparky House Publishing.

Melchjorsen, J., Sørensen, L. N., Paludan, S. R. (2003). Expression and function of chemokines during viral infections: from molecular mechanisms to in vivo function. J. Leukoc. Biol., 74(3), 331-343.

Menten, P., Wuyts, A., Van Damme, J. (2002). Macrophage inflammatory protein-1. Cytokine Growth Factor Rev., 13, 455-481.

Metges, C. C., Eberhard, M., Petzke, K. J. (2006). Synthesis and absorption of intestinal microbial lysine in humans and non-ruminant animals and impact on human estimated average requirement of dietary lysine. Curr. Opin. Clin. Nutr. Metab. Care, 9(1), 37-41.

Miettinen, M., Pietilä, T. E., Kekkonen, R. A., Kankainen, M., Latvala, S., Pirhonen, J., …, Julkunen, I. (2012). Nonpathogenic Lactobacillus rhamnosus activates the inflammasome and antiviral responses in human macrophages. Gut Microbes, 3(6), 510-522.

Mocarski, E. S., Upton, J. W., Kaiser, W. J. (2011). Viral infection and the evolution of caspase 8-regulated apoptotic and necrotic death pathways. Nat. Rev. Immunol., 12(2), 79-88.

Mohan, R., Koebnick, C., Schildt, J., Mueller, M., Radke, M., Blaut, M. (2008). Effects of Bifidobacterium lactis Bb12 supplementation on body weight, fecal pH, acetate, lactate, calprotectin, and IgA in preterm infants. Pediatr. Res., 64(4), 418-422.

Mullie, C., Yazourh, A., Thibault, H., Odou, M. F., Singer, E., Kalach, N., Kremp, O., Romond, M. B. (2004). Increased poliovirus-specific intestinal antibody response coincides with promotion of Bifidobacterium longum-infantis and Bifidobacterium breve in infants: a randomized, double-blind, placebo-controlled trial. Pediatr. Res., 56, 791-795.

Munir, M. (2010). TRIM proteins: another class of viral victims. Sci. Signal., 3(118), jc2.

Munoz, J. A., Chenoll, E., Casinos, B., Bataller, E., Ramon, D., Genoves, S., …, Rivero, M. (2011). Novel probiotic Bifidobacterium longum subsp. infantis CECT 7210 strain active against rotavirus infections. Appl. Environ. Microbiol., 77(24), 8775-8783.

Nagata, S., Asahara, T., Ohta, T., Yamada, T., Kondo, S., Bian, L., …, Nomoto, K. (2011). Effect of the continuous intake of probiotic-fermented milk containing Lactobacillus casei strain Shirota on fever in a mass outbreak of norovirus gastroenteritis and the faecal microflora in a health service facility for the aged. Br. J. Nutr., 106(4), 549-556.

Nandi, S., Chanda, S., Bagchi, P., Nayak, M. K., Bhowmick, R., Chawla-Sarkar, M. (2014). MAVS protein is attenuated by rotavirus nonstructural protein 1. PLoS One, 9(3), e92126.

Narita, Y., Murata, T., Ryo, A., Kawashima, D., Sugimoto, A., Kanda, T., …, Tsurumi, T. (2013). Pin1 interacts with the Epstein-Barr virus DNA polymerase catalytic subunit and regulates viral DNA replication. J. Virol., 87(4), 2120-2127.

Natarajan, A., Ghose, R., Hill, J. M. (2006). Structure and dynamics of ASC2, a pyrin domain-only protein that regulates inflammatory signaling. J. Biol. Chem., 281(42), 31863-31875.

Natividad, J. M., Verdu, E. F. (2013). Modulation of intestinal barrier by intestinal microbiota: pathological and therapeutic implications. Pharmacol. Res., 69(1), 42-51.

Neufeld, K. M., Kang, N., Bienenstock, J., Foster, J. A. (2011a). Effects of intestinal microbiota on anxiety-like behavior. Commun. Integr. Biol., 4(4), 492-494.

Neufeld, K. M., Kang, N., Bienenstock, J., Foster, J. A. (2011b). Reduced anxiety-like behavior and central neurochemical change in germ-free mice. Neurogastroenterol. Motil., 23(3), 255-264, e119.

Nielsen, D. S., Krych, L., Buschard, K., Hansen, C. H., Hansen, A. K. (2014). Beyond genetics. Influence of dietary factors and gut microbiota on type 1 diabetes. FEBS Lett., 588(22), 4234-4243. doi: 10.1016/j.febslet.2014.04.010

Nikonov, A., Mölder, T., Sikut, R., Kiiver, K., Männik, A., Toots, U., …, Ustav, M. (2013). RIG-I and MDA-5 detection of viral RNA-dependent RNA polymerase activity restricts positive-strand RNA virus replication. PLoS Pathog., 9(9), e1003610.

Nishino, R., Mikami, K., Takahashi, H., Tomonaga, S., Furuse, M., Hiramoto, T., …, Sudo, N. (2013). Commensal microbiota modulate murine behaviors in a strictly contamination-free environment confirmed by culture-based methods. Neurogastroenterol. Motil., 25(6), 521-528.

Norris, V., Molina, F., Gewirtz, A. T. (2013). Hypothesis: bacteria control host appetites. J. Bacteriol., 195(3), 411-416.

Obert, G., Peiffer, I., Servin, A. L. (2000). Rotavirus-induced structural and functional alterations in tight junctions of polarized intestinal Caco-2 cell monolayers. J. Virol., 74, 4645-4651.

O'Hara, A. M., Shanahan, F. (2006). The gut flora as a forgotten organ. EMBO Rep., 7(7), 688-693.

von der Ohe, M., Altstaedt, J., Gross, U., Rink, L. (2001). Human neutrophils produce macrophage inhibitory protein-1beta but not type i interferons in response to viral stimulation. J. Interf. Cytok. Res., 21, 241-247.

Olier, M., Marcq, I., Salvador-Cartier, C., Secher, T., Dobrindt, U., Boury, M., …, Oswald, E. (2012). Genotoxicity of Escherichia coli Nissle 1917 strain cannot be dissociated from its probiotic activity. Gut Microbes, 3(6), 501-509.

Ouwerkerk, J. P., de Vos, W. M., Belzer, C. (2013). Glycobiome: bacteria and mucus at the epithelial interface. Best Pract. Res. Clin. Gastroenterol., 27(1), 25-38.

Panigrahi, P., Braileanu, G. T., Chen, H., Stine, O. C. (2007). Probiotic bacteria change Escherichia coli-induced gene expression in cultured colonocytes: Implications in intestinal pathophysiology. World J. Gastroenterol., 13(47), 6370-6378.

Park, J. H., Um, J. I., Lee, B. J., Goh, J. S., Park, S. Y., Kim, W. S., Kim, P. H. (2002). Encapsulated Bifidobacterium bifidum potentiates intestinal IgA production. Cell Immunol., 219, 22-27.

Parvatiyar, K., Barber, G. N., Harhaj, E. W. (2010). TAX1BP1 and A20 inhibit antiviral signaling by targeting TBK1-IKKi kinases. J. Biol. Chem., 285(20), 4999-5009.

Pasternak, Z., Pietrokovski, S., Rotem, O., Gophna, U., Lurie-Weinberger, M. N., Jurkevitch, E. (2013). By their genes ye shall know them: genomic signatures of predatory bacteria. ISME J., 7(4), 756-769.

Pauli, E. K., Schmolke, M., Hofmann, H., Ehrhardt, C., Flory, E., Münk, C., Ludwig, S. (2009). High level expression of the anti-retroviral protein APOBEC3G is induced by influenza A virus but does not confer antiviral activity. Retrovirology, 6, 38.

Pavlidis, P., Qin, J., Arango, V., Mann, J. J., Sibille, E. (2004). Using the gene ontology for microarray data mining: a comparison of methods and application to age effects in human prefrontal cortex. Neurochem. Res., 29, 1213-1322.

Pedone, C. A., Arnaud, C. C., Postaire, E. R., Bouley, C. F., Reinert, P. (2000). Multicentric study of the effect of milk fermented by Lactobacillus casei on the incidence of diarrhoea. Int. J. Clin. Pract., 54, 568-571.

Pedron, T., Thibault, C., Sansonetti, P. J. (2003). The invasive phenotype of Shigella flexneri directs a distinct gene expression pattern in the human intestinal epithelial cell line Caco-2. J. Biol. Chem., 278, 33878-33886.

Peng, J., Narasimhan, S., Marchesi, J. R., Benson, A., Wong, F. S., Wen, L. (2014). Long term effect of gut microbiota transfer on diabetes development. J. Autoimmun., 53: 85-94. doi: 10.1016/j.jaut.2014.03.005

Pfaffl, M. W. (2001). A new mathematical model for relative quantification in real-time RT-PCR. Nucleic Acids Res., 29, e45.

Phuapradit, P., Varavithya, W., Vathanophas, K., Sangchai, R., Podhipak, A., Suthutvoravut, U., …, Haschke, F. (1999). Reduction of rotavirus infection in children receiving bifidobacteria-supplemented formula. J. Med. Assoc. Thai., 82, Suppl. 1, S43-48.

Pollicino, T., Bellinghieri, L., Restuccia, A., Raffa, G., Musolino, C., Alibrandi, A., Raimondo, G. (2013). Hepatitis B virus (HBV) induces the expression of interleukin-8 that in turn reduces HBV sensitivity to interferon-alpha. Virology, 444(1-2), 317-328.

Popp, D., Maeda, Y., Stewart, A. A., Holmes, K. C. (1991). X-ray diffraction studies on muscle regulation. Adv. Biophys., 27, 89-103.

Prakash, S., Rodes, L., Coussa-Charley, M., Tomaro-Duchesneau, C. (2011). Gut microbiota: next frontier in understanding human health and development of biotherapeutics. Biologics, 5, 71-86.

Proctor, L. M. (2011). The Human Microbiome Project in 2011 and beyond. Cell Host Microbe, 10(4), 287-291.

Putaala, H., Salusjärvi, T., Nordström, M., Saarinen, M., Ouwehand, A. C., Bech Hansen, E., Rautonen, N. (2008). Effect of four probiotic strains and Escherichia coli O157:H7 on tight junction integrity and cyclo-oxygenase expression. Res. Microbiol., 159(9-10), 692-698.

Qadri, I., Maguire, H. F., Siddiqui, A. (1995). Hepatitis B virus transactivator protein X interacts with the TATA-binding protein. Proc. Natl. Acad. Sci. USA, 92(4), 1003-1007.

Qiao, H., Duffy, L. C., Griffiths, E., Dryja, D., Leavens, A., Rossman, J., …, Locniskar, M. (2002). Immune responses in rhesus rotavirus-challenged BALB/c mice treated with bifidobacteria and prebiotic supplements. Pediatr. Res., 51, 750-755.

Qin, J., Li, R., Raes, J., Arumugam, M., Burgdorf, K. S., Manichanh, C., Wang, J. (2010). A human gut microbial gene catalogue established by metagenomic sequencing. Nature, 464(7285), 59-65.

Qin, L., Ren, L., Zhou, Z., Lei, X., Chen, L., Xue, Q., Hung, T. (2011). Rotavirus nonstructural protein 1 antagonizes innate immune response by interacting with retinoic acid inducible gene I. Virol. J., 8, 526.

Quadt, I., Günther, A. K., Voss, D., Schelhaas, M., Knebel-Mörsdorf, D. (2006). TATA-binding protein and TBP-associated factors during herpes simplex vi-

rus type 1 infection: localization at viral DNA replication sites. Virus Res., 115(2), 207-213.

Rada, B., Leto, T. L. (2008). Oxidative innate immune defenses by Nox/Duox family NADPH oxidases. Contrib. Microbiol., 15, 164-187.

Rajilić-Stojanović, M., Heilig, H. G., Tims, S., Zoetendal, E. G., de Vos, W. M. (2012). Long-term monitoring of the human intestinal microbiota composition. Environ. Microbiol., 15(4), 1146 & # 8211, 1159.

Ramirez-Farias, C., Slezak, K., Fuller, Z., Duncan, A., Holtrop, G., Louis, P. (2009). Effect of inulin on the human gut microbiota: stimulation of Bifidobacterium adolescentis and Faecalibacterium prausnitzii. Br. J. Nutr., 101(4), 541-550.

Rathinam, V. A., Jiang, Z., Waggoner, S. N., Sharma, S., Cole, L. E., Waggoner, L., …, Fitzgerald, K. A. (2010). The AIM2 inflammasome is essential for host defense against cytosolic bacteria and DNA viruses. Nat. Immunol., 11(5), 395-402.

Rautava, S., Arvilommi, H., Isolauri, E. (2006). Specific probiotics in enhancing maturation of IgA responses in formula-fed infants. Pediatr. Res., 60(2), 221-224.

Rautava, S., Salminen, S., Isolauri, E. (2009). Specific probiotics in reducing the risk of acute infections in infancy – a randomised, double-blind, placebo--controlled study. Br. J. Nutr., 101(11), 1722-1726.

Reid, G., Younes, J. A., Van der Mei, H. C., Gloor, G. B., Knight, R., Busscher, H. J. (2011). Microbiota restoration: natural and supplemented recovery of human microbial communities. Nat. Rev. Microbiol., 9(1), 27-38.

Reinhardt, C., Bergentall, M., Greiner, T. U., Schaffner, F., Ostergren-Lunden, G., Petersen, L. C., …, Bäckhed, F. (2012). Tissue factor and PAR1 promote microbiota-induced intestinal vascular remodelling. Nature, 483(7391), 627-631.

Resta-Lenert, S., Barrett, K. E. (2003). Live probiotics protect intestinal epithelial cells from the effects of infection with enteroinvasive Escherichia coli (EIEC). Gut, 52, 988-997.

Ritchie, M. E., Silver, J., Oshlack, A., Holmes, M., Diyagama, D., Holloway, A., Smyth, G. K. (2007). A comparison of background correction methods for two-colour microarrays. Bioinformatics, 23(20), 2700-2707.

Rizzello, V., Bonaccorsi, I., Dongarra, M. L., Fink, L. N., Ferlazzo, G. (2011). Role of natural killer and dendritic cell crosstalk in immunomodulation by commensal bacteria probiotics. J. Biomed. Biotechnol., ID 473097. doi: 10.1155/2011/73097

Rodríguez, L. S., Barreto, A., Franco, M. A., Angel, J. (2009). Immunomodulators released during rotavirus infection of polarized caco-2 cells. Viral Immunol., 22(3), 163-172.

Rosenberger, C. M., Scott, M. G., Gold, M. R., Hancock, R. E., Finlay, B. B. (2000). Salmonella typhimurium infection and lipopolysaccharide stimulation induce similar changes in macrophage gene expression. J. Immunol., 164, 5894-5904.

Royet, J., Charroux, B. (2013). Mechanisms and consequence of bacteria detection by the Drosophila gut epithelium. Gut Microbes, 4(3), 259-263.

Rubio, R. M., Mora, S. I., Romero, P., Arias, C. F., Lopez, S. (2013). Rotavirus prevents the expression of host responses by blocking the nucleocytoplasmic transport of polyadenylated mRNAs. J. Virol., 87(11), 6336-6345.

Ruiz, M. C., Leon, T., Diaz, Y., Michelangeli, F. (2009). Molecular biology of rotavirus entry and replication. ScientificWorldJournal, 9, 1476-1497.

Saavedra, J. M., Bauman, N. A., Oung, I., Perman, J. A., Yolken, R. H. (1994). Feeding of Bifidobacterium bifidum and Streptococcus thermophilus to infants in hospital for prevention of diarrhoea and shedding of rotavirus. Lancet, 344, 1046-1049.

Sabbah, A., Chang, T. H., Harnack, R., Frohlich, V., Tominaga, K., Dube, P. H., …, Bose, S. (2009). Activation of innate immune antiviral responses by Nod2. Nat. Immunol., 10(10), 1073-1080.

Saitoh, S., Miyake, K. (2009). Regulatory molecules required for nucleotide--sensing Toll-like receptors. Immunol. Rev., 227(1), 32-43.

Saitoh, T., Tun-Kyi, A., Ryo, A., Yamamoto, M., Finn, G., Fujita, T., …, Yamaoka, S. (2006). Negative regulation of interferon-regulatory factor 3-dependent innate antiviral response by the prolyl isomerase Pin1. Nat. Immunol., 7(6), 598-605.

Salvesen, G. S., Walsh, C. M. (2014). Functions of caspase 8: The identified and the mysterious. Semin. Immunol. 26(3), 246-252. doi: 10.1016/j.smim. 2014.03.005

Sambuy, Y., De Angelis, I., Ranaldi, G., Scarino, M. L., Stammati, A., Zucco, F. (2005). The Caco-2 cell line as a model of the intestinal barrier: influence of cell and culture-related factors on Caco-2 cell functional characteristics. Cell Biol. Toxicol., 21(1), 1-26.

Sarker, S. A., Sultana, S., Fuchs, G. J., Alam, N. H., Azim, T., Brüssow, H., Hammarström, L. (2005). Lactobacillus paracasei strain ST11 has no effect on rotavirus but ameliorates the outcome of nonrotavirus diarrhea in children from Bangladesh. Pediatrics, 116(2), e221-228.

Sasai, M., Oshiumi, H., Matsumoto, M., Inoue, N., Fujita, F., Nakanishi, M., Seya, T. (2005). Cutting edge: NF-kappaB-activating kinase-associated protein 1 participates in TLR3/Toll-IL-1 homology domain-containing adapter molecule-1-mediated IFN regulatory factor 3 activation. J. Immunol., 174, 27-30.

Sato, H., Torimura, M., Kitahara, M., Ohkuma, M., Hotta, Y., Tamura, H. (2012). Characterization of the *Lactobacillus casei* group based on the profiling of ribosomal proteins coded in S10-spc-alpha operons as observed by MALDI-TOF MS. Syst. Appl. Microbiol., 35(7), 447-454.

Sayin, S. I., Wahlström, A., Felin, J., Jäntti, S., Marschall, H. U., Bamberg, K., …, Bäckhed, F. (2013). Gut microbiota regulates bile acid metabolism by reducing the levels of tauro-beta-muricholic acid., a naturally occurring FXR antagonist. Cell Metab., 17(2), 225-235.

Schmidt, M. T., Handschuh, L., Zyprych, J., Szabelska, A., Olejnik-Schmidt, A. K., Siatkowski, I., Figlerowicz, M. (2011). Impact of DNA microarray data transformation on gene expression analysis – comparison of two normalization methods. Acta Biochim. Pol., 58(4), 573-580.

Schmittgen, T. D., Livak, K. J. (2008). Analyzing real-time PCR data by the comparative C(T) method. Nat. Protoc., 3(6), 1101-1108.

Schoggins, J. W. (2014). Interferon-stimulated genes: roles in viral pathogenesis. Curr. Opin. Virol., 6C, 40-46.

Schoggins, J. W., Wilson, S. J., Panis, M., Murphy, M. Y., Jones, C. T., Bieniasz, P., Rice, C. M. (2011). A diverse range of gene products are effectors of the type I interferon antiviral response. Nature, 472(7344), 481-485.

Sekirov, I., Russell, S. L., Antunes, L. C., Finlay, B. B. (2010). Gut microbiota in health and disease. Physiol. Rev., 90(3), 859-904.

Serino, M., Luche, E., Chabo, C., Amar, J., Burcelin, R. (2009). Intestinal microflora and metabolic diseases. Diabetes Metab., 35(4), 262-272.

Sharma, R., Young, C., Neu, J. (2010). Molecular modulation of intestinal epithelial barrier: contribution of microbiota. J. Biomed. Biotechnol. doi: 10.1155/2010/305879

Sharon, G., Segal, D., Ringo, J. M., Hefetz, A., Zilber-Rosenberg, I., Rosenberg, E. (2010). Commensal bacteria play a role in mating preference of Drosophila melanogaster. Proc. Natl. Acad. Sci. USA, 107(46), 20051-20056.

Sharon, G., Segal, D., Zilber-Rosenberg, I., Rosenberg, E. (2011). Symbiotic bacteria are responsible for diet-induced mating preference in Drosophila melanogaster., providing support for the hologenome concept of evolution. Gut Microbes, 2(3), 190-192.

Shen, J., Obin, M. S., Zhao, L. (2013). The gut microbiota, obesity and insulin resistance. Mol. Aspects Med., 34(1), 39-58.

Sheth, R., Anderson, J., Sato, T., Oh, B., Hempson, S. J., Rollo, E., …, Shaw, R. D. (1996). Rotavirus stimulates IL-8 secretion from cultured epithelial cells. Virology, 221(2), 251-259.

Shi, H. N., Walker, A. (2004). Bacterial colonization and the development of intestinal defences. Can. J. Gastroenterol., 18, 493-500.

Shu, Q., Qu, F., Gill, H. S. (2001). Probiotic treatment using Bifidobacterium lactis HN019 reduces weanling diarrhea associated with rotavirus and Escherichia coli infection in a piglet model. J. Pediatr. Gastroenterol. Nutr., 33, 171-177.

Siatkowski, I., Zyprych, J. (2008). Przegląd analiz stosowanych w eksperymencie mikromacierzowym. Colloq. Biometr., 38, 231-246.

Siggers, R. H., Hackam, D. J. (2011). The role of innate immune-stimulated epithelial apoptosis during gastrointestinal inflammatory diseases. Cell. Mol. Life Sci., 68(22), 3623-3634.

Silvestri, L. S., Taraporewala, Z. F., Patton, J. T. (2004). Rotavirus replication: plus-sense templates for double-stranded RNA synthesis are made in viroplasms. J. Virol., 78, 7763-7774.

Sjögren, K., Engdahl, C., Henning, P., Lerner, U. H., Tremaroli, V., Lagerquist, M. K., …, Ohlsson, C. (2012). The gut microbiota regulates bone mass in mice. J. Bone Miner. Res., 27(6), 1357-1367.

Smyth, G. K. (2004). Linear models and empirical bayes methods for assessing differential expression in microarray experiments. Stat. Appl. Genet. Mol. Biol., 3, 1, Article 3.

Smyth, G. K. (2005). Limma: linear models for microarray data. In: R. Gentleman, V. Carey, S. Dudoit, R. Irizarry, W. Huber (Eds.), Bioinformatics and computational biology solutions using R and bioconductor (pp. 397-420). New York: Springer.

Smyth, G. K., Speed, T. (2003). Normalization of cDNA microarray data. Methods, 31, 265-273.

Sonoda, E., Hitoshi, Y., Yamaguchi, N., Ishii, T., Tominaga, A., Araki, S., Takatsu, K. (1992). Differential regulation of IgA production by TGF-beta and IL-5: TGF-beta induces surface IgA-positive cells bearing IL-5 receptor., whereas IL-5 promotes their survival and maturation into IgA-secreting cells. Cell. Immunol., 140, 158-172.

Stępniak, P., Handschuh, L., Figlerowicz, M. (2008). Mikromacierze DNA – analiza danych. Biotechnologia, 4 (83), 68-87.

Sun, J., Gunzer, F., Westendorf, A. M., Buer, J., Scharfe, M., Jarek, M., Gössling, F., Blöcker, H., Zeng, A. P. (2005). Genomic peculiarity of coding sequences and metabolic potential of probiotic Escherichia coli strain Nissle 1917 inferred from raw genome data. J. Biotechnol., 117, 147-161.

Suzuki, M., Cela, R., Bertin, T. K., Sule, G., Cerullo, V., Rodgers, J. R., Lee, B. (2011). NOD2 signaling contributes to the innate immune response against

helper-dependent adenovirus vectors independently of MyD88 in vivo. Hum. Gene Ther., 22(9), 1071-1082.

Szajewska, H., Wanke, M., Patro, B. (2011). Meta-analysis: the effects of Lactobacillus rhamnosus GG supplementation for the prevention of healthcare-associated diarrhoea in children. Aliment. Pharmacol. Ther., 34(9), 1079-1087.

Szymański, H., Pejcz, J., Jawień, M., Chmielarczyk, A., Strus, M., Heczko, P. B. (2006). Treatment of acute infectious diarrhoea in infants and children with a mixture of three Lactobacillus rhamnosus strains – a randomized, double--blind, placebo-controlled trial. Aliment. Pharmacol. Ther., 23(2), 247-253.

Taipale, T., Pienihäkkinen, K., Isolauri, E., Larsen, C., Brockmann, E., Alanen, P., Jokela, J., Söderling, E. (2011). Bifidobacterium animalis subsp. lactis BB-12 in reducing the risk of infections in infancy. Br. J. Nutr., 105(3), 4094-16.

Takeda, S., Takeshita, M., Kikuchi, Y., Dashnyam, B., Kawahara, S., Yoshida, H., …, Kurokawa, M. (2011). Efficacy of oral administration of heat-killed probiotics from Mongolian dairy products against influenza infection in mice: alleviation of influenza infection by its immunomodulatory activity through intestinal immunity. Int. Immunopharmacol., 11(12), 1976-1983.

Tapping, R. I., Akashi, S., Miyake, K., Godowski, P. J., Tobias, P. S. (2000). Toll-like receptor 4., but not toll-like receptor 2., is a signaling receptor for Escherichia and Salmonella lipopolysaccharides. J. Immunol., 165, 5780-5787.

Tenaillon, O., Skurnik, D., Picard, B., Denamur, E. (2010). The population genetics of commensal *Escherichia coli*. Nat. Rev. Microbiol., 8(3), 207-217.

Teran, C. G., Teran-Escalera, C. N., Villarroel, P. (2009). Nitazoxanide vs. probiotics for the treatment of acute rotavirus diarrhea in children: a randomized., single-blind., controlled trial in Bolivian children. Int. J. Infect. Dis., 13(4), 518-523.

Thomas, P. D., Kejariwal, A., Guo, N., Mi, H., Campbell, M. J., Muruganujan, A., Lazareva-Ulitsky, B. (2006). Applications for protein sequence-function evolution data: mRNA/protein expression analysis and coding SNP scoring tools. Nucleic Acids Res., 34 (Web Server issue), W645-650.

Thompson, M. R., Kaminski, J. J., Kurt-Jones, E. A., Fitzgerald, K. A. (2011). Pattern recognition receptors and the innate immune response to viral infection. Viruses, 3(6), 920-940.

Trask, S. D., McDonald, S. M., Patton, J. T. (2012). Structural insights into the coupling of virion assembly and rotavirus replication. Nat. Rev. Microbiol., 10(3), 165-177.

Trask, S. D., Wetzel, J. D., Dermody, T. S., Patton, J. T. (2013). Mutations in the rotavirus spike protein VP4 reduce trypsin sensitivity but not viral spread. J. Gen. Virol., 94 (Pt 6), 1296-1300.

Tremaroli, V., Bäckhed, F. (2012). Functional interactions between the gut microbiota and host metabolism. Nature, 489(7415), 242-249.

Tuomola, E., Crittenden, R., Playne, M., Isolauri, E., Salminen, S. (2001). Quality assurance criteria for probiotic bacteria. Am. J. Clin. Nutr., 73, 393S--398S.

Velagapudi, V. R., Hezavehm R., Reigstadm, C. S., Gopalacharyulu, P., Yetukuri, L., Islam, S., …, Bäckhed, F. (2010). The gut microbiota modulates host energy and lipid metabolism in mice. J. Lipid Res., 51(5), 1101-1112.

Vereecke, L., Beyaert, R., van Loo, G. (2011). Enterocyte death and intestinal barrier maintenance in homeostasis and disease. Trends Mol. Med., 17(10), 584-593.

Victoria, J. G., Wang, C., Jones, M. S., Jaing, C., McLoughlin, K., Gardner, S., Delwart, E. L. (2010). Viral nucleic acids in live-attenuated vaccines: detection of minority variants and an adventitious virus. J. Virol., 84(12), 6033--6040.

Walker, A. W., Ince, J., Duncan, S. H., Webster, L. M., Holtrop, G., Ze, X., …, Flint, H. J. (2011). Dominant and diet-responsive groups of bacteria within the human colonic microbiota. ISME J., 5(2), 220-230.

Wang, H., Moon, S., Wang, Y., Jiang, B. (2012). Multiple virus infection alters rotavirus replication and expression of cytokines and Toll-like receptors in intestinal epithelial cells. Virus Res., 167(1), 48-55.

Wang, H. L., Akinci, I. O., Baker, C. M., Urich, D., Bellmeyer, A., Jain, M., …, Budinger, G. R. (2007). The intrinsic apoptotic pathway is required for lipopolysaccharide-induced lung endothelial cell death. J. Immunol., 179(3), 1834-1841.

Wang, J., Tian, Y., Phillips, K. L., Chiverton, N., Haddock, G., Bunning, R. A., Risbud, M. V. (2013). Tumor necrosis factor α- and interleukin-1β-dependent induction of CCL3 expression by nucleus pulposus cells promotes macrophage migration through CCR1. Arthritis Rheum., 65(3), 832-842.

Wang, X., Spandidos, A., Wang, H., Seed, B. (2012). PrimerBank: a PCR primer database for quantitative gene expression analysis. 2012 update. Nucleic Acids Res., 40 (Database issue), D1144-1149.

Wang, Y., Xie, J., Wang, N., Li, Y., Sun, X., Zhang, Y., Zhang, H. (2013). *Lactobacillus casei* Zhang modulate cytokine and toll-like receptor expression and beneficially regulate poly I:C-induced immune responses in RAW264.7 macrophages. Microbiol. Immunol., 57(1), 54-62.

Watashi, K., Khan, M., Yedavalli, V. R., Yeung, M. L., Strebel, K., Jeang, K. T. (2008). Human immunodeficiency virus type 1 replication and regulation of APOBEC3G by peptidyl prolyl isomerase Pin1. J. Virol., 82(20), 9928-9936.

Weidman, M.,K., Sharma, R., Raychaudhuri, S., Kundu, P., Tsai, W., Dasgupta, A. (2003). The interaction of cytoplasmic RNA viruses with the nucleus. Virus Res., 95(1-2), 75-85.

Weiss, G., Christensen, H. R., Zeuthen, L. H., Vogensen, F. K., Jakobsen, M., Frøkiær, H. (2011). Lactobacilli and bifidobacteria induce differential interferon-β profiles in dendritic cells. Cytokine, 56(2), 520-530.

Wen, K., Li, G., Bui, T., Liu, F., Li, Y., …, Yuan, L. (2012). High dose and low dose Lactobacillus acidophilus exerted differential immune modulating effects on T cell immune responses induced by an oral human rotavirus vaccine in gnotobiotic pigs. Vaccine, 30(6), 1198-1207.

Wexler, H. M. (2007). Bacteroides: the good., the bad., and the nitty-gritty. Clin. Microbiol. Rev., 20(4), 593-621.

Wie, S. H., Du, P., Luong, T. Q., Rought, S. E., Beliakova-Bethell, N., Lozach, J., …, Woelk, C. H. (2013). HIV downregulates interferon-stimulated genes in primary macrophages. J. Interferon. Cytokine Res., 33(2), 90-95.

Wong, J. M., de Souza, R., Kendall, C. W., Emam, A., Jenkins, D. J. (2006). Colonic health: fermentation and short chain fatty acids. J. Clin. Gastroenterol., 40(3), 235-243.

Wu, B., Peisley, A., Richards, C., Yao, H., Zeng, X., Lin, C., …, Hur, S. (2013). Structural basis for dsRNA recognition, filament formation, and antiviral signal activation by MDA5. Cell, 152(1-2), 276-289.

Wu, G. D., Chen, J., Hoffmann, C., Bittinger, K., Chen, Y. Y., Keilbaugh, S. A., …, Lewis, J. D. (2011). Linking long-term dietary patterns with gut microbial enterotypes. Science, 334(6052), 105-108.

Xu, J., Gordon, J. I. (2003). Honor thy symbionts. Proc. Natl. Acad. Sci. USA, 100, 10452-10459.

Yanagibashi, T., Hosono, A., Oyama, A., Tsuda, M., Hachimura, S., Takahashi, Y., …, Kaminogawa, S. (2009). Bacteroides induce higher IgA production than Lactobacillus by increasing activation-induced cytidine deaminase expression in B cells in murine Peyer‘s patches. Biosci. Biotechnol. Biochem., 73(2), 372-377.

Yanagibashi, T., Hosono, A., Oyama, A., Tsuda, M., Suzuki, A., Hachimura, S., …, Kaminogawa, S. (2013). IgA production in the large intestine is modulated by a different mechanism than in the small intestine: Bacteroides acidifaciens promotes IgA production in the large intestine by inducing germinal center formation and increasing the number of IgA+ B cells. Immunobiology, 218(4), 645-651.

Yang, Y. H., Dudoit, S., Luu, P., Lin, D. M., Peng, V., Ngai, J., Speed, T. P. (2002). Normalization for cDNA microarray data: a robust composite meth-

od addressing single and multiple slide systematic variation. Nucleic Acids Res., 30, e15.

Yang, Y. H., Thorne, N.,P. (2003). Normalization for two-color cDNA microarray data. In: D. R. Goldstein (Ed.). Science and statistics: A festschrift for terry speed. IMS Lecture Notes – Monograph Series, 40, 403-418. doi:10.1214/lnms/1215091155

Yoshida, R., Takaesu, G., Yoshida, H., Okamoto, F., Yoshioka, T., Choi, Y., …, Kobayashi, T. (2008). TRAF6 and MEKK1 play a pivotal role in the RIG-I-like helicase antiviral pathway. J. Biol. Chem., 283(52), 36211-36220.

Yu, J. W., Fernandes-Alnemri, T., Datta, P., Wu, J., Juliana, C., Solorzano, L., …, Alnemri, E. S. (2007). Pyrin activates the ASC pyroptosome in response to engagement by autoinflammatory PSTPIP1 mutants. Mol. Cell., 28(2), 214-227.

Yu, M., Levine, S. J. (2011). Toll-like receptor, RIG-I-like receptors and the NLRP3 inflammasome: key modulators of innate immune responses to double-stranded RNA viruses. Cytokine Growth Factor Rev., 22(2), 63-72.

Zhao, W., Pahar, B., Borda, J. T., Alvarez, X., Sestak, K. (2007). A decline in CCL3-5 chemokine gene expression during primary simian-human immunodeficiency virus infection. PLoS One, 2(8), e726.

Zhao, W., Wang, L., Zhang, M., Wang, P., Yuan, C., Qi, J., Meng, H., Gao, C. (2012). Tripartite motif-containing protein 38 negatively regulates TLR3/4- and RIG-I-mediated IFN-Î¸ production and antiviral response by targeting NAP1. J. Immunol., 188(11), 5311-5318.

Zibrik, L., Dove, W., McArdle, F., Rustom, R., Hart, C. A., Jackson, M. J. (2007). Lack of shedding of the RIX4414 live attenuated rotavirus vaccine administered to adult volunteers. Arch. Virol., 152(10), 1951-1954.

Supplemental information

Primers used for RT-qPCR for human transcripts selected from qPrimerDepot Database and literature are listed in Table S1.

In a microarray experiment a random and systemic variation can occur. Thus, in order to accurately and precisely measure gene expression changes a normalisation of the data has to be performed. This procedure adjusts data to effects that are due to variations in the technology rather than biology. These include differences in: the binding of the labels (dye biases), sample preparation, hybridization efficiency, photodetection, autofluorescence, etc. The normalisation procedure efficiency can be visualized with boxplot (Figs S2-S6). This plot consists of the central box which represents the inter-quartile range (IQR; defined as the difference between the 75th percentile and 25th percentile, i.e., the upper and lower quartiles), the line in the middle of the box represents the median (a measure of central location of the data). The whiskers show range, the highest datum still within 1.5 IQR of the 75th percentile (upper quartile) and the lowest datum still within 1.5 IQR of the 25th percentile (lower quartile). Extreme values (outlayers) not included between the whiskers are plotted individually as small circles.

Normalisation is usually applied to the log-ratios of expression described by M value ($M = \log_2 R - \log_2 G$, where R and G are the background-corrected red and green intensities for each spot). On this scale, M = 0 represents equal expression, M = 1 represents a 2-fold change between the RNA samples, M = 2 represents a 4-fold change, and so on. The normalization procedure corrects the M-values to bring their distribution around an M of 0 (the values in the array should be centered about an M equalling to 0 on the boxplot).

Table S1. Primers for quantitative Real-Time PCR analysis of human gene expression
Tabela S1. Startery zastosowane do ilościowej analizy ekspresji ludzkich genów metodą Real-Time PCR

Gene symbol	UniGene symbol	GenBank accession no.	Gene description	Primer pair sequence	Amplicon size
1	2	3	4	5	6
AIM2	Hs.733411	NM_004833	absent in melanoma 2	GGCTTTGGTTTTGTTACCGA GCAGTGATGAAGACCATTCG	119
APOBEC3G	Hs.660143	NM_021822	apolipoprotein B mRNA editing enzyme, catalytic polypeptide-like 3G	TTCCAAAAGGGAATCACGTC CAATGACACCTGGGTCCTG	126
ATG5	Hs.486063	NM_004849	ATG5 autophagy related 5 homolog (S. cerevisiae)	CAGGACGAAACAGCTTCTGA TCAATCGGAAACTCATGGAA	114
AZI2	Hs.706676	NM_022461	5-azacytidine induced 2	ATCATCTTCTACCAGTGCATCC GTTTGTTTTCGGTCCGTTTC	111
CARD8	Hs.446146	NM_014959	caspase recruitment domain family, member 8	GGAAGCGATCTTCCTCATCA CTCTCCATCCCCATCACTTC	133
CASP1	Hs.2490	NM_033292	caspase 1, apoptosis--related cysteine peptidase (interleukin 1, beta, convertase)	CACATCACAGGAACAGGCAT GCTTTCTGCTCTTCCACACC	114
CASP10	Hs.5353	NM_001230	caspase 10, apoptosis-related cysteine peptidase	CCTCTGTGGTTCCGATTCAT GAAGCCGAGTCGTATCAAGG	113
CASP8	Hs.599762	NM_001228	caspase 8, apoptosis-related cysteine peptidase	AGGCCAGATCTTCACTGTCC GGTCACTTGAACCTTGGGAA	114
CCL3	Hs.514107	NM_002983	chemokine (C-C motif) ligand 3	TGGCTGCTCGTCTCAAAGTA TGCAACCAGTTCTCTGCATC	116

1	2	3	4	5	6
CCL5	Hs.514821	NM_002985	chemokine (C-C motif) ligand 5	ACACACTTGGCGGTTCTTTC CCTGCTGCTTTGCCTACATT	125
CD40	Hs.472860	NM_001250	CD40 molecule, TNF receptor superfamily member 5	GGCACAAAGAACAGCACTGA TATGGTTCGTCTGCCTCTGC	125
CD80	Hs.838	NM_005191	CD80 molecule	TAGATGCGAGTTTGTGCCAG GCTGGCTGGTCTTTCTCACT	123
CD86	Hs.171182	NM_006889	CD86 molecule	AGAGGAGCAGCACCAGAGAG GGGAATGCTGCTGTGCTTAT	130
CHUK	Hs.198998	NM_001278	conserved helix-loop-helix ubiquitous kinase	GAATGAAGACTTTCATCAGGTGG TTTGAAGCAGCCAAGATGTTT	126
CTSB	Hs.520898	NM_001908	cathepsin B	CGACAGGGGATGGAAAGAG CTGGGCTGCAGGCTCTC	137
CTSL1	Hs.731507	NM_001912	cathepsin L1	AAAGGCAGCAAGGATGAGTG ACTCTGCTGGCCTTGAGGT	147
CTSS	Hs.181301	NM_004079	cathepsin S	GCAATCCCACAATGATTTCC CTTGTGGTTGGCTATGGTGAT	128
CXCL10	Hs.632586	NM_001565	chemokine (C-X-C motif) ligand 10	GCAGGTACAGCGTACGGTTC CAGCAGAGGAACCTCCAGTC	124
CXCL11	Hs.632592	NM_005409	chemokine (C-X-C motif) ligand 11	CCTCTTTTGAACATGGGGAA TCCAAGAAGAGCAGCAAAGC	147
CXCL9	Hs.77367	NM_002416	chemokine (C-X-C motif) ligand 9	GCTGACCTGTTTCTCCCACT CCTTCCTGCGAGAAAATTGA	117
CYLD	Hs.578973	NM_015247	cylindromatosis (turban tumor syndrome)	CTCCTTTCCTGCGTCACACT TGGGATGGAAGATTTGATGG	119

1	2	3	4	5	6
DAK	Hs.6278	NM_015533	dihydroxyacetone kinase 2 homolog (*S. cerevisiae*)	TGTCCAGGTCAGAACGGAG TTTCAGAGCCTCCACACCAT	148
DDX3X	Hs.731543	NM_001356	DEAD (Asp-Glu-Ala-Asp) box polypeptide 3, X-linked	GAATATAGCGCCCTTTGCTG GATGAGTCATGTGGCAGTGG	119
DDX58	Hs.190622	NM_014314	DEAD (Asp-Glu-Ala-Asp) box polypeptide 58	ATTGGGCCCTTGTTGTTTTT TGCAAGCCTTCCAGGATTAT	127
DHX58	Hs.55918	NM_024119	DEXH (Asp-Glu-X-His) box polypeptide 58	ATTCTCTGGGCCATGAGTTG CTATCACAGGGAGCACGTCA	118
FADD	Hs.86131	NM_003824	fas (TNFRSF6)-associated via death domain	TCTCCAATCTTTCCCCACAT GAGCTGCTCGCCTCCCT	147
FOS	Hs.25647	NM_005252	V-fos FBJ murine osteosarcoma viral oncogene homolog	GTGACCGTGGGAATGAAGTT CCGGGGATAGCCTCTCTTAC	127
HSP90 AA1	Hs.525600	NM_001017963 NM_005348	heat shock protein 90kDa alpha (cytosolic), class A member 1	ATCAACTGGGCAATTTCTGC GTCCTGTGCGGTCACTTAGC	113
IFIH1	Hs.163173	NM_022168	interferon induced with helicase C domain 1	TGACACTTCCTTCTGCCAAA TTCAACCACAGTTCAGCCAA	128
IFNA1	Hs.37026	NM_024013	interferon, alpha 1	GGAGATCACAGCCCAGAGAG CAGAGTCACCCATCTCAGCA	126
IFNA2	Hs.211575	NM_000605	interferon, alpha 2	CAGAGCAGCTTGACTTGCAG TAGGCTCACCCATTTCAACC	111
IFNAR1	Hs.529400	NM_000629	interferon (alpha, beta and omega) receptor 1	CTCCTGTTCCACCTCAGGAT GACCCTAGTGCTCGTCGC	129
IFNB1	Hs.93177	NM_002176	interferon, beta 1, fibroblast	TGGAGAAGCACAACAGGAGA AACCTTTCGAAGCCTTTGCT	111

1	2	3	4	5	6
IKBKB	Hs.597664	NM_001556	inhibitor of kappa light polypeptide gene enhancer in B-cells, kinase beta	ATCTGGATCTCCAGGCACC GGATTTGGAAATGTCATCCG	119
IL12A	Hs.673	NM_000882	interleukin 12A (natural killer cell stimulatory factor 1, cytotoxic lymphocyte maturation factor 1, p35)	GGTAAACAGGCCTCCACTGT TCAGCAACATGCTCCAGAAG	118
IL12B	Hs.674	NM_002187	interleukin 12B (natural killer cell stimulatory factor 2, cytotoxic lymphocyte maturation factor 2, p40)	GTTCCCATATGGCCACGAG AGGGCCATTGGACTCTCC	111
IL15	Hs.654378	NM_000585	interleukin 15	TCAAAGCCACGGTAAATCCT TTAGCAGATAGCCAGCCCAT	126
IL18	Hs.83077	NM_001562	interleukin 18 (interferon--gamma-inducing factor)	TGCCACAAAGTTGATGCAAT TTCGGGAAGAGGAAAGGAAC	121
IL1B	Hs.126256	NM_000576	interleukin 1, beta	CCTGAAGCCCTTGCTGTAGT AGCTGATGGCCCTAAACAGA	112
IL6	Hs.654458	NM_000600	interleukin 6 (interferon, beta 2)	CATTTGTGGTTGGGTCAGG AGTGAGGAACAAGCCAGAGC	112
IL8	Hs.624	NM_000584	interleukin 8	AGCACTCCTTGGCAAAACTG CGGAAGGAACCATCTCACTG	116
IRAK1	Hs.522819	NM_001569	interleukin-1 receptor--associated kinase 1	GTGCTTCTCAAAGCCACTCC GTGCTAGAGACCTTGGCTGG	116
IRF3	Hs.75254	NM_001571	interferon regulatory factor 3	CGGAAATTCCTCTTCCAGGT AGGATGCACAGCAGGAGG	112

1	2	3	4	5	6
IRF5	Hs.521181	NM_002200	interferon regulatory factor 5	GTGGGAGCCACTGGGATG GCAGAGCTCAGCTTGGTCC	111
IRF7	Hs.166120	NM_001572	interferon regulatory factor 7	GCCTCTGCCTCAGTCTGGT TGATGCTGCGGGATAACTC	112
ISG15	Hs.458485	NM_005101	ISG15 ubiquitin-like modifier	AGGGACACCTGGAATTCGTT GCGAACTCATCTTTGCCAGT	118
JUN	Hs.714791	NM_002228	jun oncogene	GTCCTTCTTCTCTTGCGTGG GGAGACAAGTGGCAGAGTCC	115
MAP2K1	Hs.145442	NM_002755	mitogen-activated protein kinase kinase 1	CCTCCAGCTTCTTCTGCAAG TCCAAAATGCCCAAGAAGAA	121
MAP2K3	Hs.514012	NM_002756	mitogen-activated protein kinase kinase 3	CCAGGACTCGTAAGGGAACC AGGATCAACCCAGAGCTGAA	111
MAP3K1	Hs.657756	NM_005921	mitogen-activated protein kinase kinase kinase 1	CATCAGGTCGCACAGTGAAAT TCAGGGCTATATGGTGAGAAGC	136
MAP3K7	Hs.644143	NM_003188	mitogen-activated protein kinase kinase kinase 7	CAAAGGCTCCTCTTCCAACA CTCCTCCTCCTCCTCGTCTT	122
MAPK1	Hs.431850	NM_002745	mitogen-activated protein kinase 1	CAGGGTTCTCTGGCAGTAGG CACCAACCTCTCGTACATCG	133
MAPK14	Hs.485233	NM_001315	mitogen-activated protein kinase 14	CGTAACCCCGTTTTTGTGTC GCAGGAGCTGAACAAGACAA	117
MAPK3	Hs.861	NM_002746	mitogen-activated protein kinase 3	GGTCAGTCTCCATCAGGTCC GGGAGATCCAGATCCTGCT	126
MAPK8	Hs.138211	NM_002750	mitogen-activated protein kinase 8	AAAACTCGTTCCTGCAGTCC AAGCACCTTCATTCTGCTGG	123
MAVS	Hs.570362	NM_020746	mitochondrial antiviral signalling protein	TGTCTTCAGCAAACGGCAT GGTCGCCAGGTCTCAGG	119

1	2	3	4	5	6
MEFV	Hs.632221	NM_000243	mediterranean fever	AGGAATCACGCACACAGGTA GCCCTGGAAATCCAGAACAT	114
MX1	Hs.517307	NM_002462	myxovirus (influenza virus) resistance 1, interferon--inducible protein p78 (mouse)	GCCAGCTGTAGGTGTCCTTG ACCTGATGGCCTATCACCAG	147
MYD88	Hs.82116	NM_002468	myeloid differentiation primary response gene (88)	AAAGGCTTCTCAGCCTCCTC ACTGCTCGAGCTGCTTACCA	123
NFKB1	Hs.654408	NM_003998	nuclear factor of kappa light polypeptide gene enhancer in B-cells 1	ATAACCTTTGCTGGTCCCAC ATGTATGTGAAGGCCCATCC	112
NFKBIA	Hs.81328	NM_020529	nuclear factor of kappa light polypeptide gene enhancer in B-cells inhibitor, alpha	TCATGGATGATGGCCAAGT GTCAAGGAGCTGCAGGAGAT	119
NLRP3	Hs.159483	NM_183395	NLR family, pyrin domain containing 3	TGTTGCCTCGCAGGTAAAG AGCACCTGTTGTGCAATCTG	129
NOD2	Hs.592072	NM_022162	nucleotide-binding oligomerization domain containing 2	GCCAATGGGACTGGTAATTC ATCTTCACACCGTCCCAGAG	113
OAS2	Hs.414332	NM_002535	2'-5'-oligoadenylate synthetase 2, 69/71kDa	ACCATCGGAGTTGCCTCTTA GGTGAACACCATCTGTGACG	115
PIN1	Hs.465849	NM_006221	peptidylprolyl cis/trans isomerase, NIMA-interacting 1	AAGTCCTCCTCTCCCGACTT CTGGTGAAGCACAGCCAGT	128
PSTPIP1	Hs.129758	NM_003978	proline-serine-threonine phosphatase interacting protein 1	TGCCTCAGTAGCTCCTCCAT CCCAGCTGCAGTTCAAAGAT	127

1	2	3	4	5	6
PYCARD	Hs.499094	NM_013258	PYD and CARD domain containing	CAGGACCTTCCCGTACAGAG CCTCCTCAGTCGGCAGC	117
PYDC1	Hs.58314	NM_152901	PYD (pyrin domain) containing 1	TCACAGGCGTTGCATTACTC ATGCGCATGTTGGAGGA	101
RELA	Hs.502875	NM_021975	V-rel reticuloendotheliosis viral oncogene homolog A (avian)	TTTCTCCTCAATCCGGTGAC CTCCTGTGCGTGTCTCCAT	113
RIPK1	Hs.519842	NM_003804	receptor (TNFRSF)- -interacting serine-threonine kinase 1	TCACAACTGCATTTTCGTTTG CATTTCCTGGCATTGAAGAAA	117
SPP1	Hs.313	NM_000582	secreted phosphoprotein 1	GCCACAGCATCTGGGTATTT GTGATTTGCTTTTGCCTCCT	110
STAT1	Hs.642990	NM_007315	signal transducer and activator of transcription 1, 91kDa	TGCTCTGAATATTCCCCGAC TTCAGGAAGACCCAATCCAG	117
SUGT1	Hs.281902	NM_006704	SGT1, suppressor of G2 allele of SKP1 (*S. cerevisiae*)	TTTTCCCATCTCACAGCCTC TTGAAACTGGAACTTCTTCATCC	110
TBK1	Hs.505874	NM_013254	TANK-binding kinase 1	CCCAATGCTCCAAAGATCA TCTGTATGGCACAGAAGAATATTTG	109
TICAM1	Hs.29344	NM_182919	toll-like receptor adaptor molecule 1	GTCCAGGTGTTGGCTCTGTT CTGGACGAACACTCCCAGAT	135
TLR3	Hs.657724	NM_003265	toll-like receptor 3	AGTGCACTTGGTGGTGGAG AGGAAAGGCTAGCAGTCATCC	117
TLR7	Hs.659215	NM_016562	toll-like receptor 7	AACCATCTAGCCCCAAGGAG TGCTCTGCTCTCTTCAACCA	143

1	2	3	4	5	6
TLR8	Hs.660543	NM_138636	toll-like receptor 8	CGCATAACTCACAGGAACCA GCTGCTGCAAGTTACGGAAT	118
TLR9	Hs.87968	NM_017442	toll-like receptor 9	CTGCACCAGGAGAGACAGC TGTGAAGCATCCTTCCCTGT	122
TNF	Hs.241570	NM_000594	tumor necrosis factor (TNF superfamily, member 2)	GCCAGAGGGCTGATTAGAGA TCAGCCTCTTCTCCTTCCTG	124
TRADD	Hs.460996	NM_003789	TNFRSF1A-associated via death domain	CGAGGACTCCACAAACAGGT GGAAGCGGCGGAGTAGA	138
TRAF3	Hs.510528	NM_003300	TNF receptor-associated factor 3	CGCCAGGAGAGTCCATCTT AGCAGAACGCTGCGGAC	125
TRAF6	Hs.591983	NM_004620	TNF receptor-associated factor 6	GCCACACAGCAGTCACTTTC TCCCCGCGCACTAGAAC	105
TRIM25	Hs.528952	NM_005082	tripartite motif-containing 25	GCCCCGTTGATCTGACTGTA TGGTGGAGCATAAGACCTGC	109
B2M	Hs.534255	NM_004048	beta-2-microglobulin	TGACTTTGTCACAGCCCAAGATA CGGCATCTTCAAACCTCCA	75
HPRT1	Hs.412707	NM_000194	hypoxanthine phosphoribosyltransferase 1	TGGTCAGGCAGTATAATCCAAAGA TCAAATCCAACAAAGTCTGGCTTA	100
RPLPO	Hs.523185	NM_001002 NM_053275	ribosomal protein, large, P0	CCAACTACTTCCTTAAGATCATCCAACTA ACATGCGGATCTGCTGCA	105
GAPDH	Hs.592355	NM_002046	glyceraldehyde-3-phosphate dehydrogenase	AGCCGAGCCACATCGCT TGGCAACAATATCCACTTTACCAGAGT	122
ACTB	Hs.520640	NM_001101	actin, beta	CCCCGCGAGCACAGA CCACGATGGAGGGGAAGAC	171
TBP	Hs.590872	NM_003194 NM_001172085	TATA box binding protein	GCACAGGAGCCAAGAGTGAA TCACAGCTCCCCACCATATTC	127

1	2	3	4	5	6
RN18S1	N/A	NR_003286	18S ribosomal RNA	CGGCTACCACATCCAAGGAA GCTGGAATTACCGCGGCT	187
IKBKG	Hs.43505	NM_003639	inhibitor of kappa light polypeptide gene enhancer in B-cells, kinase gamma	CTCCTGGAACTTGCACATGA TGCCTGGAGGAGAATCAAGA	138
IFI44L	Hs.389724	NM_006820	interferon-induced protein 44-like	TTCCATGTCAATCTTGTTGTCAC TTTCTGTCTCCAAACCGTGG	124
RIPK2	Hs.103755	NM_003821	receptor-interacting serine-threonine kinase 2	CAAATGTTCTCAAAACTGGTTCA TCACCGAGCACGTATGATCT	113
HERC5	Hs.26663	NM_016323	hect domain and RLD 5	CGGTGCAAGAGTTCGTCTAC GGGATGAAAGTGCTGAGGAG	130
IRF9	Hs.1706	NM_006084	interferon regulatory factor 9	TTCTGTGGAGTATGGCTGGAG GAGCTCTTCAGAACCGCCTA	131

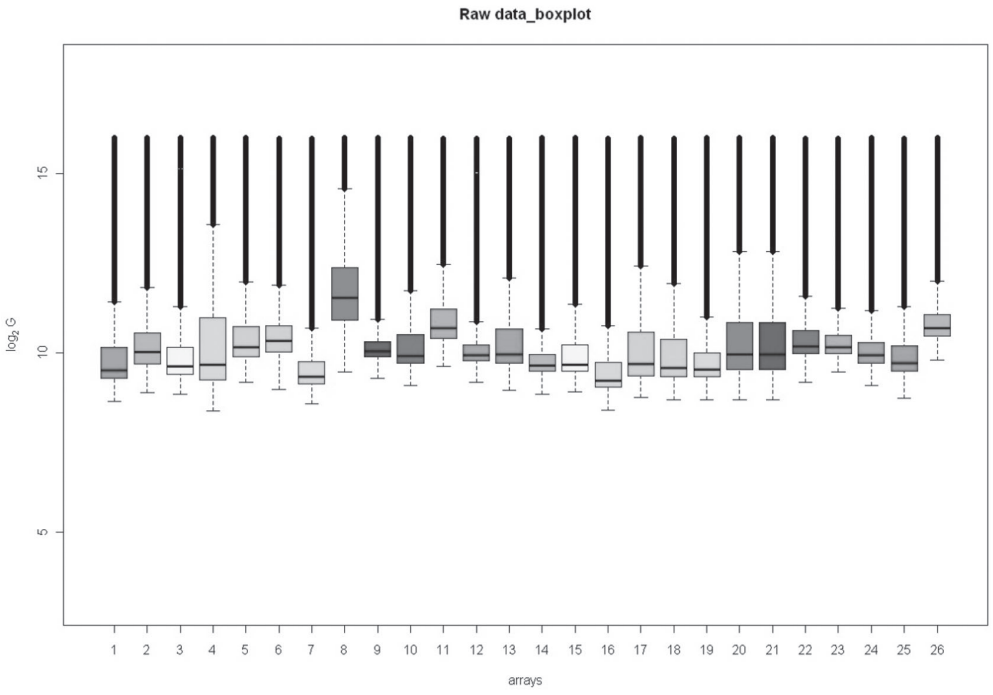

Fig. S1. Boxplot of the raw data (log, base 2 of signal intensity from green channel) of microarray experiments of transcriptome analyses of Caco-2 cells treated with: (1, 2) *L. rhamnosus GG* (ATCC 53103), (3, 4) *B. animalis* BB12, (5, 6) mixture of selected strains (*L. acidophilus* LA-5, *L. plantarum* PL02, *L. rhamnosus* KL53A, *L. delbruecki* subsp. *bulgaricus* LBY-27, *L. lactis* PB411, *B. animalis* BB12), (7, 8) *L. casei* DN114001 (Defensis), (9, 10) *B. thetaiotaomicron* ATCC 29741, (11, 12) *P. anaerobius* ATCC 27337, (13, 14) *S.* Typhimurium ATCC 14028, (15, 16) *B. animalis* MK2, (17, 18) *L. acidophilus* LA-5, (19, 20) *E. coli* ATCC 10536, (21, 22) *E. coli* Nissle 1917, (23, 24) *E. coli* O157:H7, (25, 26) *L. casei* Shirota

Ryc. S1. Wykres pudełkowy przedstawiający dane pierwotne (wartości intensywności fluorescencji mierzonej dla 555 nm przedstawionej w postaci logarytmu o podstawie 2) uzyskane w analizie mikromacierzowej transkryptomu komórek Caco-2 poddanych działaniu komórek bakterii: (1, 2) *L. rhamnosus GG* (ATCC 53103), (3, 4) *B. animalis* BB12, (5, 6) mieszaniny wybranych szczepów (*L. acidophilus* LA-5, *L. plantarum* PL02, *L. rhamnosus* KL53A, *L. delbruecki* subsp. *bulgaricus* LBY-27, *L. lactis* PB411, *B. animalis* BB12), (7, 8) *L. casei* DN114001 (Defensis), (9, 10) *B. thetaiotaomicron* ATCC 29741, (11, 12) *P. anaerobius* ATCC 27337, (13, 14) *S.* Typhimurium ATCC 14028, (15, 16) *B. animalis* MK2, (17,18) *L. acidophilus* LA-5, (19, 20) *E. coli* ATCC 10536, (21, 22) *E. coli* Nissle 1917, (23, 24) *E. coli* O157:H7, (25, 26) *L. casei* Shirota

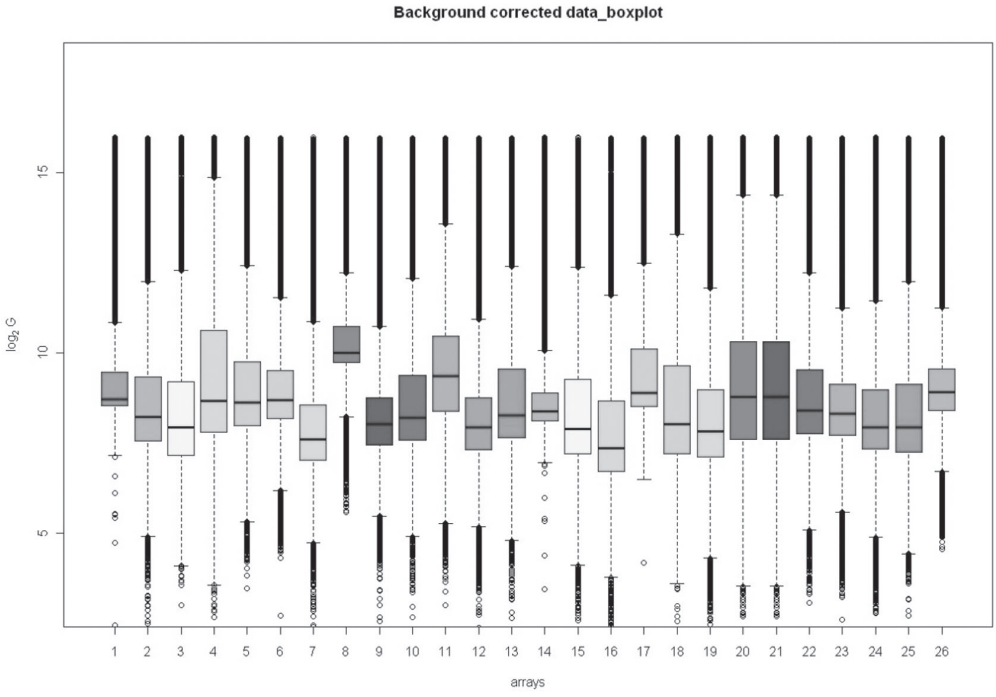

Fig. S2. Boxplot of the background corrected data with "Normexp" method (log, base 2 of signal intensity from green channel) of microarray experiments of transcriptome analyses of Caco-2 cells treated with bacteria (numbers describing experimental conditions same as in Figure S1)

Ryc. S2. Wykres pudełkowy przedstawiający dane po korekcie tła metodą „Normexp" (wartości intensywności fluorescencji mierzonej dla 555 nm przedstawionej w postaci logarytmu o podstawie 2) uzyskane w analizie mikromacierzowej transkryptomu komórek Caco-2 poddanych działaniu komórek bakterii (numeracja wariantów eksperymentalnych jak na rycinie S1)

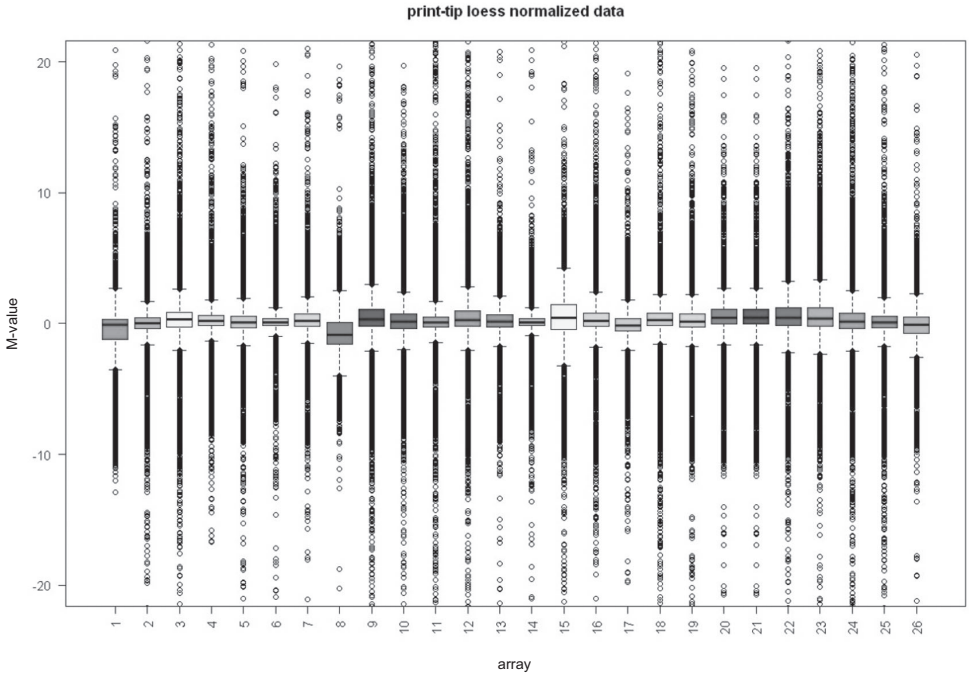

Fig. S3. Boxplot of the background corrected ("Normexp") and within-slide normalised ("Print-tip loess") *M*-values datasets of microarray experiments of transcriptome analyses of Caco-2 cells treated with bacteria (numbers describing experimental conditions same as in Figure S1)

Ryc. S3. Wykres pudełkowy przedstawiający dane po korekcie tła („Normexp") i normalizacji wewnątrz macierzy („Print-tip loess") w postaci wartości *M*, uzyskane w analizie mikromacierzowej transkryptomu komórek Caco-2 poddanych działaniu komórek bakterii (numeracja wariantów eksperymentalnych jak na rycinie S1)

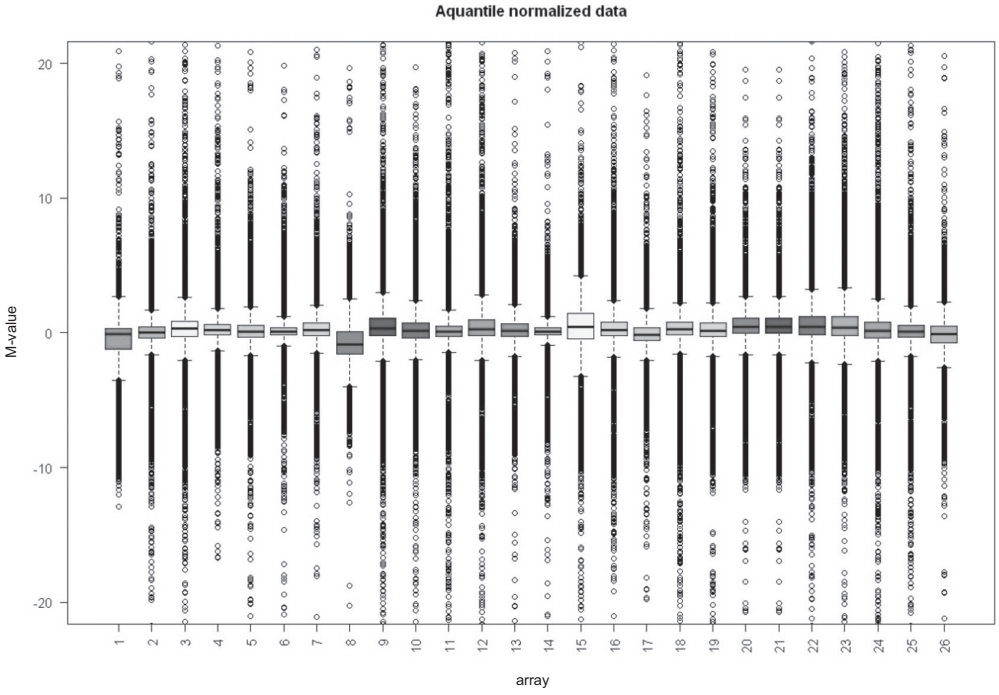

Fig. S4. Boxplot of the background corrected ("Normexp") and within-slide ("Print tip loess") and between slide ("Aquantile") normalised *M*-values datasets of microarray experiments of transcriptome analyses of Caco-2 cells treated with bacteria (numbers describing experimental conditions same as in Figure S1)

Ryc. S4. Wykres pudełkowy przedstawiający dane po korekcie tła („Normexp"), normalizacji wewnątrz macierzy („Print-tip loess") i pomiędzy macierzami („Aquantile") w postaci wartości *M*, uzyskane w analizie mikromacierzowej transkryptomu komórek Caco-2 poddanych działaniu komórek bakterii (numeracja wariantów eksperymentalnych jak na rycinie S1)

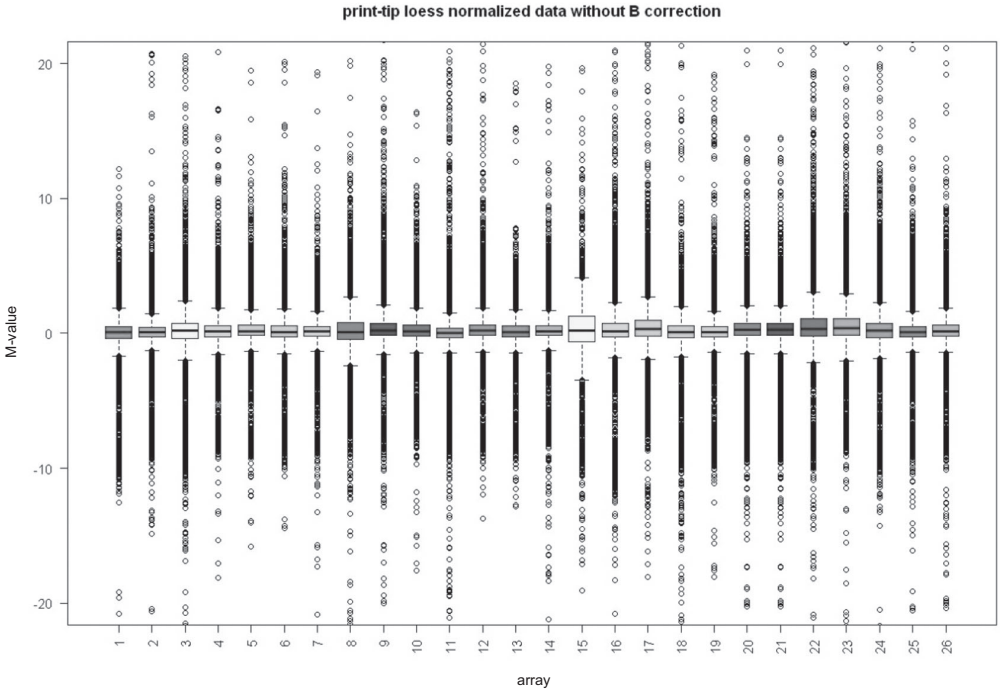

Fig. S5. Boxplot of the within-slide normalised ("Print tip loess") *M*-values datasets of microarray experiments of transcriptome analyses of Caco-2 cells treated with bacteria (numbers describing experimental conditions same as in Figure S1)

Ryc. S5. Wykres pudełkowy przedstawiający dane po normalizacji wewnątrz macierzy („Print-tip loess") w postaci wartości *M*, uzyskane w analizie mikromacierzowej transkryptomu komórek Caco-2 poddanych działaniu komórek bakterii (numeracja wariantów eksperymentalnych jak na rycinie S1)

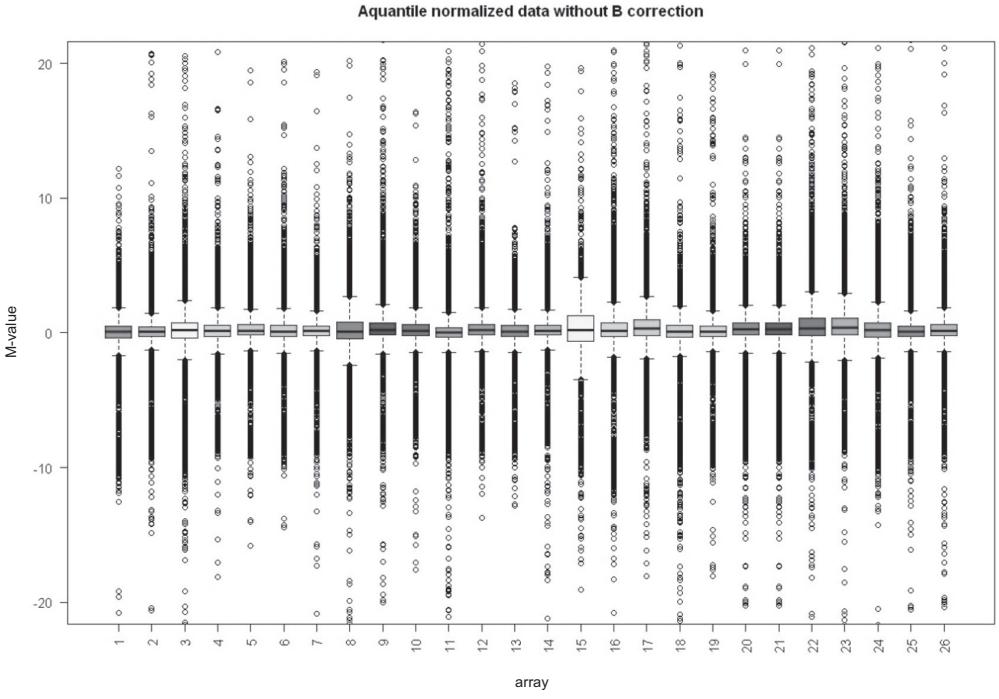

Fig. S6. Boxplot of the within-slide ("Print tip loess") and between slide ("Aquantile") normalised *M*-values datasets of microarray experiments of transcriptome analyses of Caco-2 cells treated with bacteria (numbers describing experimental conditions same as in Figure S1)

Ryc. S6. Wykres pudełkowy przedstawiający dane po normalizacji wewnątrz macierzy („Print-tip loess") i pomiędzy macierzami („Aquantile") w postaci wartości *M*, uzyskane w analizie mikromacierzowej transkryptomu komórek Caco-2 poddanych działaniu komórek bakterii (numeracja wariantów eksperymentalnych jak na rycinie S1)

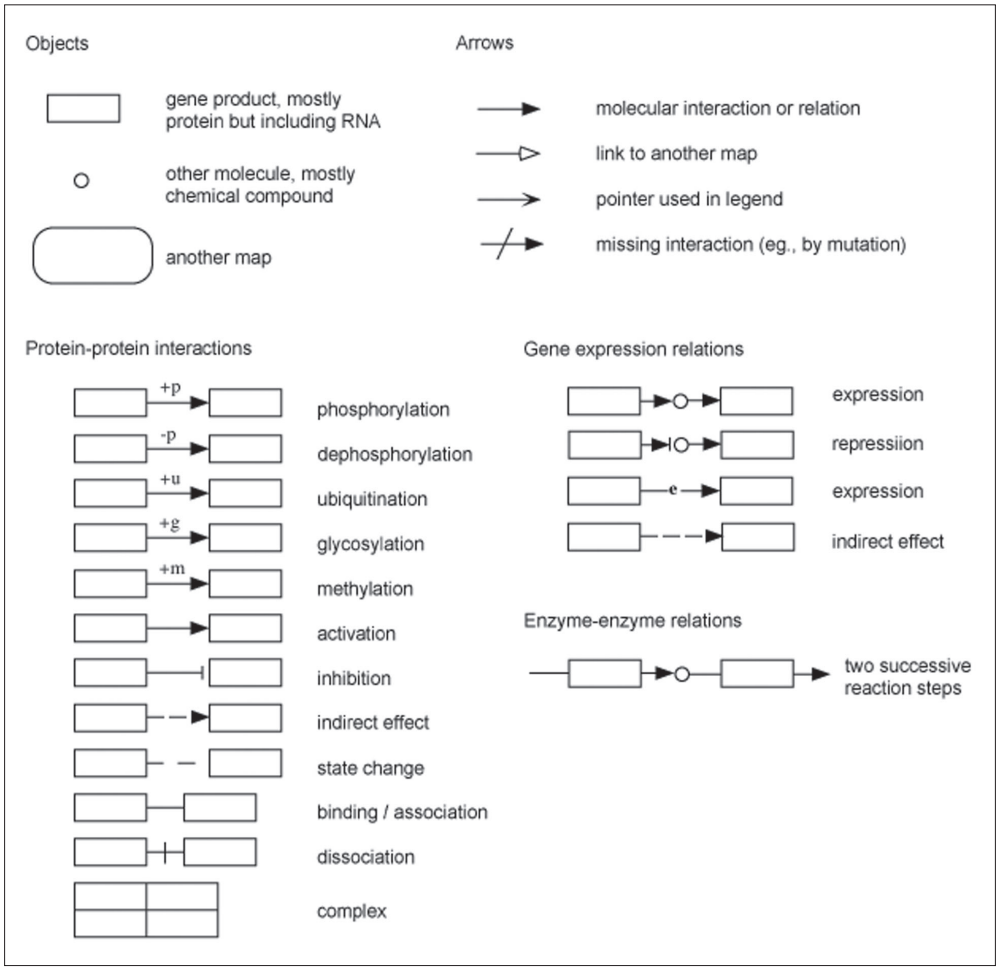

Fig. S7. Notation of objects and relations used in KEGG pathways (Kanehisa and Goto, 2000)

Ryc. S7. Oznaczenie obiektów i relacji wykorzystanych w szlakach KEGG (Kanehisa and Goto, 2000)

Table S2. Overview of the number of joint differentially expressed genes ($p < 0.05$) in Caco-2 enterocytes under the influence of tested microorganisms: *L. rhamnosus GG* ATCC 53103 (LGG), *B. animalis* BB12 (BB12), *L. acidophilus* LA-5 (Lc5), mixture (mix) of selected strains (*L. acidophilus* LA-5, *L. plantarum* PL02, *L. rhamnosus* KL53A, *L. delbruecki* subsp. *bulgaricus* LBY-27, *L. lactis* PB411, *B. animalis* BB12), *L. casei* Shirota (LcS), *L. casei* DN114001 (LcD), *E. coli* Nissle 1917 (EcN), *B. animalis* MK2 (Ba), *B. thetaiotaomicron* ATCC 29741 (Bt), *P. anaerobius* ATCC 27337 (Pa), *S.* Typhimurium ATCC 14028 (St), *E. coli* ATCC 10536 (EcF), *E. coli* O157:H7 (EcOH). Right-upper half shows the total number of joint genes in pairs of experimental conditions (∩), the left-lower half shows the numbers of joint genes that display the same expression pattern in pairs of experimental conditions: top in a cell – upregulated (↑), bottom in a cell – downregulated (↓). The overview includes the group analysis of bacteria: probiotics (prob), commensal (kom) and pathogenic (pat)

Tabela S2. Liczba wspólnych genów różnicujących ($p < 0,05$) w enterocytach Caco-2 po stymulacji badanymi mikroorganizmami: *L. rhamnosus GG* ATCC 53103 (LGG), *B. animalis* BB12 (BB12), *L. acidophilus* LA-5 (Lc5), mieszanina (mix) wybranych szczepów (*L. acidophilus* LA-5, *L. plantarum* PL02, *L. rhamnosus* KL53A, *L. delbruecki* subsp. *bulgaricus* LBY-27, *L. lactis* PB411, *B. animalis* BB12), *L. casei* Shirota (LcS), *L. casei* DN114001 (LcD), *E. coli* Nissle 1917 (EcN), *B. animalis* MK2 (Ba), *B. thetaiotaomicron* ATCC 29741 (Bt), *P. anaerobius* ATCC 27337 (Pa), *S.* Typhimurium ATCC 14028 (St), *E. coli* ATCC 10536 (EcF), *E. coli* O157:H7 (EcOH). Prawa, górna połowa zawiera całkowitą liczbę wspólnych genów różnicujących w porównaniu par warunków eksperymentalnych (∩). Lewa, dolna połowa zawiera liczby wspólnych genów różnicujących w porównaniu par warunków eksperymentalnych: górna część komórek zawiera liczby wspólnych genów o podwyższonej ekspresji (↑), dolna część komórek zawiera liczby wspólnych genów o obniżonej ekspresji (↓). Porównanie zawiera analizy grupowe dla bakterii: probiotycznych (prob), komensalnych (kom) i patogennych (pat)

↑ / ↓	∩	Probiotic								Commensal				Pathogenic			
		LGG	BB12	Lc5	mix	LcS	LcD	EcN	prob	Ba	Bt	Pa	kom	St	EcF	EcOH	pat
1	2	3	4	5	6	7	8	9	10	11	12	13	14	15	16	17	18
Probiotic	LGG		19	110	47	24	42	21	12	27	92	46	2	43	22	42	5
	BB12	8 5		81	34	29	36	35	17	22	69	46	5	37	16	34	11
	Lc5	58 32	19 18		113	67	117	107	58	117	397	167	13	145	86	245	70

1	2	3	4	5	6	7	8	9	10	11	12	13	14	15	16	17	18
Probiotic	mix	9 17	10 15	41 33		57	27	28	13	35	61	89	7	34	36	55	7
	LcS	12 9	10 12	17 19	12 28		18	49	38	19	77	68	15	61	19	35	14
	LcD	12 8	10 10	36 23	8 6	7 4		24	10	33	123	59	4	70	13	68	17
	EcN	7 7	16 16	12 53	4 19	7 37	9 6		103	27	108	89	29	137	36	61	49
	prob	4 8	6 11	7 48	3 10	3 35	3 5	14 89		8	76	52	37	72	9	29	61
Commensal	Ba	15 5	9 7	67 25	14 8	8 4	10 7	15 6	6 1		70	62	11	43	29	51	13
	Bt	11 27	18 30	27 32	4 24	17 46	30 10	24 77	5 59	11 8		161	48	192	44	142	64
	Pa	9 21	13 18	66 44	13 45	12 41	20 14	18 68	5 46	24 12	23 64		36	129	25	106	34
	kom	1 0	1 3	2 2	1 4	1 14	2 2	3 24	4 31	8 2	8 40	9 27		33	4	14	23
Pathogenic	St	17 12	7 17	16 28	5 11	8 44	21 13	50 84	4 64	13 3	53 105	36 77	3 30		25	121	65
	EcF	15 0	6 0	70 6	24 1	8 0	4 0	19 1	5 0	22 1	9 1	16 0	2 1	17 0		33	35
	EcOH	15 16	4 8	22 132	13 15	11 10	18 23	14 20	2 18	23 13	25 27	48 34	9 3	51 30	22 5		97
	pat	3 1	2 1	10 42	3 0	3 10	6 5	11 27	13 36	7 3	9 28	12 19	8 14	26 38	16 19	38 59	

Table S3. Number of differentially expressed genes in Caco-2 enterocytes under the influence of the bacteria assigned to pathway maps representing knowledge on the molecular interaction networks by KEGG database. The table contains pathways where expression of at least 10 genes was modified by one of the bacteria used. Pathways are sorted by decreasing number of genes identified. The bacterial strains used in the study were designated: LGG – *L. rhamnosus GG* ATCC 53103, BB12 – *B. animalis* BB12, Lc5 – *L. acidophilus* LA-5, mix – mixture of selected strains (*L. acidophilus* LA-5, *L. plantarum* PL02, *L. rhamnosus* KL53A, *L. delbruecki* subsp. *bulgaricus* LBY-27, *L. lactis* PB411, *B. animalis* BB12), LcS – *L. casei* Shirota, LcD – *L. casei* DN114001, EcN – *E. coli* Nissle 1917, Ba – *B. animalis* MK2, Bt – *B. thetaiotaomicron* ATCC 29741, Pa – *P. anaerobius* ATCC 27337, St – *S.* Typhimurium ATCC 14028, EcF – *E. coli* ATCC 10536, EcOH – *E. coli* O157:H7. Collection of genes overrepresented (above average for the group of bacteria used) in a pathway were written in bold letters

Tabela S3. Liczba genów różnicujących, ulegających ekspresji w enterocytach Caco-2 pod wpływem stymulacji badanymi bakteriami, przypisanych do map szlaków molekularnych oddziaływań opisanych w bazie danych KEGG. Tabela zawiera szlaki, w których co najmniej 10 genów ulegało zmianom ekspresji pod wpływem badanych bakterii. Szlaki zostały przedstawione w kolejności malejącej ilości zidentyfikowanych genów. Szczepy bakterii zastosowane w badanich zostały oznaczone: LGG – *L. rhamnosus GG* ATCC 53103, BB12 – *B. animalis* BB12, Lc5 – *L. acidophilus* LA-5, mix – mieszanina wybranych szczepów (*L. acidophilus* LA-5, *L. plantarum* PL02, *L. rhamnosus* KL53A, *L. delbruecki* subsp. *bulgaricus* LBY-27, *L. lactis* PB411, *B. animalis* BB12), LcS – *L. casei* Shirota, LcD – *L. casei* DN114001, EcN – *E. coli* Nissle 1917, Ba – *B. animalis* MK2, Bt – *B. thetaiotaomicron* ATCC 29741, Pa – *P. anaerobius* ATCC 27337, St – *S.* Typhimurium ATCC 14028, EcF – *E. coli* ATCC 10536, EcOH – *E. coli* O157:H7. Liczby genów przypisanych do danego szlaku zmienionych w ilości większej niż średnia dla badanych bakterii zostały zaznaczone pogrubioną czcionką

KEGG id	Pathway name	LGG	BB12	Lc5	mix	LcS	LcD	EcN	Ba	Bt	Pa	St	EcF	EcOH
1	2	3	4	5	6	7	8	9	10	11	12	13	14	15
hsa01100	metabolic pathways	28	24	**52**	30	16	31	24	21	**113**	**56**	**43**	16	**72**
hsa05200	pathways in cancer	9	9	11	9	**14**	8	13	11	**37**	**17**	**14**	6	**18**
hsa04151	PI3K-Akt signalling pathway	14	7	12	10	11	8	**15**	9	**35**	**19**	**15**	6	**24**
hsa05205	proteoglycans in cancer	8	5	**12**	8	8	9	5	6	**34**	**11**	**11**	5	**14**
hsa04015	Rap1 signalling pathway	9	4	8	5	9	6	7	5	**30**	**11**	**11**	5	**12**
hsa04810	regulation of actin cytoskeleton	8	5	**12**	5	6	7	3	3	**29**	**10**	6	3	7

1	2	3	4	5	6	7	8	9	10	11	12	13	14	15
hsa04010	MAPK signalling pathway	8	9	9	7	9	8	11	7	**26**	**14**	**17**	3	**18**
hsa04510	focal adhesion	7	4	**10**	**11**	5	6	7	5	**26**	**16**	5	5	7
hsa05166	HTLV-I infection	7	8	8	**12**	11	8	**13**	7	**26**	**13**	**12**	4	**16**
hsa04390	Hippo signalling pathway	3	2	**8**	5	4	3	5	**7**	**23**	**10**	**9**	1	**9**
hsa04530	tight junction	5	6	5	**7**	3	3	3	3	**21**	**8**	2	2	**13**
hsa05169	Epstein-Barr virus infection	6	4	**11**	5	3	5	**9**	3	**21**	**11**	**10**	4	**10**
hsa05206	microRNAs in cancer	**8**	4	6	6	**8**	4	7	6	**21**	**14**	6	3	**8**
hsa04014	Ras signalling pathway	6	6	8	2	7	6	**10**	4	**20**	**11**	**11**	4	**9**
hsa04670	leukocyte transendothelial migration	4	2	**6**	**5**		3	2	2	**20**	3	3		4
hsa05161	hepatitis B	5	7	6	7	5	4	7	7	**20**	**10**	**8**	6	**9**
hsa04144	endocytosis	8	7	8	8	4	**10**	4	4	**19**	**10**	**10**	3	**11**
hsa05203	viral carcinogenesis	8	5	4	**11**	8	8	**11**	4	**19**	9	**10**	7	**15**
hsa04012	ErbB signalling pathway	4	**6**	4	4	3	4	5	3	**18**	**9**	**7**	2	**7**
hsa04110	cell cycle	1	1	**9**	3	2	3	5	3	**18**	**6**	5		9
hsa04062	chemokine signalling pathway	**10**	8	7	5	3	4	**10**	**11**	**17**	**9**	**9**	8	6
hsa04068	FoxO signalling pathway	6	**7**	**9**	4	4	**7**	5	6	**17**	5	6	4	**9**
hsa04141	protein processing in ER	3	2	**10**	3	2	6	1	3	**17**	6	3		17
hsa04142	lysosome	5	1	3	2	3	3	4	2	**17**	**6**	**12**		4
hsa04919	thyroid hormone signalling pathway	**6**	4	4	4	4	3	2	3	**17**	**8**	5	3	5
hsa05164	influenza A	1	4	6	7	2	7	**11**	5	**17**	**9**	7	6	**11**
hsa04020	calcium signalling pathway	4	1	**9**	**8**	4	5	3	5	**16**	**10**	5	4	**9**

1	2	3	4	5	6	7	8	9	10	11	12	13	14	15
hsa04066	HIF-1 signalling pathway	**6**	**7**	**7**	4	3	2	5	5	**16**	5	**6**	3	**9**
hsa05100	bacterial invasion of epithelial cells		1	2	2	1	3	1	1	**16**	2	**6**		1
hsa05160	hepatitis C	5	7	**8**	**8**	2	**8**	6	4	**16**	7	7	6	**7**
hsa05202	transcriptional misregulation in cancer	**9**	2	**10**	4	2	4	**10**	3	**15**	**16**	**10**	4	**12**
hsa04668	TNF signalling pathway	6	5	6	5	4	5	**15**	8	**14**	**13**	**12**	8	7
hsa04910	insulin signalling pathway	5	3	**7**	5	3	5	1	3	**15**	**9**	**6**	4	**8**
hsa00564	glycerophospholipid metabolism	2	2	**7**		1		4	4	**14**	**6**	**5**		2
hsa05152	tuberculosis	5	3	**7**	4	5	**7**	4	2	**10**	**14**	**8**	3	**9**
hsa01200	carbon metabolism		4	**6**	3	2	2	2	2	**13**	2	**8**	2	**10**
hsa04060	cytokine-cytokine receptor interaction	**11**	**10**	7	9	7	**10**	9	**10**	**10**	9	9	7	**13**
hsa04070	phosphatidylinositol signalling system	2	2	2	2		3	3	3	**13**	**4**	3		5
hsa04120	ubiquitin mediated proteolysis	5	2	**9**	5	1	**6**	3	2	**11**	**8**	4	1	**13**
hsa04350	TGF-beta signalling pathway	2	**5**	**6**	3	3		1	4	**13**	**5**	4	1	4
hsa04514	cell adhesion molecules (CAMs)	4	4	**6**	4	4	**9**	5	2	**13**	5	**6**	1	**7**
hsa04750	inflammatory mediator regulation of TRP channels	2	1	**7**	**5**	1	3	2	2	**13**	**7**	4		3
hsa04915	estrogen signalling pathway	**8**	**5**	3	4	3	1	4	3	**13**	**8**	**5**	2	5
hsa03013	RNA transport	3	5	**10**	5	2	4	2	4	**8**	**10**	**8**	1	**12**
hsa04310	Wnt signalling pathway	3	2	**7**	4	5	4	**6**	4	**12**	**9**	5	1	**12**

1	2	3	4	5	6	7	8	9	10	11	12	13	14	15
hsa04620	toll-like receptor signalling pathway	1	4	4	**6**	3	5	**7**	**7**	**12**	**9**	**6**	4	4
hsa04912	GnRH signalling pathway	5	3	**7**	5	3	5	2	4	**12**	**6**	4	2	**7**
hsa05145	toxoplasmosis	3	2	4	4	2	**5**	4	**6**	**12**	**7**	**5**	4	**6**
hsa05146	amoebiasis	3	2	3	**5**	2	3	**6**	**5**	**12**	3	**5**	4	**7**
hsa05168	herpes simplex infection	5	4	5	**11**	5	**9**	**9**	5	**12**	**10**	**9**	4	**11**
hsa00190	oxidative phosphorylation	2		3	2	3	2	1		**11**	3	3		4
hsa00230	purine metabolism	4		1	**6**	3	3	4	4	**11**	5	**9**	3	**8**
hsa03015	mRNA surveillance pathway	3	2	**4**	**5**	1	2	2	1	**11**	**6**	**4**	1	**5**
hsa04145	phagosome	3	**5**	**6**	4	4	**7**	2	2	**11**	**6**	**6**	1	**5**
hsa04520	adherens junction	**4**	2	3	2	2	2	2	2	**11**	**6**	2	1	**5**
hsa04630	Jak-STAT signalling pathway	5	5	**7**	**7**	4	**7**	3	3	**11**	**9**	3	3	**6**
hsa05162	measles	2	4	3	5	1	2	**6**	5	**11**	**8**	**6**	4	**8**
hsa01230	biosynthesis of amino acids	1	2	**4**	3	1	3	1	1	**10**	2	**4**	2	**9**
hsa03040	spliceosome	1	3	**5**	1	1	**6**	1	2	**10**	**9**	**5**	1	**8**
hsa04064	NF-kappa B signalling pathway	1	2	3	3	4	**6**	**8**	**9**	**10**	**10**	**6**	**6**	**6**
hsa05130	pathogenic *Escherichia coli* infection		2	**3**			1	1	2	**10**	2	2		2
hsa05142	Chagas disease (trypanosomiasis)	4	**6**	3	**7**	2	2	**8**	**6**	**10**	**8**	**8**	4	5
hsa05210	colorectal cancer	**4**	**5**	1	4	1	2	3	1	**10**	**6**	3	1	1
Total (including pathways not listed):		705	606	**946**	759	592	711	765	595	**2 297**	**1 247**	**945**	437	**1 292**

Table S4. Number of differentially expressed genes ($p < 0.05$, upregulated – top in a cell, downregulated – bottom in a cell) in Caco-2 enterocytes under the influence of tested microorganisms as categorized by GO Slims. The GO Slim give a broad overview of the ontology content without the detail of the specific fine grained terms. The bacterial strains used in the study were designated: LGG – *L. rhamnosus GG* ATCC 53103, BB12 – *B. animalis* BB12, Lc5 – *L. acidophilus* LA-5, mix – mixture of selected strains (*L. acidophilus* LA-5, *L. plantarum* PL02, *L. rhamnosus* KL53A, *L. delbruecki* subsp. *bulgaricus* LBY-27, *L. lactis* PB411, *B. animalis* BB12), LcS – *L. casei* Shirota, LcD – *L. casei* DN114001, EcN – *E. coli* Nissle 1917, Ba – *B. animalis* MK2, Bt – *B. thetaiotaomicron* ATCC 29741, Pa – *P. anaerobius* ATCC 27337, St – *S.* Typhimurium ATCC 14028, EcF – *E. coli* ATCC 10536, EcOH – *E. coli* O157:H7. Significant over- and underrepresented genes in GO slim terms were determined by selecting outliers in percentages of differential genes by a Grubbs' test and are indicated by double-lined cell border regarding percentage of total differential genes in a category or in bold letters for separate calculations of up- and down-regulated genes percentages

Tabela S4. Liczba genów różnicujących ($p < 0,05$, o podwyższonej ekspresji – górny wiersz w komórce, o obniżonej ekspresji – dolny wiersz w komórce) w enterocytach Caco-2 po stymulacji mikroorganizmami w kategoriach określeń GO Slim. Określenia GO Slim dają ogólny pogląd na powiązania genów z procesami (ontologie). Szczepy bakterii stosowane w badaniach mają następujące oznaczenia: LGG – *L. rhamnosus GG* ATCC 53103, BB12 – *B. animalis* BB12, Lc5 – *L. acidophilus* LA-5, mix – mieszanina wybranych szczepów (*L. acidophilus* LA-5, *L. plantarum* PL02, *L. rhamnosus* KL53A, *L. delbruecki* subsp. *bulgaricus* LBY-27, *L. lactis* PB411, *B. animalis* BB12), LcS – *L. casei* Shirota, LcD – *L. casei* DN114001, EcN – *E. coli* Nissle 1917, Ba – *B. animalis* MK2, Bt – *B. thetaiotaomicron* ATCC 29741, Pa – *P. anaerobius* ATCC 27337, St – *S.* Typhimurium ATCC 14028, EcF – *E. coli* ATCC 10536, EcOH – *E. coli* O157:H7. Liczby genów dla danego określenia GO Slim odbiegające od trendu zaobserwowanego dla wszystkich badanych warunków eksperymentalnych wyznaczono na podstawie wartości odstających od średniego odsetka liczby genów, stosując test Grubbsa i zaznaczając podwójną linią ramki komórki (dla całkowitej liczby genów) lub stosując pogrubioną czcionkę dla obliczeń uwzględniających tylko odsetek genów o podwyższonej lub obniżonej ekspresji

GO Slim term		Number of upregulated genes ($p < 0.05$) Number of downregulated genes ($p < 0.05$)												
		probiotic							commensal			pathogenic		
		LGG	BB12	Lc5	mix	LcS	LcD	EcN	Ba	Bt	Pa	St	EcF	EcOH
1	2	3	4	5	6	7	8	9	10	11	12	13	14	15
	metabolic process	102 155	99 94	502 705	100 221	87 127	147 152	99 163	117 83	419 360	230 335	202 188	76 31	245 301

1	2	3	4	5	6	7	8	9	10	11	12	13	14	15
Biological process	biological regulation	97 136	86 86	454 538	86 201	88 119	143 145	95 147	103 71	339 348	213 299	203 194	86 19	236 234
	multicellular organismal process	70 64	40 43	252 217	59 101	52 62	75 67	65 55	70 34	158 222	133 126	125 104	51 14	126 106
	cell communication	55 73	42 39	247 219	53 104	60 59	76 72	52 67	55 41	185 194	120 131	119 103	**57** **8**	133 112
	response to stimulus	50 71	47 30	191 175	49 99	41 47	55 51	66 52	56 24	152 139	91 114	104 79	48 15	105 75
	developmental process	48 59	32 31	200 180	45 70	41 48	55 50	56 34	54 26	125 158	97 90	99 78	37 13	100 79
	cellular component organisation	29 55	30 30	163 210	34 77	34 43	49 51	44 40	39 22	161 115	81 75	80 58	28 25	92 85
	localisation	39 52	46 33	164 248	31 79	42 43	66 50	38 49	44 27	175 141	91 99	87 63	44 9	86 111
	cell proliferation	10 20	14 11	57 72	17 34	18 16	14 16	27 11	23 9	50 43	39 28	32 27	19 4	29 23
	death	14 24	14 19	67 91	15 24	14 16	21 17	28 11	13 5	74 41	32 46	43 24	16 4	41 28
	multi-organism process	11 15	8 3	34 46	11 16	10 10	12 7	**23** 5	12 6	37 29	23 20	32 16	9 8	37 11
	growth	4 12	6 11	27 26	10 11	2 11	5 11	2 5	9 4	24 20	12 18	13 12	6 4	14 8
	reproduction	13 14	8 12	47 38	8 18	16 12	12 10	21 8	15 3	36 37	20 24	24 12	11 4	28 17
	unclassified	171 151	95 151	389 384	168 261	138 154	217 215	59 122	179 97	332 657	357 445	195 306	**164** 26	285 230

1	2	3	4	5	6	7	8	9	10	11	12	13	14	15
Molecular function	protein binding	110 146	92 90	465 620	95 201	95 123	156 148	111 123	110 71	452 346	234 244	244 185	91 30	253 261
	ion binding	47 63	41 54	276 311	48 97	57 64	94 80	35 **107**	57 47	184 199	150 200	110 101	44 10	112 153
	hydrolase activity	25 44	29 19	130 176	30 53	20 36	44 36	19 33	33 22	145 82	61 77	49 38	**32** 4	54 72
	nucleic acid binding	38 62	36 49	177 292	28 78	22 51	66 62	53 **94**	42 30	127 136	97 162	75 77	19 22	108 116
	nucleotide binding	29 42	24 19	149 192	22 57	16 34	44 32	16 51	39 22	151 95	57 84	68 41	28 9	62 79
	transferase activity	25 36	28 19	120 135	22 46	16 20	32 23	21 23	34 14	74 81	51 57	42 40	19 5	51 76
	molecular transducer activity	32 39	19 18	119 76	17 42	22 33	31 36	17 29	24 13	59 105	57 48	48 54	24 1	51 36
	transcription regulator activity	16 29	15 17	93 99	16 47	12 27	27 28	**31** 34	17 12	57 67	47 60	50 39	10 1	49 54
	enzyme regulator activity	17 14	11 8	56 49	12 30	14 9	18 20	11 19	11 13	35 47	25 33	28 36	10 6	33 25
	transporter activity	14 14	14 12	58 84	9 22	19 5	23 16	11 18	12 7	65 47	33 39	36 20	17 3	29 37
	electron carrier activity	5 4	4 2	8 6	7 3	2 1	5 2	1 4	1 1	12 10	5 9	2 3	**5** 0	5 3
	structural molecule activity	6 5	3 2	26 57	5 15	6 4	9 7	4 11	2 8	44 27	17 13	18 16	2 6	17 14
	lipid binding	8 6	4 4	31 23	4 14	4 10	3 9	3 10	2 3	16 30	12 19	11 10	4 1	10 17

1	2	3	4	5	6	7	8	9	10	11	12	13	14	15
Molecular function	oxygen binding	3 1	2 0	2 2	4 0	2 0	1 1	2 **2**	2 1	2 1	3 3	2 0	2 0	1 0
	carbohydrate binding	6 5	10 0	20 7	3 5	10 6	2 9	3 2	5 3	18 27	10 7	8 10	2 2	16 9
	molecular adaptor activity	0 2	1 0	7 8	1 3	2 0	2 1	0 0	3 1	3 2	3 0	3 1	2 0	1 2
	chromatin binding	2 4	1 2	10 11	1 6	1 6	2 5	1 6	**4** 0	8 7	7 9	2 6	0 0	2 6
	antioxidant activity	0 2	1 0	0 5	0 0	2 1	0 1	0 2	1 0	6 2	0 4	0 1	0 0	3 1
	protein tag	0 0	0 0	0 0	0 0	0 0	0 0	0 0	1 0	0 0	1 0	0 0	0 0	0 0
	translation regulation activity	1 2	0 0	1 5	0 0	0 0	0 1	0 0	1 1	1 0	1 0	0 1	0 0	1 1
	nutrient reservoir activity	0 0	0 0	0 0	0 0	0 0	0 0	0 0	1 0	0 0	1 0	0 0	0 0	0 0
	unclassified	164 141	87 144	320 337	164 251	136 135	202 209	55 100	173 98	301 557	325 424	180 288	**165** 24	275 204
Cellular component	membrane	80 130	90 63	382 406	73 163	88 97	140 117	75 92	87 54	341 338	182 215	183 145	71 18	214 204
	nucleus	59 101	53 62	285 459	38 146	48 82	109 100	82 109	74 58	237 215	159 227	128 117	38 24	166 181
	macromolecular complex	37 58	38 25	152 284	27 82	31 31	63 55	43 49	32 27	186 133	95 86	88 55	27 25	101 101
	cytosol	14 17	14 11	61 132	17 31	17 20	17 21	12 19	16 14	104 47	34 39	37 25	17 12	38 51

1	2	3	4	5	6	7	8	9	10	11	12	13	14	15
Cellular component	cytoskeleton	14 21	9 13	76 91	14 33	7 13	22 25	16 18	20 16	95 65	51 30	41 26	16 **1**	40 31
	membrane-enclosed lumen	26 42	21 13	100 180	14 54	20 24	32 30	25 37	25 14	125 75	58 56	39 41	14 11	53 67
	extracellular matrix	9 4	5 1	26 10	12 2	9 4	3 5	2 4	7 3	9 13	13 10	6 8	5 2	12 11
	Golgi apparatus	10 22	15 4	55 87	12 36	11 17	18 21	11 12	18 7	69 39	19 31	27 19	9 3	22 27
	extracellular space	15 8	13 6	43 15	11 12	14 10	10 8	16 12	18 6	29 31	19 18	15 17	16 4	24 16
	endoplasmic reticulum	13 24	14 6	45 96	10 28	14 11	15 16	14 13	11 8	62 40	28 26	26 20	10 7	25 43
	mitochondrion	7 19	14 10	55 101	10 21	13 12	21 15	11 11	11 13	78 31	24 27	17 17	10 6	32 42
	cell projection	4 15	5 8	39 44	9 19	8 11	9 12	4 18	14 3	28 29	24 25	13 10	**12** 1	25 10
	endomembrane system	8 9	13 7	37 72	8 21	9 5	12 15	12 9	9 5	49 37	20 16	20 17	3 2	23 42
	vesicle	12 12	12 3	36 49	7 16	9 4	16 10	8 6	8 4	48 38	21 15	25 11	2 4	21 22
	chromosome	6 12	7 3	20 45	4 15	7 7	7 13	**21** 4	10 4	0 24	13 13	11 9	3 **15**	29 17
	endosome	8 3	3 5	20 36	2 10	7 4	11 7	6 6	6 1	24 12	9 7	11 8	1 0	10 10
	envelope	4 10	10 5	25 67	1 12	8 6	15 11	10 8	5 3	42 18	15 12	12 13	4 2	16 28

1	2	3	4	5	6	7	8	9	10	11	12	13	14	15
Cellular component	vacuole	4 4	1 1	11 23	1 5	5 4	6 5	3 6	5 3	22 5	6 10	13 6	2 0	9 5
	ribosome	1 3	1 1	5 34	0 3	1 2	2 1	0 4	1 3	11 8	3 3	3 2	0 4	4 5
	lipid particle	0 0	0 1	1 1	0 1	1 0	0 0	0 0	0 0	1 0	0 0	0 0	0 0	0 0
	microbody	0 3	1 0	6 9	0 1	0 1	2 1	2 3	0 0	8 2	2 3	2 0	0 1	5 3
	external encapsulating structure	0 0	0 0	0 0	0 0	0 0	0 0	1 0	0 0	0 0	0 0	1 0	0 0	0 0
	unclassified	182 150	99 155	365 385	164 250	126 156	219 207	44 137	163 97	320 581	347 442	165 321	**174** 24	281 229